THE UNIVERSITY
of EDINBURGH

This thesis has been submitted in fulfilment of the requirements for a postgraduate degree (e.g. PhD, MPhil, DClinPsychol) at the University of Edinburgh. Please note the following terms and conditions of use:

This work is protected by copyright and other intellectual property rights, which are retained by the thesis author, unless otherwise stated.
A copy can be downloaded for personal non-commercial research or study, without prior permission or charge.
This thesis cannot be reproduced or quoted extensively from without first obtaining permission in writing from the author.
The content must not be changed in any way or sold commercially in any format or medium without the formal permission of the author.
When referring to this work, full bibliographic details including the author, title, awarding institution and date of the thesis must be given.

Calculation of webs in non-Abelian gauge theories using unitarity cuts

Andries Waelkens

Doctor of Philosophy
The University of Edinburgh
June 2017

Abstract

When calculating scattering processes in theories involving massless gauge bosons, such as gluons in Quantum Chromodynamics (QCD), one encounters infrared (IR), or soft, divergences. To obtain precise predictions, it is important to have exact expressions for these IR divergences, which are present in any on-shell scattering amplitude. Due to their long wavelength, soft gluons factorise with respect to short-distance, or hard, interactions and can be captured by correlators of semi-infinite Wilson lines. The latter obey a renormalisation group equation, which gives rise to exponentiation. The exponent can be represented diagrammatically in terms of weighted sums of Feynman diagrams, called webs. A web with L external legs, each with n_i gluon attachments, is denoted $(n_1, n_2, \ldots, n_L)$. In this way all soft gluon interactions can be described by a soft anomalous dimension. It is currently known at three loops with lightlike kinematics, and at two loops with general kinematics. Our work is a step towards a three-loop result in general kinematics.

In recent years, much progress has been made in understanding the general physical properties of scattering amplitudes and in exploiting these properties to calculate specific amplitudes. At the same time, we have discovered a lot of structure underpinning the space of multiple polylogarithms, the functions in terms of which most known amplitudes can be written. General properties include analyticity, implying that scattering amplitudes are analytic functions except on certain branch cuts, and unitarity, or conservation of probability. These two properties are both exploited by unitarity cuts. Unitarity cuts provide a diagrammatic way of calculating the discontinuities of a Feynman diagram across its branch cuts, which is often simpler than calculating the diagram itself. From this discontinuity, the original function can be reconstructed by performing a dispersive integral.

In this work, we extend the formalism of unitarity cuts to incorporate diagrams involving Wilson-line propagators, where the inverse propagator is linear in the loop momenta, rather than the quadratic case which has been studied

before. To exploit this for the calculation of the soft anomalous dimension, we first found a suitable momentum-space IR regulator and corresponding prescription, and then derived the appropriate *largest time equation* (LTE). We find that, as in the case of the scalar diagrams, most terms contributing to the LTE turn out to be zero, albeit for different reasons. This simplifies calculations considerably.

This formalism is then applied to the calculation of webs with non-lightlike Wilson lines. As a test, we first looked at webs that have been previously studied using other methods. It emerges that, when using the correct variables, the dispersive integrals one encounters here are trivial, illustrating why unitarity cuts are a particularly useful tool for the calculation of webs. We observe that our technique is especially efficient when looking at diagrams involving three-gluon vertices, such as the $(1,1,1)$ web and the Y diagram between two lines.

We then focus on three-loop diagrams connecting three or four external non-lightlike lines and involving a three-gluon vertex. We calculate the previously unknown three-loop three-leg $(1,1,3)$ web in general kinematics. We obtain a result which agrees with the recently calculated lightlike limit. We also develop a technique to test our results numerically using the computer program SecDec, and we find agreement with our analytical result.

The result for the $(1,1,3)$ web can then be exploited to gain insight into the more complicated three-loop four-leg $(1,1,1,2)$ web. Indeed, the $(1,1,1,2)$ web reduces to the $(1,1,3)$ web in a certain collinear limit. We propose an ansatz for the $(1,1,1,2)$ web in general kinematics, based on a conjectured basis of multiple polylogarithms. The result for the $(1,1,3)$ web, together with the known result for the lightlike limit of the $(1,1,1,2)$ web, imposes strong constraints on the ansatz. Using these constraints, we manage to fix all but four coefficients in the ansatz. We fit the remaining coefficients numerically, but find that the quality of the fit is not good. We find possible explanations for this poor quality. This calculation is still a work in progress.

Our results provide a major step towards the full calculation of the three-loop soft anomalous dimension for non-lightlike Wilson lines. We calculated new results for three-loop webs, and also deepened the understanding of webs in general. We confirm a conjecture about the functional dependence of the soft anomalous dimension on the cusp angles. We also confirm earlier findings about the symbol alphabet of the relevant functions. This confirms the remarkable simplicity found earlier in the expressions for the soft anomalous dimension.

Lay summary

Quantum field theory (QFT) has proven to be a successful framework in which the theory of particle physics can be formulated [1]. Different QFT models exist to describe different aspects of particle physics. This thesis focuses on Quantum Chromodynamics (QCD), which describes the strong force between fundamental particles. This force explains why such fundamental particles form lumps of matter we are more familiar with, such as protons and neutrons. The strong force is probed experimentally by performing scattering experiments, for example at the Large Hadron Collider (LHC) in Geneva. To interpret experimental measurements, it is important to make accurate predictions of what we expect to happen, based on current theoretical knowledge.

The goal of this thesis is to advance the understanding of such theoretical predictions. Because of the complexity involved, this is a large collaborative effort, where calculations are subdivided into simpler parts. We focus on one part which involves interactions between particles with very low energies, the *soft anomalous dimension*. This soft anomalous dimension can be represented diagrammatically in terms of so-called *webs*. We calculate webs using a technique called *unitarity cuts*. Unitarity cuts provide a diagrammatic way of understanding the mathematical structure of the expressions involved. We first extend the existing framework, so that it can also be used to calculate contributions to the soft anomalous dimension. We then perform explicit calculations and obtain an independent confirmation of known results. Our calculations provide extra insights and simplifications compared to the use of other techniques. Finally, we also obtain some new results. These results will improve the precision of theoretical predictions, and give us a deeper understanding of QCD.

Declaration

I declare that this thesis was composed by myself, that the work contained herein is my own except where explicitly stated otherwise in the text, and that this work has not been submitted for any other degree or professional qualification except as specified.

(*Andries Waelkens, June 2017*)

Acknowledgements

I am very grateful to my supervisor Einan Gardi for his expert guidance during the past four years. He has been willing to answer every question I had, and thereby showed his incredible knowledge of and insight in particle physics, and also a lot of patience. I thoroughly enjoyed his enthusiasm, his positive outlook through challenges, and solving problems together.

I would also like to thank Eric Laenen for his hospitality when hosting me at Nikhef, and the exchange of ideas both during that visit and in Edinburgh. Many thanks go to Robbert Rietkerk for the very enjoyable collaboration, during which he introduced me to many useful concepts. I also want to thank Andrei, Jacopo, Gerben, and many others, for making my stay in Amsterdam a lot of fun.

I want to thank Gudrun Heinrich for her willingness to answer all questions about SecDec, which helped me greatly. I also want to thank Claude Duhr for the use of the Mathematica package PolyLogTools, which made hard calculations possible. Samuel Abreu, Mark Harley, Øyvind Almelid and Gustav Mogull were also always willing to help.

It was very nice to share offices with James, James, Rafa, Susi, Ava, Gustav, Jack, Øyvind and Vlad. Ava deserves a special mention for bearing with me for four years, during which I learnt to truly appreciate parrots.

Also thanks to Susi, Chistian, Joel, Joep, Anthony, Sjoerd, Iwan, and many others for the great cycling trips. I am particularly grateful to Susi for starting it all, and for her friendship. It was a great pleasure to live with Sjoerd, while constantly making fun of each other.

I owe a special thanks to my parents. Without the curiosity they fostered in each of us, I would never have started on this journey. I also want to thank my siblings Servaas, Johanna, Beatrijs, Hadewijch, and their families for their support, and for giving me a different perspective on life.

Finally, I want to thank my girlfriend Tiffany for all the good times we had together in the past four years, and for knowing when I need encouragement. Your support means a lot to me.

Contents

List of Figures

Chapter 1

Introduction

1.1 Divergences in QFT

Feynman diagrams provide a diagrammatic way of calculating scattering amplitudes in Quantum Field Theories. When calculating Feynman diagrams, one encounters divergences. Three types of divergences occur. Firstly, there are high-energy divergences, also called ultraviolet (UV) or hard divergences. Theories with massless particles, such as gauge bosons in gauge theories, exhibit low-energy, or soft, divergences. Finally, diagrams involving massless external particles also admit collinear divergences. Collinear and soft divergences together are known as infrared (IR) divergences. It is possible to obtain finite predictions of physical observables via a process called renormalisation [1, 2]. To apply renormalisation, a thorough understanding of divergences is required, so we look at them in more detail.

The three types of divergences can be studied independently via a process called *factorisation* [3, 4]. An amplitude $\mathcal{M}$ with n external legs can be decomposed into different colour contributions:

$$\mathcal{M} = \sum_L C^L \mathcal{M}^L \ . \tag{1.1}$$

These colour contributions can be factorised as follows [5, 6]:

$$\mathcal{M}^L = \sum_K \mathcal{H}_K \mathcal{S}^{KL}_{\text{ren}} \prod_{i=1}^{n} \frac{J_i}{\mathcal{J}_i} \ . \tag{1.2}$$

The different factors have the following meaning:

- $\mathcal{H}_K$ captures the hard part of the interaction. It is a vector in colour space. It contains ultraviolet divergences.

- J_i and $\mathcal{J}_i$ are the jet function and Eikonal jet respectively. They capture any collinear divergences.

- $\mathcal{S}^{KL}_{\text{ren}}$ is the *soft factor*. It captures the soft divergences. It is a matrix in colour space. The reason why we include the subscript *ren* will become clear in the next section.

This factorisation is illustrated on the left-hand side of figure 1.1.

Ultraviolet divergences can be regularised. In this work, we use dimensional regularisation in $d = 4 - 2\epsilon$ dimensions. Analytical expressions for infrared divergences are thus needed for the calculation of observables [5, 7–18]. The infrared divergences then disappear when integrating over phase space, so that observables such as cross sections and decay rates are free of divergences. However, the divergences often contribute to the finite part of the cross section via so-called large logarithms, which need resummation [19–22]. Apart from such phenomenological reasons, the calculation of infrared divergences is also interesting from a purely theoretical point of view.

Therefore, in this thesis we focus on the calculation of infrared divergences. We will work with massive external particles. As mentioned above, there are no collinear divergences in this case, so that the soft and infrared divergences are the same. We thus focus on the soft part of the amplitude. We can study it in isolation from the hard and jet parts, as illustrated on the right-hand side of figure 1.1. Diagrams of this kind involve hard external particles, exchanging low-energy gluons. We look at them in more detail in the next section.

1.2 Soft divergences in gauge theories

1.2.1 Eikonal lines and Wilson lines

The fact that we are looking for divergences caused by emissions of soft gluons from hard external legs allows us to make some simplifications, leading to the so-called Eikonal rules. We derive these rules for an incoming hard fermion.

In momentum space We study an incoming high-energy fermion with momentum p absorbing a soft gluon with momentum k, so that $p \gg k$. There will be a contribution to the integrand of the Feynman diagram coming from the fermion

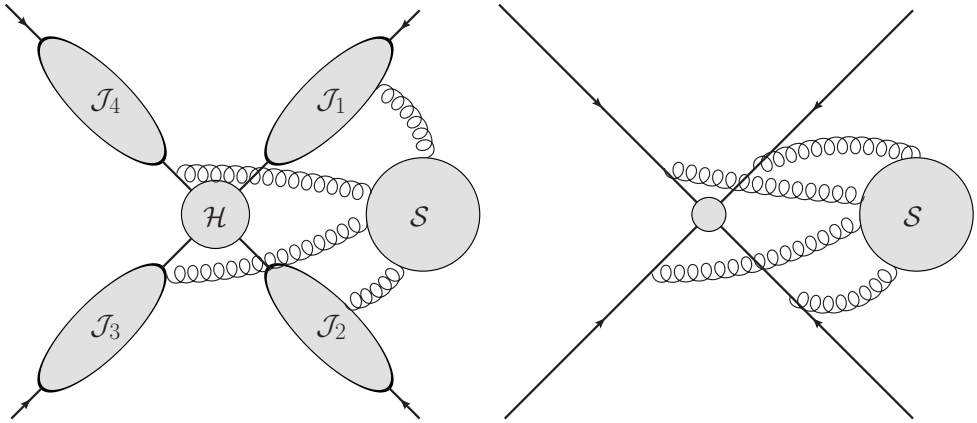

(a) *An amplitude factorises into a soft part, a hard part, and jets.*

(b) *The soft part only*

Figure 1.1 *Factorisation allows us to look at the soft part of an amplitude in isolation.*

propagator, the vertex and the external fermion as follows:

$$\frac{i(\not{p}+\not{k}+m)}{(p+k)^2-m^2+i\epsilon}(ig)\gamma^\mu u(p)\ . \tag{1.3}$$

The $i\epsilon$ in the denominator is called the *Feynman prescription*. ϵ has an infinitesimal positive value. It shifts the poles of the propagator in the k_0 plane, so that they are slightly above or below the real axis. This determines which poles we pick up when we calculate the k_0-integral as a contour integral. We will see below that this is closely related to causality.

Since the gluon is soft, we can ignore the $\not{k}$ and k^2 terms. We are left with

$$\begin{aligned}
\frac{i(\not{p}+m)}{(p+k)^2-m^2+i\epsilon}\,(ig)\gamma^\mu u(p) &= \frac{i(p^\nu\gamma_\nu+m)}{k^2-2p\cdot k+p^2-m^2+i\epsilon}(ig)\gamma^\mu u(p)\\
&= -g\frac{p_\nu(-\gamma^\mu\gamma^\nu+2g^{\mu\nu})+m\gamma^\mu}{2p\cdot k+m^2-m^2+i\epsilon}u(p)\\
&= -g\frac{-\gamma^\mu\not{p}+2p^\mu+m\gamma^\mu}{2p\cdot k+i\epsilon}u(p)\\
&= \frac{ip^\mu}{p\cdot k+i\epsilon}(ig)u(p)\\
&= \frac{i\beta_p^\mu}{\beta_p\cdot k+i\epsilon}(ig)u(p)\ ,
\end{aligned} \tag{1.4}$$

where we used the Dirac equation and defined $\beta_p=\frac{p}{\sqrt{p^2}}$. We thus see we can replace the combination of the vertex and propagator by an effective propagator,

called the Eikonal propagator:

$$E^{\mu}(k) = \frac{i\beta_p^{\mu}}{\beta_p \cdot k + i\epsilon}(ig) \ . \tag{1.5}$$

For the emission of a gluon, we replace $k \to -k$ in (1.5).

We can similarly derive rules for bosonic hard particles. Surprisingly, these give the same, spin-independent, result. This is the case because the wavelength of the low-energy gluon is too long to resolve the spin of the high-energy particle.

In configuration space By taking the Fourier transform of equation (1.5), Eikonal propagators can be studied in configuration space. It turns out that every hard line is represented by a Wilson line, defined as

$$\Phi_{\beta_i} = \mathcal{P} \exp\left(ig_s \int_0^{\infty} dt \ \beta_i \cdot A(t\beta_i) \right) \ , \tag{1.6}$$

where $\mathcal{P}$ indicates path ordering, and t is a parameter that indicates the position along the Wilson line. This correspondence is proven in chapter 2.

Notice that equation (1.5) is invariant under a rescaling $\beta_p \to \lambda\beta_p$. Likewise, (1.6) is invariant under $\beta_p \to \lambda\beta_p, t \to \frac{t}{\lambda}$. Since we are working with timelike β, we can thus always set $\beta^2 = 1$. Correlators will thus be independent of the value of β^2 and can only depend on

$$\gamma_{ij} = 2\beta_i \cdot \beta_j \quad , \ i \neq j \ . \tag{1.7}$$

1.2.2 Soft divergences

We argued in the previous section that in the kinematic region where soft divergences are generated, we can replace the hard external particles by Wilson lines[1], and we will obtain the same soft divergences. We thus define the soft function as a correlator of Wilson lines [23]

$$S(\gamma_{ij}, \alpha_s) = \langle \Phi_{\beta_1} \otimes \Phi_{\beta_2} \otimes ... \otimes \Phi_{\beta_n} \rangle \ . \tag{1.8}$$

The soft divergences of the soft function S will be equal to the soft divergences of the soft factor S_{ren}. However, S also contains ultraviolet divergences. These

[1] Or by Eikonal lines if we work in momentum space.

can be renormalised multiplicatively [9, 23–27]:

$$S_{\text{ren}}\big(\gamma_{ij}, \alpha_s(\mu), \epsilon_{\text{IR}}\big) = Z\big(\epsilon_{\text{UV}}, \gamma_{ij}, \alpha_s(\mu)\big) S\big(\gamma_{ij}, \alpha_s(\mu)\big) \ , \tag{1.9}$$

where α_s is the strong coupling constant, which depends on the energy scale μ. $\epsilon_{\text{UV}} = \epsilon_{\text{IR}}$; the notation ϵ_{IR} implies that the function S_{ren} has infrared divergences, which can be regularised by the dimensional regulator ϵ. ϵ_{UV} has a similar meaning.

Equation (1.9) can now be simplified by realising that

$$S\big(\gamma_{ij}, \alpha_s(\mu)\big) = 1 \ . \tag{1.10}$$

Indeed, all quantum corrections to (1.8) will consist of scaleless integrals, which vanish in dimensional regularisation. This leaves us with

$$S_{\text{ren}}\big(\gamma_{ij}, \alpha_s(\mu), \epsilon_{\text{IR}}\big) = Z\big(\epsilon_{\text{UV}}, \gamma_{ij}, \alpha_s(\mu)\big) \ . \tag{1.11}$$

Equation (1.9) tells us that we can calculate the infrared divergences of the soft factor S_{ren} as an ultraviolet renormalisation factor Z. This is a useful property, since there are more techniques known to calculate ultraviolet divergences than infrared ones.

Since we want to interchange infrared divergences for ultraviolet ones, we define the infrared regulated version of equation (1.8):

$$\mathcal{S}(\gamma_{ij}, \alpha_s, m, \epsilon_{\text{IR}}) = \left\langle \Phi^{(m)}_{\beta_1} \otimes \Phi^{(m)}_{\beta_2} \otimes ... \otimes \Phi^{(m)}_{\beta_n} \right\rangle \ , \tag{1.12}$$

where m is an infrared regulator. In chapter 2, we will pay more attention to the definition of such a regulator. From the analysis above, $\mathcal{S}$ is ultraviolet divergent, and can be regulated via

$$\mathcal{S}(\gamma_{ij}, \alpha_s, m, \epsilon_{\text{IR}}) Z\big(\epsilon_{\text{UV}}, \gamma_{ij}, \alpha_s(\mu)\big) = \mathcal{S}_{\text{ren}}(\gamma_{ij}, \alpha_s, m, \epsilon) \ , \tag{1.13}$$

so that $\mathcal{S}_{\text{ren}}(\gamma_{ij}, \alpha_s, m, \epsilon)$ is finite.

We now define the *soft anomalous dimension* Γ via a renormalisation group equation:

$$\frac{dZ}{d\ln\mu} = -Z\Gamma \ . \tag{1.14}$$

Γ is finite and matrix valued. It encodes all the divergences contained in Z, and

thus also the soft divergences in S_{ren}. Γ can be expanded in orders of α_s as

$$\Gamma = \sum_{n=1}^{\infty} \Gamma_s^{(n)} (\alpha_s)^n \tag{1.15}$$

Notice that $\mathcal{S}(\gamma_{ij}, \alpha_s, m, \epsilon), Z\big(\epsilon, \gamma_{ij}, \alpha_s(\mu)\big), S_{\text{ren}}\big(\gamma_{ij}, \alpha_s(\mu), \epsilon\big)$ and Γ all contain the same information about the soft divergences of an amplitude. We can thus choose how we prefer to calculate them. In fact, we will calculate them using an even different approach, in terms of webs.

1.2.3 Webs

It is convenient to study the exponentiation of equation (1.12):

$$\mathcal{S} = \exp\big(w\big) = \exp\left(\sum_n w^{(n)} \alpha_s^n\right) = \exp\left(\sum_{n,k} w^{(n,k)} \alpha_s^n \epsilon^k\right) . \tag{1.16}$$

It is again clear that knowledge of w is equivalent to knowledge of the soft anomalous dimension. Explicit relations can be found in [27].

The exponent w has some remarkable properties. The non-Abelian exponentiation theorem gives a diagrammatic approach to calculate w in terms of so-called webs [27–39]. Webs consist of sets of diagrams that only differ by the interchange of the order of gluon attachments along a Wilson line. They are labelled by the number of gluon attachments on the different Wilson lines: a web with L external legs, each with n_i gluon attachments, is denoted $(n_1, n_2, ..., n_L)$. For example, diagrams in the $(1, 3, 1)$ web, represented in figure 1.2, have one gluon attachment on leg i, three attachments on leg j, and one attachment on leg k. The three diagrams differ by the interchange of the order of gluon attachments on leg j. According to the non-Abelian exponentiation theorem, diagrams contribute to the exponent with a modified colour factor. Such colour factors correspond to connected graphs [40]. For example, looking at the example of the $(1, 3, 1)$ web, the diagrams contribute to the exponent via a factor of

$$\mathcal{W}_{(1,3,1)} = c_1 f_1 + c_2 f_2 \ , \tag{1.17}$$

with

$$c_1 = f^{bcd} f^{cae} T_i^a T_j^{de} T_k^b$$
$$c_2 = f^{bcd} f^{ade} T_i^a T_j^{ec} T_k^b$$

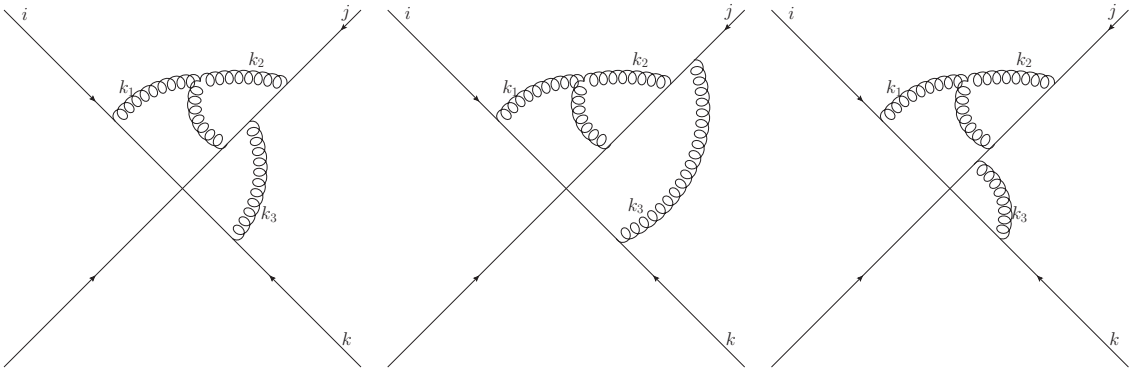

(a) $\mathcal{F}_1$ **(b)** $\mathcal{F}_2$ **(c)** $\mathcal{F}_3$

Figure 1.2 *The diagrams in the* $(1,3,1)$ *web.*

$$f_1 = \frac{1}{2}\big(-\mathcal{F}_1 - \mathcal{F}_2 + \mathcal{F}_3\big)$$
$$f_2 = \frac{1}{2}\big(-\mathcal{F}_1 + \mathcal{F}_2 - \mathcal{F}_3\big)\ . \tag{1.18}$$

The concept of webs can be related to equation (1.16) via

$$w^{(n)}\alpha_s^n = \sum_{(n_1,\ldots,n_L)} \mathcal{W}^{(n)}_{(n_1,\ldots,n_L)}\ , \tag{1.19}$$

i.e. $w^{(n)}$ is equal to the sum of all webs at $\mathcal{O}(\alpha_s^n)$. All two-loop webs are known, which implies that the soft anomalous dimension is currently known to $\mathcal{O}(\alpha_s^2)$ in general kinematics [15]. If we restrict ourself to two external lines, Γ is known as the cusp anomalous dimension, and is known at three loops [41]. In the case of massless external particles, Γ has recently been calculated to three-loop accuracy [28, 42]. The calculations in this thesis are a step towards a three-loop result in general kinematics.

1.2.4 Some remarks

In some cases, it is more useful to look at *subtracted* webs $\bar{w}$, in which commutators of subloops are subtracted from a multi-loop web w [27].

All multi-leg subtracted webs that have been calculated, obey a remarkable factorisation conjecture. Let us define the cusp parameter α_{ij} via

$$\gamma_{ij} = -\alpha_{ij} - \frac{1}{\alpha_{ij}} \tag{1.20}$$

The factorisation conjecture then states that

Conjecture 1 *Every subtracted web can be expressed as a sum of products of polylogarithms* [2] *of the form* $G(\mathbf{a}, \alpha_{ij})$*, with* $\mathbf{a}$ *a constant vector.*

This conjecture been found to be true even for very entangled webs. There are stronger versions of this conjecture, claiming that it also holds for unsubtracted webs, or even for all Feynman diagrams contributing to webs. These stronger versions of the conjecture have also been found to be true for all known diagrams, but might break down for very complicated webs.

An interesting notion is that of a multiple gluon exchange web. This is a web in which there are no three-gluon vertices. This type of web is very well understood [30].

In this thesis, we will represent webs diagrammatically as in figure 1.2. These diagrams include a spectator leg that represents a hard particle that is not participating in the soft interactions. However, the hard particle is interacting with the other legs via the hard interaction, represented by the blob in the middle of the diagram. This means that non-zero momentum and colour charge can flow through this spectator leg. We thus can not assume conservation of momentum and colour when we restrict ourselves to the particles involved in the soft interaction. Drawing the spectator leg helps us to keep this in mind.

Because the diagrams that contribute to webs are described by the Eikonal Feynman rules in momentum space, we will often refer to them as Eikonal diagrams.

We will calculate diagrams as a Laurent series in the dimensional regulator ϵ. In this expansion, we refer to the leading order in ϵ as the LO part, the next-to-leading order in ϵ as the NLO part, and so on.

1.3 Multiple polylogarithms

1.3.1 Definition

We have argued above why we are interested in the calculation of Feynman diagrams, such as webs. A logical next step is then to investigate which type of functions we expect as a result of a Feynman integral. An interesting discussion of this topic can be found in reference [43]. Most known amplitudes, and all known webs, can be expressed in terms of a class of functions called multiple polylogarithms [44, 45]. Starting from two loops, such as in the case of the so-called sunset diagram, a more general class of functions is needed [46–48].

[2] Polylogarithms are defined in the next section.

However, for the purposes of this thesis, introducing the multiple polylogarithms suffices. They are a generalisation of logarithms, and are defined recursively via [44, 45]

$$G(a_1, a_2, ..., a_n; z) = \int_0^z \frac{dt}{t - a_1} G(a_2, ..., a_n; t) \ , \tag{1.21}$$

and $G(z) = 1$. When all a_i are zero, we define

$$G(\mathbf{0}_n; z) = \frac{1}{n!} \ln^n z \ . \tag{1.22}$$

If all the entries of $\mathbf{a}$ are elements of $\{-1, 0, 1\}$, we say that $G(\mathbf{a}, z)$ is a harmonic polylogarithm.

It is clear from the definition that, just like logarithms, polylogarithms will have branch cuts. The a_i are the branch points of the resulting function. We say that $G(a_1, a_2, ..., a_n; z)$ has transcendental weight n.

1.3.2 Applications

Understanding of multiple polylogarithms, and their applications in particle physics has improved dramatically in the past twenty years. Techniques for efficient numerical evaluation, in particular for harmonic polylogarithms, have been developed [49–53]. This is very useful when using the analytical expressions for amplitudes to interpret experimental data. Moreover, polylogarithms are the perfect language to apply differential equation methods to the calculation of amplitudes [54, 55]. This is in particular the case if the chosen basis consists of uniform weight functions. Such a basis can be obtained by working with integrals with unit leading singularity, i.e. when the maximal cut equals one [41, 56, 57]. A third breakthrough, and one that we will use extensively in this thesis, is the simplification allowed by the use of the symbol algebra. This simplification was first discovered when in references [58, 59] the so-called two-loop six-point remainder function in $\mathcal{N} = 4$ SYM was evaluated, and consisted of a 17-page-long sum of harmonic polylogarithms of weight four. In [60], this was rewritten as a one-line sum of classical polylogarithms.

We now study the symbol map in more detail.

1.3.3 Symbols

The symbol algebra allows to discover functional relations between different polylogarithms. It is part of the more general coproduct structure of polylogarithms [43]. The symbol is defined as follows [60, 61]. Suppose F_w is a transcendental

function of weight w. Its total differential can then be written as

$$dF_w = \sum_i F_{i,w-1} d\ln R_i \tag{1.23}$$

for R_i some rational function and $F_{i,w-1}$ a transcendental function of weight $w-1$. We then define the symbol S recursively via

$$S(F_w) = \sum_i S(F_{i,w-1}) \otimes R_i \tag{1.24}$$

and have starting point $S(\ln f) = f$. From the way the symbol has been defined one can deduce some useful properties. Since every entry can be regarded as the argument of a logarithm, it is easy to see that

$$... \otimes (a \cdot b) \otimes ... = ... \otimes a \otimes ... + ... \otimes b \otimes ... \tag{1.25}$$

This property allows us to decompose the symbol of a function into very simple building blocks.

It is also clear that the symbol map is a linear map. This allows to simplify a sum of symbols of polylogarithms via the application of linear algebra. We conclude that the symbol of a large expression containing polylogarithms will be simpler than the expression itself.

This raises the question whether it is possible to *integrate* this symbol, with the goal of obtaining a sum of polylogarithms that is equal to the original expression, but simpler.

Such a method to integrate symbols indeed exists [62]. This algorithm is based on simple linear algebra. Suppose we want to rewrite the function f. First, we find a basis of functions of a given weight $f_1, f_2, ..., f_n$. Then, we calculate the symbol of the basis functions $S(f_1), ..., S(f_n)$. We then write the symbol of the function f as a linear combination of the symbols of the basis functions:

$$S(f) = \sum_i c_i S(f_i) \ . \tag{1.26}$$

This is always possible since the functions f_i form a basis. The linearity of the symbol calculus now guarantees that

$$S(f) = S\left(\sum_i c_i f_i \right) \ . \tag{1.27}$$

We thus have found a different function with the same symbol. Does this imply that

$$f \stackrel{?}{=} \sum_i c_i f_i \ . \tag{1.28}$$

An equivalent question is: if a function of weight k has symbol zero, does this imply that the function equals zero? The answer is no. However, the only functions of weight k with symbol zero are the ones that contain π or a multiple zeta value [61]. Instead of (1.28), we then have that

$$f = \sum_i c_i f_i + \pi g_1 + \sum_{j=2}^{k} \zeta_j g_k \ . \tag{1.29}$$

We now have to find the functions g_j. Notice that the transcendental weight of g_j is equal to $k - j$. The new unknown factors thus have a lower weight than the original ones. They can be found by looking at other parts of the coproduct. We will not go into details about how this is done, details can be found in [61]. However, it should be clear that in every iterative step, we are reducing the weight of the unknown functions, so that the process will terminate eventually. It is also clear that the algorithm consists of simple linear algebra and hence can be automated easily. It has been implemented in the Mathematica package Polylogtools, which is used extensively in this thesis.

1.3.4 Example

We give a simple example to illustrate the functional equations between polylogarithms, and how useful they are when performing iterated integrals. In the calculation of the cuts of the $(1, 3, 1)$ web, our results will include a term

$$\begin{aligned} f(\alpha_{ij}) = G\left(-1, -1, \frac{1-\alpha_{ij}^2}{\alpha_{ij}^2+1}\right) - G\left(-1, 1, \frac{1-\alpha_{ij}^2}{\alpha_{ij}^2+1}\right) \\ - G\left(1, -1, \frac{1-\alpha_{ij}^2}{\alpha_{ij}^2+1}\right) + G\left(1, 1, \frac{1-\alpha_{ij}^2}{\alpha_{ij}^2+1}\right) \ . \end{aligned} \tag{1.30}$$

When we calculate its symbol, we find remarkable simplicity:

$$S(f) = 4\alpha_{ij} \otimes \alpha_{ij} \ . \tag{1.31}$$

We recognise this as the symbol of a logarithm squared:

$$S(f) = S\big(2\ln^2 \alpha_{ij}\big) \ . \tag{1.32}$$

We then know that

$$f(\alpha_{ij}) = 2\ln^2 \alpha_{ij} + \pi g_1 + \pi^2 g_2 \ . \tag{1.33}$$

By plugging in a few values of α_{ij} numerically, we can easily find that $g_1 = g_2 = 0$, and thus

$$f(\alpha_{ij}) = 2\ln^2 \alpha_{ij} = 4G(0,0,\alpha_{ij}) \ . \tag{1.34}$$

This result is a lot simpler than the expression (1.30). It is especially useful when we want to integrate $f(\alpha_{ij})$ divided by a linear denominator. Indeed, this will be trivial using the definition of polylogarithms (1.21):

$$\int_0^z d\alpha_{ij} \frac{f(\alpha_{ij})}{\alpha_{ij} - t} = G(t,0,0,z) \ , \tag{1.35}$$

whereas it would have been a very tricky integral using the expression (1.30).

It is clear that this technique is very useful, not only to simplify final results as in reference [60], but also to simplify intermediate expressions when performing iterated integrals. It will be an invaluable tool when performing multi-loop calculations in what follows. We will omit the details of the simplifications involved, because they are trivial when using the PolyLogTools package.

1.4 Dispersive integrals

We mentioned in the previous section that polylogarithms, and therefore many amplitudes, have branch cuts, and therefore also discontinuities across these branch cuts. It would be very useful to be able to reconstruct diagrams based on their discontinuities. This is indeed possible via a *dispersive*, or *spectral*, integral.

Let us look at a function $f(\alpha)$ which has a branch cut for $\alpha > \alpha_0$, as represented in figure 1.3. We then calculate the contour integral of $\frac{f(\alpha')}{\alpha'-\alpha}$ along the contour illustrated in diagram 1.3. The parts of the contour along the branch cut are infinitesimally above and below the axis. We assume that f goes to zero at infinity sufficiently quickly, so that the contribution along the circular part of

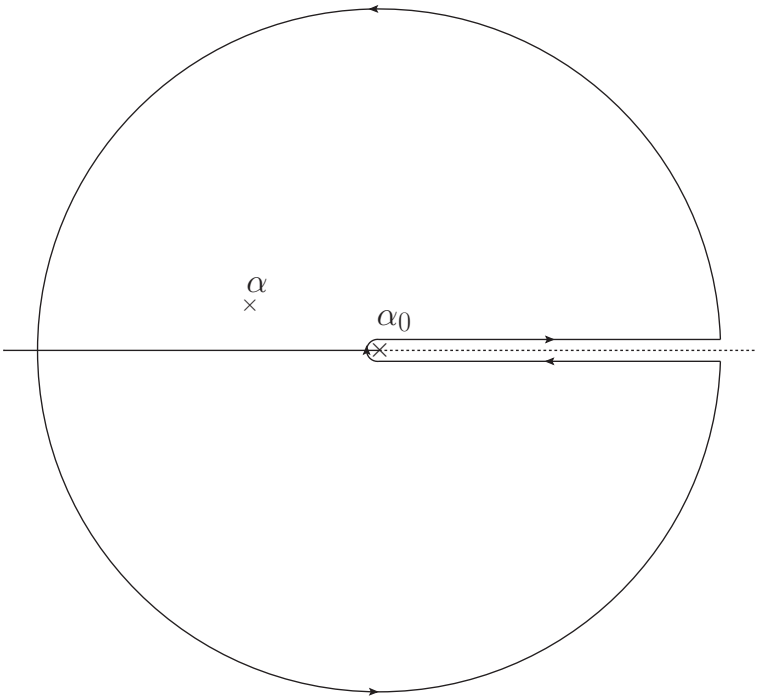

Figure 1.3 *An integration contour*

the contour vanishes. We define

$$I(\alpha) = \oint d\alpha' \frac{f(\alpha')}{\alpha' - \alpha} \ . \tag{1.36}$$

By application of Cauchy's formula, this is

$$I(\alpha) = 2\pi i f(\alpha) \ . \tag{1.37}$$

We can also calculate the contour integral explicitly. Because the part at infinity vanishes, it will be equal to

$$I(\alpha) = \int_{\infty - i\epsilon}^{\alpha_0 - i\epsilon} d\alpha' \frac{f(\alpha')}{\alpha' - \alpha} + \int_{\alpha_0 - i\epsilon}^{\alpha_0 + i\epsilon} d\alpha' \frac{f(\alpha')}{\alpha' - \alpha} + \int_{\alpha_0 + i\epsilon}^{\infty + i\epsilon} d\alpha' \frac{f(\alpha')}{\alpha' - \alpha} \ . \tag{1.38}$$

We split up the contour into three parts. The second one can be ignored:

$$I_2(\alpha) = \int_{\alpha_0 - i\epsilon}^{\alpha_0 + i\epsilon} d\alpha' \frac{f(\alpha')}{\alpha' - \alpha} = 0 \ . \tag{1.39}$$

Indeed, the contour has only a length of 2ϵ, and there is no pole along the contour. It will thus tend to zero for $\epsilon \to 0$.

Let us look at the third contribution:

$$I_3(\alpha) = \int_{\alpha_0+i\epsilon}^{\infty+i\epsilon} d\alpha' \frac{f(\alpha')}{\alpha' - \alpha} \tag{1.40}$$

We perform a change of variables where $a = \alpha' - i\epsilon$. This leads to

$$I_3(\alpha) = \int_{\alpha_0}^{\infty} da \frac{f(a + i\epsilon)}{a + i\epsilon - \alpha} \tag{1.41}$$

We now want to eliminate the $i\epsilon$ from the denominator. We have that

$$\frac{1}{a + i\epsilon - \alpha} = \mathrm{PV}\frac{1}{a - \alpha} - i\pi\delta(a - \alpha) \tag{1.42}$$

We now notice that α has been chosen away from the branch cut. The delta function will thus not have support on our region of integration, and the principal value integral will be the same as the normal integral. We thus conclude that

$$I_3(\alpha) = \int_{\alpha_0}^{\infty} da \frac{f(a + i\epsilon)}{a - \alpha} \ . \tag{1.43}$$

Likewise, we can prove that

$$I_1(\alpha) = \int_{\infty-i\epsilon}^{\alpha_0-i\epsilon} d\alpha' \frac{f(\alpha')}{\alpha' - \alpha} = -\int_{\alpha_0}^{\infty} da \frac{f(a - i\epsilon)}{a - \alpha} \ . \tag{1.44}$$

Combining equations (1.44) and (1.43), we can conclude that

$$\begin{aligned} I(\alpha) &= \int_{\alpha_0}^{\infty} d\alpha' \frac{f(\alpha' + i\epsilon) - f(\alpha' - i\epsilon)}{\alpha' - \alpha} \\ &= \int_{\alpha_0}^{\infty} d\alpha' \frac{\mathrm{Disc}_{\alpha'} f(\alpha')}{\alpha' - \alpha} \end{aligned} \tag{1.45}$$

By combining the equations (1.37) and (1.45), we thus obtain a way to obtain a function from its discontinuity:

$$f(\alpha) = \frac{1}{2\pi i} \int_{\alpha_0}^{\infty} d\alpha' \frac{\mathrm{Disc}_{\alpha'} f(\alpha')}{\alpha' - \alpha} \tag{1.46}$$

Notice that we made a strong assumption when deriving (1.46), namely that the contribution from the contour at infinity would vanish. This is not the case for the simplest example that we can imagine, namely $f(\alpha) = \ln \alpha$. By consequence, equation (1.46) does not converge for $\mathrm{Disc}_{\alpha'} f(\alpha') = 2\pi i$. We can resolve this problem by introducing another pole in our contour integral, making it more

convergent:

$$I'(\alpha) = \oint d\alpha' \frac{f(\alpha')}{(\alpha' - \alpha)\alpha'} \ . \tag{1.47}$$

Another application of Cauchy's theorem tells us that

$$I'(\alpha) = \frac{2\pi i}{\alpha}\big(f(\alpha) - f(0)\big) \ . \tag{1.48}$$

At the same time, we have that

$$I'(\alpha) = \int_{\alpha_0}^{\infty} d\alpha' \frac{\mathrm{Disc}_{\alpha'} f(\alpha')}{(\alpha' - \alpha)\alpha'} \ , \tag{1.49}$$

so that

$$f(\alpha) = f(0) + \frac{\alpha}{2\pi i} \int_{\alpha_0}^{\infty} d\alpha' \frac{\mathrm{Disc}_{\alpha'} f(\alpha')}{(\alpha' - \alpha)\alpha'} \ . \tag{1.50}$$

This is called a *subtracted* dispersive integral.

If we now apply this to $f(\alpha) = \ln(1 - \alpha)$, so that $\mathrm{Disc}_{\alpha'} f(\alpha') = -2\pi i$, we see that indeed

$$\ln(1 - \alpha) = 0 - \alpha \int_{1}^{\infty} d\alpha' \frac{1}{(\alpha' - \alpha)\alpha'} \ . \tag{1.51}$$

Notice that it is only possible to obtain this result because the value of $f(0)$ is known. We can in general make the dispersive integrals more convergent at infinity by introducing more poles in the integrand. However, we then have to know more boundary values of the function f.

When comparing the formulas for dispersive integrals, (1.46) and (1.50), to the definition of multiple polylogarithms (1.21), we see they obey a similar structure. This implies that dispersive integrals will be particularly simple when dealing with multiple polylogarithms, as we will exploit later.

1.5 Cuts

We saw in the previous sections that many Feynman diagrams can be expressed in terms of polylogarithms, and that these in turn can be reconstructed from their discontinuities. It would thus be helpful to have a procedure that allows to calculate the discontinuity of Feynman diagrams, instead of the diagrams themselves. Such a procedure indeed exists for non-Eikonal diagrams, via the

calculation of unitarity cuts [63–67]. We discuss this topic in more detail in chapter 2, when we extend the framework to include Eikonal diagrams.

1.6 Basis of functions for webs

As mentioned above, all currently known webs can be written in terms of multiple polylogarithms. In terms of multiple-gluon-exchange webs, a basis of functions describing all results has been conjectured in [30]. The basis functions are defined as

$$M_{k,l,n}(\alpha) = \frac{1}{r(\alpha)} \int_0^1 dx p_0(x,\alpha) \ln^k \left(\frac{q(x,\alpha)}{x^2} \right) \ln^l \left(\frac{x}{1-x} \right) \ln^n \tilde{q}(x,\alpha) \ , \quad (1.52)$$

where

$$\begin{aligned} r(\alpha) &= \frac{1+\alpha^2}{1-\alpha^2} \\ \ln \tilde{q}(x,\alpha) &= \ln\left(\frac{1}{x} + \alpha - 1\right) - \ln\left(\frac{1}{x} + \frac{1}{\alpha} - 1\right) \\ p_0(x,\alpha) &= r(\alpha)\left[\frac{1}{x - \frac{1}{1-\alpha}} - \frac{1}{x + \frac{\alpha}{1-\alpha}}\right] . \end{aligned} \quad (1.53)$$

The reasons for conjecturing this basis are explained in [30]. The basis functions have some interesting properties:

- For all of them, $M_{k,l,n}(1) = 0$.
- Their symbol entries are α and $\frac{\alpha}{1-\alpha^2}$.
- $M_{k,l,n}(\alpha)$ has uniform weight $w = k + l + n + 1$.
- For odd n, $M_{k,l,n}(\alpha)$ is symmetric under $\alpha \to \frac{1}{\alpha}$. For even n, it is antisymmetric under this exchange.
- It is actually a spanning set rather than a basis, since not all $M_{k,l,n}$ are independent. However, we can eliminate some elements to turn it into a basis.

In this thesis, we calculate some diagrams which do involve three-gluon vertices. The basis is only conjectured to be a basis for multiple-gluon-exchange webs, but it will be interesting to see if it also generates more general diagrams.

1.7 Outlook

We showed in this introduction that the calculation of soft divergences is very relevant to the understanding of gauge theories. We explained that the most elegant way of calculating such divergences is via the calculation of webs. These webs can be expressed in terms of generalised polylogarithms, which have an interesting branch cut structure. This branch cut structure allows us to reconstruct the full expression of a polylogarithm from the discontinuity via a dispersive integral. In the next chapter, we will derive cutting rules for webs, which will give us a direct way of calculating discontinuities. In chapter 3, we apply this to the calculation of various webs of increasing difficulty. In the fourth chapter, we will then move on to the calculation of the previously unknown $(1, 3, 1)$ web. We find an expression which is numerically proven to be correct. Using this result, we then try to calculate the $(1, 1, 1, 2)$ web via a bootstrap approach.

Chapter 2

Cutting rules for Eikonal diagrams

In this chapter we derive the cutting rules for Eikonal diagrams. They will give us a diagrammatic way to calculate the discontinuity across the branch cut of a Feynman integral involving a correlator of semi-infinite Wilson lines. We first find a convenient infrared regulator in momentum space. We use the resulting Feynman rules to then derive the so-called largest time equation. We then use this largest time equation to derive Cutkosky [63] cutting rules, in a similar way to [67]. We finally study the cutting rules in more detail, by finding categories of cuts that vanish, and illustrate the resulting simplifications in the case of the three-gluon vertex diagram forming the $(1, 1, 1)$ web.

2.1 Infrared regulator in momentum space

The goal of the work carried out in this thesis is to calculate the infrared divergences of correlators of semi-infinite Wilson lines. As explained in section 1.2, the resulting Feynman diagrams are scaleless integrals, so these infrared divergences are equal to the ultraviolet divergences. We choose to regularise the infrared divergences, so that we are left with the ultraviolet divergences only, and then calculate these. The calculations can be performed in terms of so-called webs.

To carry out this procedure, we need to define an appropriate infrared regulator for the webs. Ideally, this regulator should respect the symmetries of the problem and should be easy to deal with computationally. To find such a regulator, we look at conventional regulators in configuration space. Indeed, most recent calculations of Wilson-line correlators have been carried out in configuration space, such that we can learn from the approach used there [27–

29, 35, 40, 42, 68–70]. In configuration-space Feynman diagrams, the emission of a soft gluon by a Wilson line is represented by a one-dimensional integral of the point of emission along the Wilson line. Infrared divergences are generated when this point of emission goes to infinity. A convenient way to regularise such divergences was introduced in [35] as follows:

$$(ig_s)\beta_i^\mu \int_0^\infty d\lambda \;\; (\ldots) \to (ig_s)\beta_i^\mu \int_0^\infty d\lambda \;\; e^{-im\lambda\sqrt{\beta_i^2 - i\epsilon}}(\ldots) \; . \tag{2.1}$$

Here, $m > 0$ is the infrared regulator. We notice that (2.1) is invariant under a rescaling $\beta_i^\mu \to a\beta_i^\mu, \lambda \to \frac{\lambda}{a}$. This was also the case for the Eikonal propagator without a regulator, as discussed above equation (1.7). The regulator m respects the rescaling symmetry. We will work with timelike β_i, so can choose to rescale β_i^μ such that $\beta_i^2 = 1$. In this case (2.1) simplifies to

$$(ig_s)\beta_i^\mu \int_0^\infty d\lambda \;\; (\ldots) \to (ig_s)\beta_i^\mu \int_0^\infty d\lambda \;\; e^{-im\lambda}(\ldots) \; . \tag{2.2}$$

To ensure suppression for large values of λ, we choose the following implicit prescription:

$$m \to m - i\epsilon \; . \tag{2.3}$$

We now address the question of finding the equivalent of this regulator in momentum space. We can find out by taking the Fourier transform.

2.1.1 Single gluon emission

We start by looking at a generic diagram $\mathcal{D}$ which has one gluon emission from the leg i, represented on the left-hand side of figure 2.1. The large grey blob represents some generic soft interactions involving the other legs of the diagram, the black blob at the centre represents the hard interactions which we ignore in the calculation of the soft function. $\mathcal{D}$ will depend on the coupling g_s, on the infrared regulator m and on the external velocities $\{\beta_j\}_{j\neq i}$:

$$\mathcal{D}(g_s, m, \{\beta_j\}_{j\neq i}) = (ig_s)\beta_i^\mu \int_0^\infty d\lambda \;\; e^{-im\lambda} F_\mu(\lambda\beta_i, \{\beta_j\}_{j\neq i}) \; , \tag{2.4}$$

where $F(\lambda\beta_i, \{\beta_j\}_{j\neq i})$ is a generic factor representing the rest of the diagram, the grey blob in the figure. The gluon emission along the Wilson line is represented by the parameter λ. We can replace this by a spacetime point x by including a

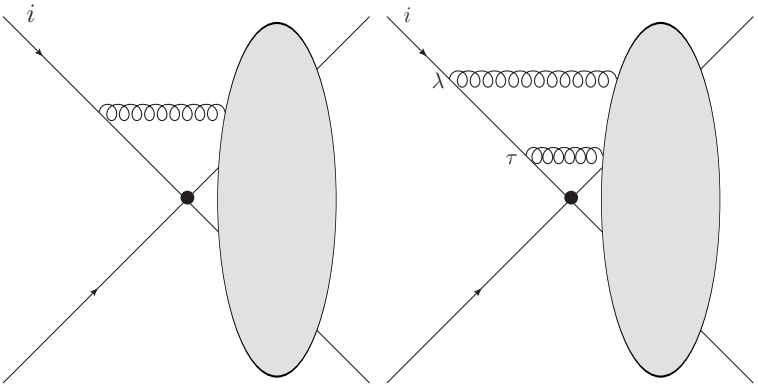

(a) *One gluon emission* **(b)** *Two gluon emissions*

Figure 2.1 *Generic diagrams involving gluon emissions.*

d-dimensional delta function:

$$\begin{aligned}\mathcal{D}(g_s, m, \{\beta_j\}_{j\neq i}) &= (ig_s)\beta_i^\mu \int_0^\infty d\lambda \int d^d x \delta^d(x - \lambda\beta_i) \;\; e^{-im\lambda} F_\mu(\lambda\beta_i, \{\beta_j\}_{j\neq i}) \\ &= (ig_s)\beta_i^\mu \int_0^\infty d\lambda \int d^d x \delta^d(x - \lambda\beta_i) \;\; e^{-im\lambda} F_\mu(x, \{\beta_j\}_{j\neq i}) \; .\end{aligned} \tag{2.5}$$

If we now Fourier transform both F and the delta function, this becomes

$$\begin{aligned}\mathcal{D}(g_s, m, \{\beta_j\}_{j\neq i}) &= (ig_s)\beta_i^\mu \int_0^\infty d\lambda \int d^d x \int \frac{d^d k}{(2\pi)^d} \int \frac{d^d q}{(2\pi)^d} e^{ik\cdot(x-\beta_i\lambda)} \\ &\qquad \times \;\; e^{-im\lambda} \tilde{F}_\mu(q, \{\beta_j\}_{j\neq i}) e^{-iq\cdot x} \\ &= (ig_s)\beta_i^\mu \int_0^\infty d\lambda \int \frac{d^d k}{(2\pi)^d} e^{-ik\cdot\beta_i\lambda} e^{-im\lambda} \tilde{F}_\mu(-k, \{\beta_j\}_{j\neq i}) \\ &= (ig_s) \int \frac{d^d k}{(2\pi)^d} \frac{i\beta_i^\mu}{-k\cdot\beta_i - m + i\epsilon} \tilde{F}_\mu(-k, \{\beta_j\}_{j\neq i}) \; .\end{aligned} \tag{2.6}$$

In the last step, we made the $i\epsilon$ prescription of m explicit.

This shows us how to regulate the Feynman rule E^μ for the emission of a gluon of momentum k along a Wilson line with momentum β_i (1.5) [1]:

$$E^\mu(k) = \frac{i\beta_i^\mu}{-k\cdot\beta_i + i\epsilon} \to \frac{i\beta_i^\mu}{-k\cdot\beta_i - m + i\epsilon} \; . \tag{2.7}$$

We see that the $i\epsilon$ prescription for m corresponds to the one we would expect for an Eikonal propagator. The regulator can be interpreted as giving a small mass

[1] We include the β^μ part of the vertex in the Eikonal propagator, and use ig_s as the vertex factor from now on.

to the Wilson line.

If we would not have assumed that $\beta_i^2 = 1$, the same calculation would have given us

$$E^\mu(k) = \frac{i\beta_i^\mu}{-k\cdot\beta_i + i\epsilon} \to \frac{i\beta_i^\mu}{-k\cdot\beta_i - m\sqrt{\beta_i^2 - i\epsilon}} \,. \tag{2.8}$$

We thus recover the invariance under a rescaling of β_i which was evident in (2.1).

2.1.2 Multiple gluon emission

We now want to generalise the Feynman rule to the case where multiple gluons are emitted from the Wilson line. For the emission of two gluons, we have in configuration space

$$\mathcal{D}(g_s, m, \{\beta_j\}_{j\neq i}) = (ig_s)^2\beta_i^\mu\beta_i^\nu \int_0^\infty d\lambda \int_0^\infty d\tau \;\; \theta(\lambda-\tau) \;\; e^{-im\lambda}e^{-im\tau} \times F_{\mu\nu}(\lambda\beta_i, \tau\beta_i, \{\beta_j\}_{j\neq i}) \,, \tag{2.9}$$

where the theta function specifies the order of emission. This is represented graphically on the right-hand side of figure 2.1.

We notice that we regularise both gluon attachments. This is not strictly necessary: it would suffice to only regularise the emission removed furthest from the hard interaction, namely the one with parameter λ. Indeed, if we regularise the long-distance divergence of the point furthest removed from the hard interaction, we have implicitly also regularised all points closer to the hard interaction. We expect these two different choices to yield the same results for the infrared divergences. This is because we calculate the infrared divergences as ultraviolet divergences, which are independent of the specific choice of infrared regulator. However, when looking at the finite part of such diagrams, there might be differences between the two approaches. It turns out that regularising all gluon emissions as in (2.9) is computationally convenient. Therefore, this choice was introduced in [35] and used in [27–29, 40, 42, 68–70]. We will also use this approach to find the equivalent regulator in momentum space.

We look at (2.9) in more detail:

$$\begin{aligned}&\mathcal{D}(g_s, m, \{\beta_j\}_{j\neq i}) \\ &= (ig_s)^2\beta_i^\mu\beta_i^\nu \int_0^\infty d\lambda \int_0^\infty d\tau \;\; \theta(\lambda-\tau) e^{-im\lambda}e^{-im\tau} F_{\mu\nu}(\lambda\beta_i, \tau\beta_i, \{\beta_j\}_{j\neq i})\end{aligned}$$

$$= (ig_s)^2 \beta_i^\mu \beta_i^\nu \int_0^\infty d\lambda \int_0^\infty d\tau \int d^d x \int d^d y \; \theta(\lambda - \tau) \delta(x - \lambda\beta_i) \delta(y - \tau\beta_i) \\ \times e^{-im\lambda} e^{-im\tau} F_{\mu\nu}(x, y, \{\beta_j\}_{j\neq i}) \; . \quad (2.10)$$

We now Fourier transform terms to momentum space. In particular, we use the following representation for the theta function

$$\theta(\lambda - \tau) = \int_{-\infty}^{\infty} dt \frac{e^{it(\lambda-\tau)}}{2\pi i(t - i\epsilon)} \; , \quad (2.11)$$

to obtain

$$\begin{aligned}
&\mathcal{D}(g_s, m, \{\beta_j\}_{j\neq i}) \\
&= (ig_s)^2 \beta_i^\mu \beta_i^\nu \int_0^\infty d\lambda \int_0^\infty d\tau \int d^d x \int d^d y \int_{-\infty}^\infty dt \frac{e^{it(\lambda-\tau)}}{2\pi i(t - i\epsilon)} \\
&\qquad \times \int \frac{d^d k}{(2\pi)^d} e^{ik\cdot(x-\beta_i\lambda)} \int \frac{d^d l}{(2\pi)^d} \; e^{il\cdot(y-\beta_i\tau)} \\
&\qquad \times \int \frac{d^d p}{(2\pi)^d} e^{ip\cdot x} \int \frac{d^d q}{(2\pi)^d} e^{iq\cdot y} \tilde{F}_{\mu\nu}(p, q, \{\beta_j\}_{j\neq i}) \; e^{-im\lambda} e^{-im\tau} \\
&= (ig_s)^2 \beta_i^\mu \beta_i^\nu \int_0^\infty d\lambda \int_0^\infty d\tau \int_{-\infty}^\infty dt \frac{e^{it(\lambda-\tau)}}{2\pi i(t - i\epsilon)} e^{-im\lambda} e^{-im\tau} \\
&\qquad \times \int \frac{d^d k}{(2\pi)^d} e^{-ik\cdot\beta_i\lambda} \int \frac{d^d l}{(2\pi)^d} \; e^{-il\cdot\beta_i\tau} \tilde{F}_{\mu\nu}(-k, -l, \{\beta_j\}_{j\neq i}) \\
&= (ig_s)^2 \beta_i^\mu \beta_i^\nu \int \frac{d^d k}{(2\pi)^d} \int \frac{d^d l}{(2\pi)^d} \int_{-\infty}^\infty dt \tilde{F}_{\mu\nu}(-k, -l, \{\beta_j\}_{j\neq i}) \\
&\qquad \times \; \frac{1}{2\pi i(t - i\epsilon)} \frac{i}{-k\cdot\beta_i + t - m + i\epsilon} \frac{i}{-l\cdot\beta_i - t - m + i\epsilon} \; . \quad (2.12)
\end{aligned}$$

We can now perform the t integral via contour integration. We can choose whether to close our contour in the upper-half or lower-half plane, since the integral converges in both cases. There are poles at

$$\begin{aligned}
t &= i\epsilon \\
t &= k\cdot\beta_i + m - i\epsilon \\
t &= -l\cdot\beta_i - m + i\epsilon \; . \quad (2.13)
\end{aligned}$$

There is only one pole in the lower-half plane, so we choose to close the contour that way. We then obtain

$$\mathcal{D}(g_s, m, \{\beta_j\}_{j\neq i}) = \int \frac{d^d p}{(2\pi)^d} \int \frac{d^d q}{(2\pi)^d} \tilde{F}_{\mu\nu}(-k, -l, \{\beta_j\}_{j\neq i}) \times \frac{(ig_s)\beta_i^\mu i}{-k\cdot\beta_i - m + i\epsilon} \frac{(ig_s)\beta_i^\nu i}{-\beta_i\cdot(k+l) - 2m + i\epsilon} \ . \tag{2.14}$$

We see that the first part of the Eikonal line looks exactly like the single-emission case. However, in the second part we see that the expected regulator m has been replaced by a factor of $2m$. One can prove in a similar way that in general, for the part of the Wilson line after the emission of n gluons with momenta $k_1, ..., k_n$ the Feynman rule becomes

$$\frac{i\beta_i^\mu}{-\beta_i\cdot(k_1 + ... + k_n) + i\epsilon} \to \frac{i\beta_i^\mu}{-\beta_i\cdot(k_1 + ... + k_n) - nm + i\epsilon} \ . \tag{2.15}$$

We notice that this is different from the choice of regulator in [57], where a single regulator $m = \frac{1}{2}$ is being used for each Eikonal line, independent of the number of emitted gluons. From the derivation above, it is clear that this choice corresponds to the case where only the outer gluon emission point on each Wilson line is regularised. We have to keep this in mind when comparing results of our calculations; we only expect the divergent parts of the result to be equal.

2.2 Positive and negative time components of propagators

When deriving the largest time equation, it will be useful to split up the configuration-space Feynman propagator into a positive and negative time component.

2.2.1 Quadratic denominator

We look at a Feynman propagator with a quadratic denominator:

$$\tilde{\Delta}_F(k) = \frac{i}{k^2 - m^2 + i\epsilon} \ . \tag{2.16}$$

In configuration space, this becomes

$$\begin{aligned}\Delta_F(x) &= \int \frac{d^dk}{(2\pi)^d} e^{-ik\cdot x}\tilde{\Delta}_F(k) \\ &= \int \frac{d^dk}{(2\pi)^d} \frac{e^{-ik\cdot x} i}{k^2 - m^2 + i\epsilon} \ .\end{aligned} \tag{2.17}$$

We want to integrate over k_0 via contour integration. There are two poles, at

$$k_0 = \pm\big(\sqrt{\mathbf{k}^2 + m^2} - i\epsilon\big) \ . \tag{2.18}$$

We choose our integration contour to be a semicircle. We want the contribution from the circular part of the contour to vanish, so that we are left with only residues when calculating (2.17). For that to be the case, the factor of $e^{-ix^0k_0}$ needs to go to zero. This implies that semicircle will be closed in the upper-half plane when $x^0 < 0$ and in the lower-half plane when $x^0 > 0$. This leads to

$$\begin{aligned}\Delta_F(x) = i\theta(x^0) &\int \frac{d^{d-1}k}{(2\pi)^{d-1}} \frac{e^{-i\sqrt{\mathbf{k}^2+m^2}x^0 + i\mathbf{k}\cdot\mathbf{x}}}{2\sqrt{\mathbf{k}^2+m^2}} i \\ + i\theta(-x^0) &\int \frac{d^{d-1}k}{(2\pi)^{d-1}} \frac{e^{i\sqrt{\mathbf{k}^2+m^2}x^0 + i\mathbf{k}\cdot\mathbf{x}}}{2\sqrt{\mathbf{k}^2+m^2}} i \ .\end{aligned} \tag{2.19}$$

This can be simplified further. Let us look at the following integral

$$\mathcal{I} = \int \frac{d^dk}{(2\pi)^d} e^{-ik\cdot x}\delta(k^2 - m^2)\theta(k_0) \ . \tag{2.20}$$

We can solve the delta function for k_0, and obtain

$$\delta(k^2 - m^2) = \frac{\delta(k_0 - \sqrt{\mathbf{k}^2+m^2})}{2\sqrt{\mathbf{k}^2+m^2}} + \frac{\delta(k_0 + \sqrt{\mathbf{k}^2+m^2})}{2\sqrt{\mathbf{k}^2+m^2}} \ . \tag{2.21}$$

This means that

$$\mathcal{I} = \int \frac{d^{d-1}k}{(2\pi)^d} \frac{e^{-i\sqrt{\mathbf{k}^2+m^2}x^0 + i\mathbf{k}\cdot\mathbf{x}}}{2\sqrt{\mathbf{k}^2+m^2}} \ . \tag{2.22}$$

We can prove similarly that

$$\int \frac{d^dk}{(2\pi)^d} e^{-ik\cdot x}\delta(k^2 - m^2)\theta(-k_0) = \int \frac{d^{d-1}k}{(2\pi)^d} \frac{e^{i\sqrt{\mathbf{k}^2+m^2}x^0 + i\mathbf{k}\cdot\mathbf{x}}}{2\sqrt{\mathbf{k}^2+m^2}} \ . \tag{2.23}$$

Combining equations (2.19), (2.22) and (2.23) then gives

$$\begin{aligned}\Delta_F(x) &= \theta(x^0)\int \frac{d^dk}{(2\pi)^d} e^{-ik\cdot x}(2\pi i)\delta(k^2-m^2)i\theta(k_0) \\ &\quad + \theta(-x^0)\int \frac{d^dk}{(2\pi)^d} e^{-ik\cdot x}(2\pi i)\delta(k^2-m^2)i\theta(-k_0) \\ &= \theta(x^0)\Delta_F^+(x) + \theta(-x^0)\Delta_F^-(x)\ . \end{aligned} \tag{2.24}$$

In what follows, we denote

$$\delta(k^2)\theta(\pm k_0) = \delta^\pm(k^2)\ . \tag{2.25}$$

We also define $\tilde{\Delta}_F^\pm(k)$ via

$$\tilde{\Delta}_F^\pm(k) = \int \frac{d^dx}{(2\pi)^d} e^{ik\cdot x}\Delta_F^\pm(x)\ , \tag{2.26}$$

so that in momentum space we have

$$\tilde{\Delta}_F^\pm(k) = (2\pi i)\delta^\pm(k^2-m^2)i\ . \tag{2.27}$$

We can interpret (2.24) as positive energy particles travelling forwards in time, and negative energy particles travelling backwards.

It is straightforward to find the equivalent of (2.24) for a propagator with a different numerator. For example, we find for gluons that in the Feynman gauge

$$\Delta_{F,\mu\nu}^\pm(x) = (-ig_{\mu\nu})\int \frac{d^dk}{(2\pi)^d} e^{-ik\cdot x}(2\pi i)\delta^\pm(k^2)\ . \tag{2.28}$$

Therefore, we have in momentum space

$$\tilde{\Delta}_{F,\text{ gluon}}^\pm(k) = (-ig_{\mu\nu})(2\pi i)\delta^\pm(k^2)\ . \tag{2.29}$$

This expression will be useful when interpreting the largest time equation.

2.2.2 Linear denominator

We now perform a similar calculation for an Eikonal propagator. According to (2.15), it has a denominator which is linear in the loop momenta, which changes our analysis.

We look at an Eikonal propagator which is part of a Wilson line with

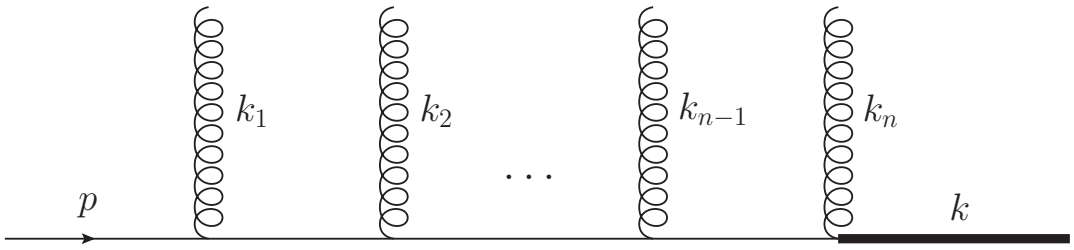

Figure 2.2 *An Eikonal propagator*

incoming momentum p and has emitted n gluons with momenta $k_1, ..., k_n$. It is represented by the thick line in figure 2.2. By conservation of momentum, we have that

$$k = p - \sum_{i=1}^{n} k_i \ . \tag{2.30}$$

Following (2.15), the configuration-space propagator is

$$\begin{aligned} E^\mu(x) &= \int \frac{d^d k}{(2\pi)^d} e^{-ik\cdot x} E^\mu(k) \\ &= \int \frac{d^d k}{(2\pi)^d} e^{-ik\cdot x} \frac{i\beta_i^\mu}{-\beta_i \cdot (k_1 + ... + k_n) - nm + i\epsilon} \\ &= \int \frac{d^d k}{(2\pi)^d} e^{-ik\cdot x} \frac{i\beta_i^\mu}{\beta_i \cdot k - \beta_i \cdot p - nm + i\epsilon} \ . \end{aligned} \tag{2.31}$$

We again want to integrate over k_0 by contour integration. Because the denominator is linear in k, there will be only one pole, situated at

$$k_0 = \frac{\mathbf{k}\cdot\boldsymbol{\beta}_i + \beta_i \cdot p + nm - i\epsilon}{\beta_i^0} \ . \tag{2.32}$$

This equation tells us that the sign of β_i^0 determines whether the pole is situated in the upper-half or lower-half plane. If for example we have an incoming particle i such that $\beta_i^0 > 0$, (2.32) implies that the pole lies in the lower half of the complex k_0 plane. This means that in this case there is only a positive time component, and the negative time component is equal to zero. Likewise, for an outgoing particle, $\beta_i^0 < 0$ and we will only have a negative time component.

We can make this more concrete by performing the k_0 integral in (2.31) explicitly. The residue is a $d-1$-dimensional integral, which can again be replaced

by a d-dimensional integral over a delta function as in (2.24):

$$\begin{aligned} E^\mu(x) &= \theta(x^0) \int \frac{d^d k}{(2\pi)^d} e^{-ik\cdot x} \theta(\beta_i^0)(2\pi i) i\beta_i^\mu \delta(\beta_i \cdot k - \beta_i \cdot p - nm) \\ &+ \theta(-x^0) \int \frac{d^d k}{(2\pi)^d} e^{-ik\cdot x} \theta(-\beta_i^0)(2\pi i) i\beta_i^\mu \delta(\beta_i \cdot k - \beta_i \cdot p - nm) \\ &= \theta(x^0) E^{\mu,+}(x) + \theta(-x^0) E^{\mu,-}(x) \ . \end{aligned} \tag{2.33}$$

In momentum space, this implies

$$\begin{aligned} E^{\mu,\pm}(k) &= \theta(\pm\beta_i^0)(2\pi i) i\beta_i^\mu \delta(\beta_i \cdot k - \beta_i \cdot p - nm) \\ &= \theta(\pm\beta_i^0)(2\pi i) i\beta_i^\mu \delta(-\beta_i \cdot (k_1 + k_2 + ... + k_n) - nm) \ . \end{aligned} \tag{2.34}$$

We see that in the Eikonal approximation, the difference between positive and negative time components is decided by the external energy flow β_i^0 via the factor $\theta(\beta_i^0)$. This contrasts with non-Eikonal propagators. For example, assume that the external particle i is a quark and we use the exact expression for the propagator. It is a fermion propagator, which has a quadratic denominator. As (2.27) shows, in this case the difference between positive and negative time components is decided by the energy flow k_0 in the propagator itself via a factor $\theta(k_0)$, not by the external energy flow β_i^0. This difference can be understood by looking at the kinematics in which we derived the Eikonal approximation. In that region, the energy of all the emitted gluons goes to zero, so that the energy flow in the external particle β_i^0 is very close to the energy flow in the propagator k_0. However, this similarity does not hold any more when we integrate over all possible gluon momenta.

We can conclude that the propagator of an incoming Eikonal particle only has a positive time component and the propagator of an outgoing Eikonal particle only has a negative time one. This will be useful when interpreting the largest time equation.

2.3 Largest time equation

We derive the largest time equation in the same way as in [67]. We start by defining configuration-space Feynman diagrams with coloured vertices. We denote a generic Feynman propagator by Δ_F. Lorentz indices are ignored; Δ_F could thus correspond to a propagator with Lorentz indices such as E_F^μ.

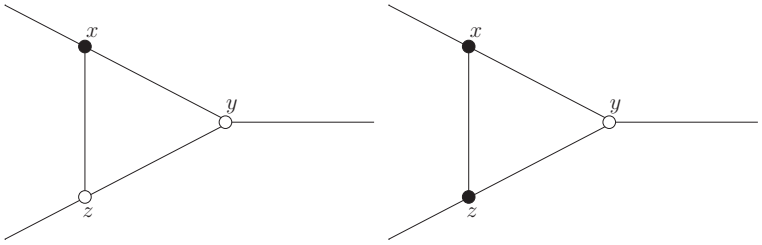

(a) *A diagram with coloured vertices*

(b) *The same diagram, with the colour of vertex z changed.*

Figure 2.3 *Diagrams with coloured vertices*

- A propagator connecting two white vertices x_i and x_j will contribute the usual factor of $\Delta_F(x_j - x_i)$.
- A propagator connecting two black vertices x_i and x_j will contribute a factor of $\Delta_F^*(x_j - x_i)$.
- A propagator connecting a white vertex x_i to a black vertex x_j will contribute a factor of $\Delta_F^+(x_j - x_i)$.
- A propagator connecting a black vertex x_i to a white vertex x_j will contribute a factor of $\Delta_F^-(x_j - x_i)$.
- A black vertex contributes the complex conjugate of a white vertex. For a scalar vertex with coupling g, this means that a white vertex contributes a factor of ig, and a black one a factor of $-ig$.

For example, the integrand of the diagram on the left-hand side of figure 2.3 will be

$$\mathcal{I}_{\text{triangle}}(x, y, z, g) = (ig)^2(-ig)\Delta_F(y - z)\Delta_F^-(z - x)\Delta_F^-(y - x) \ . \tag{2.35}$$

Note that complex conjugation swaps positive and negative time components:

$$\Delta_F^*(x) = \theta(x^0)\Delta_F^-(x) + \theta(-x^0)\Delta_F^+(x) \ . \tag{2.36}$$

Also note that the rules imply that energy flows from white to black vertices.

Let us now look at a generic Feynman diagram $F(p_1, ..., p_k)$ involving k external particles with momenta $p_1, ..., p_k$. In configuration space, we have n vertices $x_1, ..., x_n$ with $k \leq n$. Particle 1 is connected to vertex x_1 and so on, so

that momentum k_i is conjugate to point x_i. We define the integrand $\mathcal{I}(x_1, ..., x_n)$, related to $F(p_1, ..., p_k)$ via

$$F(p_1, ..., p_k) = \int d^d x_1 \int d^d x_2 ... \int d^d x_n \prod_{i=1}^{k} e^{-ik_i \cdot x_i} \mathcal{I}(x_1, ..., x_n) \ . \tag{2.37}$$

We label the vertex with the largest time component x_k, so that

$$x_{i_0} < x_{k_0} \qquad \forall i \neq k \ . \tag{2.38}$$

We now want to know what happens to $F(p_1, ..., p_k)$ when we change the colour of vertex x_k from white to black. We first investigate the behaviour of the integrand $\mathcal{I}(x_1, ..., x_n)$. When changing the colour of x_k, $\mathcal{I}$ changes as follows:

- We obtain an extra factor of -1 from the complex conjugation of the vertex.
- For all white vertices x_i that are connected to x_k via a propagator, this propagator changes from $\Delta_F(x_k - x_i)$ to $\Delta_F^+(x_k - x_i)$. However, since $x_{k_0} > x_{i_0}$, $\Delta_F(x_k - x_i) = \Delta_F^+(x_k - x_i)$, so nothing changes.
- For all black vertices x_j that are connected to x_k via a propagator, this propagator changes from $\Delta_F^-(x_k - x_i)$ to $\Delta_F^*(x_k - x_i)$. However, since $x_{k_0} > x_{j_0}$, $\Delta_F^*(x_k - x_j) = \Delta_F^-(x_k - x_i)$, so nothing changes.

We see that we obtain an overall minus sign. This means that if we keep the other colours constant, we have

$$\mathcal{I}(x_1, ..., x_n)_{x_k \text{white}} + \mathcal{I}(x_1, ..., x_n)_{x_k \text{black}} = 0 \ . \tag{2.39}$$

We can again illustrate this with the example of figure 2.3. Assume vertex z has the largest time component. The diagram obtained by colouring the vertex z black, represented on the right-hand side, has as integrand

$$\begin{aligned} \mathcal{I}_{\text{triangle,2}}(x, y, z, g) &= (ig)(-ig)^2 \Delta_F^-(y - z) \Delta_F^*(z - x) \Delta_F^-(y - x) \\ &= (ig)(-ig)^2 \Delta_F(y - z) \Delta_F^-(z - x) \Delta_F^-(y - x) \\ &= -\mathcal{I}_{\text{triangle}}(x, y, z, g) \ . \end{aligned} \tag{2.40}$$

This agrees with (2.39).

Let us now look at the sum over all 2^n possible colourings of the vertices. We can split up the 2^n terms into 2^{n-1} pairs, where the diagrams in each pair have the same colouring for all vertices except for x_k: one has x_k white, and one

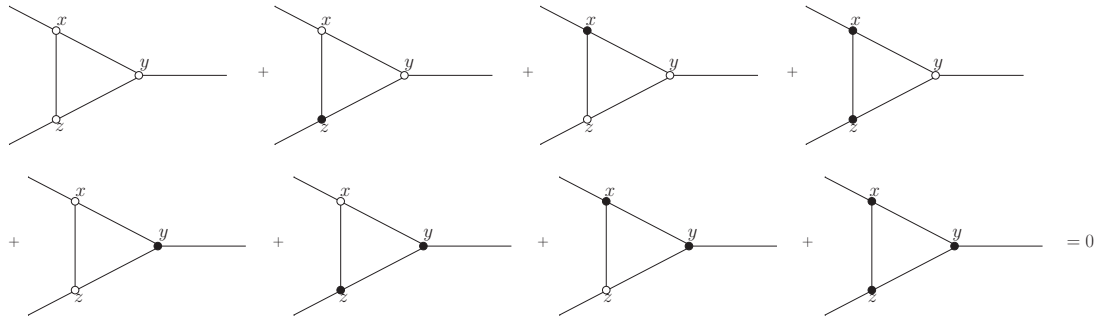

Figure 2.4 *The largest time equation*

has x_k black. Because of (2.39), all pairs will vanish so the result is zero.

$$\begin{aligned}\sum_{\text{colourings } x_i} \mathcal{I}(x_1,...,x_n) &= \sum_{\text{colourings } x_i,\ i\neq k} \left(\mathcal{I}(x_1,...,x_n)_{x_k \text{ white}} + \mathcal{I}(x_1,...,x_n)_{x_k \text{ black}}\right) \\ &= \sum_{\text{colourings } x_i,\ i\neq k} 0 \\ &= 0\ . \end{aligned} \tag{2.41}$$

Equation (2.41) was derived in a specific frame and is valid at the level of the integrand. However, the equation is frame-independent and hence will be valid in any frame. This means that we can integrate (2.41) to obtain an equation at the level of the Feynman diagram itself:

$$\sum_{\text{colourings } x_i} F(p_1,...,p_k) = 0\ . \tag{2.42}$$

Equation (2.42) is called the largest time equation (LTE).
It is illustrated in the case of a triangle diagram in figure 2.4. If we again assume that vertex z has the largest time component, the cancellation at the level of the integrand will happen pairwise between adjacent diagrams.

2.4 Interpretation

We now want to interpret the LTE (2.42). It is instructive to single out two terms in the sum: the one with all vertices white, and the one with all vertices black. They correspond to the original diagram F and its complex conjugate F^*. Rearranging (2.42) then gives

$$F(p_1,...,p_k) + F^*(p_1,...,p_k) = -\sum_{\text{mixed colourings}} F(p_1,...,p_k)\ . \tag{2.43}$$

We now want to interpret equation (2.43). We start with the left-hand side. In momentum space, there is an explicit overall factor of i in each diagram, due to the Fourier transformation [71]. When performing explicit calculations, this factor of i manifests itself via the Wick rotation. Taking the complex conjugate will thus incur an extra minus sign. Moreover, it also corresponds to changing the $i\epsilon$ prescription. The left-hand side of (2.43) thus becomes $F(+i\epsilon) - F(-i\epsilon)$. If we work in a region where we are on the branch cut of a certain kinematic channel s, this will correspond to the discontinuity across this channel. We conclude that the left-hand side of (2.43) is in momentum space equal to

$$\begin{aligned} F(p_1, ..., p_k) + F^*(p_1, ..., p_k) &= F(p_1, ..., p_k)_{+i\epsilon} - F(p_1, ..., p_k)_{-i\epsilon} \\ &= \text{Disc}_s\big(F(p_1, ..., p_k)\big) \ . \end{aligned} \tag{2.44}$$

The terms on the right-hand side of (2.43) all include at least one factor of $\Delta^{\pm}$. We call such diagrams cut diagrams and the propagators cut propagators; it will later become clear why. We usually represent cut propagators by a dashed line going through them.

Equation (2.43) thus becomes in momentum space

$$\text{Disc}_s F(p_1, ..., p_k) = -\sum_{\text{cuts}} F(p_1, ..., p_k) \ . \tag{2.45}$$

The derivation of the LTE above also tells us how to calculate cuts in momentum space:

- white vertices correspond to the usual vertex factor for the theory, black vertices are complex conjugated.
- Propagators between two white vertices correspond to usual Feynman rules, propagators between two black vertices are complex conjugated.
- Propagators between a white and a black vertex are replaced by $\Delta^{\pm}$. (2.27) and (2.34) show that in momentum space, these correspond to delta functions. Energy flows from white to black vertices. This energy flow refers to the energy of the propagator k_0 for quadratic propagators, and to the energy of the external particle β_i^0 for Eikonal propagators.

Using these rules, (2.45) provides us with a diagrammatic way of calculating the discontinuity of a Feynman diagram in a given channel. We notice that this seems a very inefficient way of calculating the discontinuity of a Feynman diagram. Indeed, for a diagram involving n vertices, there will be $2^n - 2$ cuts contributing

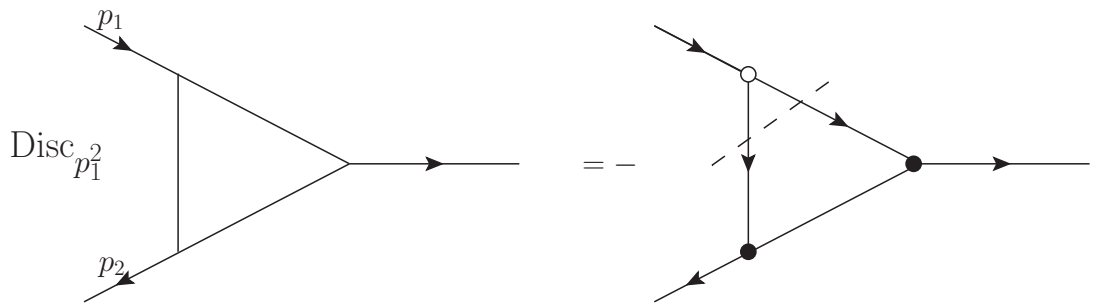

Figure 2.5 *The largest time equation applied to a triangle diagram*

to the discontinuity. However, it has been observed earlier that in the case of diagrams with quadratic propagators almost all of the cuts vanish. In reference [67], it is proven that for diagrams with quadratic propagators, the following theorem holds.

Theorem 1 *A diagram containing black vertices gives rise to a non-zero contribution if and only if the black vertices contain connected regions that contain one or more outgoing lines. And also the white vertices must form connected regions involving incoming lines.*

We can cut such a diagram into two parts, one containing only white vertices, the other one only containing black vertices. This explains why we call such diagrams *cuts*. Energy flows from the white part, corresponding to incoming particles, to the black part, corresponding to outgoing particles.

This is illustrated in figure 2.5 for the triangle diagram with quadratic propagators we studied before. If we work in the kinematic region where

$$\begin{aligned} p_1^2 &> 0 \\ p_{1_0} &> 0 \\ p_2^2 &< 0 \\ (p_1+p_2)^2 &< 0 \\ p_{2_0} &< -p_{1_0} \ , \end{aligned} \tag{2.46}$$

we have that particle 1 is the only incoming particle. We expect to have a discontinuity in the p_1^2 channel, and no discontinuity in the other channels. There is one cut contributing to this discontinuity. This cut has indeed a white and a black part, with the energy flowing from the white to the black part.

2.5 Vanishing cuts for Eikonal diagrams

In the proof of theorem 1, explicit use is made of the energy flow inside the diagram determined by factors of $\Delta_F^{\pm}$. As noticed before, in the case of Eikonal diagrams, factors of $E^{\mu,\pm}$ only determine the external energy flow, not the internal one. The proof in reference [67] hence does not apply. We now find rules similar to theorem 1 for Eikonal diagrams. We illustrate these general rules by looking at the example of the $(1,1,1)$ web involving a three-gluon vertex. We work in the region where particles i and j are incoming and particle k is outgoing, so that we expect a discontinuity in the s_{ij} channel. The diagram has five vertices, so we start out with thirty cuts.

2.5.1 Cuts violating conservation of energy

A first set of vanishing cuts consists of cuts which violate conservation of energy. An example is the leftmost cut in figure 2.6. It will include a factor of

$$\delta^+(k_1^2)\delta^+(k_2^2)\delta^+(k_3^2)\delta^{(d)}(k_1+k_2+k_3)\ . \tag{2.47}$$

The first three delta functions imply that there is net energy flowing into the vertex, which violates the last delta function enforcing conservation of momentum. We conclude that the delta functions are incompatible and hence will integrate to zero.

We notice that this type of argument does not make use of the specific form of the Eikonal factors, but only involves gluons. In fact, this is the type of argument used to prove theorem 1 [67].

In the case of the $(1,1,1)$ web, four possible colourings obey this pattern, for example the leftmost one in figure 2.6. We have only 26 possible cuts left.

2.5.2 Cuts involving vanishing $E^{\mu,+}_{\text{out}}$ and $E^{\mu,-}_{\text{in}}$.

Incoming Wilson line particles have $\beta^0 > 0$, outgoing ones $\beta^0 < 0$. Hence, it follows from (2.33) that

$$\begin{aligned} E^{\mu,+}_{\text{out}} &= 0 \\ E^{\mu,-}_{\text{in}} &= 0\ . \end{aligned} \tag{2.48}$$

Cuts involving these propagators will consequently vanish. Notice that this is a mechanism that is directly caused by the fact that the denominator has only one

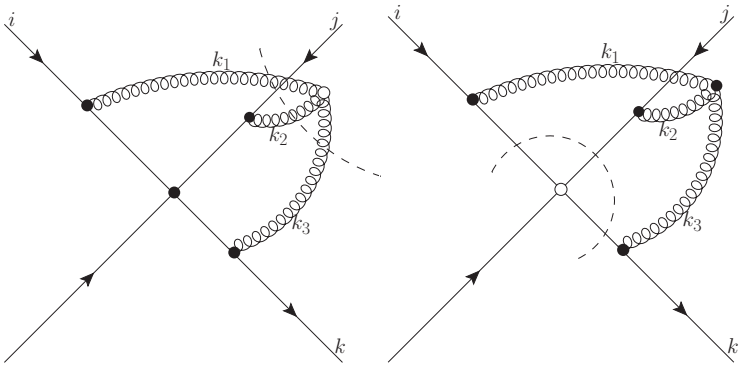

(a) *A cut violating conservation of momentum*

(b) *This cut has a factor of $E_i^{\mu,-} E_j^{\nu,-} E_k^{\rho,+}$. Because i and j are incoming, this vanishes.*

Figure 2.6 *Examples of vanishing cuts*

pole, which is unique to Eikonal diagrams.

An application to the $(1,1,1)$ web can be found on the right-hand side of figure 2.6. It includes a factor of

$$E_i^{\mu,-} = 0 \ , \tag{2.49}$$

where i is an incoming Eikonal particle. In fact, the vanishing factor only depends on the colour of the two vertices on the Wilson line i. The colour of the three other vertices did not matter. This argument thus implies that eight cuts will vanish this way. One of these was already excluded by conservation of momentum, so we have seven genuinely new vanishing cuts.

Similar arguments hold for cuts involving $E_{\mathrm{j}}^{\mu,-}$ and $E_{\mathrm{k}}^{\mu,+}$. This way eleven more cuts vanish, so that eight remain to consider.

2.5.3 Cut of an Eikonal line together with an emitted gluon

Let us now look at the case where we cut one Eikonal line, together with the gluon it emits. In the case of the $(1,1,1)$ web, we find an example of such a cut in figure 2.7. It includes a factor of

$$\delta(-\beta_i \cdot k_1 - m)\delta^+(k_1^2) \ . \tag{2.50}$$

Using that particle i is incoming so that $\beta_i^0 > 0$, and $\beta_i^2 = 1$, we can use the following parametrisation

$$\begin{aligned} k_1 &= (k_{10}, k_{11}\mathbf{v}_{d-1}), \quad \mathbf{v}^2 = 1 \\ \beta_i &= (\cosh\phi, \sinh\phi\mathbf{v}'), \quad \mathbf{v}'^2 = 1 \\ \mathbf{v}\cdot\mathbf{v}' &= \cos\sigma \ . \end{aligned} \tag{2.51}$$

Here $\mathbf{v}$ and $\mathbf{v}'$ are unit vectors. We use polar coordinates so they are integrated out, except for the angle σ between them.

The $\delta^+(k_1^2)$ then tells us that

$$k_{10} = k_{11} > 0 \ . \tag{2.52}$$

This gives us

$$-\beta_i \cdot k_1 - m = -k_{10}(\cosh\phi - \sinh\phi\cos\sigma) - m < 0 \ . \tag{2.53}$$

This quantity is negative for all values of σ [2]. This means that we can not satisfy the first constraint in (2.50). The two delta functions are incompatible and will integrate to zero.

This rule is another example that is unique to cuts of Eikonal diagrams. If we used a non-Eikonal expression for the propagator of the incoming particle i, the cut on the left-hand side of figure 2.7 would have represented the discontinuity with respect to the squared mass of the external particle i. However, we saw earlier that correlators of Wilson lines are independent of the value of β_i^2. Therefore, it makes sense physically that cuts of this type vanish for Eikonal diagrams.

Of the eight remaining cuts of the $(1,1,1)$ web, four vanish for this reason. We only have four non-vanishing cuts left.

2.5.4 Cut of an Eikonal line together with multiple emitted gluons

The rule described in the previous section also applies to the emission of multiple gluons from one Wilson line. More specifically, the cut vanishes if and only if we cut all gluons emitted further away from the hard interaction than the cut

[2] Notice that for this argument to hold, we need to choose $m > 0$. We indeed made this choice in the discussion after equation (2.1).

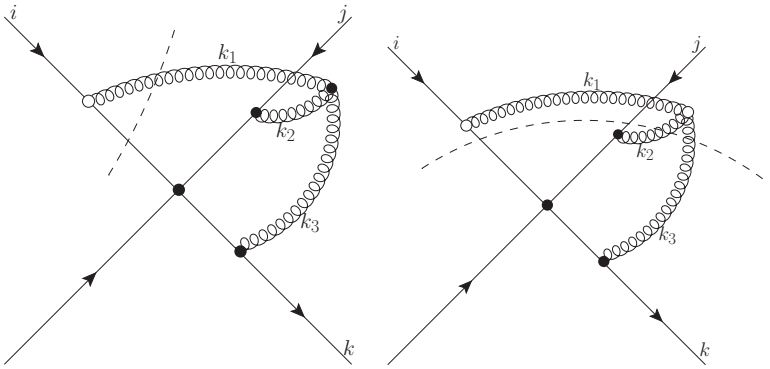

(a) *An Eikonal line cut with an emitted gluon* **(b)** *An Eikonal line cut with emitted gluons*

Figure 2.7 *More examples of vanishing cuts.*

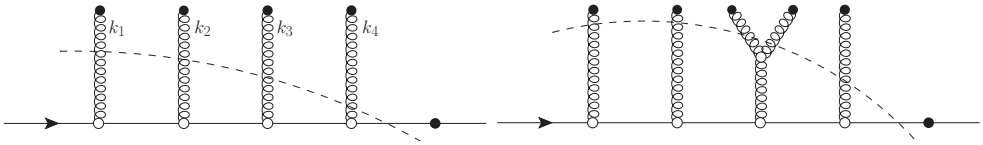

(a) **(b)**

Figure 2.8 *More examples of vanishing cuts*

Wilson line itself. This even holds if the gluons split up into other gluons before they are cut. Examples are given in figure 2.8.
The reason is exactly the same as in the case of the single-gluon emission. The cuts give a factor of

$$\delta(-\beta \cdot (k_1 + ... + k_n) - nm)\delta^+(k_1^2)\delta^+(k_2^2)...\delta^+(k_n^2) \ . \tag{2.54}$$

These delta functions are mutually exclusive, so any cut including them will be equal to zero.

In the case of the $(1, 1, 1)$ web, an application of this rule can be found on the right-hand side of figure 2.7. The gluon emitted from leg i splits into two other gluons, both of which are cut. Therefore, the situation is the same as on the right-hand side of figure 2.8. There are two more cuts of this kind, involving gluon emissions from legs j and k respectively. They all have to vanish, so that there is just one non-vanishing cut left. We can conclude that the discontinuity is equal to only one cut, as described in figure 2.9. In fact, the same conclusion would have been reached by applying theorem 1. The same conclusion is reached for all the other diagrams that are studied in this thesis. It is thus a logical step to conjecture the following:

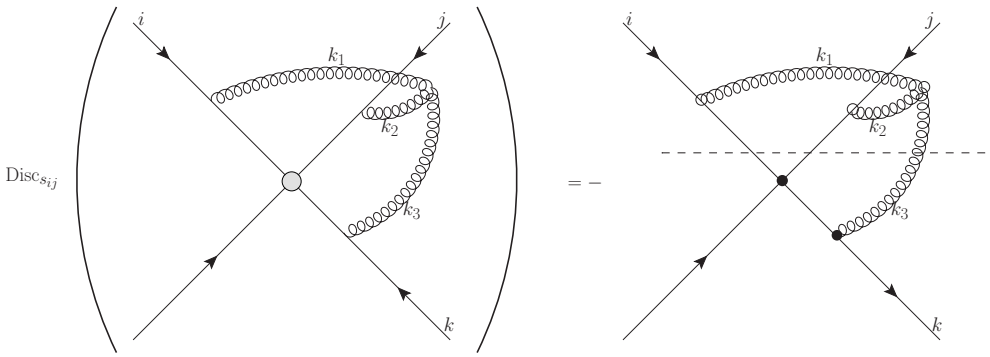

Figure 2.9 *Relation between* $\text{Disc}_{s_{ij}}$ *and* $\text{Cut}_{s_{ij}}$.

Conjecture 2 *Theorem 1 also applies to Eikonal diagrams.*

We have been able to verify conjecture 2 for all diagrams that we have calculated, but have not found a general proof. A possible proof could come from looking at the theorem for diagrams with a quadratic propagator, and then taking the Eikonal limit at the level of the integrand. However, it is not completely clear if this would incur some order-of-limit issues.

2.6 Conclusion

In this chapter, we derived a diagrammatic way to calculate discontinuities of correlators of Wilson lines. We started by introducing a momentum-space regulator for Wilson lines. We chose a regulator which is equivalent to the configuration-space regulator introduced in [34]. We then derived the largest time equation, and studied its consequences for Wilson-line correlators. We found several classes of cuts that vanish, and concluded that the non-vanishing cuts look similar to the remaining ones in the case of quadratic denominators, although the mechanisms involved are very different. We applied this framework to find a diagrammatic expression for the discontinuity of the $(1, 1, 1)$ web. We will calculate this cut and web in detail in the next chapter.

In what follows, we apply the framework of cuts to calculate diagrams contributing to webs. We will omit the colouring of all the vertices and only draw the non-vanishing cuts. We represent the cuts by a dashed line, as in diagram 2.9.

Chapter 3

Calculation of webs via cuts

We have built up a framework to calculate the discontinuities of Eikonal diagrams using cuts. We also showed how to obtain the diagram itself from the discontinuity using a dispersive integral. We now demonstrate how to apply this framework to calculate webs consisting of Eikonal diagrams in practice. All the webs in this chapter have been calculated earlier, using other techniques. This allows us to check our results.

Because this is the first time that we illustrate some techniques, we will go into a fair amount of detail. When these techniques are applied a second time, we will refer to the appendix and just state the results.

3.1 One-loop web

We first look at the easiest possible web, the one-loop one. It is represented on the left-hand side of figure 3.1 [1], and is the same as the calculation of the cusp anomalous dimension at one loop, up to self-energy corrections [9, 72–74].

[1] From now on, the black blob at the centre of the diagram represents the hard interactions that we ignore. It has nothing to do with complex conjugation as in the previous chapter.

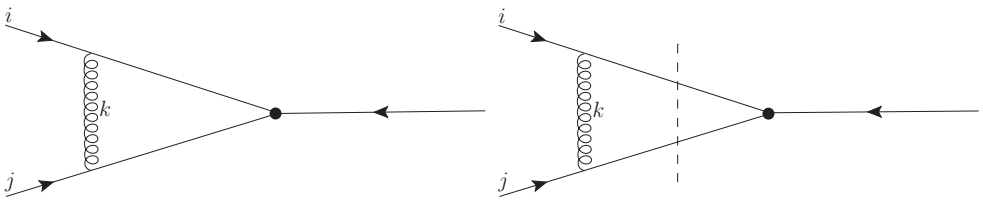

(a) *The one-loop web* **(b)** *The cut of the one-loop web*

Figure 3.1 *The one-loop web and its cut. The diagram forms a web by itself.*

This web consists of a single diagram. It can be written as

$$\mathcal{W}_{(1,1)} = \mathcal{C}_{(1,1)}\mathcal{F}_{(1,1)} \ , \tag{3.1}$$

where the colour factor is equal to

$$\mathcal{C}_{(1,1)} = T_i \cdot T_j \ . \tag{3.2}$$

We now perform the computation of the kinematic part. Using the Feynman rules that we derived before, it is equal to

$$\mathcal{F}_{(1,1)}(g_s, m, \mu, \{\beta\}) = \mu^{2\epsilon}(ig_s)^2 \int \frac{d^dk}{(2\pi)^d} \frac{i\beta_i^\mu}{-\beta_i \cdot k - m + i\epsilon} \ \frac{-ig_{\mu\nu}}{k^2 + i\epsilon} \ \frac{i\beta_j^\nu}{\beta_j \cdot k - m + i\epsilon} \ , \tag{3.3}$$

where $\{\beta\}$ still represents the relevant external velocities. We will assume again that $\beta^2 = 1$, so that there is only one kinematic variable, namely $\beta_i \cdot \beta_j$. It turns out that it is more convenient to express our results in terms of the variable α_{ij} defined via

$$\beta_i \cdot \beta_j = -\frac{1}{2\alpha_{ij}} - \frac{\alpha_{ij}}{2} \ . \tag{3.4}$$

We notice there is an ambiguity in this definition, because each value of $\beta_i \cdot \beta_j$ corresponds to two values of α_{ij}. We choose α_{ij} such that

$$|\alpha_{ij}| \leq 1 \ . \tag{3.5}$$

For what follows, it will also be convenient to define

$$r(\alpha_{ij}) = \frac{1 + \alpha_{ij}^2}{1 - \alpha_{ij}^2} \tag{3.6}$$

Looking at the expression (3.3), we notice that we can eliminate the m dependence from the integrand by rescaling the loop momentum. This leads to

$$\mathcal{F}_{(1,1)}(g_s, m, \mu, \{\beta\}) = \frac{\mu^{2\epsilon}}{m^{2\epsilon}} g_s^2 \mathcal{F}_{(1,1)}(\alpha_{ij}, \epsilon) \ . \tag{3.7}$$

In the other webs we calculate, we will usually apply the same procedure. We scale out the infrared regulator m and calculate our result as a function of the relevant α. When we are dealing with a multi-leg problem, there will be multiple

α variables.

3.1.1 Calculation of cut

We define

$$\begin{aligned} s_{ij} &= (\beta_i + \beta_j)^2 \\ &= \frac{(1-\alpha_{ij})^2}{-\alpha_{ij}} \ . \end{aligned} \tag{3.8}$$

From equation (3.8), we can see that

$$s_{ij} \pm i\epsilon \leftrightarrow \alpha_{ij} \pm i\epsilon \ . \tag{3.9}$$

This means that s_{ij} and α_{ij} discontinuities are equivalent:

$$\text{Disc}_{s_{ij}} \mathcal{F}_{(1,1)}(s_{ij}) = \text{Disc}_{\alpha_{ij}} \mathcal{F}_{(1,1)}(\alpha_{ij}) \ . \tag{3.10}$$

We can thus calculate the α_{ij} discontinuity by cutting on the s_{ij} channel. This will also apply to all the other webs we calculate below. This is one of the reasons why α is a convenient variable to use.

To find the cuts of the one-loop diagram in the variable s_{ij}, we have to work in the correct kinematic region. This is the one where

$$s_{ij} \in (4, \infty) \ . \tag{3.11}$$

By using equation (3.8), we can map this to the region where

$$\alpha_{ij} \in (-1, 0) \tag{3.12}$$

It is easy to check that this will be the case when both particles are incoming or outgoing at once, and will not be the case when we have one ingoing and one outgoing particle. Again, the same applies to all diagrams below, even if they have multiple kinematic variables. If for example we have three external particles i, j, k, and work in the region where i, j are incoming and k is outgoing, we will have that

$$-1 < \alpha_{ij} < 0 < \{\alpha_{ik}, \alpha_{jk}\} < 1 \ . \tag{3.13}$$

We thus expect a discontinuity on the α_{ij} channel, but not on the α_{ik} and α_{jk}

channels. We will always have to explicitly state the region we are calculating the cut in.

Working with the α_{ij} variables changes the subtracted dispersive integral as follows. From equation (1.50), we have that

$$\mathcal{F}_{(1,1)}(s_{ij}) - \mathcal{F}_{(1,1)}(s_{ij}=0) = \frac{s_{ij}}{2\pi i}\int_4^\infty \frac{ds'_{ij}}{s'_{ij}(s'_{ij}-s_{ij})}\text{Disc}_{s'_{ij}}\mathcal{F}_{(1,1)} \ . \tag{3.14}$$

We can rephrase this in terms of α_{ij} using (3.8). Equation (3.10) allows us to rewrite the integral as follows:

$$\begin{aligned}&\mathcal{F}_{(1,1)}(\alpha_{ij}) - \mathcal{F}_{(1,1)}(\alpha_{ij}=1)\\ &= \frac{(1-\alpha_{ij})^2}{-2\pi i\alpha_{ij}}\int_{-1}^0 \frac{d\alpha'_{ij}(1-\alpha'^2_{ij})}{\alpha'^2_{ij}}\frac{-\alpha'_{ij}\,\text{Disc}_{\alpha'_{ij}}\big(\mathcal{F}_{(1,1)}\big)}{(1-\alpha'_{ij})^2\left(\frac{(1-\alpha'_{ij})^2}{-\alpha'_{ij}}-\frac{(1-\alpha_{ij})^2}{-\alpha_{ij}}\right)} \ .\end{aligned} \tag{3.15}$$

In what follows, we will find that for the class of diagrams we calculate [2], we can always write the discontinuity as

$$\text{Disc}_{\alpha'_{ij}}\big(\mathcal{F}_{(1,1)}\big) = r(\alpha'_{ij})F(-\alpha'_{ij}) + G(-\alpha'_{ij}) \ , \tag{3.16}$$

where $F(-\alpha'_{ij})$ and $G(-\alpha'_{ij})$ are polylogarithms of the form $G(\mathbf{a},-\alpha'_{ij})$, with $\mathbf{a}$ a vector with constant entries. The dispersive integral (3.15) can then be calculated as

$$\begin{aligned}&\mathcal{F}_{(1,1)}(\alpha_{ij}) - \mathcal{F}_{(1,1)}(\alpha_{ij}=1)\\ &= \frac{1}{2\pi i}\Bigg[\int_{-1}^0 d\alpha'_{ij}\big(\frac{2}{1-\alpha'_{ij}}+\frac{1}{\alpha'_{ij}-\alpha_{ij}}+\frac{\alpha_{ij}}{\alpha_{ij}\alpha'_{ij}-1}\big)G(-\alpha'_{ij})\\ &\quad -\int_{-1}^0 d\alpha'_{ij}\left(\frac{-2}{(1-\alpha'_{ij})^2}+r(\alpha_{ij})\big(\frac{1}{\alpha_{ij}-\alpha'_{ij}}+\frac{\alpha_{ij}}{\alpha_{ij}\alpha'_{ij}-1}\big)\right)F(-\alpha'_{ij})\Bigg] \ .\end{aligned} \tag{3.17}$$

Because of the construction of polylogarithms as iterated integrals, the integral in (3.17) is trivial to perform. This is a very useful property, because often the calculation of dispersive integrals is very complicated, as in reference [75]. In what follows, we will thus be able to omit the details of the dispersive integrals. We will denote them as

[2] Except for the all-order calculation of the one-loop diagram.

$$\mathcal{F}_{(1,1)}(\alpha_{ij}) - \mathcal{F}_{(1,1)}(\alpha_{ij}=1) = \int_{\text{Disp},\alpha_{\text{ij}}} \text{Disc}_{\alpha_{ij}}\big(\mathcal{F}\big)$$
$$= -\sum_{\text{Cuts } i} \int_{\text{Disp},\alpha_{\text{ij}}} \text{Cut}_{\alpha_{ij},i}\big(\mathcal{F}\big) \qquad (3.18)$$

instead of using the full expression (3.17).

When working with two incoming particles, the largest time equation is very easy to interpret. There are $2^3 - 2 = 6$ cuts to start with. Of these, the ones where the central vertex is white will contain a factor of $E^{\mu,-}_{\text{in}} = 0$. The non-vanishing cuts will thus have a black central vertex. There are three such cuts. Two of these will include a combination of a cut of an Eikonal line and an emitted gluon, so are zero as well. Hence there is only one relevant cut contributing to discontinuity of the one-loop diagram, the one on the right-hand side of figure 3.1:

$$\begin{aligned}\text{Disc}_{\alpha_{ij}}\left(\mathcal{F}_{(1,1)}(\alpha_{ij})\right) &= -\text{Cut}\left(\mathcal{F}_{(1,1)}(\alpha_{ij})\right) \\ &= \frac{\mu^{2\epsilon}}{m^{2\epsilon}}(ig_s)^2(2\pi i)^2(i)^2\beta_i\cdot\beta_j \\ &\times \int \frac{d^dk}{(2\pi)^d}\delta(-\beta_i\cdot k-1)\frac{-i}{k^2+i\epsilon}\delta(\beta_j\cdot k-1)\ . \end{aligned} \qquad (3.19)$$

In the rest of this calculation, we drop the $i\epsilon$ prescription of the gluon propagator. This is allowed because there will not be any poles in our region of integration, so that the prescription does not matter. Indeed, it turns out below that the delta functions constrain the possible values of k^2 in such a way that it is spacelike, i.e. negative. The absence of the pole implies that the cut is purely imaginary. This is a phenomenon which we will observe in most cuts that we calculate. It allows us to drop the $i\epsilon$ for almost all cuts calculated in this chapter. The exception is the cut of the Y diagram discussed below.

To perform the loop integral, we choose an explicit parametrisation for the loop momentum and the external momenta. We choose the following one:

$$\begin{aligned}\beta_i &= (1, \mathbf{0}_3) \\ \beta_j &= (\cosh\theta, \sinh\theta, \mathbf{0}_2) \\ k &= (k_0, k_1, k_2\mathbf{v}_{d-2})\ , \mathbf{v}^2_{d-2} = 1\ , \end{aligned} \qquad (3.20)$$

where again $\mathbf{v}$ is a $(d-2)$-dimensional unit vector which can be integrated out.

This parametrisation is convenient for multiple reasons:

- It respects the constraints $\beta^2 = 1$.
- It corresponds to two incoming external particles. Outgoing external particles are parametrised by negative energy components.
- It is easy to go from this parametrisation to the variable α_{ij} via $\theta = -\ln(-\alpha_{ij})$.

In terms of our parametrisation, we have

$$r(\alpha_{ij}) = \frac{\cosh\theta}{\sinh\theta} \ . \tag{3.21}$$

The measure is equal to [3]

$$d^d k = \frac{2\pi^{1-\epsilon}}{\Gamma(1-\epsilon)} dk_0 dk_1 dk_2 k_2^{1-2\epsilon} \ , \tag{3.22}$$

such that

$$\begin{aligned}
&\text{Disc}\left(\mathcal{F}_{(1,1)}\right)(\alpha_{ij}) \\
&= \frac{\mu^{2\epsilon}}{m^{2\epsilon}} g_s^2 \frac{-1}{(2\pi)^{2-2\epsilon}} \cosh\theta \frac{2\pi^{1-\epsilon}}{\Gamma(1-\epsilon)} \int_{-\infty}^{\infty} dk_0 dk_1 \int_0^{\infty} dk_2 k_2^{1-2\epsilon} \delta(-k_0 - 1) \\
&\qquad\qquad \times \frac{-i}{k_0^2 - k_1^2 - k_2^2} \delta(\cosh\theta k_0 - \sinh\theta k_1 - 1) \\
&= -2^{2\epsilon+2} \pi i \frac{\kappa}{\Gamma(1-\epsilon)^2} r(\alpha_{ij}) \int_0^{\infty} dk_2 k_2^{1-2\epsilon} \frac{1}{1 - (1+\cosh\theta)^2/\sinh^2\theta - k_2^2} \ ,
\end{aligned} \tag{3.23}$$

where we introduced the constant κ, as defined in [27]

$$\kappa = -\frac{\mu^{2\epsilon}}{m^{2\epsilon}} g_s^2 \frac{\Gamma(1-\epsilon)}{8\pi^{2-\epsilon}} \ . \tag{3.24}$$

We will see later that every $n-$loop diagram comes with a factor of κ^n, and will always extract a factor of $\Gamma(2n\epsilon)\kappa^n$ before expanding our result in powers of ϵ.

We notice that the k_2 integral depends on only one variable, namely

$$(1+\cosh\theta)^2/\sinh^2\theta - 1 = \frac{-4\alpha_{ij}}{(1+\alpha_{ij})^2} \ . \tag{3.25}$$

[3] For an explanation on how to derive the measure for the parametrisations we use, see appendix A.

We can rescale the loop momentum and obtain

$$\begin{aligned}
\mathrm{Disc}\left(\mathcal{F}_{(1,1)}\right)(\alpha_{ij}) &= 2^{2\epsilon+2}\pi i\frac{\kappa}{\Gamma(1-\epsilon)^2}r(\alpha_{ij})\left(\frac{-4\alpha_{ij}}{(1+\alpha_{ij})^2}\right)^{-\epsilon} \\
&\quad\times\int_0^\infty dk_2 k_2^{1-2\epsilon}\frac{1}{1+k_2^2} \\
&= 2^{2\epsilon+2}\pi i\frac{\kappa}{\Gamma(1-\epsilon)^2}r(\alpha_{ij})\left(\frac{-4\alpha_{ij}}{(1+\alpha_{ij})^2}\right)^{-\epsilon}\frac{\pi}{2\sin(\epsilon\pi)} \\
&= 2\pi i\frac{\kappa}{\Gamma(1-\epsilon)}r(\alpha_{ij})\left(\frac{-\alpha_{ij}}{(1+\alpha_{ij})^2}\right)^{-\epsilon}\Gamma(\epsilon) \qquad (3.26)\\
&= (2\pi i)2\kappa\Gamma(2\epsilon)r(\alpha_{ij})+\mathcal{O}(\epsilon^0)\ . \qquad (3.27)
\end{aligned}$$

3.1.2 Dispersive integral

Now that we have an expression for the discontinuity of the web (3.26), we want to calculate the web itself via a (subtracted) dispersive integral. Since we are only interested in the $\frac{1}{\epsilon}$ divergent part of the web [4], we could calculate the dispersive integral of the $\frac{1}{\epsilon}$ part of the Laurent expansion only. When we calculate multi-loop webs, this will indeed be our approach. However, it turns out that in the one-loop case, the dispersive integral can be performed to all orders in ϵ. We can hence check if we obtain the all-orders result calculated in [27]. To demonstrate the calculation technique we will use in the multi-loop case, we then perform the integration for the $\frac{1}{\epsilon}$ part of the Laurent series as well.

All orders in ϵ

The formula (3.15) can be applied to equation (3.26):

$$\begin{aligned}
&\mathcal{F}_{(1,1)}(\alpha_{ij})-\mathcal{F}_{(1,1)}(\alpha_{ij}=1) \\
&=\frac{(1-\alpha_{ij})^2}{-2\pi i\alpha_{ij}}\int_{-1}^0\frac{d\alpha'_{ij}(1-\alpha'^2_{ij})}{\alpha'^2_{ij}}\frac{-\alpha'_{ij}\,\mathrm{Disc}_{\alpha'_{ij}}\left(\mathcal{F}_{(1,1)}\right)}{(1-\alpha'_{ij})^2\left(\frac{(1-\alpha'_{ij})^2}{-\alpha'_{ij}}-\frac{(1-\alpha_{ij})^2}{-\alpha_{ij}}\right)} \\
&=-\frac{(1-\alpha_{ij})^2}{\alpha_{ij}}\frac{\kappa\Gamma(\epsilon)}{\Gamma(1-\epsilon)}\int_0^1 d\alpha'_{ij}\frac{(1+\alpha'^2_{ij})\left(\frac{\alpha'_{ij}}{(1-\alpha'_{ij})^2}\right)^{-\epsilon}}{(1+\alpha'_{ij})^2\left((1+\alpha'_{ij})^2-\frac{(1-\alpha_{ij})^2\alpha'_{ij}}{-\alpha_{ij}}\right)}\ . \qquad (3.28)
\end{aligned}$$

[4] In fact, we will later need the $\mathcal{O}(1)$ part in a different calculation.

We can now split this into partial fractions. The integrals then evaluate to hypergeometric functions.

$$
\begin{aligned}
&\mathcal{F}_{(1,1)}(\alpha_{ij}) - \mathcal{F}_{(1,1)}(\alpha_{ij}=1) \\
&= \frac{\kappa\Gamma(\epsilon)}{\Gamma(1-\epsilon)}\Bigg(-\frac{r(\alpha_{ij})}{\alpha_{ij}}\frac{\Gamma(1-\epsilon)\Gamma(1+2\epsilon)}{\Gamma(2+\epsilon)}\,{}_2F_1\left[1,1-\epsilon,2+\epsilon,-\frac{1}{\alpha_{ij}}\right] \\
&+ \frac{4^\epsilon\Gamma(1-\epsilon)\Gamma(1/2+\epsilon)}{\sqrt{\pi}} + \alpha_{ij}r(\alpha_{ij})\frac{\Gamma(1-\epsilon)\Gamma(1+2\epsilon)}{\Gamma(2+\epsilon)}\,{}_2F_1\left[1,1-\epsilon,2+\epsilon,-\alpha_{ij}\right]\Bigg) \\
&= \kappa\Gamma(2\epsilon)\left(\frac{4^\epsilon\Gamma(1/2+\epsilon)\Gamma(\epsilon)}{\Gamma(2\epsilon)\sqrt{\pi}} + 2\beta_i\cdot\beta_j\,{}_2F_1\left[1,1-\epsilon,3/2,\frac{\beta_i\cdot\beta_j}{2}+1/2\right]\right) \\
&= \kappa\Gamma(2\epsilon)\left(2 + 2\beta_i\cdot\beta_j\,{}_2F_1\left[1,1-\epsilon,3/2,\frac{\beta_i\cdot\beta_j}{2}+1/2\right]\right)\,. \qquad (3.29)
\end{aligned}
$$

This result seems very suggestive: it has a part which has a dependence on α_{ij} and a part which does not. It is reasonable to suggest that the former is $\mathcal{F}_{(1,1)}(\alpha_{ij})$ and the latter is the constant $\mathcal{F}_{(1,1)}(\alpha_{ij}=1)$:

$$
\begin{aligned}
\mathcal{F}_{(1,1)}(\alpha_{ij}) &= \kappa\Gamma(2\epsilon)2\beta_i\cdot\beta_j\,{}_2F_1\big(1,1-\epsilon,3/2,\frac{\beta_i\cdot\beta_j}{2}+1/2\big)\,. \qquad (3.30)\\
\mathcal{F}_{(1,1)}(\alpha_{ij}=1) &= -2\kappa\Gamma(2\epsilon) \qquad (3.31)
\end{aligned}
$$

We check this assumption by calculating the diagram numerically using SecDec [76], a toolbox for numerical integration of Feynman integrals. SecDec provides us with a Laurent series of the diagram. We compare the three leading orders of this Laurent series to the series obtained by expanding (3.30) and find agreement. Equation (3.30) also agrees with reference [27].

In reference [27], a convenient expansion of (3.30) is also presented:

$$
\begin{aligned}
\mathcal{F}_{(1,1)}(\alpha_{ij}) &= 2\kappa\Gamma(2\epsilon)r(\alpha_{ij})\big(R_0(\alpha_{ij}) + \epsilon R_1(\alpha_{ij}) + \mathcal{O}(\epsilon^2)\big) \\
R_0(\alpha_{ij}) &= \ln\alpha_{ij} \\
R_1(\alpha_{ij}) &= 2\mathrm{Li}_2(-\alpha_{ij}) + 2\ln\alpha_{ij}\ln(1+\alpha_{ij}) - \frac{1}{2}\ln^2(\alpha_{ij}) + \zeta_2\,. \qquad (3.32)
\end{aligned}
$$

Laurent series in ϵ

When we look at the $\frac{1}{\epsilon}$ part of the Laurent series only, the dispersive integral becomes

$$
\begin{aligned}
&\mathcal{F}^{(-1)}_{(1,1)}(\alpha_{ij}) - \mathcal{F}^{(-1)}_{(1,1)}(\alpha_{ij}=1) \\
&= -\frac{(1-\alpha_{ij})^2}{\alpha_{ij}}\kappa \int_0^1 d\alpha'_{ij} \frac{(1+\alpha'^2_{ij})}{(1+\alpha'_{ij})^2\big((1+\alpha'_{ij})^2 - \frac{(1-\alpha_{ij})^2\alpha'_{ij}}{-\alpha_{ij}}\big)} \\
&= r(\alpha_{ij}) \ln \alpha_{ij} + 1 \ , \qquad (3.33)
\end{aligned}
$$

suggesting that

$$
\begin{aligned}
\mathcal{F}^{(-1)}_{(1,1)}(\alpha_{ij}) &= \kappa r(\alpha_{ij}) \ln \alpha_{ij} \\
\mathcal{F}^{(-1)}_{(1,1)}(\alpha_{ij}=1) &= -\kappa \ . \qquad (3.34)
\end{aligned}
$$

This can indeed be confirmed numerically by using SecDec, and is consistent with our all-orders result (3.30).

Another issue with subtracted dispersive integrals is that they only give the result up to a constant $\mathcal{F}(\alpha = 1)$. In a few cases, such as the Y diagram below, this constant is trivial to evaluate. In other cases, we work as in the one-loop case: the dispersive integral usually suggests a reasonable guess for $\mathcal{F}(\alpha = 1)$. We then check this guess numerically. In all the diagrams we studied, this approach led to the correct result.

3.2 Two-loop webs

Now that we demonstrated in detail how we can calculate a web using cuts, we move on to more interesting examples. The first two-loop case we study is the simplest one, the $(1, 2, 1)$ web. Afterwards, we look at diagrams involving three-gluon vertices, namely the Y diagram and the $(1, 1, 1)$ web.

3.2.1 The $(1, 2, 1)$ web

The $(1, 2, 1)$ web consists of two diagrams, both represented in figure 3.2. They occur with the following colour factor [27]:

$$
\begin{aligned}
\mathcal{W}_{(1,2,1)} &= \frac{1}{2}\big(\mathcal{C}_A - \mathcal{C}_B\big)\big(\mathcal{F}_A - \mathcal{F}_B\big) \\
&= -\frac{1}{2} i f^{abc} T^a_i T^b_j T^c_k \big(\mathcal{F}_A - \mathcal{F}_B\big) \ . \qquad (3.35)
\end{aligned}
$$

This web has been calculated earlier in [14, 27, 77, 78].

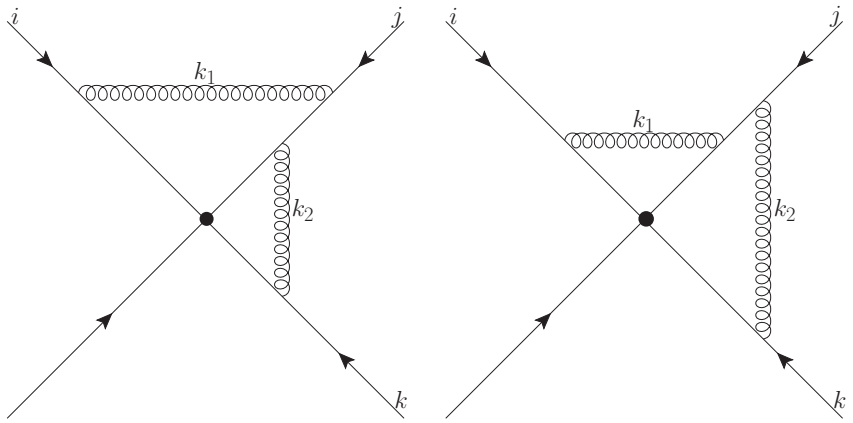

(a) A **(b)** B

Figure 3.2 *The diagrams contributing to the* $(1, 2, 1)$ *web.*

We use cuts as a way of calculating individual diagrams, rather than linear combinations of diagrams occurring in webs. We will hence have to determine both contributing diagrams individually to calculate the web. However, in what follows we will see that to calculate the discontinuity of the two diagrams, we have to calculate only one relevant cut.

The cuts of the $(1, 2, 1)$ web

The $(1, 2, 1)$ web is a function of two cusp angles, α_{ij} and α_{jk}, defined in the same way as in equation (3.4). We calculate the cuts in the α_{ij} channel of the diagrams that form the web. We work in the region where particles i and j are incoming and particle k is outgoing, so that this channel becomes the only one in which there is a discontinuity. In terms of the α variables, the cut occurs in the region

$$-1 < \alpha_{ij} < 0 < \alpha_{jk} < 1 \ . \tag{3.36}$$

Diagram A has two non-vanishing cuts, diagram B only one (see figure 3.3):

$$\begin{aligned} \mathrm{Disc}_{\alpha_{ij}} \mathcal{F}_A(\alpha_{ij}, \alpha_{jk}) &= -\mathrm{Cut}_{A_1}(\alpha_{ij}, \alpha_{jk}) - \mathrm{Cut}_{A_2}(\alpha_{ij}, \alpha_{jk}) \\ \mathrm{Disc}_{\alpha_{ij}} \mathcal{F}_B(\alpha_{ij}, \alpha_{jk}) &= -\mathrm{Cut}_B(\alpha_{ij}, \alpha_{jk}) \ . \end{aligned} \tag{3.37}$$

We can find some structure in these cuts by looking at the expressions in more detail.

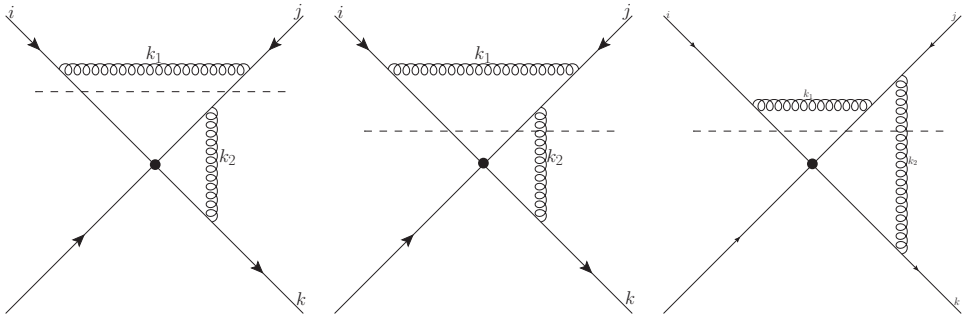

(a) Cut_{A_1} **(b)** Cut_{A_2} **(c)** Cut_B

Figure 3.3 *The cuts of the diagrams in the* $(1, 2, 1)$ *web.*

Calculation of Cut_{A_1}

Looking at the first cut, we have

$$\begin{aligned}
&\mathrm{Cut}_{A_1}(\alpha_{ij}, \alpha_{jk}) \\
&= -\frac{\mu^{4\epsilon}}{m^{4\epsilon}}(ig_s)^2(-ig_s)^2(2\pi i)^2 \int \frac{d^dk_1}{(2\pi)^d}\frac{d^dk_2}{(2\pi)^d} i\beta_i^\mu \delta\big(-\beta_i\cdot k_1 - 1\big)\frac{-ig_{\mu\nu}}{k_1^2+i\epsilon} \\
&\times i\beta_j^\nu \delta\big(\beta_j\cdot k_1 - 1\,\big)\frac{-i\beta_j^\rho}{\beta_j\cdot(k_1-k_2)-2-i\epsilon}\frac{ig_{\rho\sigma}}{k_2^2-i\epsilon}\frac{-i\beta_k^\sigma}{\beta_k\cdot k_2 - 1 - i\epsilon} \\
&= -\frac{\mu^{4\epsilon}}{m^{4\epsilon}} g_s^4(2\pi i)^2 \beta_i\cdot\beta_j \int \frac{d^dk_1}{(2\pi)^d}\delta\big(-\beta_i\cdot k_1 - 1\big)\frac{-i}{k_1^2+i\epsilon}\delta\big(\beta_j\cdot k_1 - 1\,\big) \\
&\times \beta_j\cdot\beta_k \int \frac{d^dk_2}{(2\pi)^d}\frac{1}{-\beta_j\cdot k_2 - 1 - i\epsilon}\frac{i}{k_2^2-i\epsilon}\frac{1}{\beta_k\cdot k_2 - 1 - i\epsilon}\,,
\end{aligned} \tag{3.38}$$

where we made use of the $\delta\big(\beta_j\cdot k_1 - 1\,\big)$ to simplify the first denominator on the second line. Notice that the propagators on the second line are complex conjugated because they are on the other side of the cut.

We notice that the two loop integrals decouple completely. Moreover, we recognise the first line of equation (3.38) as the cut of the one-loop web, whereas the second line corresponds to the complex conjugate of the original one-loop diagram. From equation (3.30) we see that the one-loop diagram is real valued, so that the complex conjugate equals the diagram itself. For a diagrammatical interpretation, see figure 3.4. Because we have all-order expressions for the two ingredients of Cut_{A_1}, namely (3.26) and (3.30), we could also give an all-order expression for Cut_{A_1}. However, since we will only be able to write the other cuts in the $(1, 2, 1)$ web as a Laurent series in ϵ, we do the same for this one. We can

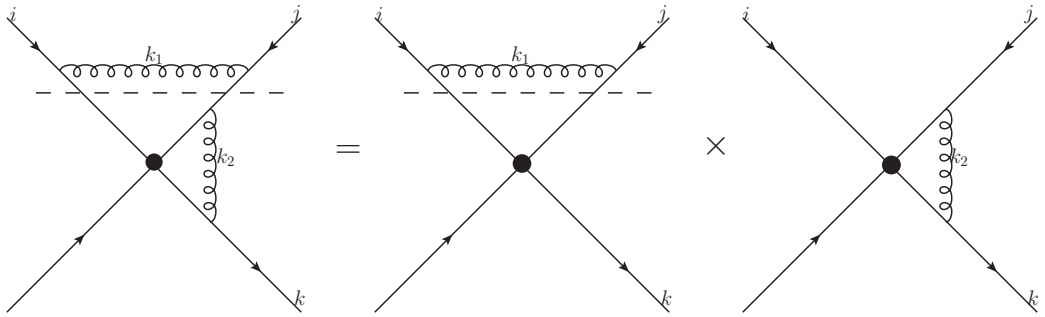

Figure 3.4 Cut_{A_1} *factorises into known one-loop expressions.*

write thus Cut_{A_1} as

$$\begin{aligned}\mathrm{Cut}_{A_1}(\alpha_{ij},\alpha_{jk}) =& \mathrm{Cut}\left(\mathcal{F}_{(1,1)}\right)(\alpha_{ij}) \times \mathcal{F}_{(1,1)}(\alpha_{jk}) \\ =& -8\pi i \frac{\kappa^2\Gamma(4\epsilon)}{\epsilon} r(\alpha_{ij}) r(\alpha_{jk}) \\ & \times \left[\ln\alpha_{jk} + \epsilon\left(\ln\left(\frac{(1+\alpha_{ij})^2}{-\alpha_{ij}}\right)\ln\alpha_{jk} + R_1(\alpha_{jk}\right)\right] + \mathcal{O}(1)\ ,\end{aligned} \tag{3.39}$$

where we made use of the Laurent series of (3.26) and of (3.32). We extracted the factor of $\kappa^2\Gamma(4\epsilon)$ before expanding in powers of ϵ, as we will for a generic two-loop diagram.

Other cuts

We have two cuts left to calculate, namely Cut_{A_2} and Cut_B. It is again instructive to give an explicit expression for them:

$$\begin{aligned}\mathrm{Cut}_{A_2}(\alpha_{ij},\alpha_{jk}) =& -\frac{\mu^{4\epsilon}}{m^{4\epsilon}}(ig_s)^3(-ig_s)(2\pi i)^3 \int \frac{d^dk_1}{(2\pi)^d}\frac{d^dk_2}{(2\pi)^d} i\beta_i^\mu \delta\big(-\beta_i\cdot k_1 - 1\big) \\ & \times \frac{i\beta_j^\nu}{\beta_j\cdot k_1 - 1 + i\epsilon}\ \frac{-ig_{\mu\nu}}{k_1^2 + i\epsilon}\ i\beta_j^\rho \delta\big(\beta_j\cdot(k_1-k_2) - 2\big) \\ & \times \big(-ig_{\rho\sigma}\big)\delta^+\big(k_2^2\big)\frac{-i\beta_k^\sigma}{\beta_k\cdot k_2 - 1 - i\epsilon}\end{aligned} \tag{3.40}$$

$$\begin{aligned}\mathrm{Cut}_{B}(\alpha_{ij},\alpha_{jk}) =& -\frac{\mu^{4\epsilon}}{m^{4\epsilon}}(ig_s)^3(-ig_s)(2\pi i)^3 \int \frac{d^dk_1}{(2\pi)^d}\frac{d^dk_2}{(2\pi)^d} i\beta_i^\mu \delta\big(-\beta_i\cdot k_1 - 1\big) \\ & \times \frac{i\beta_j^\nu}{-\beta_j\cdot k_2 - 1 + i\epsilon}\ \frac{-ig_{\mu\nu}}{k_1^2 + i\epsilon}\ i\beta_j^\rho \delta\big(\beta_j\cdot(k_1-k_2) - 2\big) \\ & \times \big(-ig_{\rho\sigma}\big)\delta^+\big(k_2^2\big)\frac{-i\beta_k^\sigma}{\beta_k\cdot k_2 - 1 - i\epsilon}\ .\end{aligned} \tag{3.41}$$

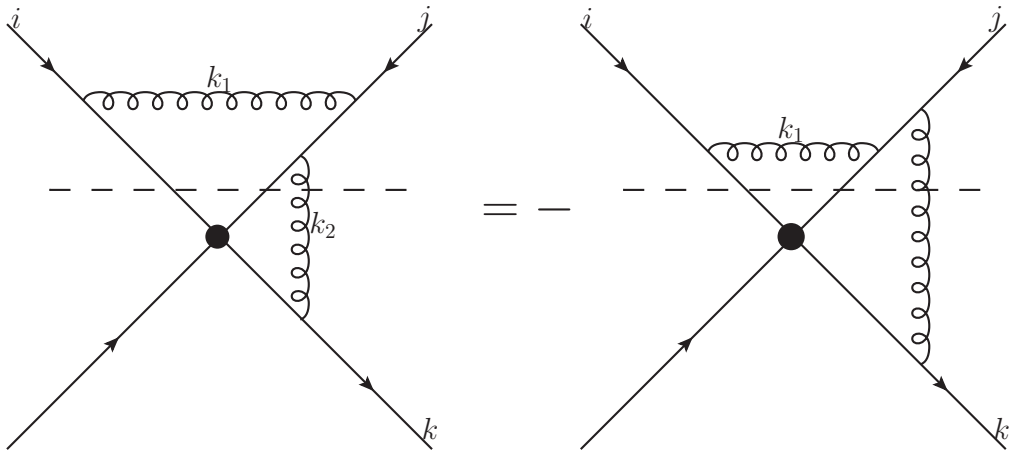

Figure 3.5 *Relation between* Cut_{A_2} *and* Cut_B.

We see that the only difference between the two expressions is the denominator of the β_j^ν part. However, these denominators can be related by making use of the $\delta\big(\beta_j \cdot (k_1 - k_2) - 2\big)$:

$$\frac{\beta_j^\nu}{\beta_j \cdot k_1 - 1 + i\epsilon}\delta\big(\beta_j \cdot (k_1 - k_2) - 2\big) = -\frac{\beta_j^\nu}{-\beta_j \cdot k_2 - 1 + i\epsilon}\delta\big(\beta_j \cdot (k_1 - k_2) - 2\big) \ , \tag{3.42}$$

so we can conclude that

$$\mathrm{Cut}_{A_2}(\alpha_{ij}, \alpha_{jk}) = -\mathrm{Cut}_B(\alpha_{ij}, \alpha_{jk}) \ . \tag{3.43}$$

This is represented diagrammatically in figure 3.5.

We see that, instead of having to calculate three separate cuts to calculate the diagrams in the $(1, 2, 1)$ web, we only have to calculate one genuinely new cut. We proved this by exploiting the delta functions in the expressions for the cuts as much as possible. We now move on to the calculation of the final remaining cut.

Calculation of Cut_B

In the calculations below, we will again see that the delta functions ensure that we do not have any poles in the region of integration. We can thus safely omit the $i\epsilon$ prescription from the denominators.

When contracting the Lorentz indices in (3.41), we obtain

$$
\begin{aligned}
&\mathrm{Cut}_B(\alpha_{ij},\alpha_{jk})\\
&=-(2\pi)^3 i\frac{\mu^{4\epsilon}}{m^{4\epsilon}}g_s^4\beta_i\cdot\beta_j\beta_j\cdot\beta_k\int\frac{d^dk_1}{(2\pi)^d}\frac{d^dk_2}{(2\pi)^d}\delta\big(-\beta_i\cdot k_1-1\big)\frac{1}{k_1^2}\\
&\times\frac{1}{-\beta_j\cdot k_2-1}\delta\big(\beta_j\cdot(k_1-k_2)-2\big)\delta^+\big(k_2^2\big)\frac{1}{\beta_k\cdot k_2-1}\\
&=-(2\pi)^3 i\frac{\mu^{4\epsilon}}{m^{4\epsilon}}g_s^4\beta_j\cdot\beta_k\int\frac{d^dk_2}{(2\pi)^d}\frac{1}{-\beta_j\cdot k_2-1}\delta^+\big(k_2^2\big)\frac{1}{\beta_k\cdot k_2-1}\mathrm{Cut}_{B_{k_1}}\ ,
\end{aligned}
\tag{3.44}
$$

where $\mathrm{Cut}_{B_{k_1}}$ is the k_1 subintegral:

$$
\begin{aligned}
&\mathrm{Cut}_{B_{k_1}}(\beta_i\cdot k_1,\beta_j\cdot k_1,\alpha_{ij},k_1^2)\\
&=\beta_i\cdot\beta_j\int\frac{d^dk_1}{(2\pi)^d}\delta\big(-\beta_i\cdot k_1-1\big)\frac{1}{k_1^2}\delta\big(\beta_j\cdot(k_1-k_2)-2\big)\ .
\end{aligned}
\tag{3.45}
$$

We choose to perform this one first, because it is very similar to the one-loop integral and can be calculated to all orders in ϵ. We then plug this result back into (3.44).
We work in the following frame:

$$
\begin{aligned}
\beta_j&=(1,\mathbf{0}_3)\\
\beta_i&=(\cosh\theta,\sinh\theta,\mathbf{0}_2)\\
k_1&=(k_{10},k_{11},k_{12}\mathbf{v}_{d-2})\ ,\mathbf{v}^2=1\\
d^dk_1&=\frac{2\pi^{1-\epsilon}}{\Gamma(1-\epsilon)}dk_{10}dk_{11}dk_{12}k_{12}^{1-2\epsilon}\ .
\end{aligned}
\tag{3.46}
$$

The delta functions can be solved immediately, giving

$$
\begin{aligned}
k_{10}&=\beta_j\cdot k_2+2\\
k_{11}&=\frac{\cosh\theta(\beta_j\cdot k_2+2)+1}{\sinh\theta}\ .
\end{aligned}
\tag{3.47}
$$

We also notice that $\beta_j\cdot k_2=k_{20}$. Since the k_2 integrand includes a factor of $\delta^+(k_2^2)$, we know that $k_{20}>0$, and hence $\beta_j\cdot k_2>0$. This leads to the following inequality

$$
k_{11}>k_{10}=\beta_j\cdot k_2+2>0\ .
\tag{3.48}
$$

such that $k_1^2<0$ and we do not have a pole in the denominator, as claimed.

Plugging (3.47) into (3.45), we obtain

$$\begin{aligned}
&\mathrm{Cut}_{B_{k_1}}(\beta_i\cdot k_1,\beta_j\cdot k_1,\alpha_{ij},k_1^2)\\
&=r(\alpha_{ij})\frac{2\pi^{1-\epsilon}}{(2\pi)^d\Gamma(1-\epsilon)}\int_0^\infty dk_{12}{k_{12}}^{1-2\epsilon}\frac{1}{(\beta_j\cdot k_2+2)^2-\big(\frac{\cosh\theta(\beta_j\cdot k_2+2)+1}{\sinh\theta}\big)^2-{k_{12}}^2}\\
&=-r(\alpha_{ij})\frac{\Gamma(\epsilon)\pi^{1-\epsilon}}{(2\pi)^d}\bigg(\big(\frac{\cosh\theta(\beta_j\cdot k_2+2)+1}{\sinh\theta}\big)^2-(\beta_j\cdot k_2+2)^2\bigg)^{-\epsilon}\,. \qquad (3.49)
\end{aligned}$$

This result is written in a Lorentz invariant way, and hence is valid in general. We now insert this into (3.44). We again perform the calculation in a specific frame, namely

$$\begin{aligned}
\beta_j&=(1,\mathbf{0}_3)\\
\beta_k&=(-\cosh\phi,\sinh\phi\mathbf{v}_{d-1})\ ,\mathbf{v}^2=1\\
k_2&=(k_{20},k_{21}{\mathbf{v}'}_{d-1})\ ,{\mathbf{v}'}^2=1\\
\mathbf{v}\cdot\mathbf{v}'&=\cos\tau\\
d^dk_2&=\frac{2\pi^{1-\epsilon}}{\Gamma(1-\epsilon)}dk_{20}dk_{21}{k_{21}}^{2-2\epsilon}d\cos\tau(\sin\tau)^{-2\epsilon}\ , \qquad (3.50)
\end{aligned}$$

so that

$$\begin{aligned}
&\mathrm{Cut}_B(\alpha_{ij},\alpha_{jk})\\
&=r(\alpha_{ij})\frac{\Gamma(\epsilon)\pi^{1-\epsilon}}{(2\pi)^{1-2\epsilon}}i\frac{\mu^{4\epsilon}}{m^{4\epsilon}}g_s^4\beta_j\cdot\beta_k\int\frac{d^dk_2}{(2\pi)^d}\frac{1}{-\beta_j\cdot k_2-1}\delta^+\big(k_2^2\big)\frac{1}{\beta_k\cdot k_2-1}\\
&\times\bigg(\big(\frac{\cosh\theta(\beta_j\cdot k_2+2)+1}{\sinh\theta}\big)^2-(\beta_j\cdot k_2+2)^2\bigg)^{-\epsilon}\\
&=r(\alpha_{ij})\frac{\Gamma(\epsilon)\pi^{1-2\epsilon}}{(2\pi)^{4-4\epsilon}\Gamma(1-\epsilon)}i\frac{\mu^{4\epsilon}}{m^{4\epsilon}}g_s^4\beta_j\cdot\beta_k\int_{-\infty}^\infty dk_{20}\int_0^\infty dk_{21}{k_{21}}^{2-2\epsilon}\\
&\times\int_{-1}^1 d\cos\tau(\sin\tau)^{-2\epsilon}\frac{1}{-k_{20}-1}\frac{\delta^+\big(k_{20}^2-{k_{21}}^2\big)}{-\cosh\phi k_{20}-\sinh\phi\cos\tau k_{21}-1}\\
&\times\bigg(\big(\frac{\cosh\theta(k_{20}+2)+1}{\sinh\theta}\big)^2-(k_{20}+2)^2\bigg)^{-\epsilon}\\
&=r(\alpha_{ij})\frac{\Gamma(\epsilon)\pi^{1-2\epsilon}}{2(2\pi)^{4-4\epsilon}\Gamma(1-\epsilon)}i\frac{\mu^{4\epsilon}}{m^{4\epsilon}}g_s^4\beta_j\cdot\beta_k\int_0^\infty dk_{21}{k_{21}}^{1-2\epsilon}\\
&\times\int_{-1}^1 d\cos\tau(\sin\tau)^{-2\epsilon}\frac{1}{-k_{21}-1}\frac{1}{-\cosh\phi k_{21}-\sinh\phi\cos\tau k_{21}-1}\\
&\times\bigg(\big(\frac{\cosh\theta(k_{21}+2)+1}{\sinh\theta}\big)^2-(k_{21}+2)^2\bigg)^{-\epsilon}\,. \qquad (3.51)
\end{aligned}$$

It is again clear that this integrand does not have poles, as claimed before.

We now have to choose whether to perform the τ or k_{21} integral next. The τ integral can be performed exactly, but has to be expressed in terms of hypergeometric functions, which are hard to integrate. We do not calculate the k_{21} integral exactly; since we are only interested in the Laurent series of the answer, we can calculate it via an asymptotic expansion.

We notice that the integrand in (3.51) has a divergence for $k_{21} \to \infty$. We hence are interested in the leading behaviour in this region. We see that

$$\begin{aligned}
&\left(\left(\frac{\cosh\theta(k_{21}+2)+1}{\sinh\theta}\right)^2 - (k_{21}+2)^2 \right)^{-\epsilon} \\
&= k_{21}^{-2\epsilon}\big(r(\alpha_{ij})^2-1\big)^{-\epsilon} \\
&\times \left(1 + \frac{(4k_{21}+4)\sinh^2\theta(r(\alpha_{ij})^2-1) + 2r(\alpha_{ij})(k_{21}+2)\sinh\theta + 1}{k_{21}^2(r(\alpha_{ij})^2-1)\sinh^2\theta}\right)^{-\epsilon} \\
&= k_{21}^{-2\epsilon}\big(r(\alpha_{ij})^2-1\big)^{-\epsilon}\left(1+\frac{ak_{21}+b}{k_{21}^2}\right)^{-\epsilon} \to k_{21}^{-2\epsilon}\big(r(\alpha_{ij})^2-1\big)^{-\epsilon}\,, \qquad (3.52)
\end{aligned}$$

where a and b are defined implicitly. This asymptotic expansion was allowed because we are only interested in the two leading divergences in ϵ. Indeed, the leading correction to (3.52) is proportional to

$$\int_0^\infty \frac{dk_{21}k_{21}^{-4\epsilon}}{1+k_{21}} \ln\left(1+\frac{ak_{21}+b}{k_{21}^2}\right) = \mathcal{O}(1)\,, \qquad (3.53)$$

so that we can ignore it. Therefore, we are left with

$$\begin{aligned}
&\mathrm{Cut}_B(\alpha_{ij},\alpha_{jk}) \\
&= r(\alpha_{ij})\frac{\Gamma(\epsilon)\pi^{1-2\epsilon}}{2(2\pi)^{4-4\epsilon}\Gamma(1-\epsilon)} i\frac{\mu^{4\epsilon}}{m^{4\epsilon}} g_s^4 \beta_j\cdot\beta_k \int_0^\infty dk_{21}k_{21}^{1-2\epsilon} \\
&\times \int_{-1}^1 d\cos\tau(\sin\tau)^{-2\epsilon}\frac{1}{-k_{21}-1}\frac{1}{-\cosh\phi k_{21}-\sinh\phi\cos\tau k_{21}-1} \\
&\times k_{21}^{-2\epsilon}\big(r(\alpha_{ij})^2-1\big)^{-\epsilon} + \mathcal{O}(1)\,. \qquad (3.54)
\end{aligned}$$

We can now partial fraction this, and calculate the k_{21} integral

$$\begin{aligned}
\mathrm{Cut}_B(\alpha_{ij},\alpha_{jk}) =& r(\alpha_{ij})\frac{\Gamma(\epsilon)\pi^{1-2\epsilon}}{2(2\pi)^{4-4\epsilon}\Gamma(1-\epsilon)} i\frac{\mu^{4\epsilon}}{m^{4\epsilon}} g_s^4\beta_j\cdot\beta_k\big(r(\alpha_{ij})^2-1\big)^{-\epsilon} \\
&\int_0^\infty dk_{21}k_{21}^{-4\epsilon} d\cos\tau(\sin\tau)^{-2\epsilon}\frac{1}{\cosh\phi+\sinh\phi\cos\tau-1} \\
&\times\left(\frac{1}{k_{21}+1} - \frac{1}{\cosh\phi k_{21}+\sinh\phi\cos\tau k_{21}+1}\right) + \mathcal{O}(1)
\end{aligned}$$

$$
\begin{aligned}
=&r(\alpha_{ij})\frac{\Gamma(\epsilon)\Gamma(4\epsilon)\Gamma(1-4\epsilon)\pi^{1-2\epsilon}}{2(2\pi)^{4-4\epsilon}\Gamma(1-\epsilon)}i\frac{\mu^{4\epsilon}}{m^{4\epsilon}}g_s^4\beta_j\cdot\beta_k\big(r(\alpha_{ij})^2-1\big)^{-\epsilon}\\
&\int_0^\infty d\cos\tau(\sin\tau)^{-2\epsilon}\frac{1}{\cosh\phi+\sinh\phi\cos\tau-1}\\
&\times\left(1-\big(\cosh\phi+\sinh\phi\cos\tau\big)^{-1+4\epsilon}\right)+\mathcal{O}(1)\ . \qquad (3.55)
\end{aligned}
$$

The remaining τ integral is finite, so we can now expand this in powers of ϵ. Up to finite corrections, this gives

$$
\begin{aligned}
&\mathrm{Cut}_B(\alpha_{ij},\alpha_{jk})\\
&=\ r(\alpha_{ij})\frac{\Gamma(\epsilon)\Gamma(4\epsilon)\Gamma(1-4\epsilon)\pi^{1-2\epsilon}}{2(2\pi)^{4-4\epsilon}\Gamma(1-\epsilon)}i\frac{\mu^{4\epsilon}}{m^{4\epsilon}}g_s^4\beta_j\cdot\beta_k\big(r(\alpha_{ij})^2-1\big)^{-\epsilon}\\
&\int_0^\infty d\cos\tau\left(\frac{1}{\cosh\phi+\sinh\phi\cos\tau}-\frac{\epsilon\ln(1-\cos^2\tau)}{\cosh\phi+\sinh\phi\cos\tau}\right.\\
&\left.-\frac{4\epsilon\ln(\cosh\phi+\sinh\phi\cos\tau)}{(\cosh\phi+\sinh\phi\cos\tau)(\cosh\phi+\sinh\phi\cos\tau-1)}\right)\\
&=2\pi i\kappa^2 r(\alpha_{ij})r(\alpha_{jk})\frac{\Gamma(\epsilon)\Gamma(4\epsilon)\Gamma(1-4\epsilon)}{\Gamma(1-\epsilon)^3}2^{2\epsilon}\big(\frac{-\alpha_{ij}}{1-\alpha_{ij}^2}\big)^{-2\epsilon}\\
&\left(-2\ln\alpha_{jk}+\epsilon\big(4\ln 2\ln\alpha_{jk}-4G(-1,0,\alpha_{jk})+4G(1,0,\alpha_{jk})-\pi^2\big)\right)\\
&=-4\pi i\frac{\kappa^2\Gamma(4\epsilon)}{\epsilon}r(\alpha_{ij})r(\alpha_{jk})\left(\ln\alpha_{jk}+\epsilon\big(2G(-1,0,\alpha_{jk})-2G(1,0,\alpha_{jk})\right.\\
&\left.+\pi^2/2-2\ln\alpha_{jk}\ln\big(\frac{-\alpha_{ij}}{1-\alpha_{ij}^2}\big)\big)\right)\ . \qquad (3.56)
\end{aligned}
$$

In what follows, we will often reuse the same tools. We will calculate exact integrals until closed form integrals are not obvious any more. We then extract the overall divergence via an asymptotic expansion, and expand the remaining finite angular integrals in powers of ϵ. Now that we showed the explicit calculations once, we will delegate the details to the appendix in what follows.

By finishing the calculation of Cut_B, we now have all the ingredients of the cuts of the $(1,2,1)$ web.

Spectral integrals

We now perform the spectral integrals to calculate the diagrams in the $(1,2,1)$ web. Since we only have calculated the discontinuities as Laurent series, we will now integrate these Laurent series. We have to integrate the respective

discontinuities

$$\begin{aligned}
\mathrm{Disc}_{\alpha_{ij}}\mathcal{F}_A(\alpha_{ij},\alpha_{jk}) &= -\mathrm{Cut}_{A_1}(\alpha_{ij},\alpha_{jk}) - \mathrm{Cut}_{A_2}(\alpha_{ij},\alpha_{jk}) \\
&= -\mathrm{Cut}\left(\mathcal{F}_{(1,1)}\right)(\alpha_{ij}) \times \mathcal{F}_{(1,1)}(\alpha_{jk}) + \mathrm{Cut}_B(\alpha_{ij},\alpha_{jk}) \\
\mathrm{Disc}_{\alpha_{ij}}\mathcal{F}_B(\alpha_{ij},\alpha_{jk}) &= -\mathrm{Cut}_B(\alpha_{ij},\alpha_{jk}) \ .
\end{aligned} \tag{3.57}$$

It is easiest to start with the calculation of $\mathcal{F}_B$, using the notation introduced in equation (3.18):

$$\begin{aligned}
&\mathcal{F}_B(\alpha_{ij},\alpha_{jk}) - \mathcal{F}_B(\alpha_{ij}=1,\alpha_{jk}) \\
&= -\int_{\mathrm{Disp},\alpha_{ij}} \mathrm{Cut}_B \\
&= 2\frac{\kappa^2\Gamma(4\epsilon)}{\epsilon} r(\alpha_{jk})\Bigg[\big(r(\alpha_{ij})\ln\alpha_{ij}+1\big)\ln\alpha_{jk} + \epsilon\Bigg(\big(r(\alpha_{ij})\ln\alpha_{ij}+1\big) \\
&\times \big(2G(-1,0,\alpha_{jk}) - 2G(1,0,\alpha_{jk}) + \pi^2/2\big) + \ln\alpha_{jk}\Bigg(-2 \\
&+ 2r(\alpha_{ij})\big(G(-1,0,\alpha_{ij}) - G(0,0,\alpha_{ij}) + G(1,0,\alpha_{ij}) - \frac{\pi^2}{12}\big)\Bigg)\Bigg)\Bigg] + \mathcal{O}(1) \ .
\end{aligned} \tag{3.58}$$

This seems to suggest that, up to $\mathcal{O}(1)$ corrections,

$$\begin{aligned}
\mathcal{F}_B(\alpha_{ij},\alpha_{jk}) =& 2\frac{\kappa^2\Gamma(4\epsilon)}{\epsilon} r(\alpha_{ij})r(\alpha_{jk})\Bigg[\ln\alpha_{ij}\ln\alpha_{jk} \\
&+ \epsilon\Bigg(\ln\alpha_{ij}\big(2G(-1,0,\alpha_{jk}) - 2G(1,0,\alpha_{jk}) + \pi^2/2\big) \\
&+ \ln\alpha_{jk}\big(2G(-1,0,\alpha_{ij}) - 2G(0,0,\alpha_{ij}) + 2G(1,0,\alpha_{ij}) - \frac{\pi^2}{6}\big)\Bigg)\Bigg] \\
\mathcal{F}_B(\alpha_{ij}=1,\alpha_{jk}) =& -2\frac{\kappa^2\Gamma(4\epsilon)}{\epsilon} r(\alpha_{jk})\Bigg[\ln\alpha_{jk} \\
&+ \epsilon\Bigg(\big(2G(-1,0,\alpha_{jk}) - 2G(1,0,\alpha_{jk}) + \pi^2/2\big) - 2\ln\alpha_{jk}\Bigg)\Bigg] \ .
\end{aligned} \tag{3.59}$$

This indeed agrees with numerical calculations using SecDec. Looking at $\mathcal{F}_A$, we have

$$\begin{aligned}
&\mathcal{F}_A(\alpha_{ij},\alpha_{jk}) - \mathcal{F}_A(\alpha_{ij}=1,\alpha_{jk}) \\
&= -\int_{\mathrm{Disp},\alpha_{ij}} \Big(\mathrm{Cut}_{A_1} + \mathrm{Cut}_{A_2}\Big)
\end{aligned}$$

$$
\begin{aligned}
&= -\int_{\text{Disp},\alpha_{ij}} \text{Cut}_{A_1} - \int_{\text{Disp},\alpha_{ij}} \text{Cut}_{A_2} \\
&= -\mathcal{F}_{(1,1)}(\alpha_{jk}) \int_{\text{Disp},\alpha_{ij}} \text{Cut}\left(\mathcal{F}_{(1,1)}\right)(\alpha_{ij}) + \int_{\text{Disp},\alpha_{ij}} \text{Cut}_B \\
&= \mathcal{F}_{(1,1)}(\alpha_{jk})\big(\mathcal{F}_{(1,1)}(\alpha_{ij}) - \mathcal{F}_{(1,1)}(\alpha_{ij}=1)\big) + \int_{\text{Disp},\alpha_{ij}} \text{Cut}_B \ . \qquad (3.60)
\end{aligned}
$$

We see that to calculate the dispersive integral of Cut_{A_1}, we can recycle the one-loop result. For the dispersive integral of Cut_{A_2}, we recycle the calculation of $\mathcal{F}_B$. We obtain, up to finite corrections,

$$
\begin{aligned}
\mathcal{F}_A(\alpha_{ij},\alpha_{jk}) &= \mathcal{F}_{(1,1)}(\alpha_{jk})\mathcal{F}_{(1,1)}(\alpha_{ij}) - \mathcal{F}_B(\alpha_{ij}) \\
&= 2\kappa^2 r(\alpha_{ij})r(\alpha_{jk})\Gamma(2\epsilon)^2\Bigg[\ln\alpha_{ij}\ln\alpha_{jk} \\
&+ \epsilon\Bigg(\ln\alpha_{jk}\big(2G(-1,0,\alpha_{ij}) - 2G(1,0,\alpha_{ij}) + \pi^2/2\big) \\
&\quad + \ln\alpha_{ij}\big(2G(-1,0,\alpha_{jk}) - 2G(0,0,\alpha_{jk}) + 2G(1,0,\alpha_{jk}) - \frac{\pi^2}{6}\big)\Bigg)\Bigg] \ . \qquad (3.61)
\end{aligned}
$$

We see that $\mathcal{F}_A$ and $\mathcal{F}_B$ are related via a swap of variables $\alpha_{ij} \leftrightarrow \alpha_{jk}$. This symmetry is clear when looking at the geometry of the two diagrams, and provides a check on the result.

Combining the two expressions, we can calculate the linear combination which is relevant for the calculation of the $(1,2,1)$ web:

$$
\begin{aligned}
&\mathcal{F}_A(\alpha_{ij},\alpha_{jk}) - \mathcal{F}_B(\alpha_{ij},\alpha_{jk}) \\
&= 2\kappa^2\Gamma(4\epsilon)r(\alpha_{ij})r(\alpha_{jk})\Bigg(-\ln\alpha_{jk}\big(-2G(0,0,\alpha_{ij}) + 4G(1,0,\alpha_{ij}) - \frac{2\pi^2}{3}\big) \\
&\qquad + \ln\alpha_{ij}\big(-2G(0,0,\alpha_{jk}) + 4G(1,0,\alpha_{jk}) - \frac{2\pi^2}{3}\big)\Bigg) + \mathcal{O}(1) \ . \qquad (3.62)
\end{aligned}
$$

If we now define

$$
S_1(\alpha) = -2G(0,0,\alpha) + 4G(1,0,\alpha) - \frac{2\pi^2}{3} \ , \qquad (3.63)
$$

we see that (3.35) reduces to

$$
\mathcal{W}^{-1}_{(1,2,1)} = -if^{abc}T^a_i T^b_j T^c_k \frac{\alpha_s^2}{(4\pi)^{2\epsilon}}\frac{1}{2} r(\alpha_{ij})r(\alpha_{jk})\big(\ln\alpha_{ij}S_1(\alpha_{jk}) - \ln\alpha_{jk}S_1(\alpha_{ij})\big) \ . \qquad (3.64)
$$

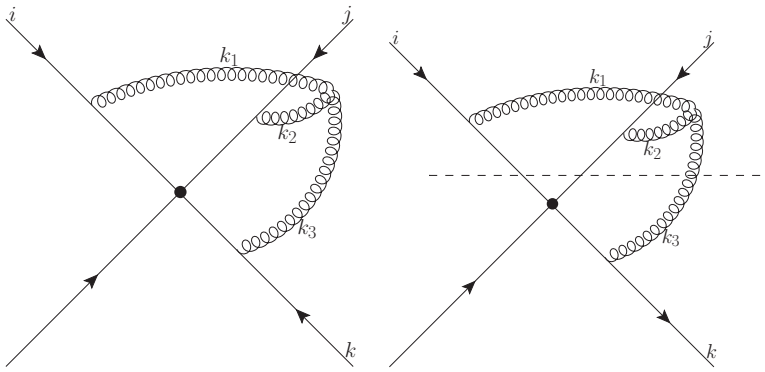

(a) $\mathcal{F}_{3g}$ **(b)** $\mathrm{Cut}_{\alpha_{ij}}(\mathcal{F}_{3g})$

Figure 3.6 *The* $(1,1,1)$ *web and its cut.*

We can also rewrite this in terms of the basis functions $M_{k,l,n}(\alpha)$. We then have

$$\begin{aligned}\mathcal{W}^{-1}_{(1,2,1)} = &-if^{abc}T^a_i T^b_j T^c_k \frac{\alpha_s^2}{(4\pi)^2\epsilon} r(\alpha_{ij})r(\alpha_{jk}) \\ &\times \left(M_{0,0,0}(\alpha_{ij})M_{1,0,0}(\alpha_{jk}) - M_{0,0,0}(\alpha_{jk})M_{1,0,0}(\alpha_{ij})\right) . \end{aligned} \tag{3.65}$$

We notice that the $\mathcal{O}(\frac{1}{\epsilon^2})$ contributions of $\mathcal{F}_A$ and $\mathcal{F}_B$ cancel. As noted in [35], leading singularities, namely $\mathcal{O}(\epsilon^{-n})$ poles at $\mathcal{O}(\alpha_s^n)$, can only come from the running coupling. Hence, the maximal subdivergences must cancel between the different diagrams of the $(1,2,1)$ web, as we observe.

This remaining $\mathcal{O}(\epsilon^{-1})$ result agrees with the one obtained in reference [27], and when written in terms of the basis functions $M_{k,l,n}(\alpha)$ it agrees with reference [30].

3.2.2 The $(1,1,1)$ web

We now move on to the calculations of diagrams involving a three-gluon vertex. These diagrams are known to be quite complex. For example, to obtain the results in reference [77], some very involved Mellin-Barnes techniques were used. The three-gluon vertex will show up as a numerator in the integrand. Below, we will see that this numerator, which is a manifestation of the gauge theory structure, allows us to simplify the calculation. The first diagram with a three-gluon vertex we look at is the $(1,1,1)$ web. The web consists of just one diagram, see figure 3.6. We extract the same colour factor as in the case of the $(1,2,1)$ web, so that

$$\mathcal{W}_{3g} = -if^{abc}T^a_i T^b_j T^c_k \mathcal{F}_{3g} . \tag{3.66}$$

We will calculate the kinematic part $\mathcal{F}_{3g}$. It is completely antisymmetric in i, j, k. To make this explicit, we write the integrand as

$$\begin{aligned}
&\mathcal{F}_{3g}(\alpha_{ij}, \alpha_{ik}, \alpha_{jk}) \\
&= i\frac{\mu^{4\epsilon}}{m^{4\epsilon}}(ig_s)^3 \int \frac{d^dk_1}{(2\pi)^d}\frac{d^dk_2}{(2\pi)^d}\frac{d^dk_3}{(2\pi)^d}(2\pi)^d\delta^{(d)}(k_1+k_2+k_3) \\
&\qquad \times \frac{i\beta_i^\mu}{-\beta_i\cdot k_1 - 1 + i\epsilon}\,\frac{i\beta_j^\nu}{-\beta_j\cdot k_2 - 1 + i\epsilon}\,\frac{i\beta_k^\rho}{-\beta_k\cdot k_3 - 1 + i\epsilon} \\
&\qquad \times \frac{-ig_{\mu\tau}}{k_1^2+i\epsilon}\,\frac{-ig_{\nu\sigma}}{k_2^2+i\epsilon}\,\frac{-ig_{\rho\phi}}{k_3^2+i\epsilon} \\
&\qquad \times g_s\Big(g^{\tau\sigma}(k_1-k_2)^\phi + g^{\sigma\phi}(k_2-k_3)^\tau + g^{\phi\tau}(k_3-k_1)^\sigma\Big) \\
&= \frac{\mu^{4\epsilon}}{m^{4\epsilon}}g_s^4 \int \frac{d^dk_1}{(2\pi)^d}\frac{d^dk_2}{(2\pi)^d}\frac{d^dk_3}{(2\pi)^d}\frac{(2\pi)^d\delta^{(d)}(k_1+k_2+k_3)}{(k_1^2+i\epsilon)(k_2^2+i\epsilon)(k_3^2+i\epsilon)} \\
&\times \frac{\beta_i\cdot\beta_j\beta_k\cdot(k_1-k_2)+\beta_j\cdot\beta_k\beta_i\cdot(k_2-k_3)+\beta_k\cdot\beta_i\beta_j\cdot(k_3-k_1)}{(-\beta_i\cdot k_1-1+i\epsilon)(-\beta_j\cdot k_2-1+i\epsilon)(-\beta_k\cdot k_3-1+i\epsilon)} \\
&= \mathcal{F}_{3g,1}(\alpha_{ij},\alpha_{ik},\alpha_{jk}) + \mathcal{F}_{3g,2}(\alpha_{ij},\alpha_{ik},\alpha_{jk}) + \mathcal{F}_{3g,3}(\alpha_{ij},\alpha_{ik},\alpha_{jk})\ , \qquad (3.67)
\end{aligned}$$

where $\mathcal{F}_{3g,1}(\alpha_{ij}, \alpha_{ik}, \alpha_{jk})$ corresponds to the first part of the numerator, and likewise for the two other parts. The antisymmetry then manifests itself via

$$\begin{aligned}
\mathcal{F}_{3g,1}(\alpha_{ij},\alpha_{ik},\alpha_{jk}) &\xrightarrow{i\leftrightarrow j} -\mathcal{F}_{3g,1}(\alpha_{ij},\alpha_{ik},\alpha_{jk}) \\
\mathcal{F}_{3g,2}(\alpha_{ij},\alpha_{ik},\alpha_{jk}) &\xrightarrow{i\leftrightarrow j} -\mathcal{F}_{3g,3}(\alpha_{ij},\alpha_{ik},\alpha_{jk}) \\
\mathcal{F}_{3g,3}(\alpha_{ij},\alpha_{ik},\alpha_{jk}) &\xrightarrow{i\leftrightarrow j} -\mathcal{F}_{3g,2}(\alpha_{ij},\alpha_{ik},\alpha_{jk})\ , \qquad (3.68)
\end{aligned}$$

and similar relations for $i \leftrightarrow k$ and $j \leftrightarrow k$. Via these relations, it is possible to deduce the complete result from only one of the three expressions.

Cut in the α_{ij} channel

As we proved in the previous chapter, there is only one cut in the α_{ij} channel. It is represented in figure 3.6. It can be written as

$$
\begin{aligned}
&\mathrm{Disc}_{\alpha_{ij}}\big(\mathcal{F}_{3g}(\alpha_{ij},\alpha_{ik},\alpha_{jk})\big)\\
&= -\mathrm{Cut}_{3g}(\alpha_{ij},\alpha_{ik},\alpha_{jk})\\
&= i\frac{\mu^{4\epsilon}}{m^{4\epsilon}}(ig_s)^2(-ig_s)\int\frac{d^dk_1}{(2\pi)^d}\frac{d^dk_2}{(2\pi)^d}\frac{d^dk_3}{(2\pi)^d}(2\pi)^d\delta^{(d)}(k_1+k_2+k_3)\\
&\times(2\pi i)^3 i\beta_i^\mu\delta(-\beta_i\cdot k_1-1)i\beta_j^\nu\delta(-\beta_j\cdot k_2-1)(-ig_{\rho\phi})\delta^-(k_3^2)\\
&\times\frac{-i\beta_k^\rho}{-\beta_k\cdot k_3-1-i\epsilon}\,\frac{-ig_{\mu\tau}}{k_1^2+i\epsilon}\,\frac{-ig_{\nu\sigma}}{k_2^2+i\epsilon}\\
&\times g_s\Big(g^{\tau\sigma}(k_1-k_2)^\phi+g^{\sigma\phi}(k_2-k_3)^\tau+g^{\phi\tau}(k_3-k_1)^\sigma\Big)\\
&= -i\frac{\mu^{4\epsilon}}{m^{4\epsilon}}g_s^4(2\pi)^3\int\frac{d^dk_1}{(2\pi)^d}\frac{d^dk_2}{(2\pi)^d}\frac{d^dk_3}{(2\pi)^d}(2\pi)^d\delta^{(d)}(k_1+k_2+k_3)\\
&\times\delta^-(k_3)^2\delta(-\beta_i\cdot k_1-1)\delta(-\beta_j\cdot k_2-1)\\
&\times\frac{\beta_i\cdot\beta_j\beta_k\cdot(k_1-k_2)+\beta_j\cdot\beta_k\beta_i\cdot(k_2-k_3)+\beta_k\cdot\beta_i\beta_j\cdot(k_3-k_1)}{(-\beta_k\cdot k_3-1)k_1^2k_2^2}\\
&= -\mathrm{Cut}_{3g,1}(\alpha_{ij},\alpha_{ik},\alpha_{jk})-\mathrm{Cut}_{3g,2}(\alpha_{ij},\alpha_{ik},\alpha_{jk})-\mathrm{Cut}_{3g,3}(\alpha_{ij},\alpha_{ik},\alpha_{jk})\ , \qquad (3.69)
\end{aligned}
$$

where we again drop the $i\epsilon$ because there are no poles in the region of integration. We split up the expression into three parts, corresponding to the three terms in the numerator. We notice that by singling out one particular channel to cut on, we have broken the total antisymmetry. We still have relations between cuts corresponding to equation (3.68) for $i\leftrightarrow j$:

$$
\begin{aligned}
\mathrm{Cut}_{3g,1}(\alpha_{ij},\alpha_{ik},\alpha_{jk}) &\xrightarrow{i\leftrightarrow j} -\mathrm{Cut}_{3g,1}(\alpha_{ij},\alpha_{ik},\alpha_{jk})\\
\mathrm{Cut}_{3g,2}(\alpha_{ij},\alpha_{ik},\alpha_{jk}) &\xrightarrow{i\leftrightarrow j} -\mathrm{Cut}_{3g,3}(\alpha_{ij},\alpha_{ik},\alpha_{jk})\\
\mathrm{Cut}_{3g,3}(\alpha_{ij},\alpha_{ik},\alpha_{jk}) &\xrightarrow{i\leftrightarrow j} -\mathrm{Cut}_{3g,2}(\alpha_{ij},\alpha_{ik},\alpha_{jk})\ . \qquad (3.70)
\end{aligned}
$$

However, there are no similar relations for $i\leftrightarrow k$ and $j\leftrightarrow k$. This means that we have two genuinely different expressions to calculate, namely $\mathrm{Cut}_{3g,1}$ and $\mathrm{Cut}_{3g,2}$. However, we can avoid one of these calculations by reconsidering how we derived the largest time equation. We only looked at the analytical structure of the denominator of the diagrams and did not need the exact expression of the numerator. When we derived which cuts are equal to zero, we again did not specify the numerator. This means that the equality

$$
\mathrm{Disc}_{\alpha_{ij}}\big(\mathcal{F}_{3g}(\alpha_{ij},\alpha_{ik},\alpha_{jk})\big) = -\mathrm{Cut}_{3g}(\alpha_{ij},\alpha_{ik},\alpha_{jk}) \qquad (3.71)
$$

is also valid with a different numerator. In particular, it is valid for each of the three separate terms in the numerator. This reasoning leads us to the conclusion that

$$\begin{aligned}
\mathrm{Disc}_{\alpha_{ij}}\big(\mathcal{F}_{3g,1}(\alpha_{ij},\alpha_{ik},\alpha_{jk})\big) &= -\mathrm{Cut}_{3g,1}(\alpha_{ij},\alpha_{ik},\alpha_{jk}) \\
\mathrm{Disc}_{\alpha_{ij}}\big(\mathcal{F}_{3g,2}(\alpha_{ij},\alpha_{ik},\alpha_{jk})\big) &= -\mathrm{Cut}_{3g,2}(\alpha_{ij},\alpha_{ik},\alpha_{jk}) \\
\mathrm{Disc}_{\alpha_{ij}}\big(\mathcal{F}_{3g,3}(\alpha_{ij},\alpha_{ik},\alpha_{jk})\big) &= -\mathrm{Cut}_{3g,3}(\alpha_{ij},\alpha_{ik},\alpha_{jk})\ . \qquad (3.72)
\end{aligned}$$

These equations provide us with a different way of calculating $\mathrm{Cut}_{3g,2}$: we can first calculate $\mathrm{Cut}_{3g,1}$, perform its dispersive integral to obtain $\mathcal{F}_{3g,1}(\alpha_{ij},\alpha_{ik},\alpha_{jk})$, change $j \leftrightarrow k$ to obtain $-\mathcal{F}_{3g,2}(\alpha_{ij},\alpha_{ik},\alpha_{jk})$, and then calculate the discontinuity to obtain $-\mathrm{Cut}_{3g,2}$. All of the operations involved are very simple. Another way of phrasing this is that the dispersive integral restores the antisymmetry between different parts of the diagram, and so removes the need to calculate both $\mathrm{Cut}_{3g,1}$ and $\mathrm{Cut}_{3g,2}$, instead letting us choose to compute the easiest of the two.

This again illustrates the simplicity that cuts bring: not only do we have only one contributing cut, we can even choose to calculate only one part of it.

Choosing which cut to calculate

We now have to choose whether we want to calculate $\mathrm{Cut}_{3g,1}$ or $\mathrm{Cut}_{3g,2}$. To see which one of the two is easier, we write explicit expressions for both. In these expressions, we solve $\delta^{(d)}(k_1+k_2+k_3)$ to eliminate one of the loop momenta. Because of the factor $\delta^-(k_3^2)$, it is convenient to keep k_3. Because of the $i \leftrightarrow j$ symmetry it is then arbitrary whether we choose to eliminate k_1 or k_2. We eliminate k_1 and then obtain

$$\begin{aligned}
\mathrm{Cut}_{3g,1}(\alpha_{ij},\alpha_{ik},\alpha_{jk}) &= i\frac{\mu^{4\epsilon}}{m^{4\epsilon}}g_s^4\int\frac{d^dk_2}{(2\pi)^d}\frac{d^dk_3}{(2\pi)^d}\frac{\beta_i\cdot\beta_j\beta_k\cdot(-k_3-2k_2)}{(-\beta_k\cdot k_3-1)(k_2+k_3)^2k_2^2} \\
&\quad\times(2\pi)^3\delta^-(k_3)^2\delta(\beta_i\cdot(k_2+k_3)-1)\delta(-\beta_j\cdot k_2-1) \\
\mathrm{Cut}_{3g,2}(\alpha_{ij},\alpha_{ik},\alpha_{jk}) &= i\frac{\mu^{4\epsilon}}{m^{4\epsilon}}g_s^4\int\frac{d^dk_2}{(2\pi)^d}\frac{d^dk_3}{(2\pi)^d}\frac{\beta_j\cdot\beta_k\beta_i\cdot(k_2-k_3)}{(-\beta_k\cdot k_3-1)(k_2+k_3)^2k_2^2} \\
&\quad\times(2\pi)^3\delta^-(k_3)^2\delta(\beta_i\cdot(k_2+k_3)-1)\delta(-\beta_j\cdot k_2-1)\ . \qquad (3.73)
\end{aligned}$$

As mentioned before, we can manipulate the numerator to arrive at a simpler expression. The easiest calculation of the two will hence be the one where we have the easiest numerator. That easiest numerator is the one in $\mathrm{Cut}_{3g,2}$, namely $\beta_i\cdot(k_2-k_3)$. The factor $\delta(\beta_i\cdot(k_2+k_3)-1)$ allows us to manipulate this factor to either one of $2\beta_i\cdot k_2-1$ and $-2\beta_i\cdot k_3+1$. This way, the numerator becomes

either independent of k_3 or k_2 respectively. That ensures that we can get rid of the numerator when performing the first loop integral, simplifying the calculation. We therefore choose to calculate $\mathrm{Cut}_{3g,2}$.

General considerations

Before we start calculating $\mathrm{Cut}_{3g,2}$, we first think some more about the expected result. We know that the diagram has to be $\mathcal{O}(\epsilon^{-1})$ divergent. Indeed, no subloop can be shrunk to the origin independently of the other subloops, indicating that there can not be any multiple divergences. Also, when performing numerical calculations of the diagram, we again see only a $\mathcal{O}(\epsilon^{-1})$ divergence.

We also know the source of the divergence: by power counting we see that we have a ultraviolet divergence when all momenta become large together. In this limit, the integral looks like

$$\int_{\Lambda}^{\infty} \frac{dk}{k^{1+4\epsilon}} = \frac{1}{4\epsilon} + \mathcal{O}(1) \ . \tag{3.74}$$

These considerations help us when calculating the diagram. The fact that the diagram is only $\mathcal{O}(\epsilon^{-1})$ divergent implies that we are only interested in the leading order part of the calculation. As before, we will parametrise the momenta explicitly, leading to both momentum-scale and angular integrals. The angular integrations will not lead to divergences, so we can ignore the dimensional regulator ϵ when performing them. In contrast, when performing the momentum-scale integrals it will be important to make sure we keep the correct ϵ-dependent power of the loop momentum, because this will influence the exact value of the divergence, as illustrated in (3.74). These considerations will guide us when performing the integrals.

Calculation of $\mathrm{Cut}_{g3,2}$

Because the techniques used are quite similar to the ones we applied for the calculation of the $(1, 2, 1)$ web, the details of this calculation can be found in the appendix.

We start from (3.73). We first perform the k_2 subintegral, hence we manipulate the numerator so that it only depends on k_3 as described above. Since we are only interested in the leading divergence coming from the region where all loop momenta are large, it suffices to calculate the subloop in this asymptotic

region. We find that

$$\begin{aligned}\mathrm{Cut}_{3g,2,k_2}(\alpha_{ij},\beta_i\cdot k_3,\beta_j\cdot k_3) &= \int\frac{d^dk_2}{(2\pi)^d}\frac{\delta(\beta_i\cdot(k_2+k_3)-1)\delta(-\beta_j\cdot k_2-1)}{(k_2+k_3)^2k_2^2}\\ &\to \frac{\pi}{(2\pi)^4}(\beta_i\cdot k_3)^{-1-2\epsilon}\frac{\ln(-\alpha_{ij})}{\beta_j\cdot k_3}+\mathcal{O}(\epsilon)\ . \end{aligned}\tag{3.75}$$

We now plug this into the remaining loop integral:

$$\begin{aligned}\mathrm{Cut}_{3g,2}(\alpha_{ij},\alpha_{ik},\alpha_{jk}) &= \frac{i}{2}\frac{\mu^{4\epsilon}}{m^{4\epsilon}}g_s^4\beta_j\cdot\beta_k\int\frac{d^dk_3}{(2\pi)^d}\frac{-2\beta_i\cdot k_3-1}{(-\beta_k\cdot k_3-1)}\\ &\quad\times\delta^-(k_3)^2(\beta_i\cdot k_3)^{-1-2\epsilon}\frac{\ln(-\alpha_{ij})}{\beta_j\cdot k_3}+\mathcal{O}(\epsilon)\\ &= 8\pi i\kappa^2\Gamma(4\epsilon)\ln(-\alpha_{ij})r(\alpha_{jk})\ln(\alpha_{jk})+\mathcal{O}(1)\ . \end{aligned}\tag{3.76}$$

Dispersive integral and final result

We can now perform the dispersive integral. We are only interested in the leading order part, so will ignore $\mathcal{O}(1)$ contributions in what follows. The dispersive integral gives

$$\begin{aligned}\mathcal{F}_{3g,2}(\alpha_{ij},\alpha_{ik},\alpha_{jk})-\mathcal{F}_{3g,2}(\alpha_{ij}=1,\alpha_{ik},\alpha_{jk}) &= -\int_{\mathrm{Disp},\alpha_{\mathrm{ij}}}\mathrm{Cut}_{3g,2}\\ &= -\frac{\kappa^2}{2\epsilon}\ln^2(\alpha_{ij})r(\alpha_{jk})\ln(\alpha_{jk})\ . \end{aligned}\tag{3.77}$$

We now have to find $\mathcal{F}_{3g,2}(\alpha_{ij}=1)$. Again, instead of calculating this explicitly, we are going to make educated guesses for this quantity and then check them numerically. The easiest possible option is that this is equal to zero. This seems to suggest that

$$\mathcal{F}_{3g,2}(\alpha_{ij},\alpha_{ik},\alpha_{jk}) = -\frac{\kappa^2}{2\epsilon}\ln^2(\alpha_{ij})r(\alpha_{jk})\ln(\alpha_{jk})\ .\tag{3.78}$$

However, this would not respect the $j\leftrightarrow k$ antisymmetry that we have observed at the level of the integrand. The logical solution to this problem is then to antisymmetrise (3.78). This would require

$$\mathcal{F}_{3g,2}(\alpha_{ij},\alpha_{ik},\alpha_{jk}) = -\frac{\kappa^2}{2\epsilon}r(\alpha_{jk})\ln(\alpha_{jk})\big(\ln^2(\alpha_{ij})-\ln^2(\alpha_{ik})\big)\tag{3.79}$$

$$\mathcal{F}_{3g,2}(\alpha_{ij}=1,\alpha_{ik},\alpha_{jk}) = \frac{\kappa^2}{2\epsilon}r(\alpha_{jk})\ln(\alpha_{jk})\ln^2(\alpha_{ik})\ .\tag{3.80}$$

When checked numerically in SecDec, this indeed proves to be correct.

We can now use the antisymmetry relations (3.68) to generate the complete result from this part:

$$\begin{aligned}\mathcal{F}_{3g}(\alpha_{ij},\alpha_{ik},\alpha_{jk}) &= \mathcal{F}_{3g,1}(\alpha_{ij},\alpha_{ik},\alpha_{jk}) + \mathcal{F}_{3g,2}(\alpha_{ij},\alpha_{ik},\alpha_{jk}) + \mathcal{F}_{3g,3}(\alpha_{ij},\alpha_{ik},\alpha_{jk}) \\ &= -\frac{\kappa^2}{2\epsilon}\Big(r(\alpha_{ij})\ln(\alpha_{ij})\big(\ln^2(\alpha_{ik}) - \ln^2(\alpha_{jk})\big) \\ &\qquad + r(\alpha_{ik})\ln(\alpha_{ik})\big(\ln^2(\alpha_{jk}) - \ln^2(\alpha_{ij})\big) \\ &\qquad + r(\alpha_{jk})\ln(\alpha_{jk})\big(\ln^2(\alpha_{ij}) - \ln^2(\alpha_{ik})\big)\Big) \ . \end{aligned} \tag{3.81}$$

We notice that from this expression it is possible to deduce $\mathrm{Cut}_{3g,1}$. However, now that we have the result of the diagram itself, there is no point in calculating this any more.

Going back to the definition of the $(1,1,1)$ web (3.66), this gives

$$\begin{aligned}\mathcal{W}_{3g}(\alpha_{ij},\alpha_{ik},\alpha_{jk}) &= -if^{abc}T_i^aT_j^bT_k^c\mathcal{F}_{3g}(\alpha_{ij},\alpha_{ik},\alpha_{jk}) \\ &= -if^{abc}T_i^aT_j^bT_k^c\frac{\kappa^2}{2\epsilon}r(\alpha_{ij})\ln(\alpha_{ij})\ln^2(\alpha_{jk}) \\ &= -if^{abc}T_i^aT_j^bT_k^c\frac{2\alpha_s^2}{(4\pi)^2\epsilon}r(\alpha_{ij})\ln(\alpha_{ij})\ln^2(\alpha_{jk}) \ , \end{aligned} \tag{3.82}$$

where we sum over i,j,k. This remarkably simple result agrees with [14, 27, 77, 79].

3.2.3 The Y diagram.

The final two-loop diagram we look at is the Y diagram, see figure 3.7 [5]. The diagram forms a web by itself, the $(1,2)$ web:

$$\mathcal{W}_{(1,2)} = -if^{abc}T_i^aT_j^bT_j^c\mathcal{F}_Y \ . \tag{3.83}$$

It includes a three-gluon vertex. We expect it is going to be $\mathcal{O}(\epsilon^{-1})$ divergent for the same reasons as the $(1,1,1)$ web: no subloop can be shrunk to the origin independently and the numerics tell us it is $\mathcal{O}(\epsilon^{-1})$ divergent.

At first glance it seems that we can obtain the Y diagram by *collinear reduction* of the $(1,1,1)$ web: if we contract two legs of the latter, we obtain a diagram that looks like the former. However, this intuition is false. By identifying two legs of the $(1,1,1)$ web, we would obtain an expression that is symmetric in

[5] This calculation has been performed in collaboration with Robbert Rietkerk.

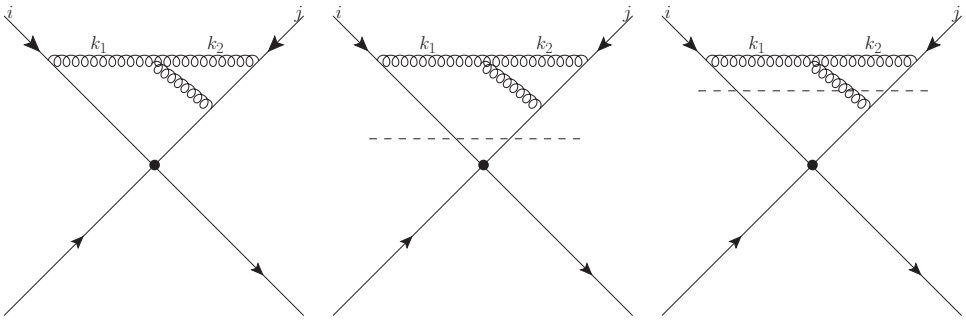

(a) $\mathcal{F}_Y$ **(b)** $\mathrm{Cut}_{Y,1}$ **(c)** $\mathrm{Cut}_{Y,2}$

Figure 3.7 *The Y diagram and its cuts. The diagram forms a web by itself.*

the gluon attachments on the leg j. In contrast, because of the antisymmetry of the three-gluon vertex, we actually want an expression that is antisymmetric in the gluon attachments. We conclude that we will have to perform explicit calculations and cannot obtain the diagram by collinearly reducing the $(1,1,1)$ web. However, the notion of collinear reduction will be useful in the discussion below.

The diagram is equal to

$$\begin{aligned}\mathcal{F}_Y(\alpha_{ij}) = (ig_s)^4 \frac{m^{4\epsilon}}{\mu^{4\epsilon}} \int \frac{d^dk_1}{(2\pi)^d} \frac{d^dk_2}{(2\pi)^d} \frac{\big(\beta_i - \beta_i\cdot\beta_j\beta_j\big)\cdot\big(k_1+2k_2\big)}{(k_1^2+i\epsilon)(k_2^2+i\epsilon)((k_1+k_2)^2+i\epsilon)} \\ \times \frac{1}{(-\beta_i\cdot k_1 - 1 + i\epsilon)(-\beta_j\cdot k_2 - 1 + i\epsilon)(\beta_j\cdot k_1 - 2 + i\epsilon)} \,. \end{aligned} \tag{3.84}$$

It has two cuts, both represented in figure 3.7:

$$\begin{aligned}\mathrm{Cut}_{Y,1}(\alpha_{ij}) = -(2\pi i)^2 g_s^4 \frac{m^{4\epsilon}}{\mu^{4\epsilon}} \int \frac{d^dk_1}{(2\pi)^d} \frac{d^dk_2}{(2\pi)^d} \frac{\big(\beta_i - \beta_i\cdot\beta_j\beta_j\big)\cdot\big(k_1+2k_2\big)}{(k_1^2+i\epsilon)(k_2^2+i\epsilon)((k_1+k_2)^2+i\epsilon)} \\ \times \frac{\delta(-\beta_i\cdot k_1 - 1)\delta(\beta_j\cdot k_1 - 2)}{(-\beta_j\cdot k_2 - 1 + i\epsilon)} \end{aligned} \tag{3.85}$$

$$\begin{aligned}\mathrm{Cut}_{Y,2}(\alpha_{ij}) = -(2\pi i)^3 g_s^4 \frac{m^{4\epsilon}}{\mu^{4\epsilon}} \int \frac{d^dk_1}{(2\pi)^d} \frac{d^dk_2}{(2\pi)^d} \frac{\big(\beta_i - \beta_i\cdot\beta_j\beta_j\big)\cdot\big(k_1+2k_2\big)}{(k_1^2+i\epsilon)(k_2^2+i\epsilon)} \\ \times \frac{\delta^+\big((k_1+k_2)^2\big)\delta(-\beta_i\cdot k_1 - 1)\delta(-\beta_j\cdot k_2 - 1)}{(\beta_j\cdot k_1 - 2 - i\epsilon)} \,. \end{aligned} \tag{3.86}$$

In what follows, we again drop the $i\epsilon$ for the second cut. However, the first cut includes an uncut loop, so we will have to take the prescription into account.

Calculation of first cut

We now calculate the first cut. We start by calculating the k_2 subloop, which does not involve any delta functions. Therefore we are dealing with a conventional Feynman integral and can use some well-known tools, such as Feynman parametrisation and reduction to basis integrals. We start with the Feynman parametrisation.

$$
\begin{aligned}
&\mathrm{Cut}_{Y,1,k_2}(\alpha_{ij},\beta_i\cdot k_1,\beta_j\cdot k_1,k_1^2)\\
&=\int\frac{d^dk_2}{(2\pi)^d}\frac{\big(\beta_i-\beta_i\cdot\beta_j\beta_j\big)\cdot\big(k_1+2k_2\big)}{(k_2^2+i\epsilon)((k_1+k_2)^2+i\epsilon)(-\beta_j\cdot k_2-1+i\epsilon)}\\
&=2\int_0^1dx\int_0^\infty dy\int\frac{d^dk_2}{(2\pi)^d}\\
&\times\frac{\big(\beta_i-\beta_i\cdot\beta_j\beta_j\big)\cdot\big(k_1+2k_2\big)}{\Big(\big(k_2+xk_1-y\beta_j/2\big)^2+xk_1^2-y-\big(xk_1-y\beta_j/2\big)^2+i\epsilon\Big)^3}\\
&=2\int_0^1dx\int_0^\infty dy\int\frac{d^dk_2}{(2\pi)^d}\frac{\big(\beta_i-\beta_i\cdot\beta_j\beta_j\big)\cdot\big(k_1+2k_2-2xk_1+y\beta_j\big)}{\Big(k_2^2+xk_1^2-y-\big(xk_1-y\beta_j/2\big)^2+i\epsilon\Big)^3}\\
&=2\big(\beta_i-\beta_i\cdot\beta_j\beta_j\big)\cdot k_1\\
&\times\int_0^1dx\int_0^\infty dy\int\frac{d^dk_2}{(2\pi)^d}\frac{1-2x}{\Big(k_2^2+xk_1^2-y-\big(xk_1-y\beta_j/2\big)^2+i\epsilon\Big)^3}\\
&=-i\frac{\Gamma(1+\epsilon)}{(4\pi)^{2-\epsilon}}\big(\beta_i-\beta_i\cdot\beta_j\beta_j\big)\cdot k_1\\
&\times\int_0^1dx\int_0^\infty dy\frac{1-2x}{\Big(-xk_1^2+y+\big(xk_1-y\beta_j/2\big)^2\Big)^{1+\epsilon}}\ .
\end{aligned}
\tag{3.87}
$$

This integral is hard to perform, but we will express it in terms of easier integrals. To do this, we introduce the following notation

$$
\begin{aligned}
F[\mathcal{N}]&=\int\frac{d^dk_2}{(2\pi)^d}\frac{\mathcal{N}(\beta_j,k_1,k_2)}{k_2^2(k_1+k_2)^2(-\beta_j\cdot k_2-1)}\\
G[\lambda]&=\int_0^1dx\int_0^\infty dy\frac{\lambda(x,y)}{\Big(-xk_1^2+y+\big(xk_1-y\beta_j/2\big)^2\Big)^{1+\epsilon}}\ ,
\end{aligned}
\tag{3.88}
$$

where $\mathcal{N}(\beta_j, k_1, k_2)$ is a polynomial in β_j, k_1, k_2 and $\lambda(x, y)$ is a linear function of x and y. Using this notation, (3.87) becomes

$$\begin{aligned}\mathrm{Cut}_{Y,1,k_2}(\alpha_{ij}, \beta_i \cdot k_1, \beta_j \cdot k_1, k_1^2) &= F[\big(\beta_i - \beta_i \cdot \beta_j \beta_j\big) \cdot \big(k_1 + 2k_2\big)] \\ &= -i\frac{\Gamma(1+\epsilon)}{(4\pi)^{2-\epsilon}}\big(\beta_i - \beta_i \cdot \beta_j \beta_j\big) \cdot k_1 G[1-2x] \ .\end{aligned} \tag{3.89}$$

It is clear that if we start with an $\mathcal{N}$ which is linear in k_2, we will end up with a λ linear in $1, x, y$. That means that if we choose our numerators wisely, three assignments of $\mathcal{N}$ should suffice to generate $G[1-2x]$. We can prove that

$$\begin{aligned}F[1] &= -i\frac{\Gamma(1+\epsilon)}{(4\pi)^{2-\epsilon}} G[1] \\ F[k_1 \cdot k_2] &= -i\frac{\Gamma(1+\epsilon)}{(4\pi)^{2-\epsilon}} G[-k_1^2(1-x) + k_1 \cdot \beta_j y/2] \\ &= -i\frac{\Gamma(1+\epsilon)}{(4\pi)^{2-\epsilon}} G[-k_1^2(1-x) + y] \\ F[-\beta_j \cdot k_2 - 1] &= -i\frac{\Gamma(1+\epsilon)}{(4\pi)^{2-\epsilon}} G[-1 + \beta_j \cdot k_1(1-x) - y/2] \\ &= -i\frac{\Gamma(1+\epsilon)}{(4\pi)^{2-\epsilon}} G[1-2x-y/2] \ ,\end{aligned} \tag{3.90}$$

where we used the delta functions $\delta(-\beta_i \cdot k_1 - 1)\delta(\beta_j \cdot k_1 - 2)$ to simplify expressions. Using linearity, it then follows that

$$F[2(-\beta_j \cdot k_2 - 1) + k_1 \cdot k_2 + k_1^2/2] = -i\frac{\Gamma(1+\epsilon)}{(4\pi)^{2-\epsilon}}\big(2 - k_1^2/2\big) G[1-2x] \ . \tag{3.91}$$

This implies that

$$\begin{aligned}&\mathrm{Cut}_{Y,1,k_2}(\alpha_{ij}, \beta_i \cdot k_1, \beta_j \cdot k_1, k_1^2) \\ &= \frac{2\big(\beta_i - \beta_i \cdot \beta_j \beta_j\big) \cdot k_1}{4 - k_1^2} F[2(-\beta_j \cdot k_2 - 1) + k_1 \cdot k_2 + k_1^2/2] \\ &= \frac{2\big(\beta_i - \beta_i \cdot \beta_j \beta_j\big) \cdot k_1}{4 - k_1^2} \int \frac{d^d k_2}{(2\pi)^d} \frac{2(-\beta_j \cdot k_2 - 1) + k_1 \cdot k_2 + k_1^2/2}{k_2^2 (k_1 + k_2)^2 (-\beta_j \cdot k_2 - 1)} \\ &= \frac{2\big(\beta_i - \beta_i \cdot \beta_j \beta_j\big) \cdot k_1}{4 - k_1^2} \bigg(\int \frac{d^d k_2}{(2\pi)^d} \frac{2}{k_2^2 (k_1 + k_2)^2} \\ &+ \int \frac{d^d k_2}{(2\pi)^d} \frac{1}{2k_2^2(-\beta_j \cdot k_2 - 1)} - \int \frac{d^d k_2}{(2\pi)^d} \frac{1}{2(k_2 + k_1)^2 (-\beta_j \cdot k_2 - 1)} \bigg) \\ &= \frac{\big(\beta_i - \beta_i \cdot \beta_j \beta_j\big) \cdot k_1}{4 - k_1^2} \bigg(4\mathcal{B}_1 + \mathcal{B}_2 - \mathcal{B}_3 \bigg) \ .\end{aligned} \tag{3.92}$$

We see that we have decomposed our original triangle with a numerator into a sum of three bubbles without a numerator. The bubbles in (3.92) can be calculated exactly.

$$\begin{aligned}
\mathcal{B}_1 &= \frac{i}{(4\pi)^{2-\epsilon}} \frac{\Gamma(1-\epsilon)^2\Gamma(\epsilon)}{\Gamma(2-2\epsilon)} \big(-k_1^2\big)^{-\epsilon} \\
\mathcal{B}_2 &= \frac{i}{(4\pi)^{2-\epsilon}} 2^{2-2\epsilon}\Gamma(1-\epsilon)\Gamma(2\epsilon-1) \\
\mathcal{B}_3 &= \big(1-\beta_j\cdot k_1\big)^{1-2\epsilon}\mathcal{B}_2 \\
&= \big(-1\big)^{1-2\epsilon}\mathcal{B}_2 \\
4\mathcal{B}_1 + \mathcal{B}_2 - \mathcal{B}_3 &= 4\ln\big(\frac{4}{k_1^2}\big) + \mathcal{O}(\epsilon)\ .
\end{aligned} \tag{3.93}$$

We can now plug (3.92) and (3.93) into (3.85).

$$\begin{aligned}
\mathrm{Cut}_{Y,1}(\alpha_{ij}) &= (2\pi i)^2 g_s^4 \frac{m^{4\epsilon}}{\mu^{4\epsilon}} \int \frac{d^dk_1}{(2\pi)^d} \frac{\delta(-\beta_i\cdot k_1 - 1)\delta(\beta_j\cdot k_1 - 2)\mathrm{Cut}_{Y,1,k_2}}{k_1^2} \\
&= (2\pi i)^2 g_s^4 \frac{m^{4\epsilon}}{\mu^{4\epsilon}} \int \frac{d^dk_1}{(2\pi)^d} \frac{\delta(-\beta_i\cdot k_1 - 1)\delta(\beta_j\cdot k_1 - 2)}{k_1^2} \\
&\qquad \times \frac{-1-2\beta_i\cdot\beta_j}{4-k_1^2} 4\bigg(\ln\big(\frac{4}{k_1^2}\big) + \mathcal{O}(\epsilon)\bigg)\ .
\end{aligned} \tag{3.94}$$

By inspection, we see that this integral will be ultraviolet finite. Indeed, for large k_1 the integrand goes as k_1^{-2}. We thus conclude that

$$\mathrm{Cut}_{Y,1}(\alpha_{ij}) = \mathcal{O}(1)\ . \tag{3.95}$$

This means that we can ignore it when calculating the $\mathcal{O}(\epsilon^{-1})$ divergence of the Y diagram.

Calculation of the second cut

We now calculate the second cut.

$$\begin{aligned}
\mathrm{Cut}_{Y,2}(\alpha_{ij}) &= -(2\pi i)^3 g_s^4 \frac{m^{4\epsilon}}{\mu^{4\epsilon}} \int \frac{d^dk_1}{(2\pi)^d} \frac{d^dk_2}{(2\pi)^d} \frac{\big(\beta_i - \beta_i\cdot\beta_j\beta_j\big)\cdot\big(k_1+2k_2\big)}{(k_1^2+i\epsilon)(k_2^2+i\epsilon)} \\
&\qquad \times \frac{\delta^+\big((k_1+k_2)^2\big)\delta(-\beta_i\cdot k_1 - 1)\delta(-\beta_j\cdot k_2 - 1)}{(\beta_j\cdot k_1 - 2 - i\epsilon)}\ .
\end{aligned} \tag{3.96}$$

When comparing this to (3.69), we see that

$$\begin{aligned}
&\lim_{\beta_k\to\beta_j}\left(\mathrm{Cut}_{3g}(\alpha_{ij},\alpha_{ik},\alpha_{jk})\right)\\
&=(2\pi i)^3\frac{\mu^{4\epsilon}}{m^{4\epsilon}}g_s^4\int\frac{d^dk_1}{(2\pi)^d}\frac{d^dk_2}{(2\pi)^d}\frac{\big(\beta_i\cdot\beta_j\beta_j-\beta_i\big)\cdot\big(k_1+2k_2\big)}{(\beta_j\cdot(k_1+k_2)-1)k_1^2k_2^2}\\
&\times\delta^+(k_1+k_2)^2\delta(-\beta_i\cdot k_1-1)\delta(-\beta_j\cdot k_2-1)\\
&=(2\pi i)^3\frac{\mu^{4\epsilon}}{m^{4\epsilon}}g_s^4\int\frac{d^dk_1}{(2\pi)^d}\frac{d^dk_2}{(2\pi)^d}\frac{\big(\beta_i\cdot\beta_j\beta_j-\beta_i\big)\cdot\big(k_1+2k_2\big)}{(\beta_j\cdot k_1-2)k_1^2k_2^2}\\
&\times\delta^+(k_1+k_2)^2\delta(-\beta_i\cdot k_1-1)\delta(-\beta_j\cdot k_2-1)\\
&=-\mathrm{Cut}_{Y,2}\ .
\end{aligned}\tag{3.97}$$

This implies that we can obtain the cut of the Y diagram by collinear reduction of the cut of the $(1,1,1)$ web, even though we already argued that at the level of the diagram itself this is not possible. We indeed saw that in the derivation of (3.97) we used one of the delta functions, which gives us some extra structure to play with compared to the diagram itself. This again illustrates that at the level of the cut, extra relations between diagrams can be exploited.

We have to raise a caveat about the limit we took when calculating (3.97). When we calculate the cut of the $(1,1,1)$ diagram, we explicitly make use of the fact that particles i,j are incoming and particle k is outgoing. Therefore, taking the limit $\beta_k\to\beta_j$ does not make sense. Physically, a more sensible limit to take is the limit $\beta_k\to-\beta_j$. In this limit, we obtain

$$\begin{aligned}
&\lim_{\beta_k\to-\beta_j}\left(\mathrm{Cut}_{3g}(\alpha_{ij},\alpha_{ik},\alpha_{jk})\right)\\
&=-(2\pi i)^3\frac{\mu^{4\epsilon}}{m^{4\epsilon}}g_s^4\int\frac{d^dk_1}{(2\pi)^d}\frac{d^dk_2}{(2\pi)^d}\frac{\big(\beta_i\cdot\beta_j\beta_j-\beta_i\big)\cdot\big(k_1+2k_2\big)}{(-\beta_j\cdot k_1)k_1^2k_2^2}\\
&\times\delta^+(k_1+k_2)^2\delta(-\beta_i\cdot k_1-1)\delta(-\beta_j\cdot k_2-1)\\
&=\mathrm{Cut}_{Y,2}(\alpha_{ij})+\mathcal{O}(1)\ .
\end{aligned}\tag{3.98}$$

In the last line we exploited that the integrand is the same as the integrand of $\mathrm{Cut}_{Y,2}$, up to a factor of $\frac{-\beta_j\cdot k_1-2}{-\beta_j\cdot k_1}$. Since the divergence is an ultraviolet one, this factor will tend to one in the region of integration where the divergence is generated. We thus have an equality, up to finite corrections. This is illustrated in figure 3.8.

Equation (3.98) now gives us a prescription to calculate the leading order

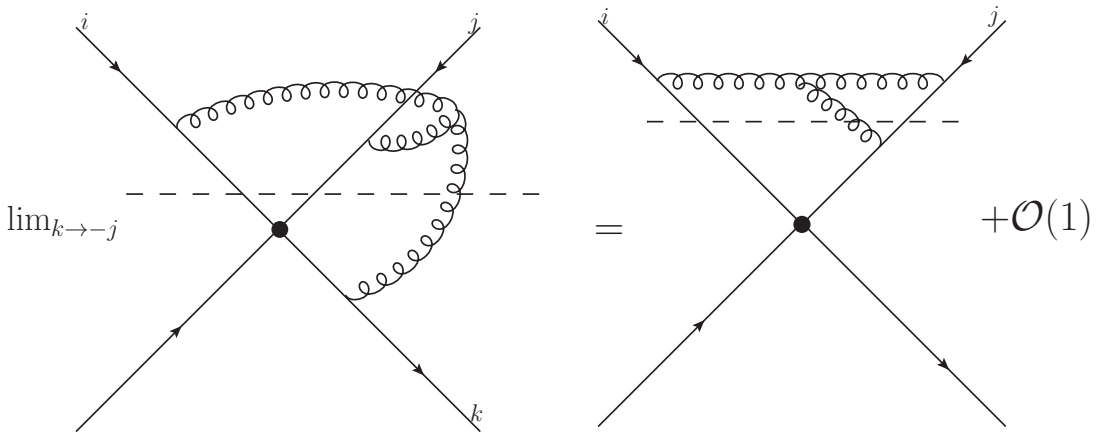

Figure 3.8 *The collinear reduction of* Cut_{3g} *gives* $\mathrm{Cut}_{Y,2}$.

part of $\mathrm{Cut}_{Y,2}$. We will again ignore subleading corrections in what follows. We first calculate $\mathrm{Cut}_{3g}(\alpha_{ij},\alpha_{ik},\alpha_{jk})$, which we know is minus the α_{ij} discontinuity of $\mathcal{F}_{3g}$

$$\begin{aligned}\mathrm{Cut}_{3g}(\alpha_{ij},\alpha_{ik},\alpha_{jk}) &= -\mathrm{Disc}_{\alpha_{ij}}\big(\mathcal{F}_{3g}\big)\\ &= \frac{\pi\kappa^2 i}{\epsilon}\bigg(r(\alpha_{ij})\big(\ln^2(\alpha_{ik})-\ln^2(\alpha_{jk})\big)\\ &\qquad + 2\ln(-\alpha_{ij})\big(r(\alpha_{jk})\ln(\alpha_{jk})-r(\alpha_{ik})\ln(\alpha_{ik})\big)\bigg)\ .\end{aligned} \tag{3.99}$$

We then take the $\beta_k \to -\beta_j$ limit. In this limit

$$\begin{aligned}&\alpha_{jk}\to 1\\ &\alpha_{ik}\to -\alpha_{ij}\ .\end{aligned} \tag{3.100}$$

This gives us

$$\begin{aligned}\mathrm{Cut}_{Y,2}(\alpha_{ij}) &= \lim_{k\to -j}\Big(\mathrm{Cut}_{3g}(\alpha_{ij},\alpha_{ik},\alpha_{jk})\Big)\\ &= \frac{\pi\kappa^2 i}{\epsilon}\bigg(r(\alpha_{ij})\ln^2(-\alpha_{ij})+2\ln(-\alpha_{ij})\big(-1-r(\alpha_{ij})\ln(-\alpha_{ij})\big)\bigg)\\ &= -\frac{\pi\kappa^2 i}{\epsilon}\bigg(r(\alpha_{ij})\ln^2(-\alpha_{ij})+2\ln(-\alpha_{ij})\bigg)\ .\end{aligned} \tag{3.101}$$

Given our earlier conclusion that $\mathrm{Cut}_{Y,1}(\alpha_{ij})=\mathcal{O}(1)$ (3.95), we can thus conclude

that

$$\begin{aligned}\mathrm{Disc}_Y(\alpha_{ij}) &= -\mathrm{Cut}_{Y,1}(\alpha_{ij}) - \mathrm{Cut}_{Y,2}(\alpha_{ij}) \\ &= \frac{\pi\kappa^2 i}{\epsilon}\bigg(r(\alpha_{ij})\ln^2(-\alpha_{ij}) + 2\ln(-\alpha_{ij})\bigg) + \mathcal{O}(1)\ . \end{aligned} \tag{3.102}$$

Dispersive integral

We can now calculate the dispersive integral of (3.102) to obtain the result for the Y diagram:

$$\begin{aligned}&\mathcal{F}_Y(\alpha_{ij}) - \mathcal{F}_Y(\alpha_{ij}=1) \\ &= \int_{\mathrm{Disp}} \mathrm{Disc}_Y \\ &= \frac{\kappa^2}{\epsilon}\bigg(r(\alpha_{ij})\big(\frac{\ln^3(\alpha_{ij})}{6} + \zeta_2\ln\alpha_{ij}\big) + \frac{\ln^2(\alpha_{ij})}{2} + \zeta_2\bigg) + \mathcal{O}(1)\ . \end{aligned} \tag{3.103}$$

In this case we actually know $\mathcal{F}_Y(\alpha_{ij}=1)$. It corresponds to the limit where $\beta_i = -\beta_j$. When taking this limit, the numerator of (3.7) becomes zero, so that

$$\mathcal{F}_Y(\alpha_{ij}=1) = 0\ . \tag{3.104}$$

Using this, equation (3.103) reduces to

$$\mathcal{F}_Y(\alpha_{ij}) = \frac{\kappa^2}{\epsilon}\bigg(r(\alpha_{ij})\big(\frac{\ln^3(\alpha_{ij})}{6} + \zeta_2\ln\alpha_{ij}\big) + \frac{\ln^2(\alpha_{ij})}{2} + \zeta_2\bigg) + \mathcal{O}(1)\ . \tag{3.105}$$

This result agrees with the result found in [72].

3.3 Conclusion

In this chapter, we have applied the unitarity cut formalism to the calculation of some one- and two-loop diagrams. To achieve this, we used a variety of techniques, such as explicit parametrisation of loop momenta, Feynman parametrisation, integral decomposition, asymptotic expansion and collinear reduction. We managed to reproduce the known results for all diagrams we attempted to calculate.

These calculations illustrate some of the benefits of the use of unitarity cuts. The main benefit is that the cuts exhibit more structure than the diagrams themselves, for example

- Cuts can decompose into lower-loop contributions, such as in the case of the $(1, 2, 1)$ web, see figure 3.4.
- Cuts can be equal to each other, as in figure 3.5.
- They can obey collinear reduction, even if the diagram itself does not, such as in (3.98).
- Sometimes they are less symmetric than the original diagrams, but the dispersive integral restores the symmetry. This can give us multiple ways to calculate a part of a cut, all leading to the same original diagram. For example, in the calculation of the $(1, 1, 1)$ web we could choose which one of two contributions to the cut we wanted to calculate.

Apart from the extra structure, another benefit is that the transcendental weight of a cut is lower than that of the diagram itself. This means that the expressions for the cut are simpler than the expression for the diagram itself. The dispersive integral then raises the weight by one. In principle this step could pose problems, but we saw that when using the correct variables it is trivial.

Another simplifying factor are the delta functions. Not only are they simple to integrate out, but they also allow us to reshuffle some terms. This is especially useful when dealing with numerators occurring in diagrams involving three-gluon vertices. We therefore focus our attention on this type of diagrams, and will calculate some as yet unknown diagrams involving three-gluon vertices in the next chapters.

Chapter 4

Calculation of the $(1,3,1)$ web

In this chapter, we use unitarity cuts to calculate the three-loop $(1,3,1)$ web. More precisely, we focus on determining the kinematic dependence associated with one of the two colour components of this web. This web has been calculated in the lightlike limit [80], but not in general kinematics. We use this lightlike limit to check our expression, and also check the result numerically, and find agreement. This result allows us some insight into the space of solutions of three-loop webs.

4.1 The $(1,3,1)$ web

There are three different diagrams contributing to the $(1,3,1)$ web, with two separate colour factors. The diagrams are represented in figure 4.1. According to reference [40]

$$\mathcal{W}_{(1,3,1)} = c_1 f_1 + c_2 f_2 \ , \tag{4.1}$$

with

$$\begin{aligned} c_1 &= f^{bcd} f^{cae} T_i^a T_j^{de} T_k^b \\ c_2 &= f^{bcd} f^{ade} T_i^a T_j^{ec} T_k^b \\ f_1 &= \frac{1}{2}\big(-\mathcal{F}_1 - \mathcal{F}_2 + \mathcal{F}_3\big) \\ f_2 &= \frac{1}{2}\big(-\mathcal{F}_1 + \mathcal{F}_2 - \mathcal{F}_3\big) \ . \end{aligned} \tag{4.2}$$

This can be rewritten in terms of a different basis of colour factors:

$$\mathcal{W}_{(1,3,1)} = c_1' \mathcal{F}_A + c_2' \mathcal{F}_B \ , \tag{4.3}$$

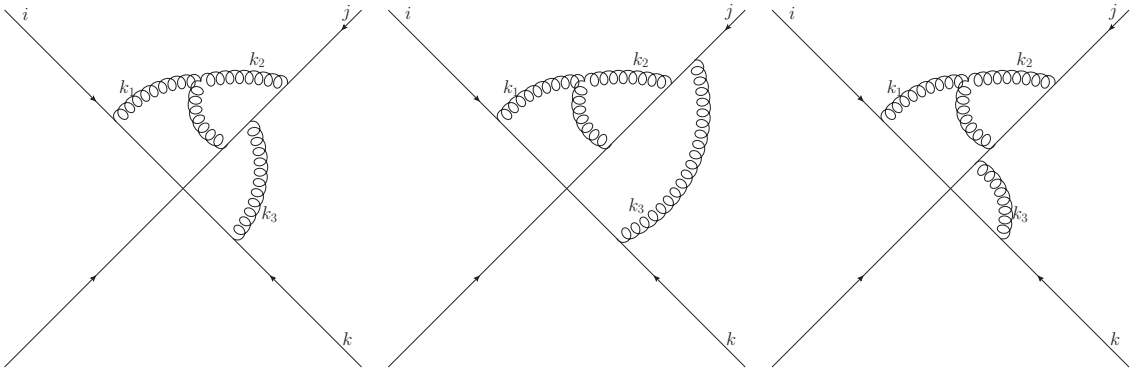

(a) $\mathcal{F}_1$ **(b)** $\mathcal{F}_2$ **(c)** $\mathcal{F}_3$

Figure 4.1 *The diagrams in the* $(1,3,1)$ *web.*

with

$$\begin{aligned}
c_1' &= \frac{i}{2}(c_1 + c_2) \\
&= \frac{i}{2} f^{bcd} f^{cae} T_i^a \left(T_j^{de} + T_j^{ed}\right) T_k^b \\
c_2' &= (c_1 - c_2) \\
&= \frac{i}{4} N_c f^{bag} T_i^a T_j^g T_k^b \\
\mathcal{F}_A &= i\mathcal{F}_1 \\
\mathcal{F}_B &= -\frac{1}{2}\left(\mathcal{F}_2 - \mathcal{F}_3\right) \ .
\end{aligned} \tag{4.4}$$

We see that in this colour basis, $\mathcal{F}_A$ forms a web by itself. Moreover, there are no subloops that can be shrunk to a point independently, and numerical calculations in SecDec indicate a $\mathcal{O}(\epsilon^{-1})$ divergence. This is in contrast to the two other diagrams contributing to $\mathcal{F}_B$, which are $\mathcal{O}(\epsilon^{-2})$ divergent.

We now decide which of the two kinematic factors we want to calculate. $\mathcal{F}_A$ seems the most natural choice. Indeed, unitarity cuts are a method for the calculation of Feynman diagrams, rather than webs. In the case of $\mathcal{F}_A$ these two notions coincide, so that the unitarity cut method seems well suited. Moreover, based on the arguments above, we would only have to calculate the LO contribution of this diagram, whereas for the calculation of $\mathcal{F}_B$ we would also have to include NLO contributions. A drawback of the calculation of $\mathcal{F}_A$ is that it is more entangled than the diagrams contributing to $\mathcal{F}_B$, as can be seen in figure 4.1. This will complicate calculations.

Based on the considerations above, we decide to focus our attention on $\mathcal{F}_A$.

4.2 $\mathcal{F}_A$ and its cuts

The expression for the diagram is

$$\begin{aligned}\mathcal{F}_A(\alpha_{ij},\alpha_{jk}) = -i\beta_j\cdot\beta_k\frac{\mu^{6\epsilon}}{m^{6\epsilon}}g_s^6\int\frac{d^dk_1}{(2\pi)^d}\frac{d^dk_2}{(2\pi)^d}\frac{d^dk_3}{(2\pi)^d}\Bigg(&\frac{1}{(k_1^2+i\epsilon)(k_2^2+i\epsilon)}\\ &\times\frac{1}{(k_3^2+i\epsilon)((k_1+k_2)^2+i\epsilon)(-\beta_j\cdot k_2-1+i\epsilon)}\\ &\times\frac{(\beta_i\cdot\beta_j\beta_j-\beta_i)\cdot(2k_2+k_1)}{(-\beta_i\cdot k_1-1+i\epsilon)(-\beta_k\cdot k_3-1+i\epsilon)}\\ &\times\frac{1}{(\beta_j\cdot(k_3-k_2)-2+i\epsilon)(\beta_j\cdot(k_1+k_3)-3+i\epsilon)}\Bigg)\,.\end{aligned} \tag{4.5}$$

When looking at the diagram $\mathcal{F}_A$, we expect that most of the complexity of the diagram will show up in the α_{ij} dependence, whereas the α_{jk} dependence should be simple: it corresponds to a single gluon exchange. Based on lower-loop calculations, we guess it will correspond to a factor of $r(\alpha_{jk})\ln\alpha_{jk}$. $\mathcal{F}_A$ is a three-loop diagram, so we expect it will have transcendental weight six at most, where we give weight 1 to each factor of ϵ^{-1}. However, because it is not maximally connected, we do not expect a uniform weight, so there might be lower weight contributions as well. In summary, we expect a result of the form

$$\mathcal{F}_A(\alpha_{ij},\alpha_{jk}) = \Gamma(6\epsilon)\kappa^3 r(\alpha_{jk})\ln\alpha_{jk}F(\alpha_{ij}) + \mathcal{O}(1)\,, \tag{4.6}$$

with $F(\alpha_{ij})$ a linear combination of contributions that have transcendental weight four and lower.

This expectation is confirmed by the lightlike limit. The lightlike limit corresponds to the region where the cusp variables α become very small [80]. The result then tends to [80] [1]

$$\begin{aligned}\mathcal{F}_A(\alpha_{ij},\alpha_{jk}) \to -\frac{8}{3}\frac{\alpha_s^3}{(4\pi)^3}\ln\alpha_{jk}&\\ \times\left(\frac{1}{3}\ln^4\alpha_{ij}+4(\zeta_3-2\zeta_2)(1+\ln\alpha_{ij})-3\zeta_4\right)&+\mathcal{O}(1)\,.\end{aligned} \tag{4.7}$$

[1] Notice that we are using a different colour factor than in reference [80].

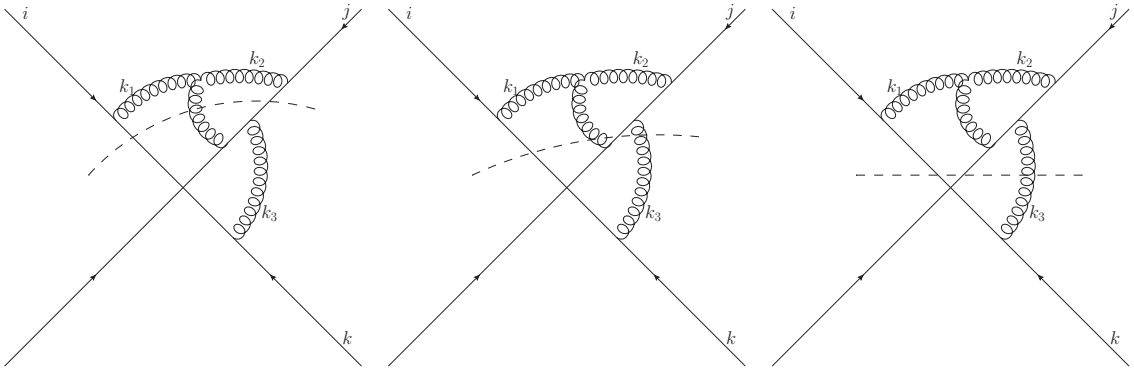

(a) $\mathrm{Cut}_1\big(\mathcal{F}_A\big)$ **(b)** $\mathrm{Cut}_2\big(\mathcal{F}_A\big)$ **(c)** $\mathrm{Cut}_3\big(\mathcal{F}_A\big)$

Figure 4.2 *The cuts of* $\mathcal{F}_A$

4.2.1 Choosing which channel to cut on

We are dealing with a function of two variables, so we can choose to cut on two different channels. Based on (4.6), the corresponding discontinuities will look like

$$\begin{aligned}\mathrm{Disc}_{\alpha_{ij}}\big(\mathcal{F}_A\big) &= \Gamma(6\epsilon)\kappa^3 r(\alpha_{jk})\ln\alpha_{jk}\mathrm{Disc}_{\alpha_{ij}}\big(F(\alpha_{ij})\big) + \mathcal{O}(1)\\ \mathrm{Disc}_{\alpha_{jk}}\big(\mathcal{F}_A\big) &= 2\pi i\Gamma(6\epsilon)\kappa^3 r(\alpha_{jk})F(\alpha_{ij}) + \mathcal{O}(1)\ .\end{aligned} \tag{4.8}$$

We thus expect that by cutting on the α_{ij} channel, and thereby reducing the weight of $F(\alpha_{ij})$ by one, we will obtain a simpler result than by cutting on the α_{jk} channel. Therefore, we calculate the cuts of the diagram in the α_{ij} channel. We work in the kinematic region where particles i and j are incoming and particle k is outgoing. There are three cuts in this channel, represented in figure 4.2. They are given by

$$\begin{aligned}\mathrm{Cut}_1\big(\mathcal{F}_A\big)(\alpha_{ij},\alpha_{jk}) = -i(2\pi i)^3\beta_j\cdot\beta_k\frac{\mu^{6\epsilon}}{m^{6\epsilon}}g_s^6\int\frac{d^dk_1}{(2\pi)^d}\frac{d^dk_2}{(2\pi)^d}\frac{d^dk_3}{(2\pi)^d}\frac{\delta^+((k_1+k_2)^2)}{(k_1^2+i\epsilon)}\\ \times\frac{\delta(-\beta_i\cdot k_1-1)\delta(-\beta_j\cdot k_2-1)}{(\beta_j\cdot(k_3-k_2)-2-i\epsilon)(\beta_j\cdot(k_1+k_3)-3-i\epsilon)}\\ \times\frac{(\beta_i\cdot\beta_j\beta_j-\beta_i)\cdot(2k_2+k_1)}{(k_2^2+i\epsilon)(k_3^2-i\epsilon)(-\beta_k\cdot k_3-1-i\epsilon)}\end{aligned} \tag{4.9}$$

$$\begin{aligned}\mathrm{Cut}_2\big(\mathcal{F}_A\big)(\alpha_{ij},\alpha_{jk}) = i(2\pi i)^4\beta_j\cdot\beta_k\frac{\mu^{6\epsilon}}{m^{6\epsilon}}g_s^6\int\frac{d^dk_1}{(2\pi)^d}\frac{d^dk_2}{(2\pi)^d}\frac{d^dk_3}{(2\pi)^d}\frac{\delta^+((k_1+k_2)^2)}{(k_1^2+i\epsilon)}\\ \times\frac{\delta^-(k_3^2)(\beta_i\cdot\beta_j\beta_j-\beta_i)\cdot(2k_2+k_1)}{(k_2^2+i\epsilon)(-\beta_j\cdot k_2-1+i\epsilon)(-\beta_k\cdot k_3-1-i\epsilon)}\\ \times\frac{\delta(\beta_j\cdot(k_3-k_2)-2)\delta(-\beta_1\cdot k_1-1)}{(\beta_j\cdot(k_1+k_3)-3-i\epsilon)}\end{aligned} \tag{4.10}$$

$$\begin{aligned}\mathrm{Cut}_3\big(\mathcal{F}_A\big)(\alpha_{ij},\alpha_{jk}) = -i(2\pi i)^3\beta_j\cdot\beta_k\frac{\mu^{6\epsilon}}{m^{6\epsilon}}g_s^6\int\frac{d^dk_1}{(2\pi)^d}\frac{d^dk_2}{(2\pi)^d}\frac{d^dk_3}{(2\pi)^d}\frac{\delta^-(k_3^2)}{(k_1^2+i\epsilon)}\\ \times\frac{(\beta_i\cdot\beta_j\beta_j-\beta_i)\cdot(2k_2+k_1)}{(k_2^2+i\epsilon)((k_1+k_2)^2+i\epsilon)(-\beta_k\cdot k_3-1-i\epsilon)}\\ \times\frac{\delta(-\beta_i\cdot k_1-1)\delta(\beta_j\cdot(k_1+k_3)-3)}{(-\beta_j\cdot k_2-1+i\epsilon)(\beta_j\cdot(k_3-k_2)-2+i\epsilon)}\,.\end{aligned} \tag{4.11}$$

We see we have two types of cuts: the first and third cuts contain an uncut subloop, the second one does not. We thus expect the $i\epsilon$ prescription to matter for the former, but not for the latter. Similarly, we see that the first and third cut have one less cut propagator, and hence one less factor of $2\pi i$, compared to the second cut. The uncut loops in the first and third cuts will contribute an extra factor of i compared to the second cut, so that we expect them all to add to a purely imaginary result.

4.2.2 Dispersive integral

When performing the calculations, we will see that it is possible to write the cuts in terms of a sum of products of polylogs of the form $G(\mathbf{a},\alpha_{ij})$ and $G(\mathbf{a},\alpha_{jk})$ separately, with $\mathbf{a}$ a vector with entries $-1,0,1$. This is by no means guaranteed before starting the calculation. Many intermediate results contain polylogs of $G(\mathbf{a},r(\alpha_{ij}))$. Individually, such polylogs can not be rewritten in terms of polylogs of the form $G(\mathbf{a},\alpha_{ij})$, but somehow the combination of polylogs that we obtain as a final expression conspires to make the simplification possible. This is an important property, because dispersive integrals of polylogs of the form $G(\mathbf{a},\alpha_{ij})$ are straightforward, but dispersive integrals of polylogs of the form $G(\mathbf{a},r(\alpha_{ij}))$ are not.

When calculating the dispersive integral, we have two options. We could combine all the cuts to generate the discontinuity of $\mathcal{F}_A$, and calculate its dispersive integral. We could also calculate the dispersive integral of the three cuts separately [2], and then combine them to obtain $\mathcal{F}_A$. The two approaches will yield the same result. We choose the latter approach, because it might give us some extra insights. We therefore define $\mathcal{F}_{A,1},\mathcal{F}_{A,2},\mathcal{F}_{A,3}$ such that

[2]Notice that in general it is not guaranteed that it is possible to calculate dispersive integrals of individual cuts, because they do not always correspond to the discontinuity of a function. However, the observation in the previous paragraph, namely that the cut can be written as a polylog of $G(\mathbf{a},\alpha_{ij})$ makes this possible.

$$\begin{aligned}
\mathrm{Disc}_{\alpha_{ij}}\big(\mathcal{F}_{A,1}\big)(\alpha_{ij},\alpha_{jk}) &= -\mathrm{Cut}_1\big(\mathcal{F}_A\big)(\alpha_{ij},\alpha_{jk}) \\
\mathrm{Disc}_{\alpha_{ij}}\big(\mathcal{F}_{A,2}\big)(\alpha_{ij},\alpha_{jk}) &= -\mathrm{Cut}_2\big(\mathcal{F}_A\big)(\alpha_{ij},\alpha_{jk}) \\
\mathrm{Disc}_{\alpha_{ij}}\big(\mathcal{F}_{A,3}\big)(\alpha_{ij},\alpha_{jk}) &= -\mathrm{Cut}_3\big(\mathcal{F}_A\big)(\alpha_{ij},\alpha_{jk}) \\
\mathcal{F}_A &= \mathcal{F}_{A,1} + \mathcal{F}_{A,2} + \mathcal{F}_{A,3} \ . \qquad (4.12)
\end{aligned}$$

When combining the three subtracted dispersive integrals, we will also have to make sure that we subtract the value of $\mathcal{F}_A(\alpha_{ij} = 1)$. This corresponds to the case where $\beta_i = -\beta_j$. In this limit, the numerator of (4.5) goes to zero, so that $\mathcal{F}_A(\alpha_{ij} = 1) = 0$. We choose also $\mathcal{F}_{A,i}(\alpha_{ij} = 1) = 0$, which is consistent with equation (4.12).

The way we deal with the calculation of the three-loop cuts is very similar to the calculation of two-loop cuts. In the case of the two-loop calculations, we first performed an exact calculation of a subloop in terms of the other loop momentum. We then plugged this expression into the remaining loop integral, and calculated this integral as a Laurent series via an asymptotic expansion. It turns out that we can use a similar strategy in the three-loop case. The delta functions will allow us to decouple some subloops. That way, we can calculate two subloops in terms of the third loop momentum. We then calculate the remaining integral via an asymptotic expansion. There will be a few extra complications compared to the calculations we performed at two loops.

To lighten the notation, we denote

$$\mathrm{Cut}_1\big(\mathcal{F}_A\big)(\alpha_{ij},\alpha_{jk}) = \mathcal{C}_1(\alpha_{ij},\alpha_{jk}) \ , \qquad (4.13)$$

and similarly for the two other cuts.

4.3 Calculation of $\mathcal{C}_1$

From (4.9), we have

$$\begin{aligned}
\mathcal{C}_1(\alpha_{ij},\alpha_{jk}) = -i(2\pi i)^3 \beta_j\cdot\beta_k \frac{\mu^{6\epsilon}}{m^{6\epsilon}} g_s^6 \int \frac{d^dk_1}{(2\pi)^d}\frac{d^dk_2}{(2\pi)^d}\frac{d^dk_3}{(2\pi)^d}\frac{\delta^+((k_1+k_2)^2)}{(k_1^2+i\epsilon)} \\
\times \frac{(\beta_i\cdot\beta_j\beta_j-\beta_i)\cdot(2k_2+k_1)}{(k_2^2+i\epsilon)(k_3^2-i\epsilon)(-\beta_k\cdot k_3-1-i\epsilon)} \\
\times \frac{\delta(-\beta_i\cdot k_1-1)\delta(-\beta_j\cdot k_2-1)}{(\beta_j\cdot(k_3-k_2)-2-i\epsilon)(\beta_j\cdot(k_1+k_3)-3-i\epsilon)}
\end{aligned}$$

$$= -i(2\pi i)^3 \beta_j \cdot \beta_k \frac{\mu^{6\epsilon}}{m^{6\epsilon}} g_s^6 \int \frac{d^d k_1}{(2\pi)^d} \frac{d^d k_2}{(2\pi)^d} \frac{d^d k_3}{(2\pi)^d} \frac{\delta^+((k_1+k_2)^2)}{(k_1^2+i\epsilon)} \times \frac{(\beta_i \cdot \beta_j \beta_j - \beta_i) \cdot (2k_2+k_1)}{(k_2^2+i\epsilon)(k_3^2-i\epsilon)(-\beta_k \cdot k_3 - 1 - i\epsilon)} \times \frac{\delta(-\beta_i \cdot k_1 - 1)\delta(-\beta_j \cdot k_2 - 1)}{(\beta_j \cdot k_3 - 1 - i\epsilon)(\beta_j \cdot (k_1+k_3) - 3 - i\epsilon)}$$

$$= (2\pi i)^3 \frac{\mu^{4\epsilon}}{m^{4\epsilon}} g_s^4 \int \frac{d^d k_1}{(2\pi)^d} \frac{\delta(-\beta_i \cdot k_1 - 1)}{(k_1^2+i\epsilon)} \mathcal{C}_{1,k_2} \mathcal{C}_{1,k_3} \ , \tag{4.14}$$

where we used the delta functions in (4.9), to replace

$$\frac{1}{(\beta_j \cdot (k_3 - k_2) - 2 - i\epsilon)} \to \frac{1}{(\beta_j \cdot k_3 - 1 - i\epsilon)} \tag{4.15}$$

in the integrand, and defined

$$\mathcal{C}_{1,k_2}(k_1^2, \beta_i \cdot k_1, \beta_j \cdot k_1, \beta_i \cdot \beta_j) = \int \frac{d^d k_2}{(2\pi)^d} \frac{\delta^+((k_1+k_2)^2)\delta(-\beta_j \cdot k_2 - 1)}{(k_2^2+i\epsilon)} \times (\beta_i \cdot \beta_j \beta_j - \beta_i) \cdot (2k_2 + k_1) \tag{4.16}$$

$$\mathcal{C}_{1,k_3}(\beta_j \cdot k_1, \beta_j \cdot \beta_k) = -i \frac{\mu^{2\epsilon}}{m^{2\epsilon}} g_s^2 \int \frac{d^d k_3}{(2\pi)^d} \frac{\beta_j \cdot \beta_k}{(-\beta_k \cdot k_3 - 1 - i\epsilon)(k_3^2 - i\epsilon)} \times \frac{1}{(\beta_j \cdot k_3 - 1 - i\epsilon)(\beta_j \cdot (k_1+k_3) - 3 - i\epsilon)} \ . \tag{4.17}$$

We see that the delta functions indeed allow us to rewrite the integral in terms of subloops $\mathcal{C}_{1,k_2}$, independent of k_3, and $\mathcal{C}_{1,k_3}$, independent of k_2. These can now be calculated in terms of k_1 and $\{\beta_n\}_{n=i,j,k}$, and then plugged into the k_1 integral (4.14), which we then calculate via an asymptotic expansion. Without the delta functions, we would have had a factor of $\frac{1}{(\beta_j \cdot (k_3 - k_2) - 2 - i\epsilon)}$ in the integrand, which would have forbidden this approach.

4.3.1 Calculation of $\mathcal{C}_{1,k_2}$

We can decompose $\mathcal{C}_{1,k_2}$ into two simpler integrals. We first define

$$\mathcal{C}^{\mu}_{1,k_2}(k_1^2, \beta_j \cdot k_1) = \int \frac{d^d k_2}{(2\pi)^d} \frac{\delta^+((k_1+k_2)^2)\delta(-\beta_j \cdot k_2 - 1)}{(k_2^2+i\epsilon)} (2k_2 + k_1)^{\mu} \ . \tag{4.18}$$

It is then easy to prove that

$$\mathcal{C}_{1,k_2}(k_1^2,\beta_i\cdot k_1,\beta_j\cdot k_1,\beta_i\cdot\beta_j)=\frac{(\beta_i\cdot\beta_j\beta_j-\beta_i)\cdot k_1}{(\beta_j\cdot k_1)^2-k_1^2}\Big(-\mathcal{B}_{1,k_2}(k_1^2,\beta_j\cdot k_1) \\ +\beta_j\cdot k_1(\beta_j\cdot k_1-2)\mathcal{T}_{1,k_2}(k_1^2,\beta_j\cdot k_1)\Big)\ , \tag{4.19}$$

where

$$\mathcal{T}_{1,k_2}(k_1^2,\beta_j\cdot k_1)=\int\frac{d^dk_2}{(2\pi)^d}\frac{\delta^+((k_1+k_2)^2)\delta(-\beta_j\cdot k_2-1)}{(k_2^2+i\epsilon)}\ , \tag{4.20}$$

and

$$\mathcal{B}_{1,k_2}(k_1^2,\beta_j\cdot k_1)=\int\frac{d^dk_2}{(2\pi)^d}\delta^+((k_1+k_2)^2)\delta(-\beta_j\cdot k_2-1)\ . \tag{4.21}$$

These integrals are calculated in appendix C. We use the results (C.6) and (C.3):

$$\mathcal{T}_{1,k_2}(k_1^2,\beta_j\cdot k_1)=\theta(\beta_j\cdot k_1-1)(\beta_j\cdot k_1-1)^{1-2\epsilon}T_{1,k_2}\ , \tag{4.22}$$

where

$$T_{1,k_2}=\frac{\pi^{1-\epsilon}}{(2\pi)^d\Gamma(1-\epsilon)}\int_{-1}^{1}d\cos\sigma \\ \times\frac{(\sin\sigma)^{-2\epsilon}}{k_1^2-2(\beta_j\cdot k_1-1)(\beta_j\cdot k_1-\sqrt{(\beta_j\cdot k_1)^2-k_1^2}\cos\sigma+i\epsilon)}\ , \tag{4.23}$$

and

$$\mathcal{B}_{1,k_2}(k_1^2,\beta_j\cdot k_1)=\theta(\beta_j\cdot k_1-1)(\beta_j\cdot k_1-1)^{1-2\epsilon}B_{1,k_2}\ , \tag{4.24}$$

with

$$B_{1,k_2}=\frac{\pi^{3/2-\epsilon}}{(2\pi)^d\Gamma(3/2-\epsilon)}\ , \tag{4.25}$$

so that

$$\mathcal{C}_{1,k_2}=\frac{(\beta_i\cdot\beta_j\beta_j-\beta_i)\cdot k_1}{(\beta_j\cdot k_1)^2-k_1^2}\theta(\beta_j\cdot k_1-1)(\beta_j\cdot k_1-1)^{1-2\epsilon}\big(B_{1,k_2}+T_{1,k_2}\big)\ . \tag{4.26}$$

4.3.2 Calculation of $\mathcal{C}_{1,k_3}$

By definition

$$\mathcal{C}_{1,k_3}(\beta_j\cdot k_1,\beta_j\cdot\beta_k) = -i\frac{\mu^{2\epsilon}}{m^{2\epsilon}}g_s^2\beta_j\cdot\beta_k\int\frac{d^dk_3}{(2\pi)^d}\frac{1}{(-\beta_k\cdot k_3-1-i\epsilon)(k_3^2-i\epsilon)} \times\frac{1}{(\beta_j\cdot k_3-1-i\epsilon)(\beta_j\cdot(k_1+k_3)-3-i\epsilon)}\ . \tag{4.27}$$

We can partial fraction this as

$$\mathcal{C}_{1,k_3}(\beta_j\cdot k_1,\beta_j\cdot\beta_k) = \frac{1}{-\beta_j\cdot k_1-2}\big(\mathcal{C}_{1,k_3,1}(\beta_j\cdot k_1,\beta_j\cdot\beta_k)+\mathcal{C}_{1,k_3,2}(\alpha_{jk})\big)\ , \tag{4.28}$$

where

$$\mathcal{C}_{1,k_3,2}(\alpha_{jk}) = i\frac{\mu^{2\epsilon}}{m^{2\epsilon}}g_s^2\beta_j\cdot\beta_k\int\frac{d^dk_3}{(2\pi)^d}\frac{1}{(-\beta_k\cdot k_3-1-i\epsilon)(k_3^2-i\epsilon)}\frac{1}{(\beta_j\cdot k_3-1-i\epsilon)}$$

$$\mathcal{C}_{1,k_3,1}(\beta_j\cdot k_1,\beta_j\cdot\beta_k) = -i\frac{\mu^{2\epsilon}}{m^{2\epsilon}}g_s^2\beta_j\cdot\beta_k\int\frac{d^dk_3}{(2\pi)^d}\frac{1}{(-\beta_k\cdot k_3-1-i\epsilon)(k_3^2-i\epsilon)} \times\frac{1}{(\beta_j\cdot(k_3+k_1)-3-i\epsilon)}\ . \tag{4.29}$$

Comparing equation (4.29) to equation (3.3), we recognise $\mathcal{C}_{1,k_3,2}$ as the complex conjugate of the one-loop diagram :

$$\begin{aligned}\mathcal{C}_{1,k_3,2}(\alpha_{jk}) &= \big(\mathcal{F}_{(1,1)}(\alpha_{jk})\big)^*\\ &= 2\kappa\Gamma(2\epsilon)r(\alpha_{jk})\big(R_0(\alpha_{jk})+\epsilon R_1(\alpha_{jk})+\mathcal{O}(\epsilon^2)\big)\ ,\end{aligned} \tag{4.30}$$

where the functions R_i are defined in equation (3.32).

We can calculate $\mathcal{C}_{1,k_3,1}(\beta_j\cdot k_1,\beta_j\cdot\beta_k)$ by Fourier transforming to configuration space and then using the same approach as developed in [27]. We thus obtain

$$\begin{aligned}&\mathcal{C}_{1,k_3,1}(\beta_j\cdot k_1,\beta_j\cdot\beta_k)\\ &= -2\beta_j\cdot\beta_k\Gamma(2\epsilon)\kappa\int_0^1 dx\frac{\big((1+(1-x)(2-\beta_j\cdot k_1)+i\epsilon)\big)^{-2\epsilon}}{\big((1-x)^2+x^2-2x(1-x)\beta_j\cdot\beta_k+i\epsilon\big)^{1-\epsilon}}\ .\end{aligned} \tag{4.31}$$

When $\beta_j\cdot k_1=2$, the numerator of the integrand simplifies to 1, and the expression reduces to $-\mathcal{C}_{1,k_3,2}(\alpha_{jk})$, as we would expect. However, we are more interested in the result for general $\beta_j\cdot k_1$, and in particular the asymptotic behaviour in

the region where the overall divergence is generated. When performing the k_1 integral, we will see that the overall divergence comes from the region $\beta_j \cdot k_1 \to \infty$. We hence perform an asymptotic expansion in this kinematic region, where the $(1-x)\beta_j \cdot k_1$ part of the numerator is dominant:

$$\mathcal{C}_{1,k_3,1}(\beta_j \cdot k_1, \beta_j \cdot \beta_k) = -2\kappa\Gamma(2\epsilon)(\beta_j \cdot k_1)^{-2\epsilon} e^{-2i\pi\epsilon} X(\alpha_{jk}) + \mathcal{O}(1) \ , \tag{4.32}$$

where

$$\begin{aligned} X(\alpha_{jk}) &= \beta_j \cdot \beta_k \int_0^1 dx \frac{(1-x)^{-2\epsilon}}{\big((1-x)^2 + x^2 - 2x(1-x)\beta_j \cdot \beta_k + i\epsilon\big)^{1-\epsilon}} \\ &= r(\alpha_{jk}) \Bigg[\ln(\alpha_{jk}) + \epsilon \Bigg(2G(-1,0,\alpha_{jk}) \\ &\quad - 2G(0,0,\alpha_{jk}) + 2G(1,0,\alpha_{jk}) - \frac{\pi^2}{6} \Bigg) + \mathcal{O}(\epsilon^2) \Bigg] \\ &= r(\alpha_{jk}) \big(X_0(\alpha_{jk}) + \epsilon X_1(\alpha_{jk}) \big) + \mathcal{O}(\epsilon^2) \ , \end{aligned} \tag{4.33}$$

where the X_i are defined implicitly in the last line. Notice that X differs from R via the extra factor of $(1-x)^{-2\epsilon}$ in the numerator. This implies that

$$R_0(\alpha_{jk}) = X_0(\alpha_{jk}) \ , \tag{4.34}$$

so it seems that these two contributions cancel at leading order:

$$\begin{aligned} \mathcal{C}_{1,k_3}(\beta_j \cdot k_1, \beta_j \cdot \beta_k) &= \frac{2\kappa\Gamma(2\epsilon) r(\alpha_{jk})}{-\beta_j \cdot k_1 - 2} \Bigg(R_0(\alpha_{jk}) + \epsilon R_1(\alpha_{jk}) \\ &\quad - (\beta_j \cdot k_1)^{-2\epsilon} e^{-2i\pi\epsilon} \big(X_0(\alpha_{jk}) + \epsilon X_1(\alpha_{jk}) \big) \Bigg) + \mathcal{O}(\epsilon) \\ &= \frac{2\kappa\Gamma(2\epsilon) r(\alpha_{jk}) \epsilon}{-\beta_j \cdot k_1 - 2} \Bigg(R_1(\alpha_{jk}) - X_1(\alpha_{jk}) \\ &\quad + \big(2\ln(\beta_j \cdot k_1) + 2\pi i \big) X_0(\alpha_{jk}) \big) \Bigg) + \mathcal{O}(\epsilon) \ . \end{aligned} \tag{4.35}$$

However, (4.35) is deceptive, since we still have to perform the final k_1 integral. When performing the k_1 integral, the factor of $(\beta_j \cdot k_1)^{-2\epsilon}$ in front of $X_0(\alpha_{jk})$ will ensure this part is proportional to $(\beta_j \cdot k_1)^{1-6\epsilon}$ in the region generating the divergence, whereas the part coming with $R_0(\alpha_{jk})$ is proportional to $(\beta_j \cdot k_1)^{1-4\epsilon}$. These terms will give rise to a $\frac{1}{6\epsilon}$ and $\frac{1}{4\epsilon}$ divergence respectively, undoing the cancellation. In (4.35) this will manifest itself via terms proportional to $\epsilon^n \ln^n(\beta_j \cdot k_1)$ that we ignored now, but become leading order in ϵ upon integration over k_1.

It is thus not a good idea to expand the factor of $\beta_j \cdot k_1$ at this point. We conclude that the clearest way to present our result is not (4.35), but

$$\mathcal{C}_{1,k_3}(\beta_j \cdot k_1, \alpha_{jk}) = \frac{2\kappa\Gamma(2\epsilon) r(\alpha_{jk})}{-\beta_j \cdot k_1 - 2} \Bigg(R_0(\alpha_{jk}) + \epsilon R_1(\alpha_{jk}) \\ - e^{-2\pi i\epsilon} (\beta_j \cdot k_1)^{-2\epsilon} \big(X_0(\alpha_{jk}) + \epsilon X_1(\alpha_{jk}) \big) + \mathcal{O}(\epsilon^2) \Bigg) \,. \tag{4.36}$$

4.3.3 Final loop integral

We now put (4.14), (4.26) and (4.36) together to obtain

$$\begin{aligned} \mathcal{C}_1(\alpha_{ij}, \alpha_{jk}) = (2\pi i)^3 \frac{\mu^{4\epsilon}}{m^{4\epsilon}} g_s^4 \int \frac{d^d k_1}{(2\pi)^d} \Bigg[& \frac{\delta(-\beta_i \cdot k_1 - 1)}{(k_1^2 + i\epsilon)} \big(T_{1,k_2} + B_{1,k2} \big) \\ & \times \frac{(\beta_i \cdot \beta_j \beta_j - \beta_i) \cdot k_1}{(\beta_j \cdot k_1)^2 - k_1^2} \theta(\beta_j \cdot k_1 - 1)(\beta_j \cdot k_1 - 1)^{1-2\epsilon} \\ & \times \frac{2\kappa\Gamma(2\epsilon) r(\alpha_{jk})}{-\beta_j \cdot k_1 - 2} \Bigg(R_0(\alpha_{jk}) + \epsilon R_1(\alpha_{jk}) \\ & - e^{-2\pi i\epsilon} (\beta_j \cdot k_1)^{-2\epsilon} \big(X_0(\alpha_{jk}) + \epsilon X_1(\alpha_{jk}) \big) + \mathcal{O}(\epsilon^2) \Bigg) \Bigg] \,. \end{aligned} \tag{4.37}$$

By power counting, it is clear that we have a logarithmic divergence for large values of k_1. We want to extract this logarithmic divergence, and then perform the remaining finite integrals as a Laurent series in ϵ. To do this, we first choose a frame:

$$\begin{aligned} k_1 &= (k_{10}, k_{11}\mathbf{v}_{d-1}), \quad \mathbf{v}^2 = 1 \\ \beta_j &= (1, \mathbf{0}_3) \\ \beta_i &= (\cosh\phi, \sinh\phi \mathbf{v'}_3), \quad \mathbf{v'}^2 = 1 \\ \mathbf{v} \cdot \mathbf{v'} &= \cos\tau \\ d^d k_1 &= \frac{2\pi^{1-\epsilon}}{\Gamma(1-\epsilon)} dk_{10} dk_{11} {k_1}^{2-2\epsilon} d\cos\tau (\sin\tau)^{-2\epsilon} \,. \end{aligned} \tag{4.38}$$

We will now give an outline of how to perform the integration. This calculation was performed in Mathematica using the PolyLogTools package. It involved many lengthy intermediate results that we do not state explicitly, but we will explain all the steps, such that it should be straightforward to reproduce the intermediate results.

We will be guided by the knowledge that we have an ultraviolet divergence, coming from integration of an overall scale integral, such as k_{10} and k_{11}.

The delta function $\delta(-\beta_i \cdot k_1 - 1)$ can be used to eliminate k_{11}:

$$k_{11} = \frac{1 + \cosh \phi k_{10}}{\sinh \phi \cos \tau} \ . \tag{4.39}$$

Notice that since $k_{11} > 0$, this means that we only have a solution for $\cos \tau > 0$. In what follows we will still use the variable k_{11} because it is shorter than the expression (4.39), but implicitly we are referring to (4.39).

The ultraviolet divergence will come from the region where $k_{10} \to \infty$. Hence the first step we would like to perform is to calculate the k_{10} integral and extract the two leading orders in ϵ. We are not interested in higher order contributions, since we are only looking for the divergent part of the diagram. However, there are two characteristics of the integrand that make this not completely straightforward: the quadratic denominator of T_{1,k_2} which does not factorise without square roots, and linear factors in k_{10} raised to non-integer powers. The same issues will be encountered when calculating the other cuts of this diagram. We want to rewrite our integrand such that the k_{10} integral looks like

$$\int_1^\infty dk_{10} \frac{(k_{10} - 1)^{-6\epsilon}}{k_{10} + a} = \frac{\pi (a+1)^{-6e}}{\sin(6\pi e)} \ . \tag{4.40}$$

Dealing with quadratic denominator

The denominator of T_{1,k_2}, equation (4.23), is quite complex, which makes it harder to perform the k_{10} integral. However, when using the parametrisation (4.38), we notice that the denominator simplifies for the boundary values of σ:

$$\begin{aligned} k_{10}^2 - k_{11}^2 - 2(k_{10} - 1)(k_{10} - k_{11} \cos \sigma) &\xrightarrow{\sigma \to 1} (k_{10} - k_{11})(k_{11} - k_{10} + 2) \\ &\xrightarrow{\sigma \to -1} -(k_{10} + k_{11})(k_{11} + k_{10} - 2) \ . \end{aligned} \tag{4.41}$$

Therefore, we expect the result of the σ integral to be simple. We expand the T_{1,k_2} integrand in powers of ϵ, which is allowed because the $\cos \sigma$ integral is finite.

$$T_{1,k_2}(k_{10}, k_{11}) = T_{1,k_2,0}(k_{10}, k_{11}) + \epsilon T_{1,k_2,1}(k_{10}, k_{11}) + \mathcal{O}(\epsilon^2) \ . \tag{4.42}$$

We can drop the $i\epsilon$ prescription, because the denominator is always negative in the region where $k_{11} > k_{10}$. $T_{1,k_2,n}$ is then a polylogarithm of weight $n+1$. This can then be rewritten in terms of $n+1$ iterated integrals of a linear denominator.

For example

$$\begin{aligned} T_{1,k_2,0}(k_{10},k_{11}) &= \frac{\pi}{(2\pi)^4}\int_{-1}^{1}\frac{d\cos\sigma}{k_{10}^2-k_{11}^2-2(k_{10}-1)(k_{10}-k_{11}\cos\sigma)} \\ &= \frac{\pi}{(2\pi)^4}\frac{1}{2(k_{10}-1)k_{11}}\ln\left(\frac{(k_{11}-k_{10})(k_{11}-k_{10}+2)}{(k_{11}+k_{10})(k_{11}+k_{10}-2)}\right) \\ &= \frac{\pi}{(2\pi)^4}\frac{-1}{2(k_{10}-1)k_{11}}\int_{-1}^{1}dz\left(\frac{k_{10}}{k_{11}+zk_{10}}+\frac{k_{10}-2}{k_{11}+z(k_{10}-2)}\right)\,. \end{aligned} \tag{4.43}$$

Notice that this simplicity is caused by the fact that the boundary values of the integrand are so simple.

Likewise, $T_{1,k_2,1}$ can be represented as a double integral of a linear denominator, details can be found in the appendix. (D.4) tells us that

$$\begin{aligned} T_{1,k_2}(k_{10},k_{11}) &= \frac{\pi^{-\epsilon}}{\Gamma(1-\epsilon)}\Big((1-2\epsilon\ln 2)T_{1,k_2,0}(k_{10},k_{11})+\epsilon T_{1,k_2,1'}(k_{10},k_{11})\Big) \\ &= \frac{\pi^{-\epsilon}}{\Gamma(1-\epsilon)}\Big(2^{-\epsilon}T_{1,k_2,0}(k_{10},k_{11})+\epsilon T_{1,k_2,1'}(k_{10},k_{11})\Big)+\mathcal{O}(\epsilon^2)\,, \end{aligned} \tag{4.44}$$

where $T_{1,k_2,1'}(k_{10},k_{11})$ is a double integral of a linear denominator. We can now eliminate k_{11} and partial fraction (4.37) with respect to k_{10}.

Non-integer powers of k_{10}

There is one remaining obstacle we have to resolve before the k_{10} integral looks like (4.40): expressions that are linear in k_{10} and raised to a non-integer power. After the elimination of k_{11}, there are three such occurrences:

- ${k_1}_1^{-2\epsilon} = \left(\frac{1+\cosh\phi k_{10}}{\sinh\phi\cos\tau}\right)^{-2\epsilon}$
- $(k_{10}-1)^{-2\epsilon}$
- ${k_1}_0^{-2\epsilon}$.

We can replace them by their asymptotic limit in the region $k_{10}\to\infty$:

$$\begin{aligned} \big(\frac{1+\cosh\phi k_{10}}{\sinh\phi\cos\tau}\big)^{-2\epsilon} &\to \big(\frac{\cosh\phi}{\sinh\phi\cos\tau}\big)^{-2\epsilon}(k_{10}-1)^{-2\epsilon} \\ (k_{10}-1)^{-2\epsilon} &\to (k_{10}-1)^{-2\epsilon} \\ {k_1}_0^{-2\epsilon} &\to (k_{10}-1)^{-2\epsilon}\,. \end{aligned} \tag{4.45}$$

These manipulations are similar to the asymptotic expansion (3.52). The resulting correction will only contribute at NNLO, in the same way as in the case of the $(1,2,1)$ web (3.53). In general, this is how we will deal with factors linear in k, raised to a non-integer power.

After these manipulations, we can now perform the k_{10} integral in terms of Csc functions, as in (4.40). The remaining $\cos\sigma, z, t$ integrals do not give rise to any divergences. Therefore, we can expand our integrand as a Laurent series in ϵ and perform the remaining integrals. The expressions involved are lengthy, but the calculations are straightforward using the Mathematica package PolyLogTools. We therefore only state the final result in here.

Expression for $\mathcal{C}_1(\alpha_{ij}, \alpha_{jk})$

$$\mathcal{C}_1 = -24\pi i \frac{\Gamma(6\epsilon)\kappa^3}{\epsilon} r(\alpha_{jk}) \Big(\mathcal{C}_{1,\mathrm{LO}} + \epsilon \mathcal{C}_{1,\mathrm{NLO}} + \mathcal{O}(\epsilon^2) \Big) \ , \tag{4.46}$$

where the leading order part is a mixed weight function:

$$\mathcal{C}_{1,\mathrm{LO}}(\alpha_{ij}) = \ln \alpha_{jk} \frac{r(\alpha_{ij}) G(0,0,-\alpha_{ij}) + G(0,-\alpha_{ij})}{6} \ . \tag{4.47}$$

The NLO part is structured as follows. It has an imaginary part, coming from the factor of $e^{-2\pi i\epsilon}$ in (4.36), which is proportional to the leading order part. There is also a part which is similar to the leading order part but with the factor of $\ln \alpha_{jk}$ replaced by a weight two function of α_{jk}. This weight two function is composed of the functions R_1, X_1 defined in equations (3.32) and (4.33). Finally, there is a part proportional to $\ln \alpha_{jk}$, times a mixed weight function of α_{ij}:

$$\begin{aligned} \mathcal{C}_{1,\mathrm{NLO}}(\alpha_{ij}) = & \frac{\big(r(\alpha_{ij}) G(0,0,-\alpha_{ij}) + G(0,-\alpha_{ij})\big) \big(3R_1(\alpha_{jk}) - 2X_1(\alpha_{jk}) + 4\pi i \ln \alpha_{jk}\big)}{6} \\ & + \ln \alpha_{jk} \Big(\mathcal{C}_{1,\mathrm{NLO},1}(\alpha_{ij}) + \mathcal{C}_{1,\mathrm{NLO},2}(\alpha_{ij}) + \mathcal{C}_{1,\mathrm{NLO},3}(\alpha_{ij}) \Big) \ , \end{aligned} \tag{4.48}$$

where

$$\begin{aligned} \mathcal{C}_{1,\mathrm{NLO},1}(\alpha_{ij}) &= \frac{\ln(-\alpha_{ij})}{3} \ , \\ \mathcal{C}_{1,\mathrm{NLO},2}(\alpha_{ij}) &= \frac{1}{36} \Big(12G(0,-1,-\alpha_{ij}) + 24G(-1,0,-\alpha_{ij}) - 36G(0,0,-\alpha_{ij}) \\ &\quad + 12G(0,1,-\alpha_{ij}) + 24G(1,0,-\alpha_{ij}) - \pi^2 \Big) + \frac{2r(\alpha_{ij}) G(0,0,-\alpha_{ij}))}{3} \ , \end{aligned}$$

$$\mathcal{C}_{1,\mathrm{NLO},3}(\alpha_{ij}) = r(\alpha_{ij})\bigg(-\frac{1}{36}\pi^2 G(0,-\alpha_{ij}) + \frac{1}{3}G(-1,0,0,-\alpha_{ij}) + \frac{2}{3}G(0,-1,0,-\alpha_{ij}) + \frac{1}{3}G(0,0,-1,-\alpha_{ij}) - \frac{4}{3}G(0,0,0,-\alpha_{ij}) + \frac{1}{3}G(0,0,1,-\alpha_{ij}) + \frac{2}{3}G(0,1,0,-\alpha_{ij}) + \frac{1}{3}G(1,0,0,-\alpha_{ij}) - \frac{\zeta(3)}{6}\bigg) . \tag{4.49}$$

As claimed earlier, it is possible to write these expressions as a sum of products of polylogs of the form $G(\mathbf{a}, -\alpha_{ij})$ and $G(\mathbf{a}, \alpha_{jk})$ separately, with $\mathbf{a}$ a vector with entries $-1, 0, 1$. We also notice that -1 and 1 never occur in the same $\mathbf{a}$. We could thus eliminate -1 from the entries at the cost of introducing functions of the form $G(-\mathbf{a}, \alpha_{ij})$, by making use of the equality $G(\mathbf{a}, -\alpha_{ij}) = G(-\mathbf{a}, \alpha_{ij})$.

It is also worth looking at the $r(\alpha_{ij})$ structure of this expression. $\mathcal{C}_{1,\mathrm{NLO},1}(\alpha_{ij})$ comes without a factor of $r(\alpha_{ij})$, $\mathcal{C}_{1,\mathrm{NLO},3}(\alpha_{ij})$ comes with a factor of $r(\alpha_{ij})$, and $\mathcal{C}_{1,\mathrm{NLO},2}(\alpha_{ij})$ has terms with and without $r(\alpha_{ij})$.

Moreover, we see that all contributions satisfy $\alpha_{ij} \to \frac{1}{\alpha_{ij}}$ antisymmetry, as we expect.

Dispersive integral

Performing the dispersive integral of (4.46) using equation (3.17) gives

$$\mathcal{F}_{A,1}(\alpha_{ij}, \alpha_{jk}) = 12\frac{\Gamma(6\epsilon)\kappa^3}{\epsilon} r(\alpha_{jk})\bigg(\mathcal{F}_{A,1,LO} + \epsilon\mathcal{F}_{A,1,\mathrm{NLO}} + \mathcal{O}(\epsilon^2)\bigg) . \tag{4.50}$$

The leading order part consists of

$$\mathcal{F}_{A,1,LO}(\alpha_{ij}, \alpha_{jk}) = \frac{1}{36}\ln\alpha_{jk}\bigg(\pi^2 r(\alpha_{ij})G(0,\alpha_{ij}) + 6r(\alpha_{ij})G(0,0,0,\alpha_{ij}) + 6G(0,0,\alpha_{ij}) + \pi^2\bigg) . \tag{4.51}$$

This contribution has a mixed weight. The next to leading part will again have a contribution which is proportional to the leading order one, and some genuinely new contributions.

$$\mathcal{F}_{A,1,\mathrm{NLO}} = \frac{1}{36}\big(3R_1(\alpha_{jk}) - 2X_1(\alpha_{jk}) + 4\pi i\ln\alpha_{jk}\big) \times \big(\pi^2 r(\alpha_{ij})G(0,\alpha_{ij}) + 6r(\alpha_{ij})G(0,0,0,\alpha_{ij}) + 6G(0,0,\alpha_{ij}) + \pi^2\big) + \ln(\alpha_{jk})\bigg(G_{2,1}(\alpha_{ij}) + G_{3,1}(\alpha_{ij}) + r(\alpha_{ij})\big(F_{3,1}(\alpha_{ij}) + F_{4,1}(\alpha_{ij})\big)\bigg) , \tag{4.52}$$

where $F_{i,1}$ is a weight i function which has a coefficient of $r(\alpha_{ij})$, and $G_{i,1}$ as a weight i function without a factor of $r(\alpha_{ij})$. X_1 and R_1 are defined in equations (4.33) and (3.32) respectively. The exact expressions for the other functions are

$$\begin{aligned}
G_{2,1}(\alpha_{ij}) &= \frac{1}{3}G(0,0,\alpha_{ij}) + \frac{\pi^2}{6} \ , \\
G_{3,1}(\alpha_{ij}) &= \pi^2\left(\frac{1}{3}G(-1,\alpha_{ij}) - \frac{7}{36}G(0,\alpha_{ij})\right) + \frac{2}{3}G(-1,0,0,\alpha_{ij}) + \frac{1}{3}G(0,-1,0,\alpha_{ij}) \\
&\quad - G(0,0,0,\alpha_{ij}) + \frac{1}{3}G(0,1,0,\alpha_{ij}) + \frac{2}{3}G(1,0,0,\alpha_{ij}) - \frac{\zeta(3)}{6} \ , \\
F_{3,1}(\alpha_{ij}) &= \frac{1}{9}\pi^2 G(0,\alpha_{ij}) + \frac{2}{3}G(0,0,0,\alpha_{ij}) \ , \\
F_{4,1}(\alpha_{ij}) &= \pi^2\left(\frac{1}{18}G(-1,0,\alpha_{ij}) + \frac{1}{3}G(0,-1,\alpha_{ij}) - \frac{1}{4}G(0,0,\alpha_{ij}) + \frac{1}{18}G(1,0,\alpha_{ij})\right) \\
&\quad - \frac{1}{6}\zeta(3)G(0,\alpha_{ij}) + \frac{1}{3}G(-1,0,0,0,\alpha_{ij}) + \frac{2}{3}G(0,-1,0,0,\alpha_{ij}) \\
&\quad + \frac{1}{3}G(0,0,-1,0,\alpha_{ij}) - \frac{4}{3}G(0,0,0,0,\alpha_{ij}) + \frac{1}{3}G(0,0,1,0,\alpha_{ij}) \\
&\quad + \frac{2}{3}G(0,1,0,0,\alpha_{ij}) + \frac{1}{3}G(1,0,0,0,\alpha_{ij}) - \frac{17\pi^4}{540} \ . \qquad (4.53)
\end{aligned}$$

Some observations

When comparing to the expected expression for $\mathcal{F}_A$, (4.6), we see a few differences.

A surprising observation is the $\mathcal{O}(\epsilon^{-2})$ divergence. Indeed, $\mathcal{F}_A$ itself is only $\mathcal{O}(\epsilon^{-1})$ divergent, and this is why we chose to calculate it. However, it is possible for cuts to be more divergent than the diagram itself [71]. We expect the $\mathcal{O}(\epsilon^{-2})$ contribution to cancel that of other cuts, leaving us with a $\mathcal{O}(\epsilon^{-1})$ result.

Another surprise are the weight-two functions of α_{jk}. We expect the final diagram to have just a $\ln \alpha_{jk}$ dependence, and so expect this weight-two contribution to cancel against other cuts as well .

It is finally worth noting that we have a complex part in $\mathcal{F}_{A,1}$, or equivalently a real part in $\mathcal{C}_1$. This is not unexpected, because there is an uncut subloop in this diagram. The real part in $\mathrm{Cut}_1\big(\mathcal{F}_A\big)$ indicates that it is possible to cut this subloop, leading to a double cut. We have not yet studied how to make use of iterated unitarity for Eikonal diagrams in practice, but it would be interesting to investigate this in the future. For scalar diagrams, a framework for using iterated unitarity has been developed in reference [71]. Since we expect $\mathcal{F}_A$ to be real, we also expect this imaginary contribution to cancel against other cuts.

The only contribution that we do not expect to cancel are the $F_{i,1}, G_{i,1}$ functions, so it is worth looking at them in a bit more detail.

The $F_{i,1}, G_{i,1}$ functions satisfy the $\alpha \to \frac{1}{\alpha}$ symmetry, as we would expect. They also again consist of functions of the form $G(\mathbf{a}, \alpha_{ij})$, where $\mathbf{a}$ is a vector with entries $-1, 0, 1$. Again, we could eliminate the entry -1, at the cost of also allowing functions of $-\alpha_{ij}$.

The symbol alphabet of the $F_{i,1}, G_{i,1}$ functions only involves the letters $\alpha_{ij}, (1 - \alpha_{ij}^2)$, as predicted in reference [27].

When calculating the other cuts, we will employ the same strategy as we used for $\mathcal{C}_1$. We first perform two subloops in terms of a remaining third loop momentum. We then rewrite any occurring quadratic denominators in terms of iterated integrals of linear denominators, and massage any factors of the loop momentum raised to a non-integer power. We then finally calculate the resulting integrals, which turn out to be relatively straightforward at this point.

However, the two other cuts pose specific problems that will require some other tools to be employed, as we will see in the next sections.

4.4 Calculation of $\mathcal{C}_2$

Looking back at (4.10), we have

$$\begin{aligned}\mathcal{C}_2(\alpha_{ij}, \alpha_{jk}) = i(2\pi i)^4 \beta_j \cdot \beta_k \frac{\mu^{6\epsilon}}{m^{6\epsilon}} g_s^6 \int \frac{d^d k_1}{(2\pi)^d} \frac{d^d k_2}{(2\pi)^d} \frac{d^d k_3}{(2\pi)^d} \frac{\delta^+((k_1+k_2)^2)\delta^-(k_3^2)}{(k_1^2 + i\epsilon)(k_2^2 + i\epsilon)} \\ \times \frac{(\beta_i \cdot \beta_j \beta_j - \beta_i) \cdot (2k_2 + k_1)}{(-\beta_j \cdot k_2 - 1 + i\epsilon)(-\beta_k \cdot k_3 - 1 - i\epsilon)} \\ \times \frac{\delta(\beta_j \cdot (k_3 - k_2) - 2)\delta(-\beta_i \cdot k_1 - 1)}{(\beta_j \cdot (k_1 + k_3) - 3 - i\epsilon)} \ . \end{aligned} \tag{4.54}$$

This cut does not have any uncut subloops, so we can ignore the $i\epsilon$ prescription. We use the factor of $\delta(\beta_j \cdot (k_3 - k_2) - 2)$ to rewrite this as

$$\begin{aligned}\mathcal{C}_2(\alpha_{ij}, \alpha_{jk}) &= i(2\pi i)^4 \beta_j \cdot \beta_k \frac{\mu^{6\epsilon}}{m^{6\epsilon}} g_s^6 \int \frac{d^d k_1}{(2\pi)^d} \frac{d^d k_2}{(2\pi)^d} \frac{d^d k_3}{(2\pi)^d} \frac{\delta^+((k_1+k_2)^2)\delta^-(k_3^2)}{k_1^2 k_2^2} \\ &\quad \times \frac{(\beta_i \cdot \beta_j \beta_j - \beta_i) \cdot (2k_2 + k_1)}{(-\beta_j \cdot k_2 - 1)(-\beta_k \cdot k_3 - 1)} \\ &\quad \times \frac{\delta(\beta_j \cdot (k_3 - k_2) - 2)\delta(-\beta_i \cdot k_1 - 1)}{(\beta_j \cdot (k_1 + k_2) - 1)} \\ &= i(2\pi i)^4 \beta_j \cdot \beta_k \frac{\mu^{6\epsilon}}{m^{6\epsilon}} g_s^6 \int \frac{d^d k_2}{(2\pi)^d} \frac{1}{k_2^2(-\beta_j \cdot k_2 - 1)} \mathcal{C}_{2,k_1} \mathcal{C}_{2,k_3} \ , \end{aligned} \tag{4.55}$$

where

$$\mathcal{C}_{2,k_1}(\beta_i\cdot k_2,\beta_j\cdot k_2,k_2^2,\beta_i\cdot\beta_j)=\int\frac{d^dk_1}{(2\pi)^d}\frac{\delta^+((k_1+k_2)^2)\delta(-\beta_i\cdot k_1-1)}{k_1^2}\times\frac{(\beta_i\cdot\beta_j\beta_j-\beta_i)\cdot(2k_2+k_1)}{(\beta_j\cdot(k_1+k_2)-1)} \tag{4.56}$$

$$\mathcal{C}_{2,k_3}(\beta_j\cdot\beta_k,\beta_j\cdot k_2)=\int\frac{d^dk_3}{(2\pi)^d}\frac{\delta^-(k_3^2)\delta(\beta_j\cdot(k_3-k_2)-2)}{(-\beta_k\cdot k_3-1)}\ . \tag{4.57}$$

4.4.1 Calculation of $\mathcal{C}_{2,k_3}$

Via (C.9), we know that

$$\mathcal{C}_{2,k_3}(\beta_j\cdot\beta_k,\beta_j\cdot k_2)=\theta(-\beta_j\cdot k_2-2)(-\beta_j\cdot k_2-2)^{1-2\epsilon}C_{2,k_3}\ , \tag{4.58}$$

where

$$C_{2,k_3}=\frac{\pi^{1-\epsilon}}{\Gamma(1-\epsilon)(2\pi)^d}\int_{-1}^{1}d\cos\sigma\frac{(\sin\sigma)^{-2\epsilon}}{(\beta_j\cdot k_2+2)(\cosh\theta-\sinh\theta\cos\sigma)-1)}\ ,$$
$$\beta_j\cdot\beta_k=-\cosh\theta\ . \tag{4.59}$$

4.4.2 Calculation of $\mathcal{C}_{2,k_1}$

$\mathcal{C}_{2,k_1}$ can not be decomposed as easily as $\mathcal{C}_{1,k_2}$ in (4.19), because its dependence on β_i and β_j is more complicated. The best we can do is to decompose the numerator as follows:

$$\begin{aligned}&\mathcal{C}_{2,k_1}(\beta_i\cdot k_2,\beta_j\cdot k_2,k_2^2,\beta_i\cdot\beta_j)\\&=\beta_i\cdot\beta_j\mathcal{T}_{2,k_1}+\beta_i\cdot\beta_j(\beta_j\cdot k_2+1)\mathcal{B}_{2,k_1}+(1-2\beta_i\cdot k_2)\mathcal{B}_{2,k_1}\ ,\end{aligned} \tag{4.60}$$

where

$$\mathcal{T}_{2,k_1}=\int\frac{d^dk_1}{(2\pi)^d}\frac{\delta^+((k_1+k_2)^2)\delta(-\beta_i\cdot k_1-1)}{k_1^2}$$
$$\mathcal{B}_{2,k_1}=\int\frac{d^dk_1}{(2\pi)^d}\frac{\delta^+((k_1+k_2)^2)\delta(-\beta_i\cdot k_1-1)}{k_1^2(\beta_j\cdot(k_1+k_2)-1)}\ . \tag{4.61}$$

The reason why we split up the $\mathcal{B}_{2,k_1}$ coefficient into two parts, is that $(\beta_j\cdot k_2+1)$ cancels a denominator in (4.55), so that the resulting integral becomes easier. Looking at $\mathcal{T}_{2,k_1}$, we see it is the same integral as $\mathcal{T}_{1,k_2}$. We can thus use (C.6) to

obtain

$$\mathcal{T}_{2,k_1}(k_2^2, \beta_i \cdot k_2) = \theta(\beta_i \cdot k_2 - 1)(\beta_i \cdot k_2 - 1)^{1-2\epsilon} T_{2,k_1} \ , \tag{4.62}$$

where

$$\begin{aligned} T_{2,k_1} = & \frac{\pi^{1-\epsilon}}{(2\pi)^d \Gamma(1-\epsilon)} \int_{-1}^{1} d\cos\sigma \\ & \times \frac{(\sin\sigma)^{-2\epsilon}}{(k_2^2 - 2(\beta_i \cdot k_2 - 1)(\beta_i \cdot k_2 - \sqrt{(\beta_i \cdot k_2)^2 - k_2^2}\cos\sigma)} \ . \end{aligned} \tag{4.63}$$

From (C.18) it follows that

$$\begin{aligned} & \mathcal{B}_{2,k_1}(k_2^2, \beta_i \cdot k_2, \beta_j \cdot k_2, \beta_i \cdot \beta_j) \\ & = \theta(\beta_i \cdot k_2 - 1)(\beta_i \cdot k_2 - 1)^{1-2\epsilon} B_{2,k_1} \ , \end{aligned} \tag{4.64}$$

where

$$\begin{aligned} B_{2,k_1} = & \int_{-1}^{1} dx \ d\cos\tau \frac{(\sin\tau)^{-1-2\epsilon}\sqrt{1-x^2}^{-2\epsilon}}{(\cosh\phi(\beta_i \cdot k_2 - 1) - \sinh\phi x(\beta_i \cdot k_2 - 1) - 1)} \\ & \frac{\pi^{1/2-\epsilon}}{\Gamma(1/2-\epsilon)(2\pi)^d} \frac{1}{k_2^2 - 2(\beta_i \cdot k_2 - 1)\big(k_{20} - x k_{21} - \sqrt{1-x^2} k_{22}\cos\tau\big)} \ , \end{aligned} \tag{4.65}$$

with

$$\begin{aligned} \cosh\phi &= \beta_i \cdot \beta_j \\ k_{20} &= \beta_i \cdot k_2 \\ k_{21} &= \frac{\cosh\phi k_{20} - \beta_j \cdot k_2}{\sinh\phi} \\ k_{22} &= \sqrt{k_{20}^2 - k_{21}^2 - k_2^2} \ . \end{aligned} \tag{4.66}$$

4.4.3 Final loop integral

We can now plug equations (4.58) and (4.60) into equation (4.55):

$$\begin{aligned} \mathcal{C}_2(\alpha_{ij}, \alpha_{jk}) = & \, i(2\pi i)^4 \beta_j \cdot \beta_k \frac{\mu^{6\epsilon}}{m^{6\epsilon}} g_s^6 \int \frac{d^d k_2}{(2\pi)^d} \frac{1}{k_2^2(-\beta_j \cdot k_2 - 1)} \mathcal{C}_{2,k_3} \\ & \times \Big(\beta_i \cdot \beta_j \mathcal{T}_{2,k_1} + \beta_i \cdot \beta_j (\beta_j \cdot k_2 + 1)\mathcal{B}_{2,k_1} + (1 - 2\beta_i \cdot k_2)\mathcal{B}_{2,k_1} \Big) \\ = & \, \mathcal{C}_{2,\mathcal{T}}(\alpha_{ij}, \alpha_{jk}) + \mathcal{C}_{2,\mathcal{B},1}(\alpha_{ij}, \alpha_{jk}) + \mathcal{C}_{2,\mathcal{B},2}(\alpha_{ij}, \alpha_{jk}) \ , \end{aligned} \tag{4.67}$$

where we implicitly define

$$\mathcal{C}_{2,\mathcal{T}}(\alpha_{ij},\alpha_{jk}) = i(2\pi i)^4 \beta_j\cdot\beta_k \frac{\mu^{6\epsilon}}{m^{6\epsilon}} g_s^6 \int \frac{d^d k_2}{(2\pi)^d} \frac{1}{k_2^2(-\beta_j\cdot k_2 - 1)} \mathcal{C}_{2,k_3}\beta_i\cdot\beta_j \mathcal{T}_{2,k_1} \ , \tag{4.68}$$

and similarly for $\mathcal{C}_{2,\mathcal{B},1}(\alpha_{ij},\alpha_{jk})$ and $\mathcal{C}_{2,\mathcal{B},2}(\alpha_{ij},\alpha_{jk})$.

We again want to calculate these three expressions as a Laurent series via an asymptotic expansion.

Calculation of $\mathcal{C}_{2,\mathcal{T}}(\alpha_{ij},\alpha_{jk})$

We calculate $\mathcal{C}_{2,\mathcal{T}}(\alpha_{ij},\alpha_{jk})$ in a frame where

$$\begin{aligned}
\beta_i &= (1,\mathbf{0}_3) \\
\beta_j &= (\cosh\phi, \sinh\phi \mathbf{v}_3), \quad \mathbf{v}^2 = 1 \\
k_2 &= (k_{20}, k_{21}\mathbf{v'}_{d-1}), \quad \mathbf{v'}^2 = 1 \\
\mathbf{v}\cdot\mathbf{v}' &= \cos\gamma \\
d^d k_2 &= \frac{2\pi^{1-\epsilon}}{\Gamma(1-\epsilon)} dk_{20} dk_{21} k_{21}^{2-2\epsilon} d\cos\gamma (\sin\gamma)^{-2\epsilon} \ .
\end{aligned} \tag{4.69}$$

We saw earlier how in this frame we can rewrite $\mathcal{T}_{2,k_1}(\alpha_{ij},\alpha_{jk})$ in terms of iterated integrals of linear denominators, so that we can partial fraction the integrand.

One difference with the calculation of $\mathcal{C}_1$ is that we do not have a delta function to eliminate k_{21}. We thus have two remaining scales, and hence two ultraviolet divergent integrals, the k_{20} and k_{21} ones. Instead of delta functions, we now have two theta functions $\theta(k_{10}-1)\theta(k_{21}\sinh\phi\cos\gamma - k_{20}\cosh\phi - 2)$. This can be represented as

$$\begin{aligned}
\mathcal{C}_{2,\mathcal{T}}(\alpha_{ij},\alpha_{jk}) &= \int_{-\infty}^{\infty} dk_{20} \int_0^{\infty} dk_{21} k_{21}^{2-2\epsilon} \int_{-1}^{1} d\cos\gamma \ \theta(k_{10}-1) \\
&\qquad \times \theta(k_{21}\sinh\phi - k_{20}\cosh\phi - 2) \mathcal{I}_{2,\mathcal{T}}(\alpha_{ij},\alpha_{jk},k_{20},k_{21}) \\
&= \int_1^{\infty} dk_{20} \int_0^1 d\cos\gamma \int_{\frac{r(\alpha_{ij})}{\cos\gamma} k_{20} + \frac{2}{\sinh\phi\cos\gamma}}^{\infty} dk_{21} \mathcal{I}_{2,\mathcal{T}}(\alpha_{ij},\alpha_{jk},k_{20},k_{21}) \ ,
\end{aligned} \tag{4.70}$$

where

$$\mathcal{I}_{2,\mathcal{T}}(\alpha_{ij},\alpha_{jk},k_{20},k_{21}) = i(2\pi i)^4 \frac{2\pi^{1-\epsilon}}{\Gamma(1-\epsilon)} \frac{\mu^{6\epsilon}}{m^{6\epsilon}} g_s^6 \beta_i\cdot\beta_j\beta_j\cdot\beta_k (\sin\gamma)^{-2\epsilon} \\ \times \frac{(\beta_i\cdot k_1 - 1)^{1-2\epsilon}}{k_2^2(-\beta_j\cdot k_2 - 1)} T_{2,k_1}(-\beta_j\cdot k_2 - 2)^{1-2\epsilon} C_{2,k_3} \quad (4.71)$$

captures the rest of the integrand.

The lower integration boundary for k_{21} seems to suggest to change variables via

$$k_{21} = \alpha + \beta k_{20}, \qquad \alpha = \frac{2}{\sinh\phi\cos\gamma} \ , \quad (4.72)$$

so that

$$\mathcal{C}_{2,\mathcal{T}}(\alpha_{ij},\alpha_{jk}) = \int_1^\infty dk_{20} \int_0^1 d\cos\gamma \int_{\frac{r(\alpha_{ij})}{\cos\gamma}}^\infty d\beta \quad k_{20}\mathcal{I}_{2,\mathcal{T}}(\alpha_{ij},\alpha_{jk},k_{20},\beta) \ . \quad (4.73)$$

When inspecting the resulting integrand $k_{20}\mathcal{I}_{2,\mathcal{T}}(\alpha_{ij},\alpha_{jk},k_{20},\beta)$, we see that the k_{20} integral generates a divergence in the region where $k_{20}\to\infty$, and the β integral generates a divergence for $\beta\to\frac{r(\alpha_{ij})}{\cos\gamma}$. This tells us how to perform the asymptotic expansion for the terms raised to a non-integer power in the integrand:

$$\begin{aligned} {k_2}_1^{-2\epsilon} &= (\alpha+\beta k_{20})^{-2\epsilon} \\ &\to \beta^{-2\epsilon}(k_{20}-1)^{-2\epsilon} \\ (\beta_i\cdot k_2 - 1)^{-2\epsilon} &= (k_{20}-1)^{-2\epsilon} \\ &\to (k_{20}-1)^{-2\epsilon} \\ (-\beta_j\cdot k_2 - 2)^{-2\epsilon} &= (\cos\gamma\sinh\phi k_{21} - \cosh\phi k_{20} - 2)^{-2\epsilon} \\ &= \big(\sinh\phi\cos\gamma(\beta - r(\alpha_{ij}))k_{20}\big)^{-2\epsilon} \\ &\to (\sinh\phi\cos\gamma)^{-2\epsilon}(\beta - r(\alpha_{ij})^{-2\epsilon}(k_{10}-1)^{-2\epsilon} \ . \end{aligned} \quad (4.74)$$

These replacements will again give us the correct LO and NLO results. The other factors raised to a non-integer power do not need an asymptotic expansion because they do not give rise to divergences.

Using (4.74), we can now perform the k_{20} integral in (4.73) in terms of csc functions. This leaves us with

$$\mathcal{C}_{2,\mathcal{T}}(\alpha_{ij},\alpha_{jk}) = \int_0^1 d\cos\gamma \int_{\frac{r(\alpha_{ij})}{\cos\gamma}}^\infty d\beta \quad \mathcal{I}'_{2,\mathcal{T}}(\alpha_{ij},\alpha_{jk},\beta) \ , \quad (4.75)$$

where $\mathcal{I}'_{2,\mathcal{T}}(\alpha_{ij},\alpha_{jk},\beta)$ is the resulting integrand.

We now calculate the remaining divergent integral in the variable β. It suffices to calculate this as a Laurent series, because all the other integrals are finite.

For values of β close to $\frac{r(\alpha_{ij})}{\cos\gamma}$, we have

$$\mathcal{I}'_{2,\mathcal{T}}(\alpha_{ij},\alpha_{jk},\beta) \to (\beta - \frac{r(\alpha_{ij})}{\cos\gamma})^{6\epsilon-1}\mathcal{I}''_{2,\mathcal{T}}(\alpha_{ij},\alpha_{jk},\frac{r(\alpha_{ij})}{\cos\gamma}) \ . \tag{4.76}$$

It is thus convenient to manipulate (4.75) as follows:

$$\mathcal{C}_{2,\mathcal{T}}(\alpha_{ij},\alpha_{jk}) = \mathcal{C}_{2,\mathcal{T},1} + \mathcal{C}_{2,\mathcal{T},2} \ , \tag{4.77}$$

where

$$\begin{aligned}
\mathcal{C}_{2,\mathcal{T},1} &= \int_{\frac{r(\alpha_{ij})}{\cos\gamma}}^{\infty} d\beta \ \ \frac{r(\alpha_{ij})}{\cos\gamma\beta}(\beta - \frac{r(\alpha_{ij})}{\cos\gamma})^{6\epsilon-1}\mathcal{I}''_{2,\mathcal{T}}(\alpha_{ij},\alpha_{jk},r(\alpha_{ij})) \\
\mathcal{C}_{2,\mathcal{T},2} &= \int_{\frac{r(\alpha_{ij})}{\cos\gamma}}^{\infty} d\beta \Bigg(\mathcal{I}'_{2,\mathcal{T}}(\alpha_{ij},\alpha_{jk},\beta) \\
&\qquad - \frac{r(\alpha_{ij})}{\cos\gamma\beta}(\beta - \frac{r(\alpha_{ij})}{\cos\gamma})^{6\epsilon-1}\mathcal{I}''_{2,\mathcal{T}}(\alpha_{ij},\alpha_{jk},\frac{r(\alpha_{ij})}{\cos\gamma}) \Bigg) \ .
\end{aligned} \tag{4.78}$$

$\mathcal{C}_{2,\mathcal{T},1}$ will then capture the divergence for $\beta \to \frac{r(\alpha_{ij})}{\cos\gamma}$, with the extra factor of $\frac{r(\alpha_{ij})}{\beta\cos\gamma}$ included to ensure finiteness when $\beta \to \infty$. Its dependence on β is very simple, so that it can be calculated exactly:

$$\mathcal{C}_{2,\mathcal{T},1} = \frac{\pi}{\sin(6\epsilon\pi)}\mathcal{I}''_{2,\mathcal{T}}(\alpha_{ij},\alpha_{jk},r(\alpha_{ij}))\left(\frac{r(\alpha_{ij})}{\cos\gamma}\right)^{6\epsilon} \ . \tag{4.79}$$

The β integral of $\mathcal{C}_{2,\mathcal{T},2}$ is finite by construction, so we can expand the integrand in powers of ϵ and perform the remaining finite integral. It is straightforward using the PolyLogTools package.

After this step, we still have to perform the finite integrals over the parameters $\cos\sigma, z, t$. However, these are also straightforward using PolyLogTools. We thus only give the final result.

Expression for $\mathcal{C}_{2,\mathcal{T}}\big(\mathcal{F}_A\big)(\alpha_{ij},\alpha_{jk})$

We have

$$\mathcal{C}_{2,\mathcal{T}}\big(\mathcal{F}_A\big)(\alpha_{ij},\alpha_{jk}) = -24\pi i\frac{\kappa^3\Gamma(6\epsilon)}{\epsilon}r(\alpha_{jk})\bigg(\mathcal{C}_{2,\mathcal{T},LO} + \epsilon\mathcal{C}_{2,\mathcal{T},\mathrm{NLO}} + \mathcal{O}(\epsilon^2)\bigg)\ , \tag{4.80}$$

with

$$\mathcal{C}_{2,\mathcal{T},\mathrm{LO}}(\alpha_{ij}) = -\frac{r(\alpha_{ij})G(0,0,-\alpha_{ij})\ln\alpha_{jk}}{6}\ . \tag{4.81}$$

The NLO part again has a part which is similar to the leading order part but with a weight two dependence on α_{jk}, and a mixed weight part proportional to $\ln\alpha_{jk}$:

$$\begin{aligned}\mathcal{C}_{2,\mathcal{T},\mathrm{NLO}}(\alpha_{ij}) = &-\frac{r(\alpha_{ij})G(0,0,-\alpha_{ij})\big(3R_1(\alpha_{jk}) - 2X_1(\alpha_{jk})\big)}{6}\\ &+\ln\alpha_{jk}\bigg(\mathcal{C}_{2,\mathcal{T},\mathrm{NLO},1}(\alpha_{ij}) + \mathcal{C}_{2,\mathcal{T},\mathrm{NLO},2}(\alpha_{ij}) + \mathcal{C}_{2,\mathcal{T},\mathrm{NLO},3}(\alpha_{ij})\bigg)\ .\end{aligned} \tag{4.82}$$

As expected, we have a purely imaginary discontinuity. We will not provide explicit results for $\mathcal{C}_{2,\mathcal{T},\mathrm{NLO}}(\alpha_{ij})$. This expression can be deduced from $\mathcal{F}_{A,2,\mathcal{T},\mathrm{NLO}}(\alpha_{ij})$ below by calculating the discontinuity.

Dispersive integral of $\mathcal{C}_{2,\mathcal{T}}\big(\mathcal{F}_A\big)(\alpha_{ij},\alpha_{jk})$

We can again perform the dispersive integral of this part of the cut to obtain $\mathcal{F}_{A,2,\mathcal{T}}$. It has a similar structure as $\mathcal{F}_{A,1}$:

$$\mathcal{F}_{A,2,\mathcal{T}}\big(\mathcal{F}_A\big)(\alpha_{ij},\alpha_{jk}) = 12\frac{\Gamma(6\epsilon)\kappa^3}{\epsilon}r(\alpha_{jk})\bigg(\mathcal{F}_{A,2,\mathcal{T},\mathrm{LO}} + \epsilon\mathcal{F}_{A,2,\mathcal{T},\mathrm{NLO}} + \mathcal{O}(\epsilon^2)\bigg)\ , \tag{4.83}$$

where

$$\mathcal{F}_{A,2,\mathcal{T},\mathrm{LO}} = -\frac{1}{36}\ln\alpha_{jk}\left(\pi^2 r(\alpha_{ij})G(0,\alpha_{ij}) + 6r(\alpha_{ij})G(0,0,0,\alpha_{ij}) + \pi^2\right)\ . \tag{4.84}$$

The next to leading part will again have a contribution which is proportional to the leading order one, and some genuinely new contributions.

$$\begin{aligned}\mathcal{F}_{A,2,\mathcal{T},\mathrm{NLO}} = &-\frac{1}{36}\big(3R_1(\alpha_{jk}) - 2X_1(\alpha_{jk})\big)\\ &\times\big(\pi^2 r(\alpha_{ij})G(0,\alpha_{ij}) + 6r(\alpha_{ij})G(0,0,0,\alpha_{ij}) + \pi^2\big)\\ &+\ln(\alpha_{jk})\bigg(G_{2,2,\mathcal{T}}(\alpha_{ij}) + G_{3,2,\mathcal{T}}(\alpha_{ij})\\ &+ r(\alpha_{ij})\big(F_{3,2,\mathcal{T}}(\alpha_{ij}) + F_{4,2,\mathcal{T}}(\alpha_{ij})\big)\bigg)\ ,\end{aligned} \tag{4.85}$$

with

$$\begin{aligned}G_{2,2,\mathcal{T}}(\alpha_{ij}) &= -\frac{\pi^2}{18}\ ,\\ G_{3,2,\mathcal{T}}(\alpha_{ij}) &= -\frac{\zeta(3)}{3}\ ,\\ F_{3,2,\mathcal{T}}(\alpha_{ij}) &= 0\ ,\\ F_{4,2,\mathcal{T}}(\alpha_{ij}) &= \pi^2\left(-\frac{1}{18}G(-1,0,\alpha_{ij}) + \frac{1}{12}G(0,0,\alpha_{ij}) - \frac{1}{18}G(1,0,\alpha_{ij})\right)\\ &\quad - \frac{1}{3}G(-1,0,0,0,\alpha_{ij}) - \frac{1}{3}G(0,0,-1,0,\alpha_{ij}) + \frac{2}{3}G(0,0,0,0,\alpha_{ij})\\ &\quad - \frac{1}{3}G(0,0,1,0,\alpha_{ij}) - \frac{1}{3}G(1,0,0,0,\alpha_{ij}) + \frac{7\pi^4}{1080} - \frac{1}{6}\zeta(3)G(0,\alpha_{ij})\ .\end{aligned} \tag{4.86}$$

Calculation of $\mathcal{C}_{2,\mathcal{B},1}(\alpha_{ij},\alpha_{jk})$

By definition (4.67),

$$\mathcal{C}_{2,\mathcal{B},1}(\alpha_{ij},\alpha_{jk}) = -i(2\pi i)^4\beta_i\cdot\beta_j\beta_j\cdot\beta_k\frac{\mu^{6\epsilon}}{m^{6\epsilon}}g_s^6\int\frac{d^dk_2}{(2\pi)^d}\frac{1}{k_2^2}\mathcal{C}_{2,k_3}\mathcal{B}_{2,k_1}\ . \tag{4.87}$$

As before, we know how to rewrite $\mathcal{C}_{2,k_3}$ in terms of iterated integrals of a linear denominator. To deal with $\mathcal{B}_{2,k_1}$, we work in the frame in which (4.64) has been derived:

$$\begin{aligned}\beta_i &= (1,\mathbf{0}_3)\\ \beta_j &= (\cosh\phi,\sinh\phi,\mathbf{0}_2)\\ k_2 &= (k_{20},k_{21},k_{22}\mathbf{v}_{d-2}),\quad \mathbf{v}^2 = 1\ ,\end{aligned} \tag{4.88}$$

so that we can use the expression (4.64). The integral can be expressed as

$$\begin{aligned}\mathcal{C}_{2,\mathcal{B},1}(\alpha_{ij},\alpha_{jk}) &= \int_{-\infty}^{\infty} dk_{20}\int_{-\infty}^{\infty} dk_{21}\int_{0}^{\infty} dk_{22}k_{22}^{1-2\epsilon} \\ &\quad\times\theta(k_{20}-1)\theta(\sinh\phi k_{21}-\cosh\phi k_{20}-2)\mathcal{I}_{2,\mathcal{B},1} \\ &= \int_{1}^{\infty} dk_{20}\int_{r(\alpha_{ij})k_{20}+\frac{2}{\sinh\phi}}^{\infty} dk_{21}\int_{0}^{\infty} dk_{22}k_{22}^{1-2\epsilon}\mathcal{I}_{2,\mathcal{B},1}\ , \end{aligned} \tag{4.89}$$

where

$$\begin{aligned}\mathcal{I}_{2,\mathcal{B},1}(\alpha_{ij},\alpha_{jk},k_{20},k_{21},k_{22}) &= i(2\pi i)^4\frac{2\pi^{1-\epsilon}}{\Gamma(1-\epsilon)}\frac{\mu^{6\epsilon}}{m^{6\epsilon}}g_s^6\beta_i\cdot\beta_j\beta_j\cdot\beta_k \\ &\quad\times\frac{(\beta_i\cdot k_1-1)^{1-2\epsilon}}{k_2^2}B_{2,k_1}(-\beta_j\cdot k_2-2)^{1-2\epsilon}C_{2,k_3}\ .\end{aligned} \tag{4.90}$$

We can turn k_{22} into a scaleless variable as follows

$$k_{22} = \sqrt{Z}\sqrt{k_{21}^2-k_{20}^2}\ , \tag{4.91}$$

and then again write

$$k_{21} = \alpha+\beta k_{20}\ , \tag{4.92}$$

so that

$$\mathcal{C}_{2,\mathcal{B},1}(\alpha_{ij},\alpha_{jk}) = \int_{1}^{\infty} dk_{20}\ k_{20}\int_{r(\alpha_{ij})}^{\infty} d\beta\int_{0}^{\infty}\frac{dZ}{2}Z^{-\epsilon}\big((\alpha+\beta k_{20})^2-k_{20}^2\big)^{1-\epsilon}\mathcal{I}_{2,\mathcal{B},1}\ . \tag{4.93}$$

The contribution to $\mathcal{I}_{2,\mathcal{B},1}$ coming from $\mathcal{B}_{2,k_1}$ has a quadratic denominator, so we cannot perform the k_{20} integral exactly. However, we can extract the leading divergence by looking at the behaviour of our integrand in the limit $k_{20}\to\infty$:

$$k_{20}\big((\alpha+\beta k_{20})^2-k_{20}^2\big)^{1-\epsilon}\mathcal{I}_{2,\mathcal{B},1}\to k_{20}^{-1-6\epsilon}\mathcal{I}'_{2,\mathcal{B},1}\ . \tag{4.94}$$

We then find that the other integrals are finite, meaning that

$$\mathcal{C}_{2,\mathcal{B},1}(\alpha_{ij},\alpha_{jk}) = \frac{1}{6\epsilon}\int_{r(\alpha_{ij})}^{\infty} d\beta\int_{0}^{\infty}\frac{dZ}{2}Z^{-\epsilon}\mathcal{I}'_{2,\mathcal{B},1}+\mathcal{O}(1)\ . \tag{4.95}$$

This means that all the information we need to calculate the $\mathcal{O}(\epsilon^{-1})$ divergence is contained in $\mathcal{I}'_{2,\mathcal{B},1}$. Because $\mathcal{C}_{2,\mathcal{B},1}(\alpha_{ij},\alpha_{jk})$ is only $\mathcal{O}(\epsilon^{-1})$ divergent , we did not have to perform the k_{20} integral exactly, but got away with just looking at the limiting behaviour in the region $k_{20}\to\infty$.

The remaining finite integrals are again straightforward to perform using PolyLogTools, as is the dispersive integral.

Dispersive integral of $\mathcal{C}_{2,\mathcal{B},1}$

We find that

$$\mathcal{F}_{A,2,\mathcal{B}_1}\big(\mathcal{F}_A\big)(\alpha_{ij},\alpha_{jk}) = 12\Gamma(6\epsilon)\kappa^3 r(\alpha_{jk})\mathcal{F}_{A,2,\mathcal{B}_1,\mathrm{LO}} + \mathcal{O}(1)\ , \tag{4.96}$$

where

$$\mathcal{F}_{A,2,\mathcal{B}_1,\mathrm{LO}} = \ln(\alpha_{jk})\bigg(G_{2,2,\mathcal{B}_1}(\alpha_{ij}) + G_{3,2,\mathcal{B}_1}(\alpha_{ij}) + r(\alpha_{ij})\big(F_{3,2,\mathcal{B}_1}(\alpha_{ij}) + F_{4,2,\mathcal{B}_1}(\alpha_{ij})\big)\bigg)\ , \tag{4.97}$$

with

$$\begin{aligned}
G_{2,2,\mathcal{B}_1}(\alpha_{ij}) &= 0\ ,\\
G_{3,2,\mathcal{B}1}(\alpha_{ij}) &= \frac{1}{6}\left(2\pi^2\ln 2 - 3\zeta(3)\right)\ ,\\
F_{3,2,\mathcal{B}_1}(\alpha_{ij}) &= 0\ ,\\
F_{4,2,\mathcal{B}_1}(\alpha_{ij}) &= \frac{1}{120}\bigg(-40\zeta(3)G(0,\alpha_{ij}) + 40\pi^2 G(0,-1,\alpha_{ij})\\
&\qquad - 20\pi^2 G(0,0,\alpha_{ij}) + 80G(0,-1,0,0,\alpha_{ij})\\
&\qquad - 80G(0,0,0,0,\alpha_{ij}) + 80G(0,1,0,0,\alpha_{ij}) - 3\pi^4\bigg)\ .
\end{aligned} \tag{4.98}$$

Equation (4.98) is the first occurrence of a factor of $\ln 2$ in the expressions forming the $\mathcal{F}_{A,i}$. We do not expect such terms in the final result, so that this term should cancel against one of the contributions calculated below.

We also notice that this contribution is less divergent than other contributions to $\mathcal{F}_{A,2}$. We investigate why below.

Why do we only have a $\mathcal{O}(\epsilon^{-1})$ divergence?

It is remarkable that (4.96) reveals only a $\mathcal{O}(\epsilon^{-1})$ divergence, whereas when calculating $\mathcal{C}_{2,\mathcal{T}}(\alpha_{ij},\alpha_{jk})$, we had a double divergence. This divergence was

generated in the region where

$$\begin{aligned} k_{20} &\to \infty \\ \beta &\to \frac{r(\alpha_{ij})}{\cos\gamma} \ . \end{aligned} \tag{4.99}$$

In this limit

$$\begin{aligned} \beta_j \cdot k_2 &= \cosh\phi k_{20} - \sinh\phi k_{21}\cos\gamma \\ &= \cosh\phi k_{20}\big(1 - \frac{\beta\cos\gamma}{r(\alpha_{ij})}\big) - 2 \\ &\to \big(\infty \times 0\big) - 2 \ . \end{aligned} \tag{4.100}$$

This $\infty \times 0$ is not well-defined, but indicates that some interesting behaviour can happen in this limit. It is reasonable to assume that it will generate a divergence via the factor

$$\begin{aligned} \frac{1}{-\beta_j \cdot k_2 - 1} &= \frac{-1}{\cosh\phi k_{20}\big(1 - \frac{\beta\cos\gamma}{r(\alpha_{ij})}\big) - 1} \\ &\to \frac{-1}{\cosh\phi\big(1 - \frac{\beta\cos\gamma}{r(\alpha_{ij})}\big)} \ , \end{aligned} \tag{4.101}$$

where we indicated the leading order term left after the k_{20} integration. It will give a divergence when $\beta \to \frac{r(\alpha_{ij})}{\cos\gamma}$. The factor (4.101) occurs in the integrand of $\mathcal{C}_{2,\mathcal{T}}$, but is cancelled in the integrand of $\mathcal{C}_{2,\mathcal{B},1}$, via the prefactor $\beta_j \cdot k_2 + 1$. This might explain why $\mathcal{C}_{2,\mathcal{B},1}$ is less divergent than $\mathcal{C}_{2,\mathcal{T}}$. However, according to this reasoning we should again expect a $\mathcal{O}(\epsilon^{-2})$ divergence for $\mathcal{C}_{2,\mathcal{B},2}$ which is calculated in the next section.

Calculation of $\mathcal{C}_{2,\mathcal{B},2}(\alpha_{ij}, \alpha_{jk})$

By definition (4.67),

$$\begin{aligned} \mathcal{C}_{2,\mathcal{B},2}(\alpha_{ij}, \alpha_{jk}) = i(2\pi i)^4 \beta_j \cdot \beta_k \frac{\mu^{6\epsilon}}{m^{6\epsilon}} g_s^6 \int \frac{d^d k_2}{(2\pi)^d} \frac{1}{k_2^2(-\beta_j \cdot k_2 - 1)} \mathcal{C}_{2,k_3} \\ \times (1 - 2\beta_i \cdot k_2)\mathcal{B}_{2,k_1} \ . \end{aligned} \tag{4.102}$$

As in the case of $\mathcal{C}_{2,\mathcal{B},1}(\alpha_{ij}, \alpha_{jk})$, we have an integrand that includes $\mathcal{B}_{2,k_1}$. However, we expect that this cut is $\mathcal{O}(\epsilon^{-2})$ divergent, so we will have to be more careful in our calculation.

We again work in the following frame

$$\begin{aligned}\beta_i &= (1, \mathbf{0}_3)\\ \beta_j &= (\cosh\phi, \sinh\phi, \mathbf{0}_2)\\ k_2 &= (k_{20}, k_{21}, k_{22}\mathbf{v}_{d-2}), \quad \mathbf{v}^2 = 1 \ ,\end{aligned} \tag{4.103}$$

and turn k_{22} into a scaleless variable via

$$k_{22} = \sqrt{Z}\sqrt{k_{21}^2 - k_{20}^2} \ , \tag{4.104}$$

and then again write

$$k_{21} = \alpha + \beta k_{20} \ . \tag{4.105}$$

The divergences will again be generated in the region

$$\begin{aligned}k_{20} &\to \infty\\ \beta &\to r(\alpha_{ij}) \ .\end{aligned} \tag{4.106}$$

The integrals in the other variables will be finite, in particular the Z and $\cos\tau$ integrals, with the variable τ introduced in equation (4.64). We make use of this to expand the integrand in powers of ϵ, so that

$$\begin{aligned}\mathcal{C}_{2,\mathcal{B},2}(\alpha_{ij},\alpha_{jk}) &= \int_1^\infty dk_{20}\int_{r(\alpha_{ij})}^\infty d\beta k_{20}\int_0^\infty dZ\, Z^{-\epsilon}(\sin\tau)^{-2\epsilon}\mathcal{I}_{2,\mathcal{B},2,LO}\\ &= \int_1^\infty dk_{20}\int_{r(\alpha_{ij})}^\infty d\beta k_{20}\int_0^\infty dZ\ \mathcal{I}_{2,\mathcal{B},2,LO}\\ &\quad\left(1-\epsilon\big(2\ln Z + \ln(1-\cos\tau) + \ln(1+\cos\tau)\big) + \mathcal{O}(\epsilon^2)\right)\\ &= \mathcal{C}_{2,\mathcal{B},2,\mathrm{LO}}(\alpha_{ij},\alpha_{jk}) + \mathcal{C}_{2,\mathcal{B},2,\mathrm{NLO}}(\alpha_{ij},\alpha_{jk}) + \mathcal{O}(1) \ ,\end{aligned} \tag{4.107}$$

where

$$\begin{aligned}\mathcal{I}_{2,\mathcal{B},2}(\alpha_{ij},\alpha_{jk},k_{20},k_{21},Z) &= i(2\pi i)^4\frac{2\pi^{1-\epsilon}}{\Gamma(1-\epsilon)}\frac{\mu^{6\epsilon}}{m^{6\epsilon}}g_s^6\beta_j\cdot\beta_k(-\beta_j\cdot k_2 - 2)^{1-2\epsilon}\\ &\quad\times\frac{(1-2\beta_i\cdot k_2)(\beta_i\cdot k_1 - 1)^{1-2\epsilon}}{(1+Z)(k_{20}^2-k_{21}^2)(-\beta_j\cdot k_2 - 1)}B_{2,k_1}C_{2,k_3}\\ &\quad\times\left((\alpha+\beta k_{20})^2 - k_{20}^2\right)^{1-\epsilon}\\ \mathcal{C}_{2,\mathcal{B},2,\mathrm{LO}}(\alpha_{ij},\alpha_{jk}) &= \int_1^\infty dk_{20}\int_{r(\alpha_{ij})}^\infty d\beta k_{20}\int_0^\infty dZ\ \mathcal{I}_{2,\mathcal{B},2,LO}\end{aligned} \tag{4.108}$$

$$\mathcal{C}_{2,\mathcal{B},2,\mathrm{NLO}}(\alpha_{ij},\alpha_{jk}) = -\epsilon \int_1^\infty dk_{20} \int_{r(\alpha_{ij})}^\infty d\beta k_{20} \int_0^\infty dZ\ \mathcal{I}_{2,\mathcal{B},2,LO} \times \Big(2\ln Z + \ln(1-\cos\tau) + \ln(1+\cos\tau)\Big) \quad (4.109)$$

Calculation of $\mathcal{C}_{2,\mathcal{B},2,LO}(\alpha_{ij},\alpha_{jk})$

We first focus on $\mathcal{C}_{2,\mathcal{B},2,LO}(\alpha_{ij},\alpha_{jk})$. We again perform the integrals that make the integrand simpler first, with the goal of obtaining an integrand which can be partial fractioned so that we can perform the k_{20} integral exactly.

After trying some combinations, it turns out that preforming the $\cos\tau$ and Z integrals first makes the integrand simpler. When extracting the Z- and $\cos\tau$-dependent part of the integrand, we obtain

$$\begin{aligned}
&\mathcal{I}_{2,\mathcal{B},2,LO,Z}(k_{20},\beta) = \int_0^\infty dZ\ \mathcal{I}_{2,\mathcal{B},2,LO}(Z) \\
&= \int_{-1}^1 dx\ \mathcal{I}'_{2,\mathcal{B},2,LO} \int_0^\infty dZ \frac{1}{1+Z} \int_{-1}^1 \frac{d\cos\tau}{\sqrt{1-\cos^2\tau}} \\
&\times \frac{1}{(k_{20}^2-k_{21}^2)(1+Z) - 2(k_{20}-1)\big(k_{20} - xk_{21} - \sqrt{1-x^2}\sqrt{Z}\sqrt{k_{21}^2-k_{20}^2}\cos\tau\big)} \\
&= \int_{-1}^1 dx\ \mathcal{I}'_{2,\mathcal{B},2,LO} \int_0^\infty dZ \frac{1}{1+Z} \frac{1}{(k_{21}^2-k_{20}^2)\sqrt{(Z+K)^2+L^2}} \\
&= \int_{-1}^1 dx\ \mathcal{I}'_{2,\mathcal{B},2,LO} \frac{1}{k_{21}^2-k_{20}^2} \frac{\log\left(\frac{\sqrt{((K-1)^2+L^2)(K^2+L^2)}+(K-1)K+L^2}{\sqrt{(K-1)^2+L^2}+K-1}\right)}{\sqrt{(K-1)^2+L^2}}\ , \qquad (4.110)
\end{aligned}$$

where

$$\begin{aligned}
\mathcal{I}'_{2,\mathcal{B},2,LO} &= \frac{\pi^{1/2-\epsilon}}{\Gamma(1/2-\epsilon)(2\pi)^d} \frac{\sqrt{1-x^2}^{-2\epsilon}}{(\cosh\phi(\beta_i\cdot k_2 - 1) - \sinh\phi x(\beta_i\cdot k_2 - 1) - 1)} \\
&\times i(2\pi i)^4 \frac{2\pi^{1-\epsilon}}{\Gamma(1-\epsilon)} \frac{\mu^{6\epsilon}}{m^{6\epsilon}} g_s^6 \beta_j\cdot\beta_k(-\beta_j\cdot k_2 - 2)^{1-2\epsilon} \\
&\times \frac{(1-2\beta_i\cdot k_2)(\beta_i\cdot k_1 - 1)^{1-2\epsilon}}{(k_{20}^2-k_{21}^2)(-\beta_j\cdot k_2 - 1)} C_{2,k_3}\big((\alpha+\beta k_{20})^2 - k_{20}^2\big)^{1-\epsilon} \\
K &= -\frac{k_{20}^2(2x^2-1) + 2k_{20}(k_{21}x - 2x^2 + 1) + k_{21}^2 - 2k_{21}x + 2x^2 - 2}{k_{20}^2 - k_{21}^2} \\
L^2 &= -\frac{4(k_{20}-1)^2(x^2-1)\big(2(k_{20}-1)k_{21}x + (k_{20}-1)^2x^2 + k_{21}^2 - 1\big)}{\big(k_{20}^2-k_{21}^2\big)^2}\ .
\end{aligned} \quad (4.111)$$

Plugging the values (4.111) into equation (4.110) provides a remarkable simplifi-

cation

$$\mathcal{I}_{2,\mathcal{B},2,LO,Z}(k_{20},\beta) = \int_{-1}^{1} dx \mathcal{I}'_{2,\mathcal{B},2,LO} \frac{\log\left(-\frac{(k_{20}+k_{21})((k_{20}-1)x+k_{21}-1)}{(k_{20}-k_{21})((k_{20}-1)x+k_{21}+1)}\right)}{2(k_{20}-1)(k_{20}x+k_{21})} \ . \tag{4.112}$$

This logarithm can be rewritten in terms of an integral over a linear denominator. We notice that by performing the Z and $\cos\tau$ integrals, we also got rid of the square root of x, so that we are left with a purely rational integrand. We now simplify the terms with an ϵ-dependent exponent in $\mathcal{I}'_{2,\mathcal{B},2,LO}$ as follows:

$$\begin{aligned}(k_{20}-1)^{-2\epsilon} &\to (k_{20}-1)^{-2\epsilon} \\ (k_{21}^2-k_{20}^2)^{-\epsilon} &\to (\beta^2-1)^{-\epsilon}(k_{20}-1)^{-2\epsilon} \\ (\sinh\phi k_{21}-\cosh\phi k_{20}-2)^{-2\epsilon} &\to (\sinh\phi)^{-2\epsilon}(\beta-r(\alpha_{ij}))^{-2\epsilon}\end{aligned} \tag{4.113}$$

Using (4.113), we can now perform the k_{20} integral in (4.108). We still have the divergent β integral, and deal with it in the same way as in the case of the triangle (4.77). We then perform the remaining finite integrals using PolyLogTools.

Calculation of $\mathcal{C}_{2,\mathcal{B},2,\mathrm{NLO}}(\alpha_{ij},\alpha_{jk})$

We now perform the calculation of $\mathcal{C}_{2,\mathcal{B},2,NLO}(\alpha_{ij},\alpha_{jk})$. This will introduce extra complications, because the dependence on $\cos\tau$ and Z will be more complicated. However, there will also be simplifications because we only need to calculate the leading order of this contribution.

Let us split up $\mathcal{C}_{2,\mathcal{B},2,\mathrm{NLO}}(\alpha_{ij},\alpha_{jk})$, defined in (4.109), into two different parts:

$$\mathcal{C}_{2,\mathcal{B},2,\mathrm{NLO}}(\alpha_{ij},\alpha_{jk}) = \mathcal{C}_{2,\mathcal{B},2,\mathrm{NLO},1}(\alpha_{ij},\alpha_{jk}) + \mathcal{C}_{2,\mathcal{B},2,\mathrm{NLO},2}(\alpha_{ij},\alpha_{jk}) \ , \tag{4.114}$$

where

$$\begin{aligned}\mathcal{C}_{2,\mathcal{B},2,\mathrm{NLO},1}(\alpha_{ij},\alpha_{jk}) &= -\epsilon \int_1^\infty dk_{20} \int_{r(\alpha_{ij})}^\infty d\beta k_{20} \int_0^\infty dZ \ \mathcal{I}_{2,\mathcal{B},2,LO} \ln(1-\cos^2\tau) \\ \mathcal{C}_{2,\mathcal{B},2,\mathrm{NLO},2}(\alpha_{ij},\alpha_{jk}) &= -2\epsilon \int_1^\infty dk_{20} \int_{r(\alpha_{ij})}^\infty d\beta k_{20} \int_0^\infty dZ \ \mathcal{I}_{2,\mathcal{B},2,LO} \ \ln Z \ .\end{aligned} \tag{4.115}$$

Let us first look at $\mathcal{C}_{2,\mathcal{B},2,\mathrm{NLO},1}(\alpha_{ij},\alpha_{jk})$. We can again perform the $\cos\tau$ integral and obtain

$$\mathcal{C}_{2,\mathcal{B},2,\text{NLO},1}(\alpha_{ij},\alpha_{jk}) = -\epsilon \int_1^\infty dk_{20} \int_{r(\alpha_{ij})}^\infty d\beta\ k_{20} \int_{-1}^1 dx \mathcal{I}'_{2,\mathcal{B},2,LO} \times \int_0^\infty dZ \frac{\ln\big(1-\Gamma\big)}{1+Z} \frac{1}{(k_{21}^2-k_{20}^2)\sqrt{(Z+K)^2+L^2}} \tag{4.116}$$

where

$$\Gamma = \frac{2(k_{20}-1)\sqrt{1-x^2}\sqrt{Z}\sqrt{k_{21}^2-k_{20}^2}}{(k_{20}^2-k_{21}^2)(1+Z)-2(k_{20}-1)\big(k_{20}-xk_{21}\big)} \tag{4.117}$$

The extra complication of the $\ln\big(1-\Gamma\big)$ factor makes it impossible to perform the Z integral. However, we are only interested in the leading divergence of $\mathcal{C}_{2,\mathcal{B},2,\text{NLO}}(\alpha_{ij},\alpha_{jk})$. This means that in all dimensionless ratios, such as Z and K, we can take the limits $k_{20}\to\infty$ and $\beta\to r(\alpha_{ij})$. The x and Z integrals then reduce to

$$\mathcal{I}(R) = \int_{-1}^1 dx \int_0^\infty dZ \frac{1}{1+Rx} \times \frac{1}{1+Z} \frac{\ln\left(1+\frac{1}{\sqrt{1-\frac{4\left(\frac{1}{R^2}-1\right)(1-x^2)Z}{\left(\frac{Z+1}{R^2}+\frac{2x}{R}-Z+1\right)^2}}}\right)}{\sqrt{\left(\frac{Z+1}{R^2}+\frac{2x}{R}-Z+1\right)^2-4\left(\frac{1}{R^2}-1\right)(1-x^2)Z}}\ , \tag{4.118}$$

where $R=\frac{1}{r(\alpha_{ij})}$. We calculate this integral in appendix E. The result is equal to (E.16). It can not be rewritten in terms of polylogs of the form $G(\mathbf{a},\alpha_{ij})$. We can now again partial fraction and integrate with respect to k_{20}, and then extract the leading order divergence of the beta integral, to obtain a final expression for $\mathcal{C}_{2,\mathcal{B},2,\text{NLO},1}(\alpha_{ij},\alpha_{jk})$.

Calculation of $\mathcal{C}_{2,\mathcal{B},2,\text{NLO},2}(\alpha_{ij},\alpha_{jk})$

We have

$$\mathcal{C}_{2,\mathcal{B},2,\text{NLO},2}(\alpha_{ij},\alpha_{jk}) = -2\epsilon \int_1^\infty dk_{20} \int_{r(\alpha_{ij})}^\infty d\beta k_{20} \int_0^\infty dZ\ \mathcal{I}_{2,\mathcal{B},2,\text{LO}} \ln Z\ . \tag{4.119}$$

As in the case of $\mathcal{C}_{2,\mathcal{B},2,\text{NLO},1}(\alpha_{ij},\alpha_{jk})$, we first perform the $\cos\tau$ integral. We then extract the leading divergence from the k_{20} and β integrals. This leaves us with

a Z integral proportional to

$$\begin{aligned}\mathcal{C}_{2,\mathcal{B},2,\text{NLO},2}(\alpha_{ij},\alpha_{jk}) &\sim \int_0^\infty dZ \frac{\ln Z}{(1+Z)^2} \\ &= 0 \ . \end{aligned} \tag{4.120}$$

We can thus ignore this part, and conclude that we have calculated all ingredients of $\mathcal{C}_{2,\mathcal{B},2}$ (4.107). We can thus perform its dispersive integral.

Dispersive integral

We can now again perform the dispersive integral to obtain $\mathcal{F}_{A,2,\mathcal{B}_2}$.

$$\mathcal{F}_{A,2,\mathcal{B}_2}(\alpha_{ij},\alpha_{jk}) = \frac{12\Gamma(6\epsilon)\kappa^3 r(\alpha_{jk})}{\epsilon}\Big(\mathcal{F}_{A,2,\mathcal{B}_2,LO} + \epsilon\mathcal{F}_{A,2,\mathcal{B}_2,\text{NLO}} + \mathcal{O}(\epsilon^2)\Big) \ , \tag{4.121}$$

where

$$\mathcal{F}_{A,2,\mathcal{B}_2,\text{LO}} = -\frac{1}{6}\ln\alpha_{jk} G(0,0,\alpha_{ij}) \ . \tag{4.122}$$

The next to leading part will again have a contribution which is proportional to the leading order one, and some genuinely new contributions.

$$\begin{aligned}\mathcal{F}_{A,2,\mathcal{B}_2,\text{NLO}} = &-\frac{1}{6}\big(3R_1(\alpha_{jk}) - 2X_1(\alpha_{jk})\big)G(0,0,\alpha_{ij}) \\ &+ \ln(\alpha_{jk})\Big(G_{2,2,\mathcal{B}_2}(\alpha_{ij}) + G_{3,2,\mathcal{B}_2}(\alpha_{ij}) \\ &+ r(\alpha_{ij})\big(F_{3,2,\mathcal{B}_2}(\alpha_{ij}) + F_{4,2,\mathcal{B}_2}(\alpha_{ij})\big)\Big) \ , \end{aligned} \tag{4.123}$$

with

$$\begin{aligned}G_{2,2,\mathcal{B}_2}(\alpha_{ij}) &= \frac{1}{9}\left(\pi^2 - 3G(0,0,\alpha_{ij})\right) \ , \\ G_{3,2,\mathcal{B}_2}(\alpha_{ij}) &= \frac{1}{36}\Big(-12\big(-2G(-1,0,0,\alpha_{ij}) + G(0,-1,0,\alpha_{ij}) + G(0,0,0,\alpha_{ij}) \\ &\quad + G(0,1,0,\alpha_{ij}) - 2G(1,0,0,\alpha_{ij}) + \pi^2 G(0,2) - \zeta(3)\big) \\ &\quad + 12\pi^2 G(-1,\alpha_{ij}) - 5\pi^2 G(0,\alpha_{ij})\Big) \ , \\ F_{3,2,\mathcal{B}_2}(\alpha_{ij}) &= \frac{1}{18}\left(2\pi^2 G(0,\alpha_{ij}) + 12G(0,0,0,\alpha_{ij})\right) \ , \\ F_{4,2,\mathcal{B}_2}(\alpha_{ij}) &= 0 \ . \end{aligned} \tag{4.124}$$

We notice that $G_{3,2,\mathcal{B}_2}(\alpha_{ij})$ also contains a contribution proportional to $\ln 2$. This contribution cancels the one found in $G_{3,2,\mathcal{B}_1}(\alpha_{ij})$.

Expression for $\mathcal{F}_{A,2}$

We can now combine the different parts making up $\mathcal{F}_{A,2}$. We do not give an explicit expression, but we notice that when we add the $\mathcal{O}(\epsilon^{-2})$ contributions, we see that (4.84) and (4.122) cancel the contribution from $\mathcal{F}_{A,1}$ (4.51). Likewise, the weight two contributions in α_{jk} cancel when adding $\mathcal{F}_{A,1}$ and $\mathcal{F}_{A,2}$. However, the imaginary part of $\mathcal{F}_{A,1}$ (4.53) is not cancelled. Since we expect $\mathcal{F}_A$ to be $\mathcal{O}(\epsilon^{-1})$ divergent and purely real, we expect $\mathcal{F}_{A,3}$ to be also $\mathcal{O}(\epsilon^{-1})$ divergent and to have an imaginary part to cancel the one in $\mathcal{F}_{A,1}$ (4.53). This will be confirmed by the calculation in the next section.

4.5 Calculation of $\mathcal{C}_3$

Looking back at (4.11), we have

$$\begin{aligned}
\mathcal{C}_3 = &-i(2\pi i)^3 \beta_j \cdot \beta_k \frac{\mu^{6\epsilon}}{m^{6\epsilon}} g_s^6 \int \frac{d^d k_1}{(2\pi)^d} \frac{d^d k_2}{(2\pi)^d} \frac{d^d k_3}{(2\pi)^d} \frac{\delta^-(k_3^2)}{(k_1^2 + i\epsilon)(k_2^2 + i\epsilon)} \\
&\times \frac{(\beta_i \cdot \beta_j \beta_j - \beta_i) \cdot (2k_2 + k_1)}{((k_1 + k_2)^2 + i\epsilon)(-\beta_k \cdot k_3 - 1 - i\epsilon)} \\
&\times \frac{\delta(-\beta_i \cdot k_1 - 1)\delta(\beta_j \cdot (k_1 + k_3) - 3)}{(-\beta_j \cdot k_2 - 1 + i\epsilon)(\beta_j \cdot (k_3 - k_2) - 2 + i\epsilon)} \\
= &\, i(2\pi i)^3 \beta_j \cdot \beta_k \frac{\mu^{6\epsilon}}{m^{6\epsilon}} g_s^6 \int \frac{d^d k_1}{(2\pi)^d} \frac{d^d k_2}{(2\pi)^d} \frac{d^d k_3}{(2\pi)^d} \frac{\delta^-(k_3^2)}{(k_1^2 + i\epsilon)(k_2^2 + i\epsilon)} \\
&\times \frac{(\beta_i \cdot \beta_j \beta_j - \beta_i) \cdot (2k_2 + k_1)}{((k_1 + k_2)^2 + i\epsilon)(-\beta_k \cdot k_3 - 1 - i\epsilon)} \\
&\times \frac{\delta(-\beta_i \cdot k_1 - 1)\delta(\beta_j \cdot (k_1 + k_3) - 3)}{(-\beta_j \cdot k_2 - 1 + i\epsilon)(\beta_j \cdot (k_1 + k_2) - 1 - i\epsilon)} \,,
\end{aligned} \tag{4.125}$$

where we used the $\delta(\beta_j \cdot (k_1 + k_3) - 3)$ to simplify the last denominator. This allows us to perform the k_2 and k_3 integrals in terms of k_1:

$$\mathcal{C}_3 = i(2\pi i)^3 \beta_j \cdot \beta_k \frac{\mu^{6\epsilon}}{m^{6\epsilon}} g_s^6 \int \frac{d^d k_1}{(2\pi)^d} \frac{\delta(-\beta_i \cdot k_1 - 1)}{(k_1^2 + i\epsilon)} \mathcal{C}_{3,k_2} \mathcal{C}_{3,k_3} \,, \tag{4.126}$$

with

$$\mathcal{C}_{3,k_2}(k_1^2, \beta_i \cdot k_1, \beta_j \cdot k_1, \beta_i \cdot \beta_j)$$
$$= \int \frac{d^d k_2}{(2\pi)^d} \frac{(\beta_i \cdot \beta_j \beta_j - \beta_i) \cdot (2k_2 + k_1)}{(k_2^2 + i\epsilon)(-\beta_j \cdot k_2 - 1 + i\epsilon)(\beta_j \cdot (k_1 + k_2) - 1 - i\epsilon)((k_1 + k_2)^2 + i\epsilon)} , \tag{4.127}$$

and

$$\mathcal{C}_{3,k_3}(k_1^2, \beta_i \cdot k_1, \beta_j \cdot k_1) = \int \frac{d^d k_3}{(2\pi)^d} \frac{\delta^-(k_3^2)\delta(\beta_j \cdot (k_1 + k_3) - 3)}{(-\beta_k \cdot k_3 - 1 - i\epsilon)} . \tag{4.128}$$

4.5.1 Calculation of $\mathcal{C}_{3,k_3}(k_1^2, \beta_i \cdot k_1, \beta_j \cdot k_1)$

We notice that (4.128) is the same integral as the one in equation (4.57), up to a change $-\beta_j \cdot k_2 - 2 \to \beta_j \cdot k_1 - 3$. We can thus use the result (C.9):

$$\mathcal{C}_{3,k_3}(\beta_j \cdot \beta_k, \beta_j \cdot k_1) = \theta(\beta_j \cdot k_1 - 3) C_{3,k_3}(\beta_j \cdot \beta_k, \beta_j \cdot k_1) , \tag{4.129}$$

where

$$C_{3,k_3} = \frac{\pi^{1-\epsilon}}{\Gamma(1-\epsilon)(2\pi)^d} \int_{-1}^{1} d\cos\sigma \frac{(\sin\sigma)^{-2\epsilon}}{-(\beta_j \cdot k_1 - 3)(\cosh\theta - \sinh\theta\cos\sigma) - 1} . \tag{4.130}$$

4.5.2 Calculation of $\mathcal{C}_{3,k_2}(k_1^2, \beta_i \cdot k_1, \beta_j \cdot k_1)$

We can simplify this calculation by making use of the symmetries of the integrand. Changing variables via $k_2 \to -k_2 - k_1$, we have

$$\mathcal{C}_{3,k_2}(k_1^2, \beta_i \cdot k_1, \beta_j \cdot k_1, \beta_i \cdot \beta_j)$$
$$= \int \frac{d^d k_2}{(2\pi)^d} \frac{(\beta_i \cdot \beta_j \beta_j - \beta_i) \cdot (2k_2 + k_1)}{(k_2^2 + i\epsilon)(-\beta_j \cdot k_2 - 1 + i\epsilon)(\beta_j \cdot (k_1 + k_2) - 1 - i\epsilon)((k_1 + k_2)^2 + i\epsilon)}$$
$$= -\int \frac{d^d k_2}{(2\pi)^d} \frac{(\beta_i \cdot \beta_j \beta_j - \beta_i) \cdot (2k_2 + k_1)}{((k_1 + k_2)^2 + i\epsilon)(\beta_j \cdot (k_1 + k_2) - 1 + i\epsilon)(-\beta_j \cdot k_2 - 1 - i\epsilon)(k_2^2 + i\epsilon)} . \tag{4.131}$$

We see that the numerator goes to minus itself, the gluon propagators are swapped, and the Eikonal propagators are swapped. The sign of the $i\epsilon$ prescription also changes for the Eikonal propagators. This $i\epsilon$ prescription is essential: without it, we would conclude that (4.131) implies that $\mathcal{C}_{3,k_2} = 0$.

Instead, we now use

$$\frac{1}{a+i\epsilon} = \mathrm{PV}\big(\frac{1}{a}\big) - i\pi\delta(a) \ , \tag{4.132}$$

To deduce that

$$\begin{aligned}
\frac{1}{(-\beta_j\cdot k_2 - 1 - i\epsilon)} &= \frac{1}{(-\beta_j\cdot k_2 - 1 + i\epsilon)} + 2\pi i\delta(-\beta_j\cdot k_2 - 1) \\
\frac{1}{(\beta_j\cdot(k_1+k_2) - 1 + i\epsilon)} &= \frac{1}{(\beta_j\cdot(k_1+k_2) - 1 - i\epsilon)} - 2\pi i\delta(\beta_j\cdot(k_1+k_2) - 1) \ ,
\end{aligned} \tag{4.133}$$

and hence

$$\begin{aligned}
&\mathcal{C}_{3,k_2}(k_1^2, \beta_i\cdot k_1, \beta_j\cdot k_1, \beta_i\cdot\beta_j) \\
&= -\int \frac{d^dk_2}{(2\pi)^d}\frac{(\beta_i\cdot\beta_j\beta_j - \beta_i)\cdot(2k_2+k_1)}{((k_1+k_2)^2+i\epsilon)(k_2^2+i\epsilon)} \\
&\qquad\times\left(\frac{1}{(-\beta_j\cdot k_2 - 1 + i\epsilon)} + 2\pi i\delta(-\beta_j\cdot k_2 - 1)\right) \\
&\qquad\times\left(\frac{1}{(\beta_j\cdot(k_1+k_2) - 1 - i\epsilon)} - 2\pi i\delta(\beta_j\cdot(k_1+k_2) - 1)\right) \ ,
\end{aligned} \tag{4.134}$$

so that

$$\begin{aligned}
&\mathcal{C}_{3,k_2}(k_1^2, \beta_i\cdot k_1, \beta_j\cdot k_1, \beta_i\cdot\beta_j) \\
&= -\pi i\int \frac{d^dk_2}{(2\pi)^d}\frac{1}{k_2^2(k_1+k_2)^2}\frac{(\beta_i\cdot\beta_j\beta_j - \beta_i)\cdot(2k_2+k_1)\delta(-\beta_j\cdot(k_1+k_2)+1)}{(-\beta_j\cdot k_2 - 1 + i\epsilon)} \\
&+ \pi i\int \frac{d^dk_2}{(2\pi)^d}\frac{1}{k_2^2(k_1+k_2)^2}\frac{(\beta_i\cdot\beta_j\beta_j - \beta_i)\cdot(2k_2+k_1)\delta(-\beta_j\cdot k_2 - 1)}{(\beta_j\cdot(k_1+k_2) - 1 - i\epsilon)} \\
&+ 2\pi^2\int \frac{d^dk_2}{(2\pi)^d}\frac{(\beta_i\cdot\beta_j\beta_j - \beta_i)\cdot(2k_2+k_1)}{k_2^2(k_1+k_2)^2}\delta(-\beta_j\cdot k_2 - 1)\delta(-\beta_j\cdot(k_1+k_2)+1) \\
&= \frac{2\pi i}{(\beta_j\cdot k_1 - 2 - i\epsilon)(2\pi)^d}\mathcal{C}_{3,k_2,1} + \frac{2\pi^2}{(2\pi)^d}\delta(-\beta_j\cdot k_1 + 2)\mathcal{C}_{3,k_2,2} \ ,
\end{aligned} \tag{4.135}$$

where

$$\begin{aligned}
\mathcal{C}_{3,k_2,1} &= \int d^dk_2\frac{(\beta_i\cdot\beta_j\beta_j - \beta_i)\cdot(2k_2+k_1)}{k_2^2(k_1+k_2)^2}\delta(-\beta_j\cdot k_2 - 1) \\
\mathcal{C}_{3,k_2,1} &= \int d^dk_2\frac{(\beta_i\cdot\beta_j\beta_j - \beta_i)\cdot(2k_2+k_1)}{k_2^2(k_1+k_2)^2}\delta(-\beta_j\cdot k_2 - 1) \ .
\end{aligned} \tag{4.136}$$

$\mathcal{C}_{3,k_2,1}$ and $\mathcal{C}_{3,k_2,2}$ are easier to calculate than $\mathcal{C}_{3,k_2}$, because they contain more delta functions and less denominators. Moreover, when we plug our expression (4.135) into the k_1 integral, we have a factor of $\theta(\beta_j \cdot k_1 - 3)$ coming from $\mathcal{C}_{3,k_3}$. This means that the factor $\delta(-\beta_j \cdot k_1 + 2)$ multiplying $\mathcal{C}_{3,k_2,2}$ does not have support when performing the k_1 integral, so that we do not need to calculate it. The theta function also implies that the factor of $\frac{1}{\beta_j \cdot k_1 - 2 - i\epsilon}$ will not have a pole in the region of integration, so that we can drop the $i\epsilon$ prescription. We now perform the k_2 integral via Feynman parametrisation. The detailed calculations can be found in appendix C.2.3. We state the result (C.12) here:

$$\begin{aligned}
&\mathcal{C}_{3,k_2,1}(\beta_i \cdot \beta_j, \beta_i \cdot k_1, \beta_j \cdot k_1, k_1^2) \\
&= -2\pi(\beta_i \cdot \beta_j \beta_j - \beta_i) \cdot k_1 \int_0^1 d\alpha \int_0^\infty dk_{21} \frac{{k_{21}}^{-2\epsilon}(1-2\alpha)}{\left((\alpha\beta_j \cdot k_1 - 1)^2 - k_{21}^2 + \alpha(1-\alpha)k_1^2 + i\epsilon\right)} \\
&= -2\pi(\beta_i \cdot \beta_j \beta_j - \beta_i) \cdot k_1 (\beta_j \cdot k_1)^{1-2\epsilon} \\
&\times \int_0^1 d\alpha \int_0^\infty dz \frac{z^{-2\epsilon}(1-2\alpha)}{\left((\alpha\beta_j \cdot k_1 - 1)^2 - z^2(\beta_j \cdot k_1)^2 + \alpha(1-\alpha)k_1^2 + i\epsilon\right)} \ , \qquad (4.137)
\end{aligned}$$

where we turned k_{21} into a scaleless variable by rescaling it by $\beta_j \cdot k_1$:

$$k_{21} = \beta_j \cdot k_1 z \ . \qquad (4.138)$$

4.5.3 Final loop integral

We can now put equations (4.137), (4.135), (4.129) and (4.126) together:

$$\begin{aligned}
\mathcal{C}_3 &= i(2\pi i)^3 \beta_j \cdot \beta_k \frac{\mu^{6\epsilon}}{m^{6\epsilon}} g_s^6 \int \frac{d^d k_1}{(2\pi)^d} \frac{\delta(-\beta_i \cdot k_1 - 1)}{(k_1^2 + i\epsilon)} \mathcal{C}_{3,k_2} \mathcal{C}_{3,k_3} \\
&= -2\pi i \beta_j \cdot \beta_k \frac{\mu^{6\epsilon}}{m^{6\epsilon}} g_s^6 \int \frac{d^d k_1}{(2\pi)^d} \frac{\delta(-\beta_i \cdot k_1 - 1)}{(k_1^2 + i\epsilon)} \\
&\times \theta(\beta_j \cdot k_1 - 3) C_{3,k_3}(\beta_j \cdot \beta_k, \beta_j \cdot k_1) \\
&\times \frac{1}{(\beta_j \cdot k_1 - 2)} \mathcal{C}_{3,k_2,1}(\beta_i \cdot \beta_j, \beta_i \cdot k_1, \beta_j \cdot k_1, k_1^2) \ . \qquad (4.139)
\end{aligned}$$

We first study the δ and θ function above. We do this in a frame where

$$\begin{aligned}
\beta_j &= (1, \mathbf{0}_3) \\
\beta_i &= (\cosh\phi, \sinh\phi \mathbf{v}_3), \quad \mathbf{v}^2 = 1 \\
k_1 &= (k_{10}, k_{11} \mathbf{v'}_{d-1}), \quad \mathbf{v'}^2 = 1 \\
\mathbf{v} \cdot \mathbf{v'} &= \cos\sigma \ , \qquad (4.140)
\end{aligned}$$

with measure

$$d^d k_1 = \frac{2\pi^{1-\epsilon}}{\Gamma(1-\epsilon)} d_{1_0} dk_{11} k_{11}^{2-2\epsilon} d\cos\sigma (\sin\sigma)^{-2\epsilon} \ , \tag{4.141}$$

so that

$$\begin{aligned}
\mathcal{C}_3 &= -2\pi i \frac{1}{(2\pi)^3} \beta_j \cdot \beta_k \frac{\mu^{6\epsilon}}{m^{6\epsilon}} g_s^6 \int_3^\infty dk_{10} \int_0^1 d\cos\sigma \\
&\times \frac{\left(\left(\frac{1+\cosh\phi k_{10}}{\sinh\phi\cos\sigma}\right)^{2-2\epsilon}\right.}{(\sinh\phi\cos\sigma)\left(k_{10}^2 - \left(\frac{1+\cosh\phi k_{10}}{\sinh\phi\cos\sigma}\right)^2\right)} C_{3,k_3}(\beta_j\cdot\beta_k, k_{10}) \\
&\times \frac{1}{(k_{10}-2)} \mathcal{C}_{3,k_2,1}(\cosh\phi, k_{10}, \cos\sigma) + \mathcal{O}(1) \\
&= -2\pi i \frac{1}{(2\pi)^3} \beta_j \cdot \beta_k \frac{\mu^{6\epsilon}}{m^{6\epsilon}} g_s^6 \int_3^\infty dk_{10} \int_0^1 d\cos\sigma \\
&\times \frac{\left(\frac{1+\cosh\phi k_{10}}{\sinh\phi\cos\sigma}\right)^{2-2\epsilon}}{(\sinh\phi\cos\sigma)\left(k_{10}^2 - \left(\frac{1+\cosh\phi k_{10}}{\sinh\phi\cos\sigma}\right)^2\right)} C_{3,k_3}(\beta_j\cdot\beta_k, k_{10}) \\
&\times \frac{1}{(k_{10}-2)} \mathcal{C}_{3,k_2,1}(\cosh\phi, k_{10}, \cos\sigma) + \mathcal{O}(1) \ .
\end{aligned} \tag{4.142}$$

Since we are only interested in the leading divergence, we now extract this from the k_{10} integral by looking at the behaviour of the integrand for $k_{20} \to \infty$. This leaves us with

$$\begin{aligned}
\mathcal{C}_3 &= 8\pi i r(\alpha_{ij}) \kappa^3 \Gamma(6\epsilon) \int_0^1 d\cos\sigma \frac{r(\alpha_{ij}^2)}{\cos\sigma\left(\cos^2\sigma - r(\alpha_{ij})^2\right)} \\
&\times \int_0^1 d\alpha \int_0^\infty dz \frac{(1-2\alpha)}{\left(\alpha^2 - z^2 + \alpha(1-\alpha)(1 - r(\alpha_{ij})^2/\cos^2\sigma) + i\epsilon\right)} \\
&\times \cosh\theta \int_{-1}^1 d\cos\sigma \frac{1}{(\cosh\theta - \sinh\theta\cos\sigma)} + \mathcal{O}(1) \\
&= -16\pi i r(\alpha_{jk}) \ln\alpha_{jk} r(\alpha_{ij}) \kappa^3 \Gamma(6\epsilon) \int_0^1 d\cos\sigma \frac{r(\alpha_{ij}^2)}{\cos\sigma\left(\cos^2\sigma - r(\alpha_{ij})^2\right)} \\
&\times \int_0^1 d\alpha \int_0^\infty dz \frac{(1-2\alpha)}{\left(\alpha - z^2 - \alpha(1-\alpha) r(\alpha_{ij})^2/\cos^2\sigma + i\epsilon\right)} \\
&= -16\pi i r(\alpha_{jk}) \ln\alpha_{jk} r(\alpha_{ij}) \kappa^3 \Gamma(6\epsilon) \int_0^1 d\cos\sigma \frac{r(\alpha_{ij}^2)\mathcal{I}(r(\alpha_{ij}), \cos\sigma)}{\cos\sigma\left(\cos^2\sigma - r(\alpha_{ij})^2\right)} \ ,
\end{aligned} \tag{4.143}$$

where

$$\mathcal{I}(r(\alpha_{ij}),\cos\sigma)=\int_0^1 d\alpha\int_0^\infty dz\frac{(1-2\alpha)}{\big(\alpha-z^2-\alpha(1-\alpha)r(\alpha_{ij})^2/\cos^2\sigma+i\epsilon\big)}\ . \tag{4.144}$$

We now calculate $\mathcal{I}(r(\alpha_{ij}),\cos\sigma)$, and split it up in a real and an imaginary part.

$$\begin{aligned}\mathcal{I}_{\rm Re}(r(\alpha_{ij}),\cos\sigma)&=\mathrm{PV}\int_0^1 d\alpha\int_0^\infty dz\frac{(1-2\alpha)}{\big(\alpha-z^2-\alpha(1-\alpha)r(\alpha_{ij})^2/\cos^2\sigma\big)}\\&=\mathrm{PV}\int_0^1 d\alpha\int_0^\infty dz\frac{(1-2\alpha)}{\sqrt{\alpha}\big(1-z^2-(1-\alpha)r(\alpha_{ij})^2/\cos^2\sigma\big)}\ .\end{aligned} \tag{4.145}$$

We now want to rescale z^2 by $1-(1-\alpha)r(\alpha_{ij})^2/\cos^2\sigma$. The resulting z integral will depend on the sign of $1-(1-\alpha)r(\alpha_{ij})^2/\cos^2\sigma$, so we split it up as follows:

$$\begin{aligned}&\mathcal{I}_{\rm Re}(r(\alpha_{ij}),\cos\sigma)\\&=\mathrm{PV}\int_{1-\cos^2\sigma/r(\alpha_{ij})^2}^1 d\alpha\int_0^\infty dz\frac{(1-2\alpha)}{\sqrt{\alpha}\sqrt{1-(1-\alpha)r(\alpha_{ij})^2/\cos^2\sigma}\big(1-z^2\big)}\\&-\mathrm{PV}\int_0^{1-\cos^2\sigma/r(\alpha_{ij})^2} d\alpha\int_0^\infty dz\frac{(1-2\alpha)}{\sqrt{\alpha}\sqrt{(1-\alpha)r(\alpha_{ij})^2/\cos^2\sigma-1}\big(1+z^2\big)}\\&=0-\pi\int_0^{1-\cos^2\sigma/r(\alpha_{ij})^2} d\alpha\frac{(1-2\alpha)}{\sqrt{\alpha}\sqrt{(1-\alpha)r(\alpha_{ij})^2/\cos^2\sigma-1}}\\&=-\pi^2\frac{\cos^3\sigma}{r(\alpha_{ij})^3}\ .\end{aligned} \tag{4.146}$$

For the imaginary part, we have

$$\begin{aligned}\mathcal{I}_{\rm Im}(r(\alpha_{ij}),\cos\sigma)&=\mathrm{Im}\int_0^1 d\alpha\int_0^\infty dz\frac{(1-2\alpha)}{\sqrt{\alpha}\big(1-z^2-(1-\alpha)r(\alpha_{ij})^2/\cos^2\sigma\big)+i\epsilon}\\&=-i\pi\int_0^1 d\alpha\int_0^\infty dz\frac{(1-2\alpha)\delta\big(1-z^2-(1-\alpha)r(\alpha_{ij})^2/\cos^2\sigma\big)}{\sqrt{\alpha}}\ .\end{aligned} \tag{4.147}$$

The δ function can be solved for α:

$$\alpha=1+(z^2-1)\frac{\cos^2\sigma}{r(\alpha_{ij})^2}\ . \tag{4.148}$$

α will only be in the region of integration for $0 < z < 1$, so that

$$\begin{aligned}\mathcal{I}_{\mathrm{Im}}(r(\alpha_{ij}),\cos\sigma) &= -i\pi\int_0^1 dz \frac{1-2\Big(1+(z^2-1)\frac{\cos^2\sigma}{r(\alpha_{ij})^2}\Big)}{\frac{r(\alpha_{ij})^2}{\cos^2\sigma}\sqrt{1+(z^2-1)\frac{\cos^2\sigma}{r(\alpha_{ij})^2}}} \\ &= i\pi\frac{\cos^2\sigma}{r(\alpha_{ij})^2}\left(1+\frac{\cos\sigma}{r(\alpha_{ij})}\ln\big(\frac{r(\alpha_{ij})-\cos\sigma}{r(\alpha_{ij})+\cos\sigma}\big)\right) . \end{aligned} \tag{4.149}$$

We can plug equations (4.149) and (4.146) into equation (4.143):

$$\begin{aligned}\mathcal{C}_3 &= -16i\pi r(\alpha_{jk})\ln\alpha_{jk} r(\alpha_{ij})\kappa^3\Gamma(6\epsilon) \\ &\quad\times\int_0^1 d\cos\sigma\frac{r(\alpha_{ij}^2)}{\cos\sigma\big(\cos^2\sigma - r(\alpha_{ij})^2\big)} \\ &\quad\times\frac{\cos^3\sigma}{r(\alpha_{ij})^3}\left(-\pi^2 + i\pi\big(\frac{r(\alpha_{ij})}{\cos\sigma}+\frac{1}{2}\ln\big(\frac{r(\alpha_{ij})-\cos\sigma}{r(\alpha_{ij})+\cos\sigma}\big)\big)\right) \\ &= 16i\pi r(\alpha_{jk})\ln\alpha_{jk}\kappa^3\Gamma(6\epsilon)\Big(-\pi^2\big(1+G(0,-\alpha_{ij})r(\alpha_{ij})\big) \\ &\qquad + i\pi\big(r(\alpha_{ij})G(0,0,-\alpha_{ij})+G(0,-\alpha_{ij})\big)\Big) . \end{aligned} \tag{4.150}$$

4.5.4 Dispersive integral and final result

We can now perform the dispersive integral of (4.150). It gives us

$$\mathcal{F}_{A,3}(\alpha_{ij},\alpha_{jk}) = 12\Gamma(6\epsilon)\kappa^3 r(\alpha_{jk})\ln\alpha_{jk}\mathcal{F}_{A,3,\mathrm{LO}} + \mathcal{O}(1) , \tag{4.151}$$

where

$$\begin{aligned}\mathcal{F}_{A,3,\mathrm{LO}}(\alpha_{ij},\alpha_{jk}) &= -\frac{i\pi}{9}\Big(\pi^2 r(\alpha_{ij})G(0,\alpha_{ij}) + 6r(\alpha_{ij})G(0,0,0,\alpha_{ij}) \\ &\qquad + 6G(0,0,\alpha_{ij}) + \pi^2\Big) \\ &\qquad + \Big(G_{2,3}(\alpha_{ij}) + G_{3,3}(\alpha_{ij}) + r(\alpha_{ij})\big(F_{3,3}(\alpha_{ij}) + F_{4,3}(\alpha_{ij})\big)\Big) , \end{aligned} \tag{4.152}$$

where

$$\begin{aligned} G_{2,3}(\alpha_{ij}) &= 0 , \\ G_{3,3}(\alpha_{ij}) &= \frac{1}{3}\pi^2\big(G(0,\alpha_{ij}) - 2G(-1,\alpha_{ij})\big) , \end{aligned}$$

$$F_{3,3}(\alpha_{ij}) = 0 \ ,$$
$$F_{4,3}(\alpha_{ij}) = \frac{1}{3}\pi^2 \left(-2G(0,-1,\alpha_{ij}) + G(0,0,\alpha_{ij}) + \frac{\pi^2}{6} \right) \ . \tag{4.153}$$

As we expected, $\mathcal{F}_{A,3}$ indeed is only $\mathcal{O}(\epsilon^{-1})$ divergent. It also contains an imaginary part, which cancels the imaginary part found in $\mathcal{F}_{A,1}$.

4.6 Combination of the three terms

4.6.1 Expression for $\mathcal{F}_A$

Now that we have expressions for all three cuts and their dispersive integrals, we can calculate $\mathcal{F}_A$ itself. We find that

$$\begin{aligned}\mathcal{F}_A(\alpha_{ij},\alpha_{jk}) &= \mathcal{F}_{A,1}(\alpha_{ij},\alpha_{jk}) + \mathcal{F}_{A,2}(\alpha_{ij},\alpha_{jk}) + \mathcal{F}_{A,3}(\alpha_{ij},\alpha_{jk}) \\ &= 12\kappa^3\Gamma(6\epsilon) r(\alpha_{jk}) \ln \alpha_{jk} \\ &\quad \times \left(G_2(\alpha_{ij}) + G_3(\alpha_{ij}) + r(\alpha_{ij})\big(F_3(\alpha_{ij}) + F_4(\alpha_{ij})\big) \right) \ ,\end{aligned} \tag{4.154}$$

where

$$\begin{aligned}G_2(\alpha_{ij}) &= \frac{2\pi^2}{9} \ , \\ G_3(\alpha_{ij}) &= \frac{2}{3}(2G(-1,0,0,\alpha_{ij}) - 2G(0,0,0,\alpha_{ij}) + 2G(1,0,0,\alpha_{ij}) - \zeta(3)) \ , \\ F_3(\alpha_{ij}) &= \frac{2}{9}\left(\pi^2 G(0,\alpha_{ij}) + 6G(0,0,0,\alpha_{ij})\right) \ , \\ F_4(\alpha_{ij}) &= \frac{1}{180}\Big(-120\zeta(3)G(0,\alpha_{ij}) + 240G(0,-1,0,0,\alpha_{ij}) \\ &\qquad - 240G(0,0,0,0,\alpha_{ij}) + 240G(0,1,0,0,\alpha_{ij}) + \pi^4 \Big) \ .\end{aligned} \tag{4.155}$$

4.6.2 Lightlike limit

We now want to check if the result (4.155) is correct. We first calculate its lightlike limit, i.e. the non-vanishing terms in the limit where the cusp parameters go to zero:

$$\begin{aligned}\mathcal{F}_A(\alpha_{ij},\alpha_{jk}) \to 12\kappa^3\Gamma(6\epsilon)\ln\alpha_{jk}\frac{1}{180}\Big(&40\left(\pi^2 - 3\zeta(3)\right)G(0,\alpha_{ij}) - 10G(0,\alpha_{ij})^4 \\ &- 120\zeta(3) + \pi^4 + 40\pi^2 \Big)\end{aligned}$$

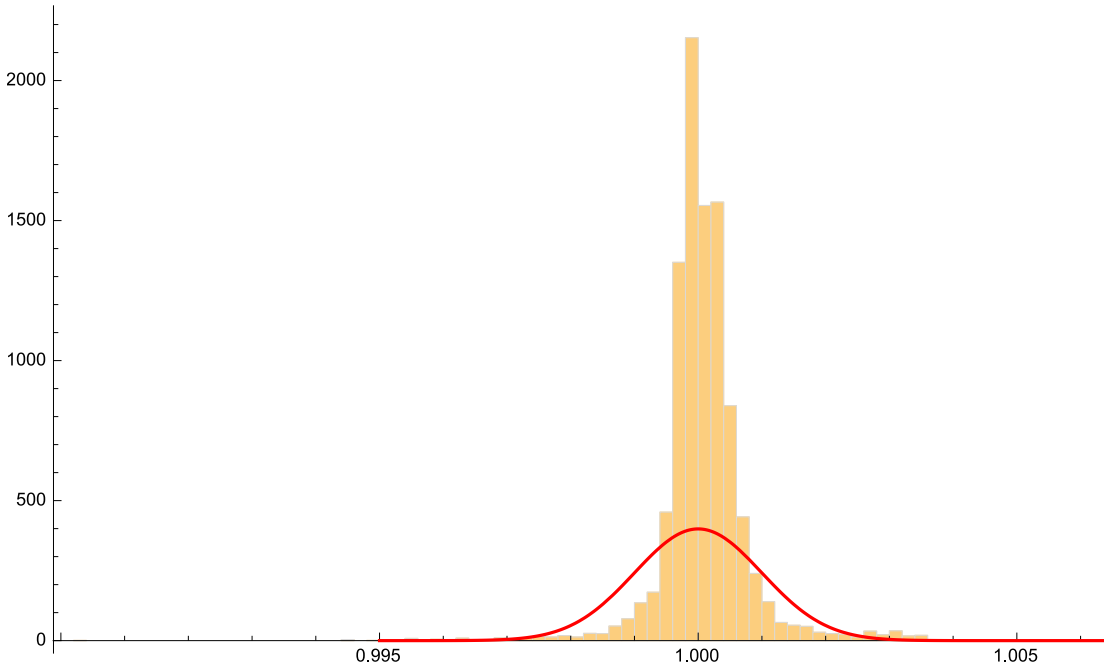

Figure 4.3 *Ratio of exact results to SecDec results. The red curve is the expected distribution.*

$$= \frac{2}{\epsilon}\left(\frac{\alpha_s}{2\pi}\right)^3 \ln\alpha_{jk}\frac{1}{180}\Bigg(40\left(\pi^2 - 3\zeta(3)\right)G(0,\alpha_{ij}) - 10G(0,\alpha_{ij})^4 - 120\zeta(3) + \pi^4 + 40\pi^2\Bigg) + \mathcal{O}(1)\ . \tag{4.156}$$

This is exactly the same as the result (4.7) obtained in [80].

4.6.3 Numerical checks

To check our result in general kinematics, we perform numerical calculations using SecDec. We calculate $\mathcal{F}_A(\alpha_{ij},\alpha_{jk})$ numerically in 9751 points on a 199×49 $(\alpha_{ij},\alpha_{jk})$ grid. SecDec requires to specify a value for the α_{ik} angle as well, even though (4.155) does not depend on it. We set $\alpha_{ik} = 0.5$ in all the points calculated. We choose a relative error of 10^{-3} when performing the SecDec calculation.

In figure 4.3, we present a histogram displaying the distribution of the ratio of the exact result obtained via (4.155) to the result obtained numerically in SecDec. Because we worked with a relative accuracy of 10^{-3}, we expect this histogram to obey a normal distribution with $(\mu,\sigma) = (1, \frac{1}{1000})$. This distribution is displayed as the red curve in figure 4.3. We see that our histogram is even more centred around one than we would have expected, indicating very good agreement between the exact result and numerics. This good agreement is reached despite large fluctuations in the value of $\mathcal{F}_A$ in our parameter space. The largest and

smallest results we obtain are

$$\begin{aligned}\mathcal{F}_A(0.005, 0.02) &= 3087.46 \\ \mathcal{F}_A(0.995, 0.98) &= 0.000132848 \ ,\end{aligned} \tag{4.157}$$

so that our results span more than seven orders of magnitude.

These numerical results confirm beyond reasonable doubt that the expression (4.155) is indeed correct. We can now analyse it in more detail.

4.6.4 Analysis of the result

We now look at the expression (4.155) in more detail.

- As expected, the F_i are antisymmetric under $\alpha_{ij} \to 1/\alpha_{ij}$, and the G_i are symmetric under this interchange. This implies that the whole expression is symmetric under $\alpha \to 1/\alpha$ transformations, as it should.

- We see that the result satisfies the factorisation conjecture 1 on page 8.

- When looking at the symbol of the expression, we see that

$$\begin{aligned}\mathcal{S}\big(G_2\big) &= 0 \ , \\ \mathcal{S}\big(G_3\big) &= \frac{4}{3}\bigg(\alpha_{ij} \otimes \alpha_{ij} \otimes (1-\alpha_{ij}^2) - \alpha_{ij} \otimes \alpha_{ij} \otimes \alpha_{ij}\bigg) \\ &= -\frac{4}{3}\alpha_{ij} \otimes \alpha_{ij} \otimes \frac{\alpha_{ij}}{1-\alpha_{ij}^2} \ , \\ \mathcal{S}\big(F_3\big) &= \frac{4}{3}\alpha_{ij} \otimes \alpha_{ij} \otimes \alpha_{ij} \ , \\ \mathcal{S}\big(F_4\big) &= \frac{4}{3}\bigg(\alpha_{ij} \otimes \alpha_{ij} \otimes (1-\alpha_{ij}^2) \otimes \alpha_{ij} - \alpha_{ij} \otimes \alpha_{ij} \otimes \alpha_{ij} \otimes \alpha_{ij}\bigg) \\ &= -\frac{4}{3}\alpha_{ij} \otimes \alpha_{ij} \otimes \frac{\alpha_{ij}}{1-\alpha_{ij}^2} \otimes \alpha_{ij} \ .\end{aligned} \tag{4.158}$$

  We find that the only letters that occur are α_{ij} and $\frac{\alpha_{ij}}{1-\alpha_{ij}^2}$. This is predicted in reference [27]. The letter $\frac{\alpha_{ij}}{1-\alpha_{ij}^2}$ occurs at most once in each symbol.

- It is clear that the expression does not have a uniform weight. This is not a surprise, because we only expect uniform weight for maximally connected diagrams. At three loops, such maximally connected diagrams connect four legs, whereas the $(1,3,1)$ web connects only three legs.

- Another interesting question is whether we can write $\mathcal{F}_A$ in terms of basis functions $M_{k,l,m}$. Since each basis function is of uniform weight and does

not contain a rational $r(\alpha)$ part, we would need to be able to write all of the F_i and G_i in terms of the basis functions. This is clearly not possible, since F_2 is a constant, not a basis function.
The next best we can aim for is to rewrite the result in terms of basis functions and multiple zeta values. This is possible, as follows:

$$\begin{aligned}
G_2(\alpha_{ij}) &= \frac{2\pi^2}{9} \ , \\
G_3(\alpha_{ij}) &= \frac{1}{12} M_{0,0,0}(\alpha_{ij}) M_{1,0,0}(\alpha_{ij}) - \frac{M_{0,1,1}(\alpha_{ij})}{6} - \zeta_3 \ , \\
F_3(\alpha_{ij}) &= \frac{M_{0,2,0}(\alpha_{ij})}{3} \\
&= \frac{M_{0,0,0}^3(\alpha_{ij}) + 4\pi^2 M_{0,0,0}(\alpha_{ij})}{36} \ , \\
F_4(\alpha_{ij}) &= M_{0,0,0}(\alpha_{ij}) \left(-\frac{1}{12} M_{0,1,1}(\alpha_{ij}) \right) + \frac{1}{24} M_{0,0,0}(\alpha_{ij})^2 M_{1,0,0}(\alpha_{ij}) \\
&\quad - \frac{3}{24} M_{1,0,2}(\alpha_{ij}) - \zeta_3 G(0, \alpha_{ij}) \\
&= M_{0,0,0}(\alpha_{ij}) \left(-\frac{1}{12} M_{0,1,1}(\alpha_{ij}) - \zeta_3/2 \right) \\
&\quad + \frac{1}{24} M_{0,0,0}(\alpha_{ij})^2 M_{1,0,0}(\alpha_{ij}) - \frac{3}{24} M_{1,0,2}(\alpha_{ij}) \ . \qquad (4.159)
\end{aligned}$$

Notice that the expressions for F_3 and F_4 are not unique. This is because by adding zeta values to the basis, we introduce some relations between basis functions:

$$\begin{aligned}
M_{0,2,0}(\alpha) &= \frac{M_{0,0,0}^3(\alpha) + 4\pi^2 M_{0,0,0}(\alpha_{ij})}{12} \\
M_{1,2,0}(\alpha) &= -\frac{1}{4} \Bigg(- 4 M_{0,0,0}(\alpha) M_{0,1,1}(\alpha) - 16\zeta(3) M_{0,0,0}(\alpha) - \frac{4}{3}\pi^2 M_{1,0,0}(\alpha) \\
&\quad + M_{0,0,0}(\alpha)^2 M_{1,0,0}(\alpha) - 4 M_{1,0,2}(\alpha) \Bigg) \ . \qquad (4.160)
\end{aligned}$$

Strictly speaking, this means that the $M_{k,l,m}$ form a spanning set, but not a basis when combined with multiple zeta values. If we eliminate $M_{0,2,0}$ and $M_{1,2,0}$ from the spanning set, we turn it into a basis again.

4.7 Conclusion

In this chapter, we calculated a three-loop web which is part of the $(1, 3, 1)$ web. The web consists of one diagram which is $\mathcal{O}(\epsilon^{-1})$ divergent. There were

three cuts contributing to the diagram. Two out of the three cuts were more divergent than the diagram itself, but this $\mathcal{O}(\epsilon^{-2})$ divergence cancelled upon combining the cuts. Likewise, two out of three cuts had a complex part, which cancelled upon combination. Finally, two out of the three cuts contained a higher-weight contribution in one of the cusp angles, which also vanished eventually. We conclude that the cuts did not provide all the simplifications that we hoped for based on two-loop calculations, but still allowed us to calculate the diagram. The result has been checked both in the lightlike limit and numerically, yielding agreement with the found expression.

By analysing the expression, we found out more about the space of functions that describe three-loop webs. We can confirm some properties conjectured based on lower-loop calculations, such as the factorisation conjecture. We then tried to rewrite the expression in terms of the basis functions $M_{k,l,m}(\alpha)$. We found that to be able to do this, we needed to extend our basis by multiple zeta values, and eliminate the now redundant functions $M_{0,2,0}$ and $M_{1,2,0}$. We need to keep this in mind when using our basis in the next chapter.

Chapter 5

Calculation of $(1, 1, 1, 2)$ web

In this chapter, we study the $(1, 1, 1, 2)$ web. We first study the web itself, cuts of the diagrams involved, and the kinematic region in which we can calculate them. We then propose an ansatz for the expression of the $(1, 1, 1, 2)$ web and constrain it using the results for the $(1, 3, 1)$ web and the lightlike limit of the $(1, 1, 1, 2)$ web. We then try to deduce the remaining parameters numerically.

5.1 The $(1, 1, 1, 2)$ web

The $(1, 1, 1, 2)$ web consists of two diagrams, represented in figure 5.1. It is equal to [40]

$$\mathcal{W}_{1,1,1,2} = \mathcal{F}_{1,1,1,2} c_{1,1,1,2} \ , \tag{5.1}$$

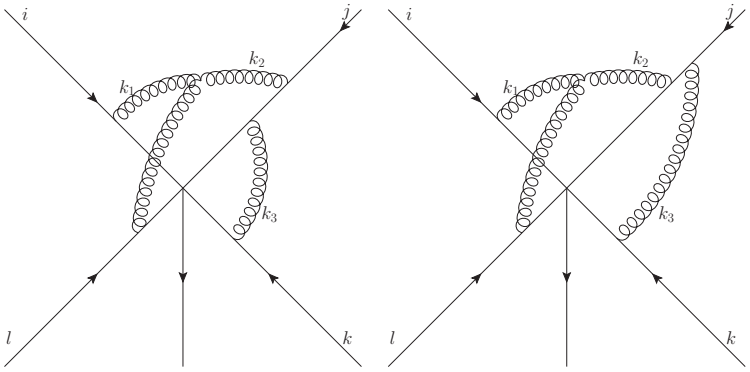

(a) $\mathcal{F}_1$ **(b)** $\mathcal{F}_2$

Figure 5.1 *The diagrams in the* $(1, 1, 1, 2)$ *web.*

where

$$\mathcal{F}_{1,1,1,2} = \frac{1}{2}\big(\mathcal{F}_2(\alpha_{ij},\alpha_{il},\alpha_{jk},\alpha_{jl}) - \mathcal{F}_1(\alpha_{ij},\alpha_{il},\alpha_{jk},\alpha_{jl})\big)$$
$$c_{1,1,1,2} = -f^{ade}f^{bce}T^a_k T^b_l T^c_i T^d_j \tag{5.2}$$

In reference [81], some first steps towards this calculation are made. Firstly, it is proven that the web is $\mathcal{O}(\epsilon^{-2})$ divergent, with leading divergence

$$\mathcal{W}^{(\epsilon^{-2})}_{1,1,1,2}(\alpha_{ij},\alpha_{il},\alpha_{jk},\alpha_{jl}) = \frac{1}{6}\left[\mathcal{W}^{(\epsilon^{-1})}_{3g}(\alpha_{ij},\alpha_{il},\alpha_{jl}),\mathcal{W}^{(\epsilon^{-1})}_{1,1}(\alpha_{jk})\right] , \tag{5.3}$$

which is in accordance with [35]. It is then remarked that at $\mathcal{O}(\epsilon^{-1})$, it is more sensible to calculate the subtracted $(1,1,1,2)$ web $\bar{\mathcal{W}}_{1,1,1,2}$:

$$\begin{aligned}\bar{\mathcal{W}}^{(\epsilon^{-1})}_{1,1,1,2}(\alpha_{ij},\alpha_{il},\alpha_{jk},\alpha_{jl}) = \mathcal{W}^{(\epsilon^{-1})}_{1,1,1,2}(\alpha_{ij},\alpha_{il},\alpha_{jk},\alpha_{jl}) \\ - \frac{1}{2}\left[\mathcal{W}^{(\epsilon^{0})}_{3g}(\alpha_{ij},\alpha_{il},\alpha_{jl}),\mathcal{W}^{(\epsilon^{-1})}_{1,1}(\alpha_{jk})\right] \\ + \frac{1}{2}\left[\mathcal{W}^{(\epsilon^{-1})}_{3g}(\alpha_{ij},\alpha_{il},\alpha_{jl}),\mathcal{W}^{(\epsilon^{0})}_{1,1}(\alpha_{jk})\right] .\end{aligned} \tag{5.4}$$

There are two ingredients in the expression (5.4) which we do not know from earlier calculations in [81]: $\mathcal{W}^{(\epsilon^{-1})}_{1,1,1,2}(\alpha_{ij},\alpha_{il},\alpha_{jk},\alpha_{jl})$ and $\mathcal{W}^{(\epsilon^{0})}_{3g}(\alpha_{ij},\alpha_{il},\alpha_{jl})$. It is then proven that these two unknowns can be combined as follows:

$$\begin{aligned}\bar{\mathcal{F}}^{(\epsilon^{-1})}_{1,1,1,2}(\alpha_{ij},\alpha_{il},\alpha_{jk},\alpha_{jl}) = \frac{i}{4}\Gamma(6\epsilon)\kappa^3 r(\alpha_{jk})\Big(M_{0,0,0}(\alpha_{jk})t_1(\alpha_{ij},\alpha_{il},\alpha_{jl}) \\ - 2M_{1,0,0}(\alpha_{jk})t_0(\alpha_{ij},\alpha_{il},\alpha_{jl})\Big) + \mathcal{O}(1) ,\end{aligned} \tag{5.5}$$

where $t_0(\alpha_{ij},\alpha_{il},\alpha_{jl})$ is proportional to the leading order contribution to the $(1,1,1)$ web:

$$\begin{aligned}t_0(\alpha_{ij},\alpha_{il},\alpha_{jl}) = 2\Big[r(\alpha_{il})\ln\alpha_{il}\big(\ln^2\alpha_{ij} - \ln^2\alpha_{jl}\big) \\ + r(\alpha_{ij})\ln\alpha_{ij}\big(\ln^2\alpha_{jl} - \ln^2\alpha_{il}\big) \\ + r(\alpha_{jl})\ln\alpha_{jl}\big(\ln^2\alpha_{il} - \ln^2\alpha_{ij}\big)\Big] .\end{aligned} \tag{5.6}$$

$t_1(\alpha_{ij},\alpha_{il},\alpha_{jl})$ is the only unknown in the expression (5.5). We know that it satisfies a $i \leftrightarrow l$ antisymmetry. It has been calculated in the lightlike limit in

reference [80]:

$$
\begin{aligned}
t_1(\alpha_{ij},\alpha_{il},\alpha_{jl}) \to \frac{2}{3}\big(\ln(\alpha_{ij})-\ln(\alpha_{jl})\big) \\
&\times\Big(4\ln(\alpha_{il})\ln(\alpha_{ij})\ln(\alpha_{jl})-3\ln^2(\alpha_{il})\ln(\alpha_{ij}) \\
&+\ln(\alpha_{il})\ln^2(\alpha_{ij})-3\ln^2(\alpha_{il})\ln(\alpha_{jl})+\ln(\alpha_{il})\ln^2(\alpha_{jl}) \\
&-6\zeta_2\ln(\alpha_{il})-\ln^3(\alpha_{il})-3\ln(\alpha_{ij})\ln^2(\alpha_{jl}) \\
&-3\ln^2(\alpha_{ij})\ln(\alpha_{jl})+6\zeta_2\ln(\alpha_{ij})+\ln^3(\alpha_{ij}) \\
&+6\zeta_2\ln(\alpha_{jl})+\ln^3(\alpha_{jl})-12\zeta(3)\Big)\,. \qquad (5.7)
\end{aligned}
$$

We now try to obtain it in general kinematics.

5.2 Calculation of $t_1(\alpha_{ij},\alpha_{il},\alpha_{jl})$ using cuts

A first possibility, in line with previous work, is to calculate $t_1(\alpha_{ij},\alpha_{il},\alpha_{jl})$ using cuts. We would go back to equation (5.4) and calculate all its ingredients. As remarked earlier, there are two unknowns: $\mathcal{W}^{(-1)}_{(1,1,1,2)}(\alpha_{ij},\alpha_{il},\alpha_{jk},\alpha_{jl})$ and $\mathcal{W}^{(0)}_{3g}(\alpha_{ij},\alpha_{il},\alpha_{jl})$.

5.2.1 Calculation of $\mathcal{W}^{(\epsilon^0)}_{3g}(\alpha_{ij},\alpha_{il},\alpha_{jl})$

We already calculated $\mathcal{W}^{(-1)}_{3g}(\alpha_{ij},\alpha_{il},\alpha_{jl})$ in chapter 3. We could go back to this calculation and calculate the NLO part of the web. From chapter 3 we know that only one cut contributes, and it is only $\mathcal{O}(\epsilon^{-1})$ divergent. To calculate $\mathcal{W}^{(0)}_{3g}(\alpha_{ij},\alpha_{il},\alpha_{jl})$, we would thus have to calculate the cut at NLO. In chapter 4 we built up experience of performing calculations of cuts at NLO. The calculations in chapter 4 involved an extra loop dependence, but dependence on one less angle. We thus expect the calculation of $\mathcal{W}^{(0)}_{3g}(\alpha_{ij},\alpha_{il},\alpha_{jl})$ to be equally difficult as the calculation of $\mathcal{W}_{(1,1,3)}$: it should be a long calculation, but doable using known techniques.

5.2.2 Calculation of $\mathcal{W}^{(\epsilon^{-1})}_{(1,1,1,2)}(\alpha_{ij},\alpha_{il},\alpha_{jk},\alpha_{jl})$

Before we can calculate the cuts of the diagrams of the $\mathcal{W}_{(1,1,1,2)}$ web, we first need to specify which variable we want to cut on. This is closely related to the choice of kinematic region. For example, for the calculation of the $(1,1,1)$ web,

we wanted to calculate the cuts on the α_{ij} channel, and hence worked in the kinematic region where

$$-1 < \alpha_{ij} < 0 < \{\alpha_{ik}, \alpha_{jk}\} < 1 \ . \tag{5.8}$$

It is essential that we worked in a region where only one α is negative, because otherwise there will be branch cuts in multiple channels at once. We worked in the kinematic region (5.8) by choosing the particles i, j to be incoming and the particle k to be outgoing.

Can we find a configuration of incoming and outgoing particles such that only one α is negative when calculating a web with four external particles? Because swapping all incoming and outgoing particles gives the same kinematic region, there are three different cases to consider:

- All four particles are incoming. In this case, all six relevant α are negative.
- Three particles are incoming and one is outgoing. In this case, we will have three negative and three positive α.
- Two particles are incoming and two are outgoing. In this case, we will have two negative and four positive α.

It therefore seems impossible to specify a kinematic region in which there is just a single α to cut on. However, this conclusion is only valid if the correlator in question depends on all six cusp parameters. This is expected to be the case for diagrams such as the $(1,1,1,1)$ webs with a four-gluon vertex, or with two three-gluon vertices. However, in the case of $\mathcal{W}^{(-1)}_{(1,1,1,2)}(\alpha_{ij}, \alpha_{il}, \alpha_{jk}, \alpha_{jl})$, we know that there is only a dependence on four out of the six possible cusp parameters. From the analysis above, it follows then that it is still impossible to have a single negative α if we choose all four particles incoming/outgoing at once, but otherwise a convenient choice can lead to a single negative α. We find that

- We can cut on α_{il} if we work in the kinematic region where particles i, k and l are incoming and j is outgoing. In this region, $\alpha_{ik}, \alpha_{il}, \alpha_{kl}$ are all negative, but because there is no dependence on α_{ik}, α_{kl}, there is only a cut on α_{il}.
- We can cut on α_{ij} if we work in the kinematic region where particles i and j are incoming and k and l outgoing. In this region, α_{ij} and α_{kl} are both negative, but because there is no dependence on α_{kl}, there is only a cut on α_{ij}.

- We can cut on α_{jl} if we work in the kinematic region where particles j and l are incoming and k and i outgoing. In this region, α_{jl} and α_{ik} are both negative, but because there is no dependence on α_{ik}, there is only a cut on α_{jl}. Because of the $i \leftrightarrow l$ antisymmetry, cutting on this variable is equivalent to cutting on the α_{ij} channel.

- It is not possible to find a kinematic region where there is only a cut on the α_{jk} channel.

We conclude that there are two truly different variables we can cut in: α_{ij} and α_{il}. We can now proceed by picking one of the two variables, calculating the cuts and then calculating the dispersive integrals. We expect that this calculation will be similar to the calculation of the $(1,3,1)$ web: it is also a three-loop calculation and we expect to again have to calculate the two leading orders of the cut. However, there are more variables the result can depend on, so we expect a few more complications.

5.2.3 Conclusion

From the considerations above, it can be concluded that it is possible to calculate the $(1,1,1,2)$ subtracted web using the techniques used in chapter four. However, this would involve lengthy calculations, and would not provide much extra insight. We therefore decide to try a different approach. This approach involves using the collinear limit of the $(1,1,1,2)$ web.

5.3 Collinear reduction of the $(1,1,1,2)$ web

Let us now take the collinear limit $l \to j$ of the $(1,1,1,2)$ web. Diagrammatically, it is clear that the result will be a part of the $(1,3,1)$ web. The colour factor goes to

$$\begin{aligned}\lim_{l\to j} c_{1,1,1,2} &= \frac{1}{2}\big(- f^{ade} f^{bce} T_k^a T_i^c T_j^b T_j^d - f^{ade} f^{bce} T_k^a T_i^c T_j^d T_j^b \big) \\ &= -\frac{1}{2} f^{bcd} f^{cae} T_i^a \big(T_j^d T_j^e + T_j^e T_j^d \big) T_k^b \\ &= i c_1^{'} \ . \end{aligned} \tag{5.9}$$

This implies that the collinear limit of the kinematic part has to be proportional to the $\mathcal{F}_A$ diagram in the $(1,3,1)$ web:

$$\lim_{l\to j}\left(\bar{\mathcal{F}}_{(1,1,1,2)}(\alpha_{ij},\alpha_{il},\alpha_{jk},\alpha_{jl})\right) = -i\mathcal{F}_A(\alpha_{ij},\alpha_{jk})\ . \tag{5.10}$$

This can also be proven using the effective vertex formalism [40].

Notice that when taking the limit $l \to j$,

$$\begin{aligned}
&\lim_{l\to j}\bar{\mathcal{F}}_{(1,1,1,2)}(\alpha_{ij},\alpha_{il},\alpha_{jk},\alpha_{jl}) = \lim_{l\to j}\mathcal{F}_{(1,1,1,2)}(\alpha_{ij},\alpha_{il},\alpha_{jk},\alpha_{jl})\\
&\lim_{l\to j}\bar{\mathcal{F}}^{(\epsilon^{-2})}_{(1,1,1,2)}(\alpha_{ij},\alpha_{il},\alpha_{jk},\alpha_{jl}) = 0\ ,
\end{aligned} \tag{5.11}$$

because in this limit $\mathcal{F}_{3g} \to 0$.
If we now make use of equation (5.5), we can rewrite equation (5.10) as

$$\begin{aligned}
\mathcal{F}_A(\alpha_{ij},\alpha_{jk}) &= -\lim_{l\to j}\left[\frac{1}{4}\Gamma(6\epsilon)\kappa^3 r(\alpha_{jk})\Big(M_{0,0,0}(\alpha_{jk})t_1(\alpha_{ij},\alpha_{il},\alpha_{jl})\right.\\
&\qquad\left. - 2M_{1,0,0}(\alpha_{jk})t_0(\alpha_{ij},\alpha_{il},\alpha_{jl})\Big) + \mathcal{O}(1)\right]\\
&= -\frac{1}{4}\Gamma(6\epsilon)\kappa^3 r(\alpha_{jk})M_{0,0,0}(\alpha_{jk})\lim_{l\to j}\Big(t_1(\alpha_{ij},\alpha_{il},\alpha_{jl})\Big) + \mathcal{O}(1)\\
&= -\frac{1}{4}\Gamma(6\epsilon)\kappa^3 r(\alpha_{jk})M_{0,0,0}(\alpha_{jk})\Big(t_1(\alpha_{ij},\alpha_{ij},1)\Big) + \mathcal{O}(1)\ .
\end{aligned} \tag{5.12}$$

Equation (5.10) provides a strong constraint on the possible expression for $t_1(\alpha_{ij},\alpha_{il},\alpha_{jl})$. It suggests a possible way to calculate the $(1,1,1,2)$ web. We can write down an ansatz for $\bar{\mathcal{F}}_{(1,1,1,2)}$, or equivalently an ansatz for $t_1(\alpha_{ij},\alpha_{il},\alpha_{jl})$. We then constrain the coefficients in this ansatz using equation (5.10). We can also use the lightlike limit of the $(1,1,1,2)$ web, equation (5.7), to constrain the result further. The final remaining coefficients can then be fitted numerically. We follow this approach in this chapter. Such an approach, where amplitudes are reconstructed using the results from simpler amplitudes, is known as a bootstrap approach. It is a popular technique of calculation, see for example references [82–87]. It was already used unsuccessfully to try to compute $\bar{\mathcal{F}}_{(1,1,1,2)}$ in reference [81]. The extra information gained from the calculation of the $(1,3,1)$ web and the lightlike limit of $\bar{\mathcal{F}}_{(1,1,1,2)}$ since, should allow us to improve on this approach.

5.4 Ansatz for the $(1,1,1,2)$ web.

We now write down an ansatz for $\mathcal{F}_{(1,1,1,2)}$, or equivalently, an ansatz for $t_1(\alpha_{ij},\alpha_{il},\alpha_{jl})$:

$$t_1(\alpha_{ij},\alpha_{il},\alpha_{jl}) = \mathcal{A}(\alpha_{ij},\alpha_{il},\alpha_{jl},a_i)\ , \tag{5.13}$$

where the a_i are free parameters that need to be fixed.

5.4.1 First ansatz

We start with an ansatz based on the following assumptions:

- It consists of a sum of products of basis functions $M_{k,l,n}(\alpha)$ and factors of $r(\alpha)$.
- It has to be of uniform weight four. We know this because the lightlike limit of t_1, equation (5.7), is a uniform weight four function, and the lightlike limit conserves weight for basis functions. Also, this diagram connects the maximum number of lines at three loops. This means that it will contribute to the $\mathcal{N}=4$ calculation of the soft anomalous dimension. This calculation has only uniform weight contributions.
- This ansatz has to satisfy a $i \leftrightarrow l$ antisymmetry. This is clear from the definition.
- For each α, it has to satisfy a $\alpha \to \alpha^{-1}$ symmetry. This follows from the definition of α.
- It has at most two factors of $r(\alpha)$. If there are two such factors, they each have a different argument. This constraint is based on experience from calculations of other webs. Every one of these $r(\alpha)$ functions has to come with a factor of $M(\alpha)$, to make sure the ansatz has a finite result in the limit $\alpha \to 1$.

These are the same assumptions that were used in reference [81], and are further justified in there. The resulting ansatz can be found in [81] and has 40 parameters $a_1, a_2, ..., a_{40}$:

$$\mathcal{A}(\alpha_{ij},\alpha_{il},\alpha_{jl},a_i) = \sum_{i=1}^{40} a_i \mathcal{A}_i(\alpha_{ij},\alpha_{il},\alpha_{jl},a_i)\ . \tag{5.14}$$

5.4.2 Generation of minimal ansatz

We have gained some extra information from our calculation of $\mathcal{F}_A$, which constrains t_1 via (5.12). Based on the analysis carried out in section 4.6.4, we can improve the ansatz (5.14) as follows:

- We also include multiple zeta values in our ansatz. This extends the ansatz by one extra function, namely $\zeta_3\big(M_{0,0,0}(\alpha_{il}) - M_{0,0,0}(\alpha_{jl})\big)$.
- The collinear limit of a function f which does not contain a factor of $r(\alpha)$ is either zero, if f depends on α_{jl}, or else a weight four function of α_{ij} which does not contain a factor of $r(\alpha_{ij})$. However, there are no such terms in (4.155). Therefore, we do not need such terms in our ansatz. This excludes seven terms.
- From section 4.6.4, we also learnt that the symbol of $\mathcal{F}_A$ contains at most one occurrence of the letter $\frac{\alpha_{ij}}{1-\alpha_{ij}^2}$. It can be proven that the collinear limit of a term which contains two letters $\frac{\alpha}{1-\alpha^2}$ in its symbol also contains two letters $\frac{\alpha_{ij}}{1-\alpha_{ij}^2}$ in its symbol. We can hence remove all eight such terms from our ansatz.
- It turns out that not all of the original forty functions $\mathcal{A}_i$ are linearly independent. This removes a further seven functions from the ansatz.

We thus have only 19 parameters left in our reduced ansatz $\mathcal{A}_{\text{minimal}}$.

It consists of five terms with two different factors of $r(\alpha)$:

$$\begin{aligned}\mathcal{A}_{r(\alpha)r(\alpha')} = M_{0,0,0}(\alpha_{il})r(\alpha_{il})\Big(& q_5\left(M_{0,0,0}(\alpha_{jl})^3 r(\alpha_{jl}) - M_{0,0,0}(\alpha_{ij})^3 r(\alpha_{ij})\right)\\ &+ q_6\left(M_{0,0,0}(\alpha_{jl})r(\alpha_{jl})M_{0,0,0}(\alpha_{ij})^2 - M_{0,0,0}(\alpha_{jl})^2 M_{0,0,0}(\alpha_{ij})r(\alpha_{ij})\right)\\ &+ q_7\big(M_{0,2,0}(\alpha_{jl})r(\alpha_{jl}) - M_{0,2,0}(\alpha_{ij})r(\alpha_{ij})\big)\Big)\\ &+ q_{12}M_{0,0,0}(\alpha_{il})^3 r(\alpha_{il})\big(M_{0,0,0}(\alpha_{jl})r(\alpha_{jl}) - M_{0,0,0}(\alpha_{ij})r(\alpha_{ij})\big)\\ &+ q_2 r(\alpha_{jl})r(\alpha_{ij})\left(M_{0,0,0}(\alpha_{jl})M_{0,0,0}(\alpha_{ij})^3 - M_{0,0,0}(\alpha_{jl})^3 M_{0,0,0}(\alpha_{ij})\right)\ ,\end{aligned} \tag{5.15}$$

13 terms with a single factor of $r(\alpha)$:

$$
\begin{aligned}
\mathcal{A}_{r(\alpha)} = &\big(M_{0,0,0}(\alpha_{jl})r(\alpha_{jl}) - M_{0,0,0}(\alpha_{ij})r(\alpha_{ij})\big) \\
&\times \big(k_1 M_{0,1,1}(\alpha_{il}) + k_2 M_{0,0,0}(\alpha_{il})M_{1,0,0}(\alpha_{il})\big) \\
&+ k_3 M_{0,0,0}(\alpha_{il})^2\big(M_{1,0,0}(\alpha_{jl})r(\alpha_{jl}) - M_{1,0,0}(\alpha_{ij})r(\alpha_{ij})\big) \\
&+ k_4 M_{1,0,0}(\alpha_{il})r(\alpha_{il})\left(M_{0,0,0}(\alpha_{jl})^2 - M_{0,0,0}(\alpha_{ij})^2\right) \\
&+ M_{0,0,0}(\alpha_{il})r(\alpha_{il})\Big(k_5\big(M_{0,1,1}(\alpha_{jl}) - M_{0,1,1}(\alpha_{ij})\big) \\
&+ k_6\big(M_{0,0,0}(\alpha_{jl})M_{1,0,0}(\alpha_{jl}) - M_{0,0,0}(\alpha_{ij})M_{1,0,0}(\alpha_{ij})\big)\Big) \\
&+ k_8\big(M_{1,2,0}(\alpha_{jl})r(\alpha_{jl}) - M_{1,2,0}(\alpha_{ij})r(\alpha_{ij})\big) \\
&+ k_9\big(M_{1,0,2}(\alpha_{jl})r(\alpha_{jl}) - M_{1,0,2}(\alpha_{ij})r(\alpha_{ij})\big) \\
&+ k_{10}\Big(M_{0,0,0}(\alpha_{jl})M_{0,1,1}(\alpha_{jl})r(\alpha_{jl}) - M_{0,0,0}(\alpha_{ij})M_{0,1,1}(\alpha_{ij})r(\alpha_{ij})\Big) \\
&+ k_{11}\Big(M_{0,0,0}(\alpha_{jl})^2 M_{1,0,0}(\alpha_{jl})r(\alpha_{jl}) - M_{0,0,0}(\alpha_{ij})^2 M_{1,0,0}(\alpha_{ij})r(\alpha_{ij})\Big) \\
&+ k_{12}\big(M_{0,1,1}(\alpha_{jl}) - M_{0,1,1}(\alpha_{ij})\big)\big(M_{0,0,0}(\alpha_{jl})r(\alpha_{jl}) + M_{0,0,0}(\alpha_{ij})r(\alpha_{ij})\big) \\
&+ k_{13}\big(M_{0,0,0}(\alpha_{jl})M_{1,0,0}(\alpha_{jl}) - M_{0,0,0}(\alpha_{ij})M_{1,0,0}(\alpha_{ij})\big) \\
&\times \big(M_{0,0,0}(\alpha_{jl})r(\alpha_{jl}) + M_{0,0,0}(\alpha_{ij})r(\alpha_{ij})\big) \\
&+ k_{14}\left(M_{0,0,0}(\alpha_{jl})^2 + M_{0,0,0}(\alpha_{ij})^2\right)\left(M_{1,0,0}(\alpha_{jl})r(\alpha_{jl}) - M_{1,0,0}(\alpha_{ij})r(\alpha_{ij})\right) ,
\end{aligned}
\tag{5.16}
$$

and finally one term with a multiple zeta value

$$
\mathcal{A}_{\zeta} = e_1\zeta(3)\big(M_{0,0,0}(\alpha_{jl})r(\alpha_{jl}) - M_{0,0,0}(\alpha_{ij})r(\alpha_{ij})\big) . \tag{5.17}
$$

To summarise

$$
\mathcal{A}_{\text{minimal}} = \mathcal{A}_{r(\alpha)} + \mathcal{A}_{r(\alpha)r(\alpha')} + \mathcal{A}_{\zeta} . \tag{5.18}
$$

Note that in the ansatz $\mathcal{A}_{\text{minimal}}$ we still used $M_{0,2,0}$ and $M_{1,2,0}$ for notational convenience. However, we made sure that all terms in $\mathcal{A}_{\text{minimal}}$ are linearly independent.

We now calculate the collinear limit of $\mathcal{A}_{\text{minimal}}$, and try to fix some coefficients so that it obeys the constraint (5.12). However, when performing the analysis in Mathematica, it turns out that this is impossible. We will thus have to add some terms to our basis to gain more freedom.

5.4.3 Extension of $\mathcal{A}_{\text{minimal}}$

To extend our ansatz $\mathcal{A}_{\text{minimal}}$, we will have to drop one of our constraints. We choose to allow terms which include two factors of the same $r(\alpha)$. Such terms have never been known to occur in the calculation of other webs, but there is no fundamental reason why it should not occur in this web. We can create four such terms that also obey the other constraints. We thus extend our basis as follows:

$$\mathcal{A}_{\text{extended}} = \mathcal{A}_{r(\alpha)} + \mathcal{A}_{r(\alpha)r(\alpha')} + \mathcal{A}_{\zeta} + \mathcal{A}_{r(\alpha)^2} \ , \tag{5.19}$$

where

$$\begin{aligned}
\mathcal{A}_{r(\alpha)^2} = {} & j_7 M_{0,0,0}(\alpha_{il})^2 \left(M_{0,0,0}(\alpha_{jl})^2 r(\alpha_{jl})^2 - M_{0,0,0}(\alpha_{ij})^2 r(\alpha_{ij})^2 \right) \\
& + j_1 \left(M_{0,0,0}(\alpha_{jl})^4 r(\alpha_{jl})^2 - M_{0,0,0}(\alpha_{ij})^4 r(\alpha_{ij})^2 \right) \\
& + j_5 \left(M_{0,0,0}(\alpha_{jl})^2 + M_{0,0,0}(\alpha_{ij})^2 \right) \\
& \times \left(M_{0,0,0}(\alpha_{jl})^2 r(\alpha_{jl})^2 - M_{0,0,0}(\alpha_{ij})^2 r(\alpha_{ij})^2 \right) \\
& + j_6 \left(M_{0,0,0}(\alpha_{jl}) M_{0,2,0}(\alpha_{jl}) r(\alpha_{jl})^2 - M_{0,0,0}(\alpha_{ij}) M_{0,2,0}(\alpha_{ij}) r(\alpha_{ij})^2 \right) \ .
\end{aligned} \tag{5.20}$$

We now have 23 parameters in our ansatz.

5.4.4 Constraining $\mathcal{A}_{\text{extended}}$

We again try to fix parameters in $\mathcal{A}_{\text{extended}}$ by solving the equation (5.12). This time it is indeed possible to solve this equation. This fixes twelve parameters, leaving eleven free ones. We then calculate the lightlike limit of the remaining result, and equate this to the result found in [80], equation (5.7). This is possible and fixes seven further parameters, leaving us with only four remaining ones:

$$\begin{aligned}
\mathcal{A}(\alpha_{ij}, \alpha_{il}, \alpha_{jl}) = {} & \mathcal{A}_0(\alpha_{ij}, \alpha_{il}, \alpha_{jl}) + k_1 \mathcal{A}_{k_1}(\alpha_{ij}, \alpha_{il}, \alpha_{jl}) + k_{11} \mathcal{A}_{k_{11}}(\alpha_{ij}, \alpha_{il}, \alpha_{jl}) \\
& + k_{13} \mathcal{A}_{k_{13}}(\alpha_{ij}, \alpha_{il}, \alpha_{jl}) + j_5 \mathcal{A}_{j_5}(\alpha_{ij}, \alpha_{il}, \alpha_{jl})
\end{aligned} \tag{5.21}$$

The expressions for the contributions to $\mathcal{A}$ are quite lengthy, so are omitted.

5.5 Numerical fit

We have exploited the analytical constraints on $\mathcal{A}$ as much as we could, leaving us with only four parameters. We now want to fix these parameters numerically.

We do this by calculating the $(1,1,1,2)$ web using SecDec. We equate the result to the result that we obtain using our ansatz. We then solve for the four unknown parameters.

5.5.1 Generation of numerical results

The calculation of the $(1,1,1,2)$ subtracted web in SecDec is computationally a lot more expensive than calculation of the $(1,3,1)$ web in SecDec. Indeed, we have to calculate four diagrams to NLO accuracy, instead of just one diagram at LO. Of those four diagrams, the two that make up the $(1,1,1,2)$ web are particularly complicated due to their dependence on four different cusp parameters.

We choose 256 points on a $4\times4\times4\times4$ grid, and calculate the four diagrams up to NLO in SecDec. Of these 256 points, we discard those where we had an estimated numerical error of more than one per cent in one of the four loop calculations. After this procedure, 59 points remain. As a check, we calculate if they obey the relation (5.3). We calculate the numerical values of

$$\mathcal{R} = \frac{6\mathcal{W}^{(\epsilon^{-2})}_{1,1,1,2}(\alpha_{ij},\alpha_{il},\alpha_{jk},\alpha_{jl})}{\left[\mathcal{W}^{(\epsilon^{-1})}_{3g}(\alpha_{ij},\alpha_{il},\alpha_{jl}),\mathcal{W}^{(\epsilon^{-1})}_{1,1}(\alpha_{jk})\right]} \ , \tag{5.22}$$

in the 59 selected points, and expect to obtain one. The obtained values are displayed in histogram 5.2, and are indeed close to one. This provides confirmation that the leading order part of the numerical results generated in SecDec is correct.

5.5.2 Fitting the parameters

Now that we have calculated all the contributions to $\bar{\mathcal{F}}^{(-1)}_{(1,1,1,2)}$ numerically in SecDec, we can combine them using equation (5.4). This gives us numerical values for $\bar{\mathcal{F}}^{(-1)}_{(1,1,1,2)}$ in 59 points. We denote them by $\bar{\mathcal{F}}_{(1,1,1,2),\text{num}}$.
Using the the ansatz for $t_1(\alpha_{ij},\alpha_{il},\alpha_{jl})$, (5.21), equation (5.5) can be rewritten as

$$\begin{aligned}\bar{\mathcal{F}}_{(1,1,1,2)}(\alpha_{ij},\alpha_{il},\alpha_{jk},\alpha_{jl}) = \frac{i}{4}\Gamma(6\epsilon)\kappa^3 r(\alpha_{jk})\Big(&M_{0,0,0}(\alpha_{jk})\mathcal{A}(\alpha_{ij},\alpha_{il},\alpha_{jl}) \\ &- 2M_{1,0,0}(\alpha_{jk})t_0(\alpha_{ij},\alpha_{il},\alpha_{jl})\Big) + \mathcal{O}(1) \ ,\end{aligned} \tag{5.23}$$

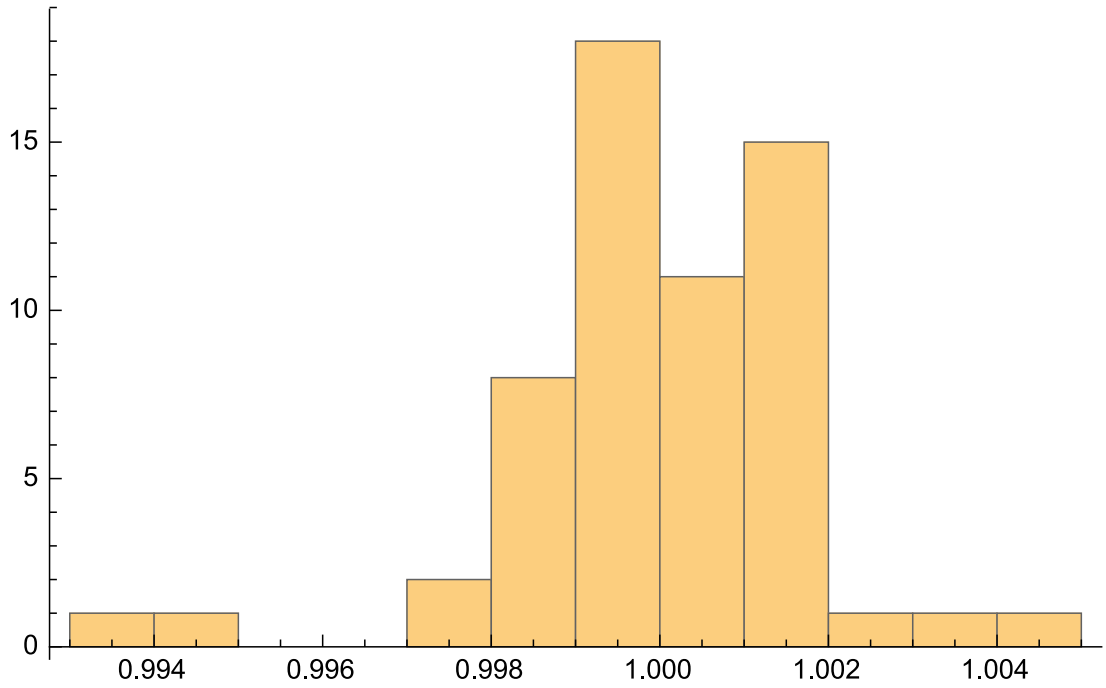

Figure 5.2 *Histogram of the numerical values of the ratio $\mathcal{R}$ calculated in 59 points using SecDec. Values around one are expected.*

or, using the explicit expression for the ansatz (5.21),

$$\begin{aligned}
&\frac{i}{4}\Gamma(6\epsilon)\kappa^3 r(\alpha_{jk})\Big(2M_{1,0,0}(\alpha_{jk})t_0(\alpha_{ij},\alpha_{il},\alpha_{jl}) - M_{0,0,0}(\alpha_{jk})\mathcal{A}_0(\alpha_{ij},\alpha_{il},\alpha_{jl})\Big) \\
&+ \bar{\mathcal{F}}_{(1,1,1,2)}(\alpha_{ij},\alpha_{il},\alpha_{jk},\alpha_{jl}) \\
&= \frac{i}{4}\Gamma(6\epsilon)\kappa^3 r(\alpha_{jk})M_{0,0,0}(\alpha_{jk})\Big(k_1\mathcal{A}_{k_1}(\alpha_{ij},\alpha_{il},\alpha_{jl}) + k_{11}\mathcal{A}_{k_{11}}(\alpha_{ij},\alpha_{il},\alpha_{jl}) \\
&+ k_{13}\mathcal{A}_{k_{13}}(\alpha_{ij},\alpha_{il},\alpha_{jl}) + j_5\mathcal{A}_{j_5}(\alpha_{ij},\alpha_{il},\alpha_{jl})\Big) + \mathcal{O}(1)\ . \qquad (5.24)
\end{aligned}$$

Using the numeric values $\bar{\mathcal{F}}_{(1,1,1,2),\text{num}}$, we can calculate the left-hand side of equation (5.24) in the 59 selected points. We can then calculate the right-hand side of equation (5.24) in the same 59 points, leaving the four unknown coefficients k_1, k_{11}, k_{13}, j_5. We then try to fit these functions numerically, using the Mathematica Fit function. We obtain that

$$\begin{aligned}
j_5 &= -0.00746503 \\
k_1 &= -521.175 \\
k_{11} &= -177.691 \\
k_{13} &= 132.878\ . \qquad (5.25)
\end{aligned}$$

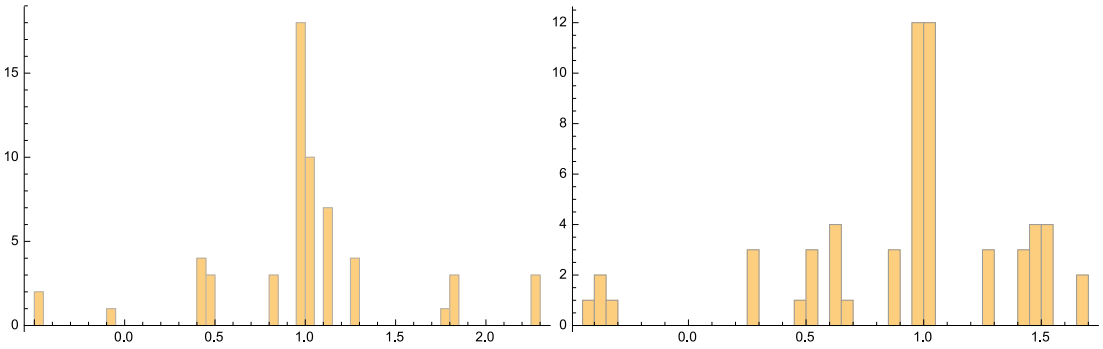

(a) *First fit.* **(b)** *Fit with an extra parameter.*

Figure 5.3 *Histograms displaying the quality of the fit of the* $(1,1,1,2)$ *web. They show the ratio of the fitted values to the numeric values in equations* (5.24) *and* (5.28) *respectively.*

When plugging these values into the ansatz, we can recalculate the right-hand side of equation (5.24). We then compare it to the numerical values of the left-hand side. A histogram displaying the distribution of the ratio of the two quantities can be found on the left-hand side of figure 5.3. The histogram has a sharp peak around one, indicating very good agreement in many points. However, it also shows many outliers, so that we have to conclude that the quality of the fit is not very good. The discrepancy can not be explained by the numerical errors of the calculations in SecDec alone, so that we have to conclude that we are missing something in this approach. We investigate in the next section what could have gone wrong.

5.6 What can be improved?

We find different causes that can explain why the fit we used is so poor, and discuss them.

5.6.1 Mistakes when performing the fit

A straightforward explanation is an error made when combining all the terms occurring in equation (5.24). We list the possible mistakes, and what we have done to check that they were not made.

Combining diagrams to calculate $\bar{\mathcal{F}}_{(1,1,1,2),\text{num}}$

Calculation of the left-hand side of equation (5.24) involved calculating $\bar{\mathcal{F}}_{(1,1,1,2),\text{num}}$ in SecDec, which involves a combination of the four diagrams occurring in

equation (5.4). One possible way to check we are combining diagrams the correct way is by checking equation (5.3). We did this in histogram (5.2). We indeed did spot a mistake this way, and corrected for it. However, this did not improve the fit.

A stronger check to see if we are combining the results correctly, would be to calculate $\bar{\mathcal{F}}_{(1,1,1,2),\text{num}}$ in the lightlike limit, and check if this agrees with the result calculated in reference [80]. However, numerical calculations in this limit are computationally expensive, so that we did not do this yet. It might be a good idea to perform this check in the future.

Relative normalisations

On the left-hand side of (5.24), we combine $\bar{\mathcal{F}}_{(1,1,1,2),\text{num}}$, which has been calculated numerically in SecDec, with terms that we have derived analytically. We have to be careful, because the different ingredients use different normalisations. The analytical ansatz is derived using both the lightlike limit in [80], where at three loops a factor of α_s^3 is extracted, and the expression (4.159) for the $(1,3,1)$ web, where at three loops we extract a factor of $\Gamma(6\epsilon)\kappa^3$. This ansatz is then added to a SecDec result, where at three loops a factor of $-i(4\pi)^{3-3\epsilon}$ is extracted. We thus have to rescale the different results before we can add them, which can easily introduce mistakes. This is particularly true for the calculation of $\bar{\mathcal{F}}_{(1,1,1,2),\text{num}}$, because we also use NLO results, so the ϵ dependence of the normalisation can matter. We ensure that we add terms correctly in two ways.

First, we prove that the ϵ dependence of the normalisation factor in SecDec does not matter. Indeed, suppose we rescale all l-loop SecDec results by a factor of $X^{l\epsilon}$ for some number X. This changes the contributions to the subtracted $(1,1,1,2)$ web as follows:

$$\begin{aligned}
\bar{\mathcal{W}}^{(\epsilon^{-1})}_{(1,1,1,2)} &\to \bar{\mathcal{W}}^{(\epsilon^{-1})}_{(1,1,1,2)} + 3\epsilon \ln X \bar{\mathcal{W}}^{(\epsilon^{-2})}_{(1,1,1,2)} \ , \\
\mathcal{W}^{(\epsilon^{0})}_{3g} &\to \mathcal{W}^{(\epsilon^{0})}_{3g} + 2\epsilon \ln X \mathcal{W}^{(\epsilon^{-1})}_{3g} \ , \\
\mathcal{W}^{(\epsilon^{0})}_{(1,1)} &\to \mathcal{W}^{(\epsilon^{0})}_{(1,1)} + \epsilon \ln X \mathcal{W}^{(\epsilon^{-1})}_{(1,1)} \ ,
\end{aligned} \tag{5.26}$$

so that

$$\begin{aligned}
\bar{\mathcal{W}}^{(-1)}_{1,1,1,2}(\alpha_{ij},\alpha_{il},\alpha_{jk},\alpha_{jl}) &\to \bar{\mathcal{W}}^{(-1)}_{1,1,1,2}(\alpha_{ij},\alpha_{il},\alpha_{jk},\alpha_{jl}) \\
&\quad + 3\epsilon \ln X \left(\bar{\mathcal{W}}^{(-2)}_{(1,1,1,2)} - \frac{1}{6}\left[\mathcal{W}^{(-1)}_{3g}(\alpha_{ij},\alpha_{il},\alpha_{jl}), \mathcal{W}^{(-1)}_{1,1}(\alpha_{jk}) \right] \right) \\
&= \bar{\mathcal{W}}^{(-1)}_{1,1,1,2}(\alpha_{ij},\alpha_{il},\alpha_{jk},\alpha_{jl}) \ ,
\end{aligned} \tag{5.27}$$

where the last equality follows from equation (5.3). This implies that we do not need to worry about the ϵ dependence of the normalisation.

However, we could still be making a mistake that does not depend on ϵ when combining the terms on the left-hand side of (5.24). To deal with this possibility, we introduce an extra coefficient k in equation (5.24) as follows:

$$\begin{aligned}
&\bar{\mathcal{F}}_{(1,1,1,2)}(\alpha_{ij},\alpha_{il},\alpha_{jk},\alpha_{jl}) \\
&= \frac{i}{4}\Gamma(6\epsilon)\kappa^3 r(\alpha_{jk})\Bigg[-k\Big(2M_{1,0,0}(\alpha_{jk})t_0(\alpha_{ij},\alpha_{il},\alpha_{jl}) - M_{0,0,0}(\alpha_{jk})\mathcal{A}_0(\alpha_{ij},\alpha_{il},\alpha_{jl})\Big) \\
&+ M_{0,0,0}(\alpha_{jk})\Big(k_1\mathcal{A}_{k_1}(\alpha_{ij},\alpha_{il},\alpha_{jl}) + k_{11}\mathcal{A}_{k_{11}}(\alpha_{ij},\alpha_{il},\alpha_{jl}) \\
&+ k_{13}\mathcal{A}_{k_{13}}(\alpha_{ij},\alpha_{il},\alpha_{jl}) + j_5\mathcal{A}_{j_5}(\alpha_{ij},\alpha_{il},\alpha_{jl})\Big)\Bigg] + \mathcal{O}(1) \ , \qquad (5.28)
\end{aligned}$$

where we expect k to equal one if we did not make a mistake, and most likely a power of two if we did miss such a factor somewhere.

When performing the fit, we do not find any improvement, as can be seen on the right-hand side of figure 5.3. Moreover, the fit reveals that

$$k = 0.201927 \ , \qquad (5.29)$$

which is not the type of factor the we can expect to have missed.

We performed more fits with even more extra parameters introduced, but none were of good quality. We conclude that this can not be the source of the poor quality of the fit.

Not enough data

It could be possible that the 59 data points do not give enough information to fit the four parameters. This problem would be easy to resolve by generating more data in SecDec. However, when performing a similar fit in reference [81], two hundred data points suffice to fix 25 parameters. It is thus highly unlikely that 59 would not suffice to fix four.

One possible way to check this, is by performing fits where we exclude some of our data points. We can then compare the quality of these fits to the quality of the fit with 59 points. This would give us an idea how adding data points improves the value of the fit.

Conclusion

From the above, we conclude that if the procedure does go wrong during the fitting itself, the most likely cause is the incorrect combination of the diagrams calculated in SecDec to form the subtracted web. It would be useful to check this by performing a numerical calculation with small values of α, and compare the result to the lightlike limit (5.7). It would also be a good idea to perform a fit with some data points excluded, to see how this influences the quality of the fit.

5.6.2 Incomplete ansatz

Another possible source of error is that the ansatz used in (5.24) might not be correct. This could have two explanations. Firstly, it could be the case that something went wrong when eliminating coefficients from $\mathcal{A}_{\text{minimal}}$. However, the constraints used to eliminate these coefficients, namely the lightlike limit of the $(1,1,1,2)$ web and the result for the $(1,3,1)$ web in general kinematics, have been proven to be correct numerically. This explanation is thus not very likely. The second possible explanation is that an assumption made when producing the ansatz $\mathcal{A}_{\text{minimal}}$ was unjustified. This way, we would have excluded from our ansatz some functions that in fact do contribute to the web, so that the resulting ansatz is incomplete. Therefore, we decide to investigate different assumptions that might not have been justified when producing $\mathcal{A}_{\text{minimal}}$.

The result is not described by the basis functions

It is possible that the ansatz is not complete, because the final result also contains functions which are not included in the basis $M_{k,l,m}(\alpha)$. However, this is highly unlikely. Indeed, when conjecturing the basis in reference [30], it is argued convincingly why webs can only be described by functions of this nature.

The result also contains functions without a factor of $r(\alpha)$

When generating the minimal ansatz, we argued that there is no need for functions without a factor of $r(\alpha)$. When taking the collinear limit of such a term, it becomes either zero or a weight four function of α_{ij}, still without a factor of $r(\alpha)$, and we do not see such a term in the result for the $(1,3,1)$ web. However, it is still possible for such terms to occur in such a way that they all cancel in the collinear limit. We could reintroduce such terms; they would be the same as $\mathcal{A}_{r(\alpha)^2}$, but without the factors of $r(\alpha)^2$. This would hence introduce four extra parameters.

Some of them might be eliminated by the constraints posed by the lightlike and collinear limits.

More than two factors of $r(\alpha)$

We could extend our ansatz by functions containing more than two factors of $r(\alpha)$. However, based on the expressions for webs that have been calculated earlier, such terms are highly unlikely to occur. There would also be a large number of them, making numerical fits very complicated. We conclude that such an extension would not be a good idea.

Other constraints

All the other constraints, such as $i \leftrightarrow l$ antisymmetry, $\alpha \to \frac{1}{\alpha}$ symmetry, having only one occurrence of the letter $(1-\alpha^2)$ in the symbol, and so on, have been proven to be necessary. They thus have to be obeyed.

5.7 Conclusion and outlook

In this chapter, we tried to calculate the subtracted $(1,1,1,2)$ web via a bootstrap approach. We started from the results in [81], where a 40-parameter ansatz is proposed. By using the result for the $(1,3,1)$ web to constrain the result further, we gained more insight into the problem. We managed to write down a reduced ansatz containing 23 parameters, and to constrain it further so that there are only four parameters left. However, when fitting these parameters numerically, we did not obtain satisfactory results. We analysed the most likely reasons for this, and how to resolve them. We found that there are three promising options to pursue. Firstly, we could check if the numerical results generated using SecDec are correct, by calculating data points in the lightlike limit and comparing them to the known analytical result. Secondly, we could find out how leaving out some data points influences the quality of the fit, so that we can find out if adding more data points would be helpful. Finally, we could extend our ansatz with functions which do not contain a factor of $r(\alpha)$.

Chapter 6

Conclusion and outlook

In this thesis, we developed new techniques for the calculation of infrared divergences in gauge theories. Such divergences are an essential contribution to the calculation of observables such as cross sections and decay rates [5, 7–18]. The calculation of infrared divergences can be phrased in terms of webs [27–39]. Our main focus was on the use of unitarity cuts to calculate webs. In chapter 2, we extended the existing framework to make this possible. We then applied this to the calculation of various one- and two-loop diagrams. We found agreement with known results, and discovered that the calculation of cuts revealed some hidden structure. This was particularly helpful when dealing with diagrams involving three-gluon vertices. In chapter 4, we continued this approach by calculating the $(1, 3, 1)$ web. We found that in this case, the cuts displayed some unexpected complexity. We were however still able to find an expression for the web, which was numerically proven to be correct. We found that the expression satisfied the factorisation conjecture 1. However, we had to extend the conjectured basis functions by multiple zeta values to describe our result. In chapter 5, we used the information gained from the calculation of the $(1, 3, 1)$ web to calculate the $(1, 1, 1, 2)$ web via a bootstrap approach. We managed to eliminate all but four parameters of our ansatz, but failed to calculate those parameters numerically. We proposed a few possible ways to resolve this problem, which is still a work in progress.

Overall, the work presented in this thesis is a step towards the calculation of the soft anomalous dimension at three loops. We were able to calculate one of the missing diagrams needed to obtain the complete result. Moreover, our work suggests that it is possible to calculate some of the remaining unknown diagrams using unitarity cuts. However, for some webs, such as the $(1, 1, 1, 1)$

web with a four-gluon vertex, a different approach will be needed. This could be the bootstrap approach, presented in chapter 5. Another method could be using differential equations, which has been successfully used to calculate the three-loop cusp anomalous dimension [57].

Appendix A

Measures for polar coordinates in d dimensions.

When we parametrise our loop momenta, we always choose some form of polar coordinates. The main difference between different parametrisations is the number of angles we have left. In this appendix, we derive what the measure becomes in these cases, and illustrate with some examples.

A.1 General case

We start from the most general measure for polar coordinates:

$$\begin{aligned} d^d k &= dk_0\, k_0^{d-1} d\theta_1\, d\cos\theta_2 ... d\cos\theta_{d-1} \sin^{d-3}\theta_{d-1} \\ k_0 &> 0 \\ 0 &< \theta_1 < 2\pi \\ 0 &< \theta_i < \pi \text{ for } i > 1 \ . \end{aligned} \tag{A.1}$$

In the problems we study, there will be some symmetries so that we can integrate out some angles. We look what the remaining measure looks like.

A.2 No angular dependence

If there is no angular dependence, we can integrate out all angles. To integrate out the angles, we make use of the formula

$$\int_0^\pi d\cos\theta \sin^{k-1}\theta = \frac{\Gamma(1/2)\Gamma((k+1)/2)}{\Gamma((k+2)/2)} \ , \tag{A.2}$$

such that

$$\begin{aligned} d^d k &= dk_0 k_0^{d-1} \int_0^{2\pi} d\theta_1 \int_0^{\pi} d\cos\theta_2 ... d\cos\theta_{d-1} \sin^{d-3}\theta_{d-1} \\ &= dk_0 k_0^{d-1} 2\pi \frac{\Gamma(1/2)\Gamma(1)}{\Gamma(3/2)} \frac{\Gamma(1/2)\Gamma(3/2)}{\Gamma(2)} ... \frac{\Gamma(1/2)\Gamma((d-1)/2)}{\Gamma(d/2)} \\ &= dk_0 k_0^{d-1} 2\pi \frac{\Gamma^{d-2}(1/2)}{\Gamma(d/2)} \\ &= 2dk_0 k_0^{d-1} \frac{\pi^{d/2}}{\Gamma(d/2)} \ . \end{aligned} \tag{A.3}$$

A.2.1 Example

A specific example is the parametrisation we use to calculate the one-loop diagram. We chose

$$k = (k_0, k_1, k_2 \mathbf{v}_{d-2}) \ . \tag{A.4}$$

We see that we left the first two components of the measure untouched, and parametrised the last $d-2$ components in terms of polar coordinates. There is no angular dependence left, so we can apply (A.3) to obtain

$$d^d k = \frac{2\pi^{1-\epsilon}}{\Gamma(1-\epsilon)} dk_0 dk_1 dk_2 k_2^{1-2\epsilon} \ . \tag{A.5}$$

A.3 One angular variable

In this case, the momentum can be parametrised as $k = (k_0 \cos\sigma, k_0 \sin\sigma \mathbf{v}_{d-1})$ where $\mathbf{v}_{d-1}$ is a $(d-1)$-dimensional unit vector that can be integrated out. The variable σ corresponds to the θ_{d-1} in the most general parametrisation. We thus obtain as measure

$$\begin{aligned} d^d k &= dk_0 k_0^{d-1} d\cos\sigma \sin^{d-3}\sigma \int_0^{2\pi} d\theta_1 \int_0^{\pi} d\cos\theta_2 ... d\cos\theta_{d-2} \sin^{d-4}\theta_{d-2} \\ &= dk_0 k_0^{d-1} d\cos\sigma \sin^{d-3}\sigma \, 2 \frac{\pi^{(d-1)/2}}{\Gamma((d-1)/2)} \ . \end{aligned} \tag{A.6}$$

A.3.1 Example

We use such a parametrisation in the calculation of the k_2 loop of the $(1,2,1)$ diagram:

$$\begin{aligned} \beta_k &= (-\cosh\phi, \sinh\phi \mathbf{v}_{d-1}) \\ k_2 &= (k_{20}, k_{21}\mathbf{v'}_{d-1}) \\ \mathbf{v}\cdot\mathbf{v'} &= \cos\tau \ . \end{aligned} \tag{A.7}$$

This parametrisation indeed uses polar coordinates and there is only one relevant angle, namely τ. The measure then becomes

$$d^d k_2 = \frac{2\pi^{1-\epsilon}}{\Gamma(1-\epsilon)} dk_{20} dk_{21}\ k_{21}^{2-2\epsilon} d\cos\tau (\sin\tau)^{-2\epsilon} \ . \tag{A.8}$$

Similarly, if we parametrise $k = (k_0, k_1, k_2\cos\sigma, k_2\sin\sigma\mathbf{v})$, the measure becomes

$$d^d k = \frac{2\pi^{1/2-\epsilon}}{\Gamma(1/2-\epsilon)} dk_0\ dk_1\ dk_2 k_2^{1-2\epsilon} d\cos\sigma (\sin\sigma)^{-1-2\epsilon} \ . \tag{A.9}$$

A.4 Two angular variables left

Finally, we look at the case where we have two angular variables left, denoted σ_1, σ_2, corresponding to $\theta_{d-1}, \theta_{d-2}$ above. We then have

$$k = (k_0\cos\sigma, k_0\sin\sigma\cos\sigma', k_0\sin\sigma\sin\sigma'\mathbf{v}_{d-2}) \ . \tag{A.10}$$

The measure then becomes

$$\begin{aligned} d^d k &= dk_0 k_0^{d-1} d\cos\sigma \sin^{d-3}\sigma d\cos\sigma' \sin^{d-4}\sigma' \\ &\times \int_0^{2\pi} d\theta_1 \int_0^{\pi} d\cos\theta_2 ... d\cos\theta_{d-3} \sin^{d-5}\theta_{d-3} \\ &= dk_0 k_0^{d-1} d\cos\sigma \sin^{d-3}\sigma\ d\cos\sigma' \sin^{d-4}\sigma'\ \frac{2\pi^{(d-2)/2}}{\Gamma((d-2)/2)} \ . \end{aligned} \tag{A.11}$$

A.4.1 Example

We used a similar parametrisation when calculating the k_3 loop integral of $\mathrm{Cut}_{3g,2}$. Indeed, we then used

$$\beta_i = (\cosh\psi, \sinh\psi\cos\rho, \sinh\psi\sin\rho\mathbf{v})$$

$$
\begin{aligned}
k_3 &= (k_{30}, k_{31}\cos\sigma, k_{31}\sin\sigma\mathbf{v}') \\
\mathbf{v}\cdot\mathbf{v}' &= \cos\tau \ .
\end{aligned} \tag{A.12}
$$

We are left with two remaining angles σ, τ, so that the measure becomes

$$
d^d k_3 = \frac{2\pi^{1/2-\epsilon}}{\Gamma(1/2-\epsilon)} dk_{30} dk_{31} k_{31}^{2-2\epsilon} d\cos\sigma (\sin\sigma)^{-2\epsilon} d\cos\tau (\sin\tau)^{-1-2\epsilon} \ . \tag{A.13}
$$

Appendix B

The $(1,1,1)$ web

We show here how to calculate the cuts of the $(1,1,1)$ web. As explained in the main text, it suffices to calculate $\mathrm{Cut}_{3g,2}$.
We start from equation (3.73). We first perform the k_2 subintegral, hence we manipulate the numerator so that it only depends on k_3 as described above. We calculate this in the frame where

$$\begin{aligned}
\beta_i &= (1, \mathbf{0}_{d-1}) \\
\beta_j &= (\cosh\theta, \sinh\theta, \mathbf{0}_{d-2}) \\
k_2 &= (k_{20}, k_{21}, k_{22}\mathbf{v}_{d-2}) \\
k_3 &= (-k_{30}, k_{30}\cos\sigma, k_{30}\sin\sigma \mathbf{v}'_{d-2}) \\
\mathbf{v}\cdot\mathbf{v}' &= \cos\tau
\end{aligned} \tag{B.1}$$

This parametrisation makes explicit use of the $\delta^-(k_3^2)$. We then have

$$\begin{aligned}
\mathrm{Cut}_{3g,2,k_2} &= \int \frac{d^d k_2}{(2\pi)^d} \frac{\delta(\beta_i\cdot(k_2+k_3)-1)\delta(-\beta_j\cdot k_2 - 1)}{(k_2+k_3)^2 k_2^2} \\
&= \frac{2\pi^{1/2-\epsilon}}{(2\pi)^d \Gamma(1/2-\epsilon)} \int dk_{20} dk_{21} dk_{22} k_{22}^{1-2\epsilon} \frac{d\cos\tau(\sin\tau)^{-1-2\epsilon}}{(k_{20}^2 - k_{21}^2 - k_{22}^2)} \\
&\times \frac{\delta(k_{20}-k_{30}-1)\delta(-k_{20}\cosh\theta + k_{21}\sinh\theta - 1)}{(k_{20}^2 - k_{21}^2 - k_{22}^2 - 2k_{20}k_{30} - 2k_{21}k_{30}\cos\sigma - 2k_{22}k_{30}\sin\sigma\cos\tau)} \\
&= \frac{2\pi^{1/2-\epsilon}}{(2\pi)^d \Gamma(1/2-\epsilon)\sinh\theta} \int_0^\infty dk_{22} d\cos\tau \frac{k_{22}^{1-2\epsilon}(\sin\tau)^{-1-2\epsilon}}{k_{20}^2 - k_{21}^2 - k_{22}^2} \\
&\times \frac{1}{k_{20}^2 - k_{21}^2 - k_{22}^2 - 2k_{20}k_{30} - 2k_{21}k_{30}\cos\sigma - 2k_{22}k_{30}\sin\sigma\cos\tau} \,,
\end{aligned} \tag{B.2}$$

where k_{20} and k_{21} are the solutions of the delta functions, namely

$$\begin{aligned} k_{20} &= 1 + k_{30} \\ k_{21} &= \frac{(1+k_{30})\cosh\theta + 1}{\sinh\theta} \ . \end{aligned} \tag{B.3}$$

The $\cos\tau$ integral is now easy to perform. Because it is a finite integral, we are only interested in the leading order part, so this simplifies to

$$\begin{aligned} \mathrm{Cut}_{3g,2,k_2} = &\frac{2}{(2\pi)^4 \sinh\theta} \int_0^\infty dk_{22} \frac{k_{22}^{1-2\epsilon}}{k_{20}^2 - k_{21}^2 - k_{22}^2} \\ &\times \frac{\pi}{\sqrt{\left(k_{20}^2 - k_{21}^2 - k_{22}^2 - 2k_{20}k_{30} - 2k_{21}k_{30}\cos\sigma\right)^2 - 4k_{22}^2 k_{30}^2 \sin^2\sigma}} \ . \end{aligned} \tag{B.4}$$

The k_{22} integral has a momentum scale, so we have to be careful about powers of ϵ. However, we can extract the scale via

$$k_{22} = \sqrt{\alpha} k_{30} \ . \tag{B.5}$$

We then only need to calculate the leading order part of the α integration.

$$\begin{aligned} \mathrm{Cut}_{3g,2,k_2} = &\frac{\pi}{(2\pi)^4 \sinh\theta} k_{30}^{2-2\epsilon} \int_0^\infty d\alpha \frac{1}{k_{20}^2 - k_{21}^2 - \alpha k_{30}^2} \\ &\times \frac{1}{\sqrt{\left(k_{20}^2 - k_{21}^2 - \alpha k_{30}^2 - 2k_{20}k_{30} - 2k_{21}k_{30}\cos\sigma\right)^2 - 4\alpha k_{30}^4 \sin^2\sigma}} \ . \end{aligned} \tag{B.6}$$

This α integration can now be performed and will give logarithms of complicated arguments. However, we can again exploit the general considerations that we made before. We are only looking for the leading order divergence, coming from the region where $k_{30} \to \infty$. This means that we only need to take the leading order contributions in k_{30} into account. We can then replace

$$\begin{aligned} k_{20} &= 1 + k_{30} \to k_{30} \\ k_{21} &= \frac{(1+k_{30})\cosh\theta + 1}{\sinh\theta} \to r(\alpha_{ij}) k_{30} \ , \end{aligned} \tag{B.7}$$

so that (B.6) becomes

$$\begin{aligned}\mathrm{Cut}_{3g,2,k_2} &\to \frac{\pi}{(2\pi)^4 \sinh\theta} k_{30}^{-2-2\epsilon} \int_0^\infty d\alpha \frac{1}{1-r(\alpha_{ij})^2-\alpha} \\ &\times \frac{1}{\sqrt{\big(1-r(\alpha_{ij})^2-\alpha-2-2r(\alpha_{ij})\cos\sigma\big)^2-4\alpha\sin^2\sigma}} \\ &= -\frac{\pi}{2(2\pi)^4 \sinh\theta} k_{30}^{-1-2\epsilon} \frac{\ln\left(\frac{1+r(\alpha_{ij})}{1-r(\alpha_{ij})}\right)}{\cos\sigma + r(\alpha_{ij})} + \mathcal{O}(1) \\ &= \frac{\pi}{(2\pi)^4} (\beta_i \cdot k_3)^{-1-2\epsilon} \frac{\ln(-\alpha_{ij})}{\beta_j \cdot k_3} + \mathcal{O}(1)\ . \end{aligned} \tag{B.8}$$

We now plug this into the remaining loop integral:

$$\begin{aligned}\mathrm{Cut}_{3g,2} = \frac{i}{2}\frac{\mu^{4\epsilon}}{m^{4\epsilon}} g_s^4 \beta_j \cdot \beta_k \int \frac{d^d k_3}{(2\pi)^d} \frac{-2\beta_i \cdot k_3 - 1}{(-\beta_k \cdot k_3 - 1)} \\ \times \delta^-(k_3)^2 (\beta_i \cdot k_3)^{-1-2\epsilon} \frac{\ln(-\alpha_{ij})}{\beta_j \cdot k_3} + \mathcal{O}(1)\ . \end{aligned} \tag{B.9}$$

We calculate this in a frame where

$$\begin{aligned}\beta_j &= (1, \mathbf{0}_{d-1}) \\ \beta_k &= (-\cosh\phi, \sinh\phi, \mathbf{0}_{d-2}) \\ \beta_i &= (\cosh\psi, \sinh\psi\cos\rho, \sinh\psi\sin\rho \mathbf{v}_{d-2}) \\ k_3 &= (k_{30}, k_{31}\cos\sigma, k_{31}\sin\sigma \mathbf{v}'_{d-2}) \\ \mathbf{v}\cdot\mathbf{v}' &= \cos\tau \\ d^d k_3 &= \frac{2\pi^{1/2-\epsilon}}{\Gamma(1/2-\epsilon)} dk_{30} dk_{31} k_{31}^{2-2\epsilon} d\cos\sigma (\sin\sigma)^{-2\epsilon} d\cos\tau (\sin\tau)^{-1-2\epsilon}\ . \end{aligned} \tag{B.10}$$

Equation (B.9) then becomes, up to finite corrections,

$$\begin{aligned}\mathrm{Cut}_{3g,2} &= \frac{i}{(2\pi)^4}\frac{\mu^{4\epsilon}}{m^{4\epsilon}} g_s^4 \beta_j \cdot \beta_k \int dk_{30} dk_{31} k_{31}^{2-2\epsilon} \frac{\ln(-\alpha_{ij})}{k_{30}} \\ &\times \int_{-1}^1 d\cos\sigma (\sin\sigma)^{-2\epsilon} d\cos\tau (\sin\tau)^{-1-2\epsilon} \frac{\delta(k_{30}+k_{31})}{2k_{31}} \\ &\times \frac{-2\big(\cosh\psi k_{30} - \sinh\psi k_{31}\cos\rho - \sinh\psi k_{31}\sin\rho\cos\tau\big) - 1}{(k_{30}\cosh\phi + k_{31}\sinh\phi\cos\sigma - 1)} \\ &\times \big(\cosh\psi k_{30} - \sinh\psi k_{31}\cos\rho - \sinh\psi k_{31}\sin\rho\cos\tau\big)^{-1-2\epsilon} \\ &= \frac{i}{(2\pi)^4}\frac{\mu^{4\epsilon}}{m^{4\epsilon}} g_s^4 \beta_j \cdot \beta_k \int_0^\infty dk_{31} k_{31}^{2-2\epsilon} \end{aligned}$$

$$
\begin{aligned}
&\times \int_{-1}^{1} d\cos\sigma (\sin\sigma)^{-2\epsilon} d\cos\tau (\sin\tau)^{-1-2\epsilon} \frac{1}{2k_{31}} \frac{\ln(-\alpha_{ij})}{-k_{31}} \\
&\times \frac{-2\big(-\cosh\psi k_{31} - \sinh\psi k_{31}\cos\rho - \sinh\psi k_{31}\sin\rho\cos\tau\big) - 1}{(-k_{31}\cosh\phi + k_{31}\sinh\phi\cos\sigma - 1)} \\
&\times \big(-\cosh\psi k_{31} - \sinh\psi k_{31}\cos\rho - \sinh\psi k_{31}\sin\rho\cos\tau\big)^{-1-2\epsilon} \\
&= i\ln(-\alpha_{ij}) \frac{1}{4\epsilon} \frac{1}{(2\pi)^4} \frac{\mu^{4\epsilon}}{m^{4\epsilon}} g_s^4 \beta_j \cdot \beta_k \int_{-1}^{1} d\cos\sigma (\sin\sigma)^{-2\epsilon} d\cos\tau \\
&\times (\sin\tau)^{-1-2\epsilon} \frac{\big(-\cosh\psi - \sinh\psi\cos\rho - \sinh\psi\sin\rho\cos\tau\big)^{-2\epsilon}}{-\cosh\phi + \sinh\phi\cos\sigma} \ . \qquad \text{(B.11)}
\end{aligned}
$$

The angular integrals now have to be performed only to leading order. This gives

$$
\begin{aligned}
&\mathrm{Cut}_{3g,2} \\
&= i\ln(-\alpha_{ij}) \frac{1}{4\epsilon} \frac{1}{(2\pi)^4} \frac{\mu^{4\epsilon}}{m^{4\epsilon}} g_s^4 \beta_j \cdot \beta_k \int_{-1}^{1} \frac{d\cos\tau}{(\sin\tau)^{-1}} \int_{-1}^{1} \frac{d\cos\sigma}{-\cosh\phi + \sinh\phi\cos\sigma} \\
&= i\ln(-\alpha_{ij}) \frac{1}{4\epsilon} \frac{\pi}{(2\pi)^4} \frac{\mu^{4\epsilon}}{m^{4\epsilon}} g_s^4 r(\alpha_{jk}) \ln\Big(\frac{\cosh\phi - \sinh\phi}{\cosh\phi + \sinh\phi}\Big) \\
&= i\ln(-\alpha_{ij}) \frac{1}{4\epsilon} \frac{2\pi}{(2\pi)^4} \frac{\mu^{4\epsilon}}{m^{4\epsilon}} g_s^4 r(\alpha_{jk}) \ln(\alpha_{jk}) \\
&= \frac{2\pi i\kappa^2}{\epsilon} \ln(-\alpha_{ij}) r(\alpha_{jk}) \ln(\alpha_{jk}) \ . \qquad \text{(B.12)}
\end{aligned}
$$

Appendix C

The $(1,3,1)$ web

We calculate some loop integrals that occur in the $(1,3,1)$ web in this chapter.

C.1 Bubbles

By bubbles, we mean Feynman integrals with two propagators. There is only one relevant bubble to calculate:

$$\begin{aligned}\mathcal{B}_{1,k_2}(k_1^2,\beta_j\cdot k_1) &= \int \frac{d^dk_2}{(2\pi)^d}\delta^+((k_1+k_2)^2)\delta(-\beta_j\cdot k_2-1)\\ &= \int \frac{d^dk_2}{(2\pi)^d}\delta^+(k_2^2)\delta(-\beta_j\cdot(k_2-k_1)-1)\ . \end{aligned}\tag{C.1}$$

We calculate it in the centre of mass frame of particle j:

$$\begin{aligned}\beta_j &= (1,\mathbf{0}_{d-1})\\ k_2 &= (k_{20},k_{21}\mathbf{v}_{d-1}),\quad \mathbf{v}^2=1\\ d^dk_2 &= \frac{2\pi^{3/2-\epsilon}}{\Gamma(3/2-\epsilon)}dk_{20}dk_{21}{k_{21}}^{2-2\epsilon}\ , \end{aligned}\tag{C.2}$$

so that

$$\begin{aligned}\mathcal{B}_{1,k_2}(k_1^2,\beta_j\cdot k_1) &= \frac{2\pi^{3/2-\epsilon}}{(2\pi)^d\Gamma(3/2-\epsilon)}\int_{-\infty}^{\infty}dk_{20}\int_0^{\infty}dk_{21}{k_{21}}^{2-2\epsilon}\\ &\quad\times\frac{\delta(k_{20}-k_{21})}{2k_{21}}\delta\big(k_{20}-(\beta_j\cdot k_1-1)\big)\\ &= \frac{\pi^{3/2-\epsilon}}{(2\pi)^d\Gamma(3/2-\epsilon)}\theta(\beta_j\cdot k_1-1)(\beta_j\cdot k_1-1)^{1-2\epsilon}\ . \end{aligned}\tag{C.3}$$

C.2 Triangles

By triangles, we mean Feynman integrals with three propagators. There are two relevant triangles to calculate.

C.2.1 $\mathcal{T}_{1,k_2}$

$$\begin{aligned}\mathcal{T}_{1,k_2}(k_1^2,\beta_j\cdot k_1) &= \int \frac{d^dk_2}{(2\pi)^d}\frac{\delta^+((k_1+k_2)^2)\delta(-\beta_j\cdot k_2-1)}{(k_2^2+i\epsilon)}\\ &= \int \frac{d^dk_2}{(2\pi)^d}\frac{\delta^+(k_2^2)\delta(\beta_j\cdot k_1-\beta_j\cdot k_2-1)}{((k_2-k_1)^2+i\epsilon)}\ .\end{aligned} \tag{C.4}$$

We calculate this in the following frame

$$\begin{aligned}\beta_j &= (1,\mathbf{0}_{d-1})\\ k_1 &= (k_{10},k_{11}\mathbf{v}_{d-1}) \quad \mathbf{v}^2=1\\ k_2 &= (k_{20},k_{21}\mathbf{v'}_{d-1}) \quad \mathbf{v'}^2=1\\ \mathbf{v}\cdot\mathbf{v'} &= \cos\sigma\\ d^dk_2 &= \frac{2\pi^{1-\epsilon}}{\Gamma(1-\epsilon)}dk_{20}dk_{21}{k_{21}}^{2-2\epsilon}d\cos\sigma(\sin\sigma)^{-2\epsilon}\ ,\end{aligned} \tag{C.5}$$

so that

$$\begin{aligned}&\mathcal{T}_{1,k_2}(k_1^2,\beta_j\cdot k_1)\\ &= \frac{2\pi^{1-\epsilon}}{(2\pi)^d\Gamma(1-\epsilon)}\int_{-\infty}^{\infty}dk_{20}\int_0^{\infty}dk_{21}{k_{21}}^{2-2\epsilon}\int_{-1}^{1}d\cos\sigma(\sin\sigma)^{-2\epsilon}\\ &\qquad\times\frac{\delta(k_{20}-k_{21})\delta\big((k_{20}-(\beta_j\cdot k_1-1)\big)}{2k_{21}(k_1^2-2(k_{10}k_{20}-k_{11}k_{21}\cos\sigma+i\epsilon)}\\ &= \frac{\pi^{1-\epsilon}}{(2\pi)^d\Gamma(1-\epsilon)}\theta(\beta_j\cdot k_1-1)(\beta_j\cdot k_1-1)^{1-2\epsilon}\int_{-1}^{1}d\cos\sigma(\sin\sigma)^{-2\epsilon}\\ &\qquad\times\frac{1}{(k_1^2-2(k_{10}(\beta_j\cdot k_1-1)-k_{11}(\beta_j\cdot k_1-1)\cos\sigma+i\epsilon)}\\ &= \frac{\pi^{1-\epsilon}}{(2\pi)^d\Gamma(1-\epsilon)}\theta(\beta_j\cdot k_1-1)(\beta_j\cdot k_1-1)^{1-2\epsilon}\int_{-1}^{1}d\cos\sigma(\sin\sigma)^{-2\epsilon}\\ &\qquad\times\frac{1}{(k_1^2-2(\beta_j\cdot k_1-1)(\beta_j\cdot k_1-\sqrt{(\beta_j\cdot k_1)^2-k_1^2}\cos\sigma+i\epsilon)}\ .\end{aligned} \tag{C.6}$$

C.2.2 $\mathcal{T}_{2,k_3}$

We calculate the integral (4.57).

$$\mathcal{T}_{2,k_3}(\beta_j\cdot\beta_k,\beta_j\cdot k_2)=\int\frac{d^dk_3}{(2\pi)^d}\frac{\delta^-(k_3^2)\delta(\beta_j\cdot(k_3-k_2)-2)}{(-\beta_k\cdot k_3-1)}\ . \tag{C.7}$$

We calculate this in the following frame

$$\begin{aligned}\beta_j&=(1,\mathbf{0}_{d-1})\\ \beta_k&=(-\cosh\theta,\sinh\theta\mathbf{v}_{d-1}),\quad \mathbf{v}^2=1\\ k_3&=(k_{30},k_{31}\mathbf{v'}_{d-1}),\quad \mathbf{v'}^2=1\\ \mathbf{v}\cdot\mathbf{v}'&=\cos\sigma\\ d^dk_3&=\frac{2\pi^{1-\epsilon}}{\Gamma(1-\epsilon)}dk_{30}dk_{31}k_{31}^{2-2\epsilon}d\cos\sigma(\sin\sigma)^{-2\epsilon}\ .\end{aligned} \tag{C.8}$$

Notice that we assumed that k is an outgoing particle, so $\beta_{k_0}<0$. Now

$$\begin{aligned}&\mathcal{C}_{2,k_3}(\beta_j\cdot\beta_k,\beta_j\cdot k_2)\\ &=\frac{2\pi^{1-\epsilon}}{\Gamma(1-\epsilon)(2\pi)^d}\int_{-\infty}^{\infty}dk_{30}\int_0^{\infty}dk_{31}k_{31}^{2-2\epsilon}\\ &\times\int_{-1}^{1}d\cos\sigma(\sin\sigma)^{-2\epsilon}\frac{\delta(k_{30}+k_{31})\delta\big(k_{30}-(\beta_j\cdot k_2+2)\big)}{2k_{31}(k_{30}\cosh\theta+k_{31}\sinh\theta\cos\sigma-1)}\\ &=\frac{\pi^{1-\epsilon}}{\Gamma(1-\epsilon)(2\pi)^d}\theta(-\beta_j\cdot k_2-2)(-\beta_j\cdot k_2-2)^{1-2\epsilon}\\ &\times\int_{-1}^{1}d\cos\sigma(\sin\sigma)^{-2\epsilon}\frac{1}{(\beta_j\cdot k_2+2)(\cosh\theta-\sinh\theta\cos\sigma)-1)}\ .\end{aligned} \tag{C.9}$$

C.2.3 $\mathcal{C}_{3,k_2,1}$

This is also a triangle, albeit one with a numerator. We Feynman parametrise immediately:

$$\begin{aligned}\mathcal{C}_{3,k_2,1}&=\int d^dk_2\frac{(\beta_i\cdot\beta_j\beta_j-\beta_i)\cdot(2k_2+k_1)\delta(-\beta_j\cdot k_2-1)}{(k_2^2+i\epsilon)((k_1+k_2)^2+i\epsilon)}\\ &=\int_0^1dx\int d^dk_2\frac{(\beta_i\cdot\beta_j\beta_j-\beta_i)\cdot(2k_2+k_1)\delta(-\beta_j\cdot k_2-1)}{\big((1-x)k_2^2+x(k_1+k_2)^2+i\epsilon\big)^2}\\ &=\int_0^1dx\int d^dk_2\frac{(\beta_i\cdot\beta_j\beta_j-\beta_i)\cdot(2k_2+k_1)\delta(-\beta_j\cdot k_2-1)}{\big(k_2^2+2xk_1\cdot k_2+xk_1^2+i\epsilon\big)^2}\\ &=\int_0^1dx\int d^dk_2\frac{(\beta_i\cdot\beta_j\beta_j-\beta_i)\cdot(2k_2+k_1)\delta(-\beta_j\cdot k_2-1)}{\big((k_2+xk_1)^2+x(1-x)k_1^2+i\epsilon\big)^2}\end{aligned}$$

$$= \int_0^1 dx \int d^d k_2 \frac{(\beta_i \cdot \beta_j \beta_j - \beta_i) \cdot (2k_2 - 2xk_1 + k_1)}{\left(k_2^2 + x(1-x)k_1^2 + i\epsilon\right)^2}$$
$$\times \delta(-\beta_j \cdot k_2 + x\beta_j \cdot k_1 - 1) \ . \tag{C.10}$$

We now calculate this again in a frame where

$$\begin{aligned} \beta_j &= (1, \mathbf{0}) \\ \beta_i &= (\cosh\phi, \sinh\phi \mathbf{v}) \\ k_2 &= (k_{20}, k_{21}\mathbf{v}') \\ \mathbf{v} \cdot \mathbf{v}' &= \cos\sigma \ . \end{aligned} \tag{C.11}$$

This gives

$$\mathcal{C}_{3,k_2,1} = \frac{2\pi^{1-\epsilon}}{\Gamma(1-\epsilon)} \int_{-1}^{\beta_j \cdot k_1 - 1} dk_{20} \int_0^\infty dk_{21} \int_{-1}^1 d\cos\sigma (\sin\sigma)^{-2\epsilon} {k_{21}}^{2-2\epsilon}$$
$$\frac{(\beta_i \cdot \beta_j \beta_j - \beta_i) \cdot k_1 (1 - 2\frac{1+k_{20}}{\beta_j \cdot k_1}) + \beta_i \cdot \beta_j k_{20} - \cosh\phi k_{20} + \sinh\phi k_{21} \cos\sigma}{\beta_j \cdot k_1 \left({k_{20}}^2 - {k_{21}}^2 + \frac{1+k_{20}}{\beta_j \cdot k_1}(1 - \frac{1+k_{20}}{\beta_j \cdot k_1}) k_1^2 + i\epsilon\right)^2} \ .$$

We see that the $\cos\sigma$ part in the numerator integrates to zero. We are then left with

$$\begin{aligned} \mathcal{C}_{3,k_2,1} &= \frac{2\pi^{1-\epsilon}}{\Gamma(1-\epsilon)} (\beta_i \cdot \beta_j \beta_j - \beta_i) \cdot k_1 \int_{-1}^{\beta_j \cdot k_1 - 1} dk_{20} \int_0^\infty dk_{21} {k_{21}}^{2-2\epsilon} \\ &\int_{-1}^1 d\cos\sigma (\sin\sigma)^{-2\epsilon} \frac{(1 - 2\frac{1+k_{20}}{\beta_j \cdot k_1})}{\beta_j \cdot k_1 \left({k_{20}}^2 - {k_{21}}^2 + \frac{1+k_{20}}{\beta_j \cdot k_1}(1 - \frac{1+k_{20}}{\beta_j \cdot k_1}) k_1^2 + i\epsilon\right)^2} \\ &= \frac{2\pi^{1-\epsilon}}{\Gamma(1-\epsilon)} (\beta_i \cdot \beta_j \beta_j - \beta_i) \cdot k_1 \int_0^{\beta_j \cdot k_1} dk_{20} \int_0^\infty dk_{21} {k_{21}}^{2-2\epsilon} \\ &\int_{-1}^1 d\cos\sigma (\sin\sigma)^{-2\epsilon} \frac{(1 - 2\frac{k_{20}}{\beta_j \cdot k_1})}{\beta_j \cdot k_1 \left((k_{20}-1)^2 - {k_{21}}^2 + \frac{k_{20}}{\beta_j \cdot k_1}(1 - \frac{k_{20}}{\beta_j \cdot k_1}) k_1^2 + i\epsilon\right)^2} \\ &= \frac{2\pi^{1-\epsilon}}{\Gamma(1-\epsilon)} (\beta_i \cdot \beta_j \beta_j - \beta_i) \cdot k_1 \int_0^1 d\alpha \int_0^\infty dk_{21} {k_{21}}^{2-2\epsilon} \\ &\int_{-1}^1 d\cos\sigma (\sin\sigma)^{-2\epsilon} \frac{(1 - 2\alpha)}{\left((\alpha\beta_j \cdot k_1 - 1)^2 - {k_{21}}^2 + \alpha(1-\alpha) k_1^2 + i\epsilon\right)^2} \\ &= 4\pi (\beta_i \cdot \beta_j \beta_j - \beta_i) \cdot k_1 \int_0^1 d\alpha \\ &\times \int_0^\infty dk_{21} \frac{{k_{21}}^{2-2\epsilon} (1 - 2\alpha)}{\left((\alpha\beta_j \cdot k_1 - 1)^2 - {k_{21}}^2 + \alpha(1-\alpha) k_1^2 + i\epsilon\right)^2} + \mathcal{O}(\epsilon) \end{aligned}$$

$$= -2\pi(\beta_i \cdot \beta_j \beta_j - \beta_i) \cdot k_1 \int_0^1 d\alpha$$
$$\times \int_0^\infty dk_{21} \frac{{k_{21}}^{-2\epsilon}(1-2\alpha)}{\left((\alpha\beta_j \cdot k_1 - 1)^2 - k_{21}^2 + \alpha(1-\alpha)k_1^2 + i\epsilon\right)} + \mathcal{O}(\epsilon) \ , \qquad \text{(C.12)}$$

where we used integration by parts in the last step. We also ignored the subleading contribution in $\cos\sigma$, because we are only interested in the leading order part of Cut_2.

C.3 Boxes

By boxes, we mean integrals with four propagators.

C.3.1 $\mathcal{B}_{2,k1}$

We calculate $\mathcal{B}_{2,k_1}$. It is equal to

$$\mathcal{B}_{2,k_1}(k_2^2, \beta_i \cdot k_2, \beta_j \cdot k_2, \beta_i \cdot \beta_j) = \int \frac{d^d k_1}{(2\pi)^d} \frac{\delta^+((k_1+k_2)^2)\delta(-\beta_i \cdot k_1 - 1)}{k_1^2(\beta_j \cdot (k_1+k_2) - 1)}$$
$$= \int \frac{d^d k_1}{(2\pi)^d} \frac{\delta^+(k_1^2)\delta(\beta_i \cdot k_2 - \beta_i \cdot k_1 - 1)}{(k_1-k_2)^2(\beta_j \cdot k_1 - 1)} \ . \qquad \text{(C.13)}$$

We choose the following frame:

$$\begin{aligned}
\beta_i &= (1, \mathbf{0}_{d-1}) \\
\beta_j &= (\cosh\phi, \sinh\phi, \mathbf{0}_{d-2}) \\
k_2 &= (k_{20}, k_{21}, k_{22}\mathbf{v}_{d-2}), \quad \mathbf{v}^2 = 1 \\
k_1 &= (k_{10}, k_{11}, k_{12}{\mathbf{v}'}_{d-2}), \quad {\mathbf{v}'}^2 = 1 \\
\mathbf{v} \cdot \mathbf{v}' &= \cos\tau \\
d^d k_1 &= \frac{2\pi^{1/2-\epsilon}}{\Gamma(1/2-\epsilon)} dk_{10} dk_{11} dk_{12} {k_{12}}^{1-2\epsilon} d\cos\tau (\sin\tau)^{-1-2\epsilon} \ ,
\end{aligned} \qquad \text{(C.14)}$$

so that

$$\mathcal{B}_{2,k_1} = \frac{2\pi^{1/2-\epsilon}}{\Gamma(1/2-\epsilon)(2\pi)^d} \int_{-\infty}^\infty dk_{10} \int_{-\infty}^\infty dk_{11} \int_0^\infty dk_{12} {k_{12}}^{1-2\epsilon} d\cos\tau (\sin\tau)^{-1-2\epsilon}$$
$$\times \frac{\delta({k_{10}}^2 - {k_{11}}^2 - {k_{12}}^2)\theta(k_{10})\delta\big(k_{10} - (\beta_i \cdot k_2 - 1)\big)}{(k_2^2 - 2k_{10}k_{20} + 2k_{11}k_{21} + 2k_{12}k_{22}\cos\tau)(\cosh\phi k_{10} - \sinh\phi k_{11} - 1)}$$
$$= \frac{2\pi^{1/2-\epsilon}}{\Gamma(1/2-\epsilon)(2\pi)^d} \theta(\beta_i \cdot k_2 - 1) \int_{-\infty}^\infty dk_{11} \int_0^\infty dk_{12} {k_{12}}^{1-2\epsilon}$$

$$\times \int_{-1}^{1} d\cos\tau (\sin\tau)^{-1-2\epsilon} \frac{1}{(\cosh\phi(\beta_i\cdot k_2 - 1) - \sinh\phi k_{11} - 1)}$$
$$\times \frac{\delta((\beta_i\cdot k_2-1)^2 - {k_{11}}^2 - {k_{12}}^2)}{(k_2^2 - 2(\beta_i\cdot k_2 - 1)k_{20} + 2k_{11}k_{21} + 2k_{12}k_{22}\cos\tau)} \ . \tag{C.15}$$

We now solve the remaining delta function for k_{12}. Notice that it only has a solution for $-(\beta_i\cdot k_2 - 1) < k_{11} < (\beta_i\cdot k_2 - 1)$.

$$\mathcal{B}_{2,k_1} = \frac{\pi^{1/2-\epsilon}}{\Gamma(1/2-\epsilon)(2\pi)^d}\theta(\beta_i\cdot k_2 - 1)$$
$$\times \int_{-(\beta_i\cdot k_2-1)}^{(\beta_i\cdot k_2-1)} dk_{11} d\cos\tau \frac{(\sin\tau)^{-1-2\epsilon}\sqrt{(\beta_i\cdot k_2-1)^2 - {k_{11}}^2}^{-2\epsilon}}{(\cosh\phi(\beta_i\cdot k_2-1) - \sinh\phi k_{11} - 1)}$$
$$\frac{1}{(k_2^2 - 2(\beta_i\cdot k_2-1)k_{20} + 2k_{11}k_{21} + 2\sqrt{(\beta_i\cdot k_2-1) - {k_{11}}^2}k_{22}\cos\tau)} \ . \tag{C.16}$$

We now rescale k_{11} by a factor of $(\beta_i\cdot k_2 - 1)$:

$$k_{11} = (\beta_i\cdot k_2 - 1) \ , \tag{C.17}$$

so that finally

$$\mathcal{B}_{2,k_1} = \frac{\pi^{1/2-\epsilon}}{\Gamma(1/2-\epsilon)(2\pi)^d}\theta(\beta_i\cdot k_2 - 1)(\beta_i\cdot k_2 - 1)^{1-2\epsilon}$$
$$\times \int_{-1}^{1} dx d\cos\tau \frac{(\sin\tau)^{-1-2\epsilon}\sqrt{1-x^2}^{-2\epsilon}}{(\cosh\phi(\beta_i\cdot k_2-1) - \sinh\phi x(\beta_i\cdot k_2-1) - 1)}$$
$$\frac{1}{k_2^2 - 2(\beta_i\cdot k_2-1)\big(k_{20} - xk_{21} - \sqrt{1-x^2}k_{22}\cos\tau\big)} \ , \tag{C.18}$$

with

$$\begin{aligned}
\cosh\phi &= \beta_i\cdot\beta_j \\
k_{20} &= \beta_i\cdot k_2 \\
k_{21} &= \frac{\cosh\phi k_{20} - \beta_j\cdot k_2}{\sinh\phi} \\
k_{22} &= \sqrt{k_{20}^2 - k_{21}^2 - k_2^2} \ .
\end{aligned} \tag{C.19}$$

Appendix D

Rewriting polylogarithms as iterated integrals

By definition, polylogarithms are iterated integrals. It is thus not surprising that we can find equations such as (4.43), where we rewrite a logarithm as an integral of a linear denominator. However, the expression that we find is more compact than expected. We now find a similar simple expression for T_{1,k_2}:

$$
\begin{aligned}
T_{1,k_2}(k_{10},k_{11}) &= -\int_{-1}^{1} d\cos\sigma \frac{\ln(1+\cos\sigma)+\ln(1-\cos\sigma)}{k_{10}^2-k_{11}^2-2(k_{10}-1)(k_{10}-k_{11}\cos\sigma)} \\
&= \frac{G\left(-\frac{-k_{10}^2+2k_{10}-k_{11}^2}{2k_{10}k_{11}-2k_{11}},-1,-1\right)}{2k_{10}k_{11}-2k_{11}} + \frac{G\left(-\frac{-k_{10}^2+2k_{10}-k_{11}^2}{2k_{10}k_{11}-2k_{11}},1,-1\right)}{2k_{10}k_{11}-2k_{11}} \\
&- \frac{G\left(-\frac{-k_{10}^2+2k_{10}-k_{11}^2}{2k_{10}k_{11}-2k_{11}},-1,1\right)}{2k_{10}k_{11}-2k_{11}} - \frac{G\left(-\frac{-k_{10}^2+2k_{10}-k_{11}^2}{2k_{10}k_{11}-2k_{11}},1,1\right)}{2k_{10}k_{11}-2k_{11}} \\
&= -2(\ln 2)T_{0,k_2} + \frac{xy}{2(x-1)}\Bigg(2G(0,-x,y) - 2G(0,x,y \\
&+ 2G\left(0,\frac{x}{2x-1},y\right) - 2G\left(0,\frac{x}{1-2x},y\right) \\
&- G(-x,-x,y) + G(-x,x,y) \\
&- G\left(-x,\frac{x}{2x-1},y\right) + G\left(-x,\frac{x}{1-2x},y\right) - G(x,-x,y) \\
&+ G(x,x,y) - G\left(x,\frac{x}{2x-1},y\right) + G\left(x,\frac{x}{1-2x},y\right) \\
&- G\left(\frac{x}{2x-1},-x,y\right) + G\left(\frac{x}{2x-1},x,y\right) \\
&- G\left(\frac{x}{2x-1},\frac{x}{2x-1},y\right) + G\left(\frac{x}{2x-1},\frac{x}{1-2x},y\right)
\end{aligned}
$$

$$
\begin{aligned}
&- G\left(\frac{x}{1-2x}, -x, y\right) + G\left(\frac{x}{1-2x}, x, y\right) \\
&- G\left(\frac{x}{1-2x}, \frac{x}{2x-1}, y\right) + G\left(\frac{x}{1-2x}, \frac{x}{1-2x}, y\right)\Big) \ , \qquad \text{(D.1)}
\end{aligned}
$$

where

$$
x = \frac{1}{k_{10}}, \quad y = \frac{1}{k_{11}} \ . \qquad \text{(D.2)}
$$

We see that (D.1) consists of pairs of polylogs that only differ by the sign of the middle entry. We can rewrite such terms as double integrals via

$$
G(a,-b,c) - G(a,b,c) = \int_0^1 dz \int_{-1}^1 dt \frac{cz}{b\left(z-\frac{a}{c}\right)\left(1-\frac{ctz}{b}\right)} \ . \qquad \text{(D.3)}
$$

Using this formula, we can re express (D.1) as

$$
\begin{aligned}
T_{1,k_2}(k_{10},k_{11}) &= -2\ln(2) T_{0,k_2}(k_{10},k_{11}) \\
&\quad - \frac{1}{2k_{11}(k_{10}-1)} \int_0^1 dz \int_{-1}^1 dt \Bigg[\frac{2k_{10}}{k_{11}\left(\frac{k_{10}tz}{k_{11}}+1\right)} \\
&\quad - \frac{k_{10}z}{k_{11}\left(\frac{k_{11}}{k_{10}}+z\right)\left(1-\frac{k_{10}tz}{k_{11}}\right)} - \frac{k_{10}z}{k_{11}\left(z-\frac{k_{11}}{k_{10}}\right)\left(1-\frac{k_{10}tz}{k_{11}}\right)} \\
&\quad - \frac{k_{10}z}{k_{11}\left(\frac{k_{11}}{(k_{10}-2)}+z\right)\left(1-\frac{k_{10}tz}{k_{11}}\right)} - \frac{k_{10}z}{k_{11}\left(z-\frac{k_{11}}{(k_{10}-2)}\right)\left(1-\frac{k_{10}tz}{k_{11}}\right)} \\
&\quad - \frac{(k_{10}-2)z}{k_{11}\left(\frac{k_{11}}{k_{10}}+z\right)\left(1-\frac{(k_{10}-2)tz}{k_{11}}\right)} - \frac{(k_{10}-2)z}{k_{11}\left(z-\frac{k_{11}}{k_{10}}\right)\left(1-\frac{(k_{10}-2)tz}{k_{11}}\right)} \\
&\quad - \frac{(k_{10}-2)z}{k_{11}\left(\frac{k_{11}}{(k_{10}-2)}+z\right)\left(1-\frac{(k_{10}-2)tz}{k_{11}}\right)} + \frac{2(k_{10}-2)}{k_{11}\left(\frac{(k_{10}-2)tz}{k_{11}}+1\right)} \\
&\quad - \frac{(k_{10}-2)z}{k_{11}\left(z-\frac{k_{11}}{(k_{10}-2)}\right)\left(1-\frac{(k_{10}-2)tz}{k_{11}}\right)} \Bigg] \\
&= -2\ln(2) T_{0,k_2}(k_{10},k_{11}) + T_{1',k_2}(k_{10},k_{11}) \ . \qquad \text{(D.4)}
\end{aligned}
$$

$T_{1',k_2}(k_{10},k_{11})$ captures the part of $T_{1,k_2}(k_{10},k_{11})$ that is not proportional to $T_{0,k_2}(k_{10},k_{11})$.

Appendix E

Calculation of a twofold integral

As part of the calculation of $\mathrm{Cut}_{2,\mathcal{B},2,NLO,1}(\alpha_{ij},\alpha_{jk})$ (4.118), we have to calculate the following twofold integral:

$$\mathcal{I}(R) = \int_{-1}^{1} dx \int_{0}^{\infty} dZ \times \frac{1}{1+Rx}\frac{1}{1+Z}\frac{\ln\left(1+\frac{1}{\sqrt{1-\frac{4\left(\frac{1}{R^2}-1\right)(1-x^2)Z}{\left(\frac{Z+1}{R^2}+\frac{2x}{R}-Z+1\right)^2}}}\right)}{\sqrt{\left(\frac{Z+1}{R^2}+\frac{2x}{R}-Z+1\right)^2-4\left(\frac{1}{R^2}-1\right)(1-x^2)Z}}\,, \tag{E.1}$$

with $0 < R < 1$. We reduce the complexity of the argument of the logarithm by introducing a new variable via

$$u^2 = 1 - \frac{4\left(\frac{1}{R^2}-1\right)(1-x^2)Z}{\left(\frac{Z+1}{R^2}+\frac{2x}{R}-Z+1\right)^2}\,. \tag{E.2}$$

This is not a one-to-one relationship: for every value of u, there will be two corresponding Z values, one for $Z > \frac{R^2+2Rx+1}{1-R^2}$ and one for $Z < \frac{R^2+2Rx+1}{1-R^2}$. We solve this by splitting up the integration region into two parts

$$\int_0^\infty dZ f(Z) = \int_0^{\frac{R^2+2Rx+1}{1-R^2}} dZ f(Z) + \int_{\frac{R^2+2Rx+1}{1-R^2}}^{\infty} dZ f(Z)\,. \tag{E.3}$$

In both regions, u will vary between $u_{\min} = \sqrt{\frac{(Rx+1)^2}{R^2+2Rx+1}}$ and one. (E.1) then becomes

$$\begin{aligned}\mathcal{I}(R) &= -\int_{-1}^{1} dx \int_{u_{\min}}^{1} du \frac{1}{(R+x)^2\left(u^2 - \frac{(1+Rx)^2}{(x+R)^2}\right)} \\ &\times \frac{R\sqrt{1-x^2}\log\left(\frac{1}{u}+1\right)}{\sqrt{(R^2+2Rx+1)}\sqrt{u^2-u_{min}^2}} \\ &= -\int_{-1}^{1} dx \int_{u_{\min}}^{1} du \int_{0}^{\frac{1}{u}} dz \frac{1}{(R+x)^2\left(u^2 - \frac{(1+Rx)^2}{(x+R)^2}\right)(1+z)} \\ &\times \frac{R\sqrt{1-x^2}}{\sqrt{(R^2+2Rx+1)}\sqrt{u^2-u_{min}^2}} \ , \end{aligned} \tag{E.4}$$

where in the last step we replaced the logarithm by an integral. We now want to integrate over u, so have to change the order of integration via

$$\int_{u_{\min}}^{1} du \int_{0}^{\frac{1}{u}} dz f(z,u) = \int_{0}^{1} dz \int_{u_{\min}}^{1} du f(z,u) + \int_{1}^{\frac{1}{u_{\min}}} dz \int_{u_{\min}}^{\frac{1}{z}} du f(z,u) \ . \tag{E.5}$$

Changing the order of integration thus implies that we have to calculate our integral in two different regions, yielding two different integrals:

$$\mathcal{I}(R) = \mathcal{I}_1(R) + \mathcal{I}_2(R) \ . \tag{E.6}$$

One of the two is straightforward to calculate:

$$\begin{aligned}\mathcal{I}_1(R) &= -\int_{-1}^{1} dx \int_{0}^{1} dz \frac{R\sqrt{1-x^2}}{\sqrt{(R^2+2Rx+1)}} \frac{1}{(R+x)^2(1+z)} \\ &\times \int_{u_{\min}}^{1} du \frac{1}{\sqrt{u^2-u_{min}^2}} \frac{1}{\left(u^2 - \frac{(1+Rx)^2}{(x+R)^2}\right)} \\ &= \int_{-1}^{1} dx \int_{0}^{1} dz \frac{R(\log(R+1) - \log(1-R))}{2(z+1)(Rx+1)^2} \\ &= \frac{R\log(2)(\log(R+1) - \log(1-R))}{1-R^2} \ . \end{aligned} \tag{E.7}$$

We now calculate the other part.

$$\mathcal{I}_2(R) = -\int_{-1}^{1} dx \int_{1}^{\frac{1}{u_{\min}}} dz \frac{R\sqrt{1-x^2}}{\sqrt{(R^2+2Rx+1)}} \frac{1}{(R+x)^2(1+z)}$$

$$
\begin{aligned}
&\times \int_{u_{\min}}^{\frac{1}{z}} du \frac{1}{\sqrt{u^2 - u_{min}^2}} \frac{1}{\left(u^2 - \frac{(1+Rx)^2}{(x+R)^2}\right)} \\
&= \int_{-1}^{1} dx \int_{1}^{\frac{1}{u_{\min}}} dz \frac{R}{2(z+1)(Rx+1)^2} \\
&\times \left(- \log \left(\sqrt{1-x^2}\sqrt{1/u_{min}^2 - z^2} + \frac{(1+Rx)}{u_{min}^2} - z(x+R) \right) \right. \\
&+ \log \left(\sqrt{1-x^2}\sqrt{1/u_{min}^2 - z^2} + \frac{(1+Rx)}{u_{min}^2} + z(x+R) \right) \\
&\left. - \log(Rxz + R + x + z) + \log(R(xz-1) - x + z) \right) . \qquad \text{(E.8)}
\end{aligned}
$$

We now want to perform integration by parts with respect to x. We again have to change the order of integration. It turns out that

$$
\int_{-1}^{1} dx \int_{1}^{\frac{1}{u_{\min}}} dz f(x,z) = \int_{1}^{\frac{1-R}{1-R^2}} dz \int_{x_{\min}}^{x_{\max}} dx f(x,z) \ , \qquad \text{(E.9)}
$$

where

$$
\begin{aligned}
x_{\max} &= \frac{\sqrt{(R^2-1)\,z^2+1} - z^2 + 1}{Rz^2} \\
x_{\min} &= \frac{-\sqrt{(R^2-1)\,z^2+1} - z^2 + 1}{Rz^2} \ . \qquad \text{(E.10)}
\end{aligned}
$$

We can then perform integration by parts with respect to x, to get rid of the logarithms in the integrand.
If we define

$$
\begin{aligned}
f' &= \frac{R}{2(z+1)(Rx+1)^2} \\
g &= \log \left(\sqrt{1-x^2}\sqrt{1/u_{min}^2 - z^2} + \frac{(1+Rx)}{u_{min}^2} + z(x+R) \right) \\
&\quad \left. - \log(Rxz + R + x + z) + \log(R(xz-1) - x + z) \right) , \qquad \text{(E.11)}
\end{aligned}
$$

and then use

$$
\int dx(f'g) = fg|_{boundary} - \int dx(g'f) \ , \qquad \text{(E.12)}
$$

it turns out that the boundary term equals zero. This then leaves us with

$$\begin{aligned}\mathcal{I}_2(R) = &\int_1^{\frac{1-R}{1-R^2}} dz \int_{x_{\min}}^{x_{\max}} dx \frac{1}{2(z+1)(Rx+1)} \\ &\times \Bigg(-\frac{Rz+1}{Rxz+R+x+z} + \frac{1-Rz}{R(-x)z+R+x-z} \\ &+ \frac{\frac{R^2x\left(\left(2x^2-1\right)z^2-1\right)+R\left(3x^2-1\right)\left(z^2-1\right)+x\left(z^2-1\right)}{\sqrt{X(R,x,z)}} + R^2z + 2R(xz+1) + z}{\sqrt{X(R,x,z)} + R^2(xz+1) + R\left(x^2z+2x+z\right) + xz + 1} \\ &- \frac{\frac{R^2x\left(\left(2x^2-1\right)z^2-1\right)+R\left(3x^2-1\right)\left(z^2-1\right)+x\left(z^2-1\right)}{\sqrt{X(R,x,z)}} + R^2z + 2R(xz-1) + z}{\sqrt{X(R,x,z)} + R^2(xz-1) + R\left(x^2z-2x+z\right) + xz - 1} \Bigg) ,\end{aligned} \tag{E.13}$$

where

$$X(R,x,z) = \left(x^2-1\right)\left(R^2\left(x^2z^2-1\right) + 2Rx\left(z^2-1\right) + z^2 - 1\right) . \tag{E.14}$$

We now swap order of integration again and perform the z integral

$$\begin{aligned}\mathcal{I}_2(R) = -\int_{-1}^{1} dx \Bigg(&\frac{-(Rx+1)\log\left(R^2+2Rx+1\right)}{2\left(x^2-1\right)(Rx+1)^2} \\ &+ \frac{(R-1)(x-1)\log(1-R) + (R+1)(x+1)\log(R+1)}{2\left(x^2-1\right)(Rx+1)^2} \Bigg) ,\end{aligned} \tag{E.15}$$

and then finally the x integral, yielding

$$\begin{aligned}\mathcal{I}_2(R) = -\frac{2R}{4\left(R^2-1\right)} \Bigg[&G\left(-1,R^2\right) G\left(-\frac{1}{R},-1\right) - 2RG\left(-1,R^2\right) G\left(-\frac{1}{R},1\right) \\ &+ RG\left(-1,-\frac{R^2+1}{2R},1\right) + G\left(-1,-\frac{R^2+1}{2R},1\right) \\ &- RG\left(1,-\frac{R^2+1}{2R},-1\right) + G\left(1,-\frac{R^2+1}{2R},-1\right) \\ &+ 2RG\left(-\frac{1}{R},-\frac{R^2+1}{2R},-1\right) - 2RG\left(-\frac{1}{R},-\frac{R^2+1}{2R},1\right) \\ &+ RG\left(-\frac{R^2+1}{2R},-1,-1\right) + G\left(-\frac{R^2+1}{2R},-1,-1\right) \\ &- RG\left(-\frac{R^2+1}{2R},1,1\right) + G\left(-\frac{R^2+1}{2R},1,1\right) \\ &+ \log(4) G\left(-1,R^2\right) - G(0,1-R) \times \left(2(R+1) G\left(-\frac{1}{R},-1\right) \right.\end{aligned}$$

$$
\begin{aligned}
&- 2(R+1)G\left(-\frac{1}{R},1\right) - 4R + R\log(4) + \log(4)\Big) \\
&- G(0,R+1)\Big(2(R-1)G\left(-\frac{1}{R},-1\right) - 2(R-1)G\left(-\frac{1}{R},1\right) \\
&+ 4R - R\log(4) + \log(4)\Big)\Big] \,. \qquad \text{(E.16)}
\end{aligned}
$$

We can now combine (E.7) and (E.16) to obtain

$$
\begin{aligned}
\mathcal{I}(R) = &-\frac{2R}{4\left(R^2-1\right)}\Big[G\left(-1,R^2\right)G\left(-\frac{1}{R},-1\right) - 2RG\left(-1,R^2\right)G\left(-\frac{1}{R},1\right) \\
&+ RG\left(-1,-\frac{R^2+1}{2R},1\right) + G\left(-1,-\frac{R^2+1}{2R},1\right) \\
&- RG\left(1,-\frac{R^2+1}{2R},-1\right) + G\left(1,-\frac{R^2+1}{2R},-1\right) \\
&+ 2RG\left(-\frac{1}{R},-\frac{R^2+1}{2R},-1\right) - 2RG\left(-\frac{1}{R},-\frac{R^2+1}{2R},1\right) \\
&+ RG\left(-\frac{R^2+1}{2R},-1,-1\right) + G\left(-\frac{R^2+1}{2R},-1,-1\right) \\
&- RG\left(-\frac{R^2+1}{2R},1,1\right) + G\left(-\frac{R^2+1}{2R},1,1\right) \\
&+ \log(4)G\left(-1,R^2\right) - G(0,1-R)\times\Big(2(R+1)G\left(-\frac{1}{R},-1\right) \\
&- 2(R+1)G\left(-\frac{1}{R},1\right) - 4R + 3R\log(4) + \log(4)\Big) \\
&- G(0,R+1)\Big(2(R-1)G\left(-\frac{1}{R},-1\right) - 2(R-1)G\left(-\frac{1}{R},1\right) \\
&+ 4R - 3R\log(4) + \log(4)\Big)\Big] \,. \qquad \text{(E.17)}
\end{aligned}
$$

We try to simplify the result (E.17) by rewriting it as a sum of polylogs of the form $G(\mathbf{a},R)$. However, this does not seem possible. We can also replace $R \to \frac{1-\alpha_{ij}^2}{1+\alpha_{ij}^2}$, and try to rewrite (E.17) in terms of functions of the form $G(\mathbf{a},\alpha_{ij})$. However, this also turns out to be impossible.

Bibliography

[1] M. E. Peskin and D. V. Schroeder, *An Introduction to quantum field theory*. 1995.

[2] K. G. Wilson and J. B. Kogut, *The Renormalization group and the epsilon expansion*, *Phys. Rept.* **12** (1974) 75–200.

[3] J. C. Collins, D. E. Soper, and G. F. Sterman, *Factorization of Hard Processes in QCD*, *Adv. Ser. Direct. High Energy Phys.* **5** (1989) 1–91, [hep-ph/0409313].

[4] G. F. Sterman, *Partons, factorization and resummation, TASI 95*, in *QCD and beyond. Proceedings, Theoretical Advanced Study Institute in Elementary Particle Physics, TASI-95, Boulder, USA, June 4-30, 1995*, pp. 327–408, 1995. hep-ph/9606312.

[5] L. J. Dixon, E. Gardi, and L. Magnea, *On soft singularities at three loops and beyond*, *JHEP* **02** (2010) 081, [0910.3653].

[6] E. Gardi and L. Magnea, *Factorization constraints for soft anomalous dimensions in QCD scattering amplitudes*, *JHEP* **03** (2009) 079, [0901.1091].

[7] G. P. Korchemsky and A. V. Radyushkin, *Loop Space Formalism and Renormalization Group for the Infrared Asymptotics of QCD*, *Phys. Lett.* **B171** (1986) 459–467.

[8] S. V. Ivanov, G. P. Korchemsky, and A. V. Radyushkin, *Infrared Asymptotics of Perturbative QCD: Contour Gauges*, *Yad. Fiz.* **44** (1986) 230–240. [Sov. J. Nucl. Phys.44,145(1986)].

[9] G. P. Korchemsky and A. V. Radyushkin, *Renormalization of the Wilson Loops Beyond the Leading Order*, *Nucl. Phys.* **B283** (1987) 342–364.

[10] S. Catani, *The Singular behavior of QCD amplitudes at two loop order*, *Phys. Lett.* **B427** (1998) 161–171, [hep-ph/9802439].

[11] T. Becher and M. Neubert, *Toward a NNLO calculation of the anti-B —¿ X(s) gamma decay rate with a cut on photon energy: I. Two-loop result for the soft function*, *Phys. Lett.* **B633** (2006) 739–747, [hep-ph/0512208].

[12] S. M. Aybat, L. J. Dixon, and G. F. Sterman, *The Two-loop soft anomalous dimension matrix and resummation at next-to-next-to leading pole*, *Phys. Rev.* **D74** (2006) 074004, [hep-ph/0607309].

[13] E. Laenen, L. Magnea, and G. Stavenga, *On next-to-eikonal corrections to threshold resummation for the Drell-Yan and DIS cross sections*, *Phys. Lett.* **B669** (2008) 173–179, [0807.4412].

[14] A. Mitov, G. F. Sterman, and I. Sung, *The Massive Soft Anomalous Dimension Matrix at Two Loops*, *Phys. Rev.* **D79** (2009) 094015, [0903.3241].

[15] T. Becher and M. Neubert, *Infrared singularities of QCD amplitudes with massive partons*, *Phys. Rev.* **D79** (2009) 125004, [0904.1021]. [Erratum: Phys. Rev.D80,109901(2009)].

[16] V. Del Duca, C. Duhr, E. Gardi, L. Magnea, and C. D. White, *An infrared approach to Reggeization*, *Phys. Rev.* **D85** (2012) 071104, [1108.5947].

[17] T. Becher and M. Neubert, *On the Structure of Infrared Singularities of Gauge-Theory Amplitudes*, *JHEP* **06** (2009) 081, [0903.1126]. [Erratum: JHEP11,024(2013)].

[18] E. Laenen, G. Stavenga, and C. D. White, *Path integral approach to eikonal and next-to-eikonal exponentiation*, *JHEP* **03** (2009) 054, [0811.2067].

[19] G. F. Sterman, *Summation of Large Corrections to Short Distance Hadronic Cross-Sections*, *Nucl. Phys.* **B281** (1987) 310–364.

[20] S. Catani, L. Trentadue, G. Turnock, and B. R. Webber, *Resummation of large logarithms in e+ e- event shape distributions*, *Nucl. Phys.* **B407** (1993) 3–42.

[21] H. Contopanagos and G. F. Sterman, *Principal value resummation*, *Nucl. Phys.* **B419** (1994) 77–104, [hep-ph/9310313].

[22] G. Bozzi, S. Catani, D. de Florian, and M. Grazzini, *Higgs boson production at the LHC: Transverse-momentum resummation and rapidity dependence*, *Nucl. Phys.* **B791** (2008) 1–19, [0705.3887].

[23] A. M. Polyakov, *Gauge Fields as Rings of Glue*, *Nucl. Phys.* **B164** (1980) 171–188.

[24] I. Ya. Arefeva, *QUANTUM CONTOUR FIELD EQUATIONS*, *Phys. Lett.* **93B** (1980) 347–353.

[25] V. S. Dotsenko and S. N. Vergeles, *Renormalizability of Phase Factors in the Nonabelian Gauge Theory*, *Nucl. Phys.* **B169** (1980) 527–546.

[26] R. A. Brandt, F. Neri, and M.-a. Sato, *Renormalization of Loop Functions for All Loops*, *Phys. Rev.* **D24** (1981) 879.

[27] E. Gardi, *From Webs to Polylogarithms*, *JHEP* **04** (2014) 044, [1310.5268].

[28] E. Gardi, O. Almelid, and C. Duhr, *Long-distance singularities in multi-leg scattering amplitudes*, *PoS* **LL2016** (2016) 058, [1606.05697].

[29] E. Gardi, *Infrared singularities in multi-leg scattering amplitudes*, *PoS* **LL2014** (2014) 069, [1407.5164].

[30] G. Falcioni, E. Gardi, M. Harley, L. Magnea, and C. D. White, *Multiple Gluon Exchange Webs*, *JHEP* **10** (2014) 10, [1407.3477].

[31] M. Dukes, E. Gardi, H. McAslan, D. J. Scott, and C. D. White, *Webs and Posets*, *JHEP* **01** (2014) 024, [1310.3127].

[32] M. Dukes, E. Gardi, E. Steingrimsson, and C. D. White, *Web worlds, web-colouring matrices, and web-mixing matrices*, *J. Comb. Theory Ser.* **A120** (2013) 1012–1037, [1301.6576].

[33] E. Gardi, E. Laenen, G. Stavenga, and C. D. White, *Webs in multiparton scattering using the replica trick*, *JHEP* **11** (2010) 155, [1008.0098].

[34] E. Gardi and C. D. White, *General properties of multiparton webs: Proofs from combinatorics*, *JHEP* **03** (2011) 079, [1102.0756].

[35] E. Gardi, J. M. Smillie, and C. D. White, *On the renormalization of multiparton webs*, *JHEP* **09** (2011) 114, [1108.1357].

[36] E. Laenen, K. J. Larsen, and R. Rietkerk, *Position-space cuts for Wilson line correlators*, *JHEP* **07** (2015) 083, [1505.02555].

[37] E. Laenen, K. J. Larsen, and R. Rietkerk, *Imaginary parts and discontinuities of Wilson line correlators*, *Phys. Rev. Lett.* **114** (2015), no. 18 181602, [1410.5681].

[38] J. G. M. Gatheral, *Exponentiation of Eikonal Cross-sections in Nonabelian Gauge Theories*, *Phys. Lett.* **133B** (1983) 90–94.

[39] J. Frenkel and J. C. Taylor, *NONABELIAN EIKONAL EXPONENTIATION*, *Nucl. Phys.* **B246** (1984) 231–245.

[40] E. Gardi, J. M. Smillie, and C. D. White, *The Non-Abelian Exponentiation theorem for multiple Wilson lines*, *JHEP* **06** (2013) 088, [1304.7040].

[41] A. Grozin, J. M. Henn, G. P. Korchemsky, and P. Marquard, *Three Loop Cusp Anomalous Dimension in QCD*, *Phys. Rev. Lett.* **114** (2015), no. 6 062006, [1409.0023].

[42] O. Almelid, C. Duhr, and E. Gardi, *Three-loop corrections to the soft anomalous dimension in multileg scattering*, *Phys. Rev. Lett.* **117** (2016), no. 17 172002, [1507.00047].

[43] C. Duhr, *Mathematical aspects of scattering amplitudes*, in *Theoretical Advanced Study Institute in Elementary Particle Physics: Journeys Through the Precision Frontier: Amplitudes for Colliders (TASI 2014) Boulder, Colorado, June 2-27, 2014*, 2014. 1411.7538.

[44] A. B. Goncharov, *Multiple polylogarithms, cyclotomy and modular complexes*, *Math. Res. Lett.* **5** (1998) 497–516, [1105.2076].

[45] A. B. Goncharov, *Multiple polylogarithms and mixed Tate motives*, math/0103059.

[46] M. Caffo, H. Czyz, S. Laporta, and E. Remiddi, *The Master differential equations for the two loop sunrise selfmass amplitudes*, *Nuovo Cim.* **A111** (1998) 365–389, [hep-th/9805118].

[47] S. Laporta and E. Remiddi, *Analytic treatment of the two loop equal mass sunrise graph*, *Nucl. Phys.* **B704** (2005) 349–386, [hep-ph/0406160].

[48] S. Bloch and P. Vanhove, *The elliptic dilogarithm for the sunset graph*, *J. Number Theor.* **148** (2015) 328–364, [1309.5865].

[49] T. Gehrmann and E. Remiddi, *Numerical evaluation of harmonic polylogarithms*, *Comput. Phys. Commun.* **141** (2001) 296–312, [hep-ph/0107173].

[50] D. Maitre, *HPL, a mathematica implementation of the harmonic polylogarithms*, *Comput. Phys. Commun.* **174** (2006) 222–240, [hep-ph/0507152].

[51] D. Maitre, *Extension of HPL to complex arguments*, *Comput. Phys. Commun.* **183** (2012) 846, [hep-ph/0703052].

[52] J. Vollinga and S. Weinzierl, *Numerical evaluation of multiple polylogarithms*, *Comput. Phys. Commun.* **167** (2005) 177, [hep-ph/0410259].

[53] S. Buehler and C. Duhr, *CHAPLIN - Complex Harmonic Polylogarithms in Fortran*, *Comput. Phys. Commun.* **185** (2014) 2703–2713, [1106.5739].

[54] A. V. Kotikov, *Differential equations method: The Calculation of vertex type Feynman diagrams*, *Phys. Lett.* **B259** (1991) 314–322.

[55] T. Gehrmann and E. Remiddi, *Differential equations for two loop four point functions*, *Nucl. Phys.* **B580** (2000) 485–518, [hep-ph/9912329].

[56] J. M. Henn, *Multiloop integrals in dimensional regularization made simple*, *Phys. Rev. Lett.* **110** (2013) 251601, [1304.1806].

[57] A. Grozin, J. M. Henn, G. P. Korchemsky, and P. Marquard, *The three-loop cusp anomalous dimension in QCD and its supersymmetric extensions*, *JHEP* **01** (2016) 140, [1510.07803].

[58] V. Del Duca, C. Duhr, and V. A. Smirnov, *An Analytic Result for the Two-Loop Hexagon Wilson Loop in N = 4 SYM*, *JHEP* **03** (2010) 099, [0911.5332].

[59] V. Del Duca, C. Duhr, and V. A. Smirnov, *The Two-Loop Hexagon Wilson Loop in N = 4 SYM*, *JHEP* **05** (2010) 084, [1003.1702].

[60] A. B. Goncharov, M. Spradlin, C. Vergu, and A. Volovich, *Classical Polylogarithms for Amplitudes and Wilson Loops*, *Phys. Rev. Lett.* **105** (2010) 151605, [1006.5703].

[61] C. Duhr, *Hopf algebras, coproducts and symbols: an application to Higgs boson amplitudes*, *JHEP* **08** (2012) 043, [1203.0454].

[62] C. Duhr, H. Gangl, and J. R. Rhodes, *From polygons and symbols to polylogarithmic functions*, *JHEP* **10** (2012) 075, [1110.0458].

[63] R. E. Cutkosky, *Singularities and discontinuities of Feynman amplitudes*, *J. Math. Phys.* **1** (1960) 429–433.

[64] L. D. Landau, *On analytic properties of vertex parts in quantum field theory*, *Nucl. Phys.* **13** (1959) 181–192.

[65] R. J. Eden, P. V. Landshoff, D. I. Olive, and J. C. Polkinghorne, *The analytic S-matrix*. Cambridge Univ. Press, Cambridge, 1966.

[66] W. L. van Neerven, *Dimensional Regularization of Mass and Infrared Singularities in Two Loop On-shell Vertex Functions*, *Nucl. Phys.* **B268** (1986) 453–488.

[67] G. 't Hooft and M. J. G. Veltman, *DIAGRAMMAR*, *NATO Sci. Ser. B* **4** (1974) 177–322.

[68] E. Gardi, *Progress on soft gluon exponentiation and long-distance singularities*, *PoS* **RADCOR2013** (2013) 043, [1401.0139].

[69] L. Magnea, V. Del Duca, C. Duhr, E. Gardi, and C. D. White, *Infrared singularities in the high-energy limit*, *PoS* **LL2012** (2012) 008, [1210.6786].

[70] V. Del Duca, C. Duhr, E. Gardi, L. Magnea, and C. D. White, *Infrared Singularities and the High-Energy Limit*, 1201.2841. [PoSRADCOR2011,038(2011)].

[71] S. Abreu, R. Britto, C. Duhr, and E. Gardi, *From multiple unitarity cuts to the coproduct of Feynman integrals*, *JHEP* **10** (2014) 125, [1401.3546].

[72] N. Kidonakis, *Two-loop soft anomalous dimensions with massive and massless quarks*, in *Particles and fields. Proceedings, Meeting of the Division of the American Physical Society, DPF 2009, Detroit, USA, July 26-31, 2009*, 2009. 0910.0473.

[73] J. M. Henn, *Analytic results for multiloop scattering amplitudes*, 1209.5879. [PoSLL2012,012(2012)].

[74] J. M. Henn and T. Huber, *Systematics of the cusp anomalous dimension*, *JHEP* **11** (2012) 058, [1207.2161].

[75] M. Dimou, J. Lyon, and R. Zwicky, *Exclusive Chromomagnetism in heavy-to-light FCNCs*, *Phys. Rev.* **D87** (2013), no. 7 074008, [1212.2242].

[76] S. Borowka, G. Heinrich, S. Jahn, S. P. Jones, M. Kerner, J. Schlenk, and T. Zirke, *pySecDec: a toolbox for the numerical evaluation of multi-scale integrals*, 1703.09692.

[77] A. Mitov, G. F. Sterman, and I. Sung, *Computation of the Soft Anomalous Dimension Matrix in Coordinate Space*, *Phys. Rev.* **D82** (2010) 034020, [1005.4646].

[78] A. Ferroglia, M. Neubert, B. D. Pecjak, and L. L. Yang, *Two-loop divergences of scattering amplitudes with massive partons*, *Phys. Rev. Lett.* **103** (2009) 201601, [0907.4791].

[79] A. Ferroglia, M. Neubert, B. D. Pecjak, and L. L. Yang, *Two-loop divergences of massive scattering amplitudes in non-abelian gauge theories*, *JHEP* **11** (2009) 062, [0908.3676].

[80] O. Almelid, *The Three-Loop Soft Anomalous Dimension of Massless Multi-Leg Scattering*. PhD thesis, University of Edinburgh, 2016.

[81] M. Harley, *Multiparton Webs in Non-abelian Gauge Theories at Three Loops and Beyond*. PhD thesis, University of Edinburgh, 2015.

[82] L. J. Dixon, J. M. Drummond, M. von Hippel, and J. Pennington, *Hexagon functions and the three-loop remainder function*, *JHEP* **12** (2013) 049, [1308.2276].

[83] L. J. Dixon and M. von Hippel, *Bootstrapping an NMHV amplitude through three loops*, *JHEP* **10** (2014) 065, [1408.1505].

[84] L. J. Dixon, J. M. Drummond, C. Duhr, M. von Hippel, and J. Pennington, *Bootstrapping six-gluon scattering in planar N=4 super-Yang-Mills theory*, *PoS* **LL2014** (2014) 077, [1407.4724].

[85] S. Caron-Huot, L. J. Dixon, A. McLeod, and M. von Hippel, *Bootstrapping a Five-Loop Amplitude Using Steinmann Relations*, *Phys. Rev. Lett.* **117** (2016), no. 24 241601, [1609.00669].

[86] L. J. Dixon, J. Drummond, T. Harrington, A. J. McLeod, G. Papathanasiou, and M. Spradlin, *Heptagons from the Steinmann Cluster Bootstrap*, *JHEP* **02** (2017) 137, [1612.08976].

[87] O. y. Almelid, C. Duhr, E. Gardi, A. McLeod, and C. D. White, *Bootstrapping the QCD soft anomalous dimension*, 1706.10162.